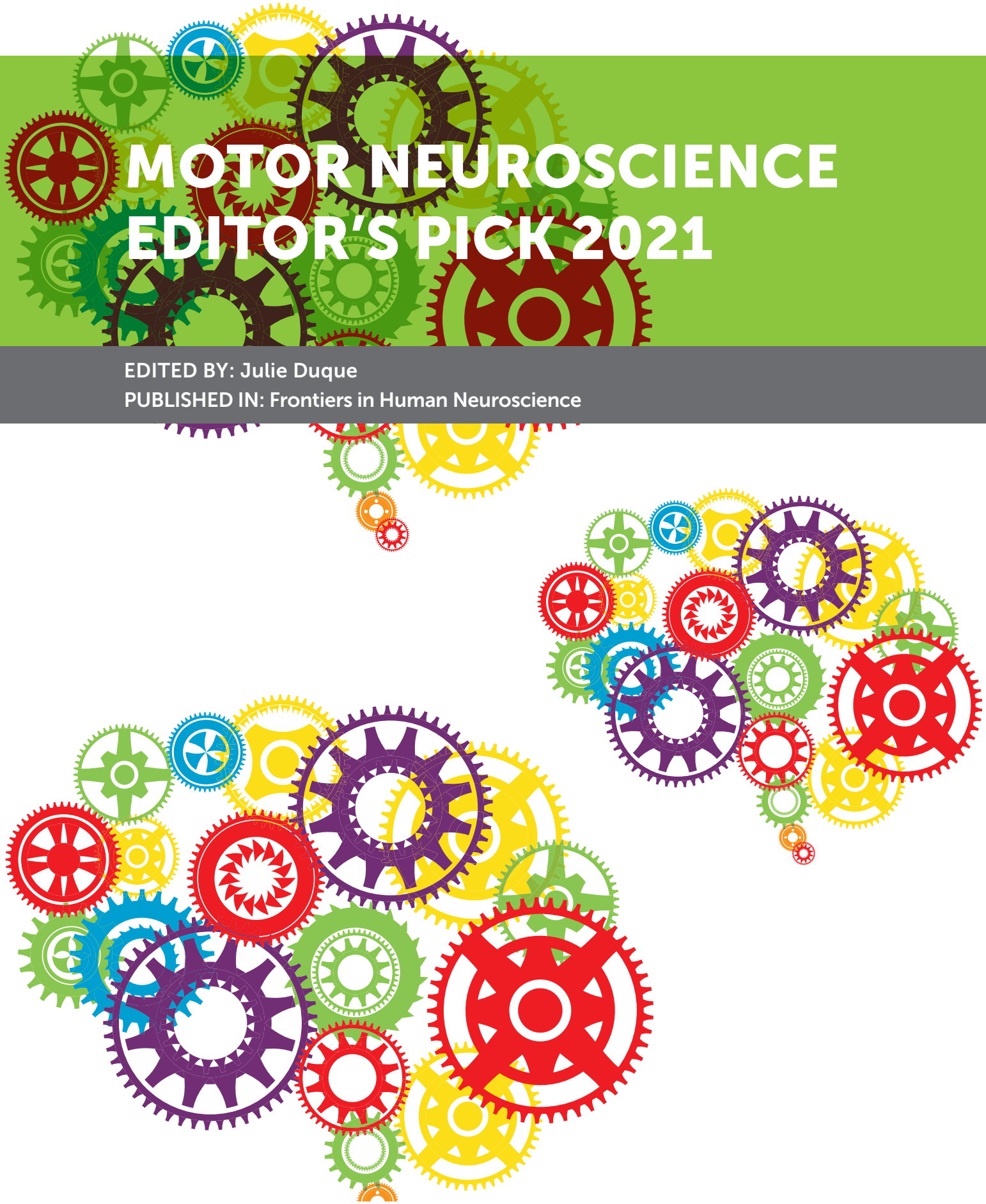

MOTOR NEUROSCIENCE EDITOR'S PICK 2021

EDITED BY: Julie Duque

PUBLISHED IN: Frontiers in Human Neuroscience

frontiers Research Topics

frontiers

ISSN 1664-8714
ISBN 978-2-88971-146-8
DOI 10.3389/978-2-88971-146-8

About Frontiers

Frontiers is more than just an open-access publisher of scholarly articles: it is a pioneering approach to the world of academia, radically improving the way scholarly research is managed. The grand vision of Frontiers is a world where all people have an equal opportunity to seek, share and generate knowledge. Frontiers provides immediate and permanent online open access to all its publications, but this alone is not enough to realize our grand goals.

Frontiers Journal Series

The Frontiers Journal Series is a multi-tier and interdisciplinary set of open-access, online journals, promising a paradigm shift from the current review, selection and dissemination processes in academic publishing. All Frontiers journals are driven by researchers for researchers; therefore, they constitute a service to the scholarly community. At the same time, the Frontiers Journal Series operates on a revolutionary invention, the tiered publishing system, initially addressing specific communities of scholars, and gradually climbing up to broader public understanding, thus serving the interests of the lay society, too.

Dedication to Quality

Each Frontiers article is a landmark of the highest quality, thanks to genuinely collaborative interactions between authors and review editors, who include some of the world's best academicians. Research must be certified by peers before entering a stream of knowledge that may eventually reach the public - and shape society; therefore, Frontiers only applies the most rigorous and unbiased reviews.
Frontiers revolutionizes research publishing by freely delivering the most outstanding research, evaluated with no bias from both the academic and social point of view. By applying the most advanced information technologies, Frontiers is catapulting scholarly publishing into a new generation.

What are Frontiers Research Topics?

Frontiers Research Topics are very popular trademarks of the Frontiers Journals Series: they are collections of at least ten articles, all centered on a particular subject. With their unique mix of varied contributions from Original Research to Review Articles, Frontiers Research Topics unify the most influential researchers, the latest key findings and historical advances in a hot research area! Find out more on how to host your own Frontiers Research Topic or contribute to one as an author by contacting the Frontiers Editorial Office: frontiersin.org/about/contact

MOTOR NEUROSCIENCE EDITOR'S PICK 2021

Topic Editor:
Julie Duque, Catholic University of Louvain, Belgium

Citation: Duque, J., ed. (2021). Motor Neuroscience Editor's Pick 2021. Lausanne: Frontiers Media SA. doi: 10.3389/978-2-88971-146-8

Table of Contents

frontiers in Human Neuroscience

ORIGINAL RESEARCH
published: 09 January 2019
doi: 10.3389/fnhum.2018.00536

Neural Substrates of Cognitive Motor Interference During Walking; Peripheral and Central Mechanisms

Emad Al-Yahya[1,2], Wala' Mahmoud[2,3], Daan Meester[2], Patrick Esser[2,4] and Helen Dawes[2,4]*

[1] School of Rehabilitation Sciences, The University of Jordan, Amman, Jordan, [2] Movement Science Group, Faculty of Health and Life Sciences, Oxford Brookes University, Oxford, United Kingdom, [3] Institute for Clinical Psychology and Behavioural Neurobiology, Eberhard Karls Universität Tübingen, Tübingen, Germany, [4] Faculty of Health and Life Sciences, Centre for Movement, Occupational and Rehabilitation Sciences, OxINMAHR, Oxford Brookes University, Oxford, United Kingdom

Current gait control models suggest that independent locomotion depends on central and peripheral mechanisms. However, less information is available on the integration of these mechanisms for adaptive walking. In this cross-sectional study, we investigated gait control mechanisms in people with Parkinson's disease (PD) and healthy older (HO) adults: at self-selected walking speed (SSWS) and at fast walking speed (FWS). We measured effect of additional cognitive task (DT) and increased speed on prefrontal (PFC) and motor cortex (M1) activation, and Soleus H-reflex gain. Under DT-conditions we observed increased activation in PFC and M1. Whilst H-reflex gain decreased with additional cognitive load for both groups and speeds, H-reflex gain was lower in PD compared to HO while walking under ST condition at SSWS. Attentional load in PFC excites M1, which in turn increases inhibition on H-reflex activity during walking and reduces activity and sensitivity of peripheral reflex during the stance phase of gait. Importantly this effect on sensitivity was greater in HO. We have previously observed that the PFC copes with increased attentional load in young adults with no impact on peripheral reflexes and we suggest that gait instability in PD may in part be due to altered sensorimotor functioning reducing the sensitivity of peripheral reflexes.

Keywords: gait control, prefrontal cortex, motor cortex, H-reflex, fNIRS, Parkinson disease, cognitive motor interference

OPEN ACCESS

Edited by:
Hidenao Fukuyama, Kyoto University, Japan

Reviewed by:
Eling D. de Bruin, Karolinska Institute (KI), Sweden
Sean Commins, Maynooth University, Ireland

****Correspondence:***
Emad Al-Yahya
e.alyahya@ju.edu.jo

Received: *25 October 2018*
Accepted: *20 December 2018*
Published: *09 January 2019*

Citation:
Al-Yahya E, Mahmoud W, Meester D, Esser P and Dawes H (2019) Neural Substrates of Cognitive Motor Interference During Walking; Peripheral and Central Mechanisms. Front. Hum. Neurosci. 12:536. doi: 10.3389/fnhum.2018.00536

INTRODUCTION

Walking, although a largely automatic process, is controlled by the cortex, brain stem and the spinal cord; with corrective reflexes modulated through integration of neural signals from central and peripheral inputs throughout the gait cycle (Nielsen, 2003; Yang and Gorassini, 2006; Meester et al., 2014; Minassian et al., 2015). Controlled experiments and studies from pathological populations demonstrate that impairments to any of these systems affect gait control (Axer et al., 2010; Takakusaki, 2017). In particular, gait adaptation to unpredictable environmental constraints is challenged by such impairments, rendering ambulation unsafe and increasing fall risks (Axer et al., 2010; Hamacher et al., 2015). However, whilst much is known about each of the systems independent working, there is less information of the integration of central and peripheral

mechanisms during walking. A better understanding of gait control mechanisms in healthy adults and in those with increased risk of falls may inform novel therapeutic approaches.

On the one hand, we know that central motor networks, including the motor, premotor, and prefrontal cortices are active during walking and that additional cognitive tasks can interfere with walking performance particularly in older adults or those with pathology (Suzuki et al., 2004; Al-Yahya et al., 2011; Hamacher et al., 2015). For example, increased prefrontal cortex (PFC) activation under dual task (DT) walking conditions has been repeatedly reported in different groups of participants (Hamacher et al., 2015; Herold et al., 2017). Previously, we have found that DT walking resulted in increased PFC activation in healthy adults and in chronic stroke survivors (Meester et al., 2014; Al-Yahya et al., 2016). In other studies, DT-related increase in PFC activation has been shown in healthy elderly (Holtzer et al., 2015) and in people with Parkinson's disease (PD) (Maidan et al., 2016; Nieuwhof et al., 2016). One suggested mechanism is through central motor networks influence on spinal reflex circuits via corticospinal inputs to alpha motor-neuron (Knikou, 2008, 2010). In particular, PFC capacity to activate the motor cortex required for task execution (Corp et al., 2013; Fujiyama et al., 2016), as activity in the motor cortex has been reported to be directly involved in leg muscles control during human walking (Petersen et al., 2001).

On the other hand, previous studies show that H-reflex gain can be modulated based on task and environment. For example, it has been reported that H-reflex is attenuated during running and narrow beam walking (Capaday and Stein, 1987; Llewellyn et al., 1990), during DT standing (Weaver et al., 2012), and in the elderly compared to young adults (Chalmers and Knutzen, 2000). Combined, these results suggest that the gain of the H-reflex is reduced, indicating a depressed spinal reflex excitability, in tasks or individuals requiring greater stability (Zehr, 2002). Perhaps, H-reflex is suppressed to prevent excessive reflex activation of motor neurons, and possible instability in the stretch reflex feedback loop, while allowing high levels of afferent signals to continue to supraspinal structures so that these signals can contribute to locomotor activity (Capaday and Stein, 1987; Llewellyn et al., 1990; Hayashi et al., 1992). In support of this hypothesis, it has been suggested that H-reflex suppression in complex postural tasks may reflect more cortical control over the task as well as to prevent unwanted oscillations in postural control (Koceja et al., 1995), and H-reflex is relatively resistance to modulation when conditioning sources are peripheral (Garrett et al., 1999; Ferris et al., 2001), suggesting a central control of reflex modulation while walking (Phadke et al., 2010).

However, brain pathologies, such as stroke or PD, lead to defective utilization of these peripheral inputs by spinal reflex circuits (Dietz, 2002; Hiraoka et al., 2005; Mullie and Duclos, 2014). In addition to the basal ganglion pathology, alterations in a widespread supraspinal locomotor network have been suggested to underlie distinctive gait dysfunctions in people with PD (Amano et al., 2013; Peterson and Horak, 2016). Moreover, impaired modulation of the Soleus H-reflex during standing (Hayashi et al., 1997) and gait initiation (Hiraoka et al., 2005) has been reported in people with PD, which might be attributed to abnormal descending control. Therefore, a better understanding of how peripheral and central mechanism are integrated to modulate spinal circuits may inform effective interventions. To date there have been no studies exploring these mechanisms simultaneously in older healthy adults and those with known gait pathology. In this study in healthy older adults and people with PD we used an additional cognitive task to interfere with the automatic processing occurring during locomotion on a treadmill by introducing a backward counting task (Al-Yahya et al., 2009). We investigated the effect of the additional demands on the PFC and motor cortex activities and on Soleus H-reflex gain alongside gait performance (Suzuki et al., 2004, 2008; McCulloch, 2007). We anticipated that differences in the involvement of peripheral and central mechanisms will emerge between people with PD and healthy older adults and these differences will be relative to the walking task.

MATERIALS AND METHODS

This study was approved by Oxford Brookes University Research Ethics Committee (UREC120604). All methods were carried out in accordance with the latest guidelines and regulations of the Declaration of Helsinki. All subjects gave informed, written consent prior to participation.

Participants

We recruited two groups of participants to take part in this cross-sectional randomized repeated measure study; people diagnosed with Parkinson's disease (PD) and age similar healthy older adults (HO). General inclusion criteria for all participants were (a) above 50 years old; (b) no named neurological condition other than PD for the experimental group; (c) mentally intact; (d) able to walk safely and continuously on a treadmill for at least 5 min; and (e) able to give written consent. People with PD were included if they were also (a) diagnosed with idiopathic PD as confirmed by a neurologist; (b) taking their prescribed anti-Parkinsonian medication; and (c) fully independent in all activities of daily living as per Hoehn and Yahr scale (Hoehn and Yahr, 1967). Healthy control were basically relatives of PD patients/interested people from local community, or university employee. They were defined healthy as per their own words. Participants were excluded if they had psychiatric comorbidity, clinical diagnosis of dementia or other clinically significant cognitive impairment, and a history of any neurological disorder that could affect their performance (other than PD).

For patients with PD, we conducted all tests within the practical self-reported "ON" medications state (roughly within 1–2 h after medication intake). PD patients were in general moderately physically active per self-report.

Study Design and Procedure

In order to standardize the assessment, we advised all participants to avoid strenuous exercise 24 h prior to the assessment. Initially, we familiarized participants with the treadmill walking (Woodway ELG 75, Germany) at varying speeds. Thus, for each participant we determined a preferred self-selected treadmill

speed, which relatively corresponds to individual's natural over-ground walking speed (Al-Yahya et al., 2009; Meester et al., 2014), hereinafter referred to as self-selected walking speed (SSWS). We then increased the SSWS by 20% to determine a faster walking (Voloshin, 2000; Meester et al., 2014), hereinafter referred to as fast-walking speed (FWS).

We then introduced participants to the cognitive (i.e., distracting) task. For the cognitive task, we utilized serial subtraction by a given number (i.e., counting backward by 7 s). Serial subtraction is a mental tracking task that loads cognitive resources of the brain that are otherwise engaged in processing attention and working memory (Al-Yahya et al., 2011). This cognitive task is also known to negatively affect walking performance, not only among the elderly and individuals with neurologic disorders but also in healthy young adults (Al-Yahya et al., 2011).

Each participant then completed two walking trials; one at SSWS and the other at FWS in a pseudo random order. Each trial consisted of five blocks of single-task (ST) walking and five blocks of dual-task (DT) walking (i.e., subtracting whilst walking) conditions. For each trial, walking tasks consisted of a 30 s task period repeated 10 times (5 blocks of ST walking and 5 blocks of DT walking) and alternated with rest periods. To avoid anticipation of walking blocks onset, the duration of rest periods ranged from 25 to 45 s in a pseudo-random order. During the DT blocks, participants were asked to count backward in sevens from a random 3-digit number. The instructions before ST and DT blocks were standardized for all participants and they were not given advice as to which task to prioritize during DT-walking. To monitor hemodynamic responses, systematic blood pressure, and heart rate were measured at the beginning and after the end of each trial.

fNIRS Imaging and Processing

Cortical brain activation was measured with the OxyMon Mk III system (Artinis Medical Systems, Netherlands). The continuous-wave multichannel system uses two wavelengths at 782 and 859 nm to estimate relative changes in the concentration of oxygenated (oxy-Hb) and deoxygenated (deoxy-Hb) hemoglobin, respectively.

In order to estimate PFC task-related activation, two identical plastic holders consisting of two optodes each (one source and one detector) with an inter optode distance of 30 mm were placed on each participant's forehead using a custom-built spring-loaded holder centered in the area linking Fp1, F3, and F7 and the area linking Fp2, F4, and F8 according to the international 10–20 EEG electrode placement system, which corresponds to the left and right PFC, respectively (Leff et al., 2008; Al-Yahya et al., 2016).

Additionally, a 4-channel arrangement (two sources and two detectors) was aligned with Cz (**Figure 1**). The four channels within this arrangement covered the area linking Cz, C3, F3, and Fz, and the area linking Cz, C4, F4, and Fz, which corresponds to left and right sensorimotor cortex (SMC), respectively, including the primary motor cortex (M1) (Okamoto et al., 2004; Koenraadt et al., 2014).

Optical signals were continuously sampled at 10 Hz, and stored according to their wavelength and location, resulting in values for changes in the concentration of oxy-Hb and deoxy-Hb from each channel. Optical data were used to quantify task-related changes of oxy-Hb and deoxy-Hb based on the modified Beer-Lambert law (Delpy et al., 1988).

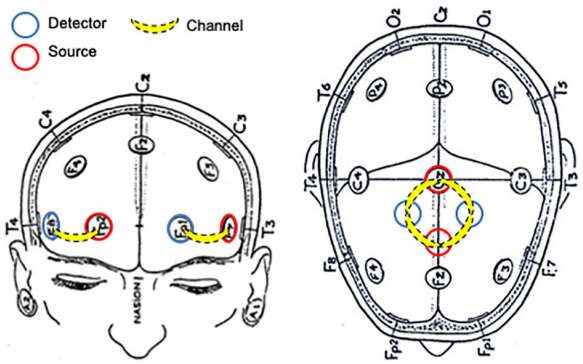

FIGURE 1 | Schematic representation of NIRS probe location.

NIRS data processing was performed using the OxySoft software (version 2.1.6). Standard pre-processing and individual-level statistical analysis was applied (Meester et al., 2014; Al-Yahya et al., 2016). Initially, traces were visually inspected by two investigators independently to identify motion artifacts. Motion artifacts were defined as sudden changes in the amplitude of the NIRS signals (oxy-Hb and deoxy-Hb) that were much larger than the expected changes and that appeared in several channels, while missing signals were characterized by flat-line appearing traces of oxy-Hb and/or deoxy-Hb changes. Blocks with motion artifacts were excluded from further analysis. To remove high frequency noise such as cardiac pulsation, NIRS signals were then low-pass filtered at a 0.67 Hz cut off frequency using a customized LabVIEW program (National Instruments, Austin, TX, United States). A moving average filter with a width of 4 s was then used to smooth the signal. Block averages of the task plus rest repetitions were calculated and the middle 10 s of each task and rest periods used for statistical analyses. To identify channels exhibiting task-related activation, average concentration changes were compared, by means of *t*-tests for all tasks to the average baseline-corrected on a block-by-block basis by subtracting the mean intensity of the 5 s preceding trial onset (i.e., last 5 s of rest block) from the overall task block. Active channels were defined as statistically different relative to baseline. For each task, signals from all repeats were averaged, and data from active channels were used for subsequent statistical analyses.

H-Reflex Measurement and Gain Calculation

H-reflexes were elicited in the right Soleus muscle (SOL) as described before (Meester et al., 2014). We utilized a constant current high voltage stimulator (Digitimer Ltd., DS7A, United Kingdom) to elicit H-reflexes and M-waves (**Figure 2**). We recorded H-reflex recruitment curves while participants were standing. In order to determine the intensity which would elicit 20–25% of Mmax (Simonsen and Dyhre-Poulsen,

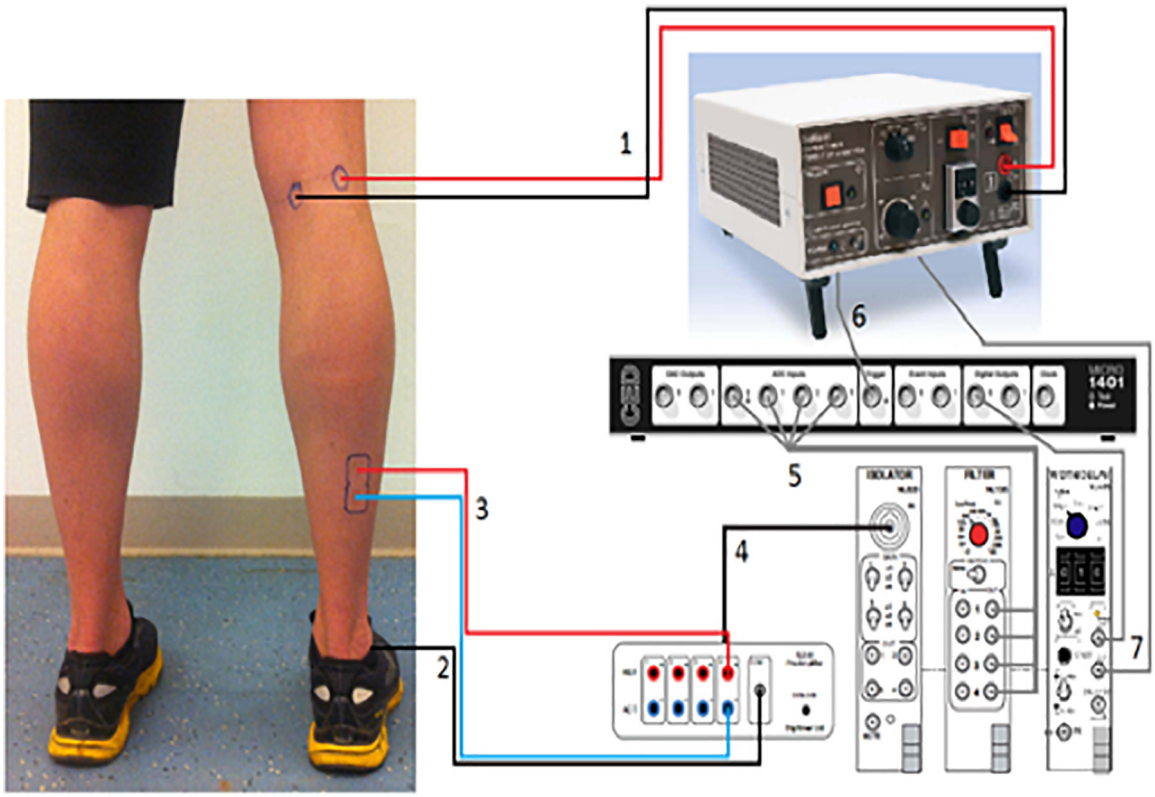

FIGURE 2 | H-reflex measurement setup. (1) The cables from the stimulator to the Tibial nerve in the popliteal fossa. (2) Reference electrode going to the lateral Malleolus. (3) The cables from the EMG-amplifier going to the Soleus. (4) The EMG-signal going to isolator which is connected with the filter. (5) The filtered EMG-signal is going to the CED-box. This box is connected with the pc. (6) The signal from the stimulator is also sent to the CED-box. (7) "Width-tool," which sends the signal to the CED-box. With a pc the signals from the CED-box can be viewed in the "Signal Software."

1999; Phadke et al., 2010) we measured Hmax and Mmax. A footswitch (Odstock Medical Ltd., United Kingdom) under the participant's right heel was used to synchronize H-reflex with the mid stance [30% (Hughes and Jacobs, 1979)] phase of the gait cycle. To prevent depression of the H-reflex and subject anticipation of the reflex, stimulations were given every 4–6 heel strikes; corresponding to an inter-stimulus-time (ISI) of 4–5 s, which is known to be long enough to measure consecutive H-reflexes (Knikou and Taglianetti, 2006; Jeon et al., 2007).

Ag–AgCl electrodes were placed on the muscle belly and as a stimulating electrode on the Tibial nerve (Konrad, 2005). The cathode was placed in the popliteal fossa with the anode at a distance of 2 cm medial to the cathode (**Figure 2**). We located the nerve using small moveable electrodes, before positioning the actual stimulation electrodes, which were secured with Velcro tape to prevent slippage during locomotion. EMG leads were attached to the leg and upper body to reduce movement artifacts and prevent subjects from tripping.

Data acquisition and initial analysis were performed using Signal software (CED Signal 3.09, United Kingdom). EMG signals were pre-amplified and high passed filtered at 42.5 Hz (NL844; Digitimer). Signals were then low pass filtered at 200 Hz (NL135; Digitimer) before H-reflexes were sampled at 1000 Hz (Tokuno et al., 2007). A customized LabVIEW program (National Instruments, Austin, TX, United States) was used to automatically detect the H-reflex and calculate its peak-to-peak amplitude.

We calculated H-reflex gain as described previously (Capaday and Stein, 1987; Edamura et al., 1991). For each measurement at 30% of the gait cycle, we calculated the average of the rectified EMG during the time frame. Then, we plotted a data point for each time frame with the corresponding H-reflex amplitude on the *y*-axis and the averaged rectified EMG on the *x*-axis. We fitted a linear least-square regression model to the data points at each walking task for each subject. Then, we calculated the slopes of the H-reflex amplitudes versus averaged background EMG regression lines.

Gait Measurement

Step time was measured using an inertial measuring unit (Philips, Eindhoven, Netherlands) comprising a tri-axial accelerometer, gyroscope and magnetometer placed on the projected center of mass located over the fourth lumbar vertebrae (Esser et al., 2012). Post-processing and analysis was performed using a customized prewritten program in LabVIEW (National Instruments, Austin, TX, United States). Step time was then estimated according to the inverted pendulum gait model (Esser et al., 2009),

and variability of step time was estimated using the standard deviation.

Statistical Analysis

Statistical analysis was performed using IBM-SPSS 25.0 (IBM SPSS, Inc., Armonk, NY, United States). At first, we performed descriptive. statistical analysis on demographics (**Tables 1**, **2**). Then, we analyzed behavioral (i.e., step time and step time variability) and physiological (i.e., H-reflex gain) gait measures by conducting a mixed-design analysis of variance (ANOVA) with task (two levels; ST-walking and DT-walking) and speed (two levels; SSWS and FWS) as the independent within-subjects variables for each measure separately, and participants' group (two levels; PD and HO) as the between-subject factor.

For the NIRS data statistical analysis, the average of relative changes in oxy-Hb and deoxy-Hb concentrations of combined activated blocks was calculated for each task and region (left PFC, left M1, and right M1). Initially, we intended to include the site (left vs. right PFC) as another factor in our NIRS analysis. Due to unforeseen technical reasons, the NIRS signals from the right PFC showed very low gain for almost all participants and, therefore, it was not included in the final analysis. For each region (i.e., left PFC, right M1, and Left M1) data from all participants were analyzed by conducting a mixed-design ANOVA with task (two levels; ST-walking and DT-walking) and speed (two levels; SSWS and FWS) as the independent within-subjects variables while participant group (two levels) was the between-subjects factor. For all statistical tests, alpha level was set at 0.05 *a priori* and SPSS-generated Bonferroni adjusted *P*-values are quoted.

RESULTS

A total number of 51 participants were recruited and evaluated according to the protocol; 29 individuals with PD and 22 HO adults. PD patients were significantly older and walk slower than HO at both speeds (**Table 1**). Due to technical difficulties, however, we could not obtain the full data set (gait data, H-reflex, and NIRS data) from all of the participants. In particular, NIRS data from the right PFC were missing for all participants as the signal to noise ratio was very low.

All PD participants were independent in their activities of daily living (**Table 2**), and the majority of them (70%) had a unilateral involvement according to the Hoehn and Yahr scale. The detailed characteristics of PD participants are summarized in **Table 2**.

TABLE 1 | Participants characteristics.

	N	Females	Age* (mean ± SD)	SSWS* (mean ± SD) m/s	FWS* (mean ± SD) m/s
Old	22	16	59.5 ± 6.8	1.04 ± 0.19	1.24 ± 0.23
PD	29	13	66.3 ± 5.9	0.89 ± 0.21	1.06 ± 0.26

**Independent samples t-test (two-tailed) revealed significant differences between groups ($p < 0.05$).*

Behavioral Gait Measures

We first examined whether counting while walking on the treadmill would interfere with gait pattern at either of the walking speed. Average and variability of step time are summarized in **Table 3**. For step time, mixed-design ANOVA revealed no significant main effect of task [$F(1,43) = 0.79$, $p = 0.38$] or group [$F(1,43) = 0.11$, $p = 0.74$]. However, mixed-design ANOVA revealed a significant main effect of speed [$F(1,43) = 4.22$, $p = 0.04$, $\eta^2 = 0.089$]. Pairwise comparisons revealed that speed effect was only significant for HO group under ST ($p < 0.001$) and DT ($p = 0.033$) conditions (**Table 3**).

For step time variability, there were no significant main effects of task [$F(1,43) = 0.68$, $p = 0.41$], speed [$F(1,43) = 0.97$, $p = 0.33$], or group [$F(1,43) = 2.59$, $p = 0.12$]. For both step variables we measured, mixed-design ANOVA revealed no significant interactions between task, speed, and group.

TABLE 2 | Parkinson's disease group detailed characteristics.

Barthel index score[1]: median (range)	**20 (19–20)**
Tripping without falling: number (%)	10 (34.5%)
Falling: number (%)	7 (24%)
FOG[2]: number (%)	7 (24%)
HY[3] stage ("ON meds"): number (%)	
HY = 1	20 (70%)
HY = 2	9 (30%)
HY = 3	0
HY = 4	0
HY = 5	0
MDS-UPDRS[4] ("ON meds") mean (SD)	
Part I (0–52)	8.6 (4.5)
Part II (0–52)	8.25 (5.1)
Part III (0–132)	16.7 (10)
Part IV (0–24)	1.65 (2.6)

[1]A scale for activity of daily living (Mahoney and Barthel, 1965). [2]Freezing of gait. [3]Hoehn-Yahr Classification of Disability Scale (Hoehn and Yahr, 1967): (1) Absent or minimal unilateral disability; (2) Minimal bilateral or midline involvement with intact balance; (3) Unsteadiness when turning or rising with some activities restrictions, patients are independent; (4) Severe symptoms and possible walking with assistance; (5) Confined to bed or wheelchair. [4]Unified Parkinson's Disease Rating Scale, a measure of disease progression (Goetz et al., 2008).

TABLE 3 | Gait measurement results (Mean ± SD).

	Old		**PD**	
	ST	**DT**	**ST**	**DT**
SSWS				
Step time (ms)*	**547 ± 69**	**553 ± 76**	530 ± 50	529 ± 82
Step time variability	81.4 ± 80	68.5 ± 72	98 ± 85	94.7 ± 99
FWS				
Step time (ms)*	**508 ± 39**	**527 ± 43**	529 ± 70	523 ± 94
Step time variability	44.7 ± 31	50.2 ± 50	103 ± 134	93.9 ± 100

**Repeated measure ANOVA revealed a significant ($p < 0.05$) main effect of speed on step time. Significant pairwise comparisons ($p < 0.05$) between SSWS and FWS for both tasks are highlighted in bold and appeared only in the old group.*

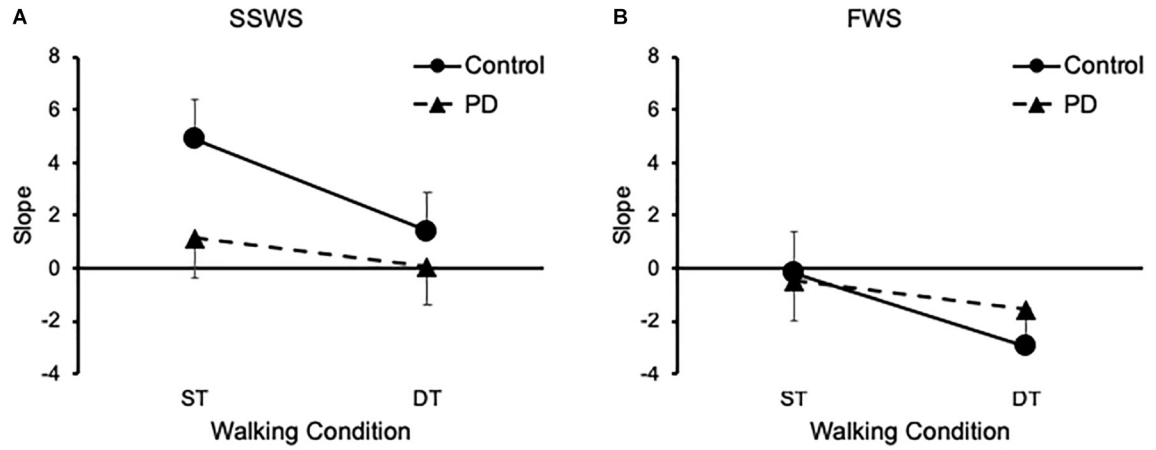

FIGURE 3 | Groups results of the Soleus H-reflex gain. **(A)** Means and standard errors of linear regressions slopes at SSWS. **(B)** Means and standard errors of linear regressions slopes at FWS. PD, Parkinson disease; SSWS, self-selected walking speed; FWS, fast walking speed; ST, single task; DT, dual task.

Physiological Gait Measures

Next we examined the effects of task, speed, and group on H-reflex gain. Our findings are illustrated on **Figure 3**. Mixed-design ANOVA revealed a significant main effect of task [$F(1,26) = 30.489$, $p < 0.001$, $\eta^2 = 0.540$] on H-reflex gain, which decreased during DT-walking compared with ST-walking for both groups and at the two walking speeds (**Figure 3**). There was no significant main effect of either speed [$F(1,26) = 2.978$, $p = 0.057$] or group [$F(1,26) = 1.106$, $p = 0.303$] on H-reflex gain. However, there was a significant interaction between task and group [$F(1,26) = 7.324$, $p = 0.012$, $\eta^2 = 0.220$]. Independent samples t-test (two-tailed) revealed that OH participants exhibited larger H-reflex gain than PD participants ($p = 0.045$) only while walking under ST condition and at SSWS (**Figure 3**).

Cortical Activations

Finally, we examined the effects of task, speed, and group on cortical brain activation. In particular, we analyzed relative concentration changes of oxy-Hb and deoxy-Hb in left PFC, left M1, and right M1. Results are illustrated on **Figure 4** and summarized in **Table 4**. For the left PFC, mixed-design ANOVA revealed a significant main effect of task on oxy-Hb relative concentration changes [$F(1,17) = 12.945$, $p = 0.003$, $\eta^2 = 0.648$], but not on deoxy-Hb [$F(1,17) = 4.137$, $P = 0.061$, $\eta^2 = 0.304$]. Also, there were no significant main effects of speed or group on either oxy-Hb or deoxy-Hb (**Figure 4A**). There was a significant main effect of task on oxy-Hb [$F(1,17) = 31.307$, $p > 0.001$, $\eta^2 = 0.423$] and deoxy-Hb [$F(1,17) = 7.428$, $p = 0.014$, $\eta^2 = 0.305$] in left M1, with no significant main effect of either group or speed (**Figure 4B**). Similarly, there was a significant main effect of task on oxy-Hb [$F(1,17) = 12.45$, $p = 0.003$, $\eta^2 = 0.480$], and deoxy-Hb [$F(1,17) = 7.45$, $p = 0.014$, $\eta^2 = 0.228$] in right M1, with no significant main effect of either speed or group (**Figure 4C**). For all measured cortical areas, there were no significant interactions between task, speed, and group.

DISCUSSION

In the present study we investigated neuronal control mechanisms affecting gait performance in people with PD and a group of healthy older adults (HO). We measured the effect of an additional cognitive task and increased walking speed on the pre-frontal and motor cortex activation, and the Soleus H-reflex gain alongside behavioral gait performance. Under DT conditions, as we expected, we observed increased cortical activation in PFC and M1 for both groups and speeds. Whilst, H-reflex gain decreased with the additional cognitive load and somehow increased speed for both groups, H-reflex gain was lower in PD compared to HO only while walking under ST condition at SSWS. Concerning behavioral gait measures, DT interference during walking at both speeds was comparable for PD and HO controls. All in all, these observations show hitherto unreported integration of central and peripheral mechanisms of gait control in PD and HO. We propose that attentional load in the PFC excites the M1, which in turn increases inhibition on H-reflex activity during walking and reduces the activity and sensitivity of peripheral reflex during the stance phase of gait. Importantly this effect on sensitivity was greater in HO. We have previously observed that the PFC appears to be able to cope with increased attentional load in young adults with no impact on peripheral reflexes (Meester et al., 2014), and we suggest that gait instability in PD may in part be due to altered sensorimotor functioning reducing the sensitivity of peripheral reflexes.

Safe, independent, and goal-directed gait is crucial for daily living and relies on complex neuronal networks encompassing supraspinal and spinal structures of the CNS. On the one hand, supraspinal structures usually participate in appropriate planning and precise control of movement (Drew and Marigold, 2015). Thus, they are indispensable for adapting gait to the behavioral goals. On the other hand, spinal circuits modulate corrective reflexes throughout the gait cycle by integrating neural signals

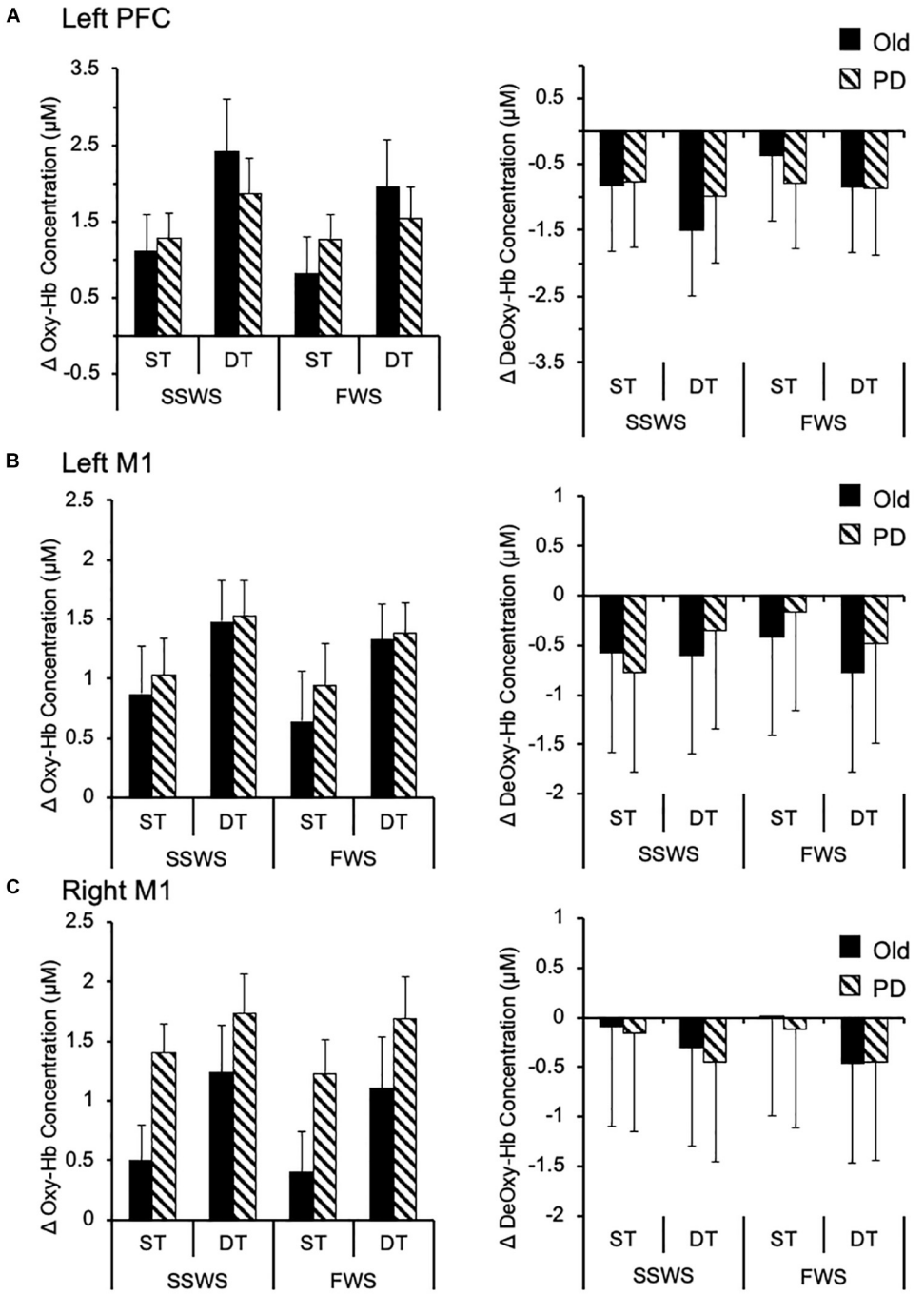

FIGURE 4 | Cortical activation while walking. Group data (means and standard errors) of task-related changes in oxy-Hb (left side) and deoxy-Hb (right side) concentrations while walking under different conditions, in **(A)** left prefrontal cortex, **(B)** left motor cortex, and **(C)** right motor cortex. oxy-Hb, oxygenated hemoglobin; deoxy-Hb, deoxygenated hemoglobin; M1, motor cortex; PFC, prefrontal cortex; PD, Parkinson disease; SSWS, self-selected walking speed; FWS, fast walking speed; ST, single task; DT, dual task.

from peripheral as well as central inputs (Nielsen, 2003; Yang and Gorassini, 2006; Meester et al., 2014; Minassian et al., 2015).

Mounting evidence from neuroimaging studies suggests that stable and goal-directed gait requires the activation of both cortical and subcortical structures of the brain (Hamacher et al., 2015; Herold et al., 2017). In particular, two cortical networks have been proposed; a direct and an indirect pathway (la Fougère et al., 2010; Zwergal et al., 2012, 2013). The direct pathway is potentially involved in the automatic control of gait via M1, cerebellum, and spinal cord. The indirect pathway emerges

TABLE 4 | Brain activation as measured by relative concentration changes (in μM) in Oxy-Hb and DeOxy-Hb (Mean ± SE).

Area	SSWS		FWS	
	ST	DT	ST	DT
Left M1				
*Oxy-Hb**				
Old	**0.876 ± 0.394**	**1.484 ± 0.345**	**0.641 ± 0.419**	**1.330 ± 0.301**
PD	**1.037 ± 0.336**	**1.529 ± 0.294**	**0.941 ± 0.358**	**1.381 ± 0.257**
*DeOxy-Hb**				
Old	−0.575 ± 0.258	−0.599 ± 0.28	**−0.412 ± 0.251**	**−0.775 ± 0.26**
PD	**−0.018 ± 0.22**	**−0.346 ± 0.239**	−0.161 ± 0.214	−0.484 ± 0.222
Right M1				
*Oxy-Hb**				
Old	0.501 ± 0.291	1.242 ± 0.39	**0.399 ± 0.338**	**1.107 ± 0.422**
PD	**1.400 ± 0.248**	**1.731 ± 0.333**	**1.223 ± 0.288**	**1.684 ± 0.36**
*DeOxy-Hb**				
Old	−0.095 ± 0.104	−0.302 ± 0.199	0.004 ± 0.192	−0.467 ± 0.249
PD	**−0.156 ± 0.089**	**−0.450 ± 0.17**	−0.117 ± 0.163	−0.447 ± 0.212
Left PFC				
*Oxy-Hb**				
Old	1.104 ± 0.49	2.422 ± 0.688	**0.814 ± 0.478**	**1.952 ± 0.62**
PD	**1.277 ± 0.33**	**1.872 ± 0.464**	1.266 ± 0.322	1.533 ± 0.418
DeOxy-Hb				
Old	−0.824 ± 0.364	−1.501 ± 0.501	−0.363 ± 0.333	−0.838 ± 0.499
PD	−0.759 ± 0.245	−0.987 ± 0.338	−0.783 ± 0.225	−0.872 ± 0.338

Repeated measure ANOVA revealed a significant ($p < 0.05$) main effect of task on cortical activation. Significant pairwise comparisons ($p < 0.05$) between ST and DT for both groups and speeds are highlighted in bold.*

in challenging situations (i.e., those that require cognitive as opposed to automatic gait control) and additionally involves prefrontal and premotor areas (Hamacher et al., 2015; Herold et al., 2017). Therefore, gait control entails a subtle balance between automatic and executive control processes, which is dependent upon task demands and individual's ability (Clark, 2015). Findings from our study support this notion; we observed increased PFC and M1 activation under DT walking compared to ST in both groups.

Increased PFC activation under DT walking conditions has been repeatedly reported in different groups of participants (Hamacher et al., 2015; Herold et al., 2017). Previously, we have found that DT walking resulted in increased PFC activation in healthy adults and in chronic stroke survivors (Meester et al., 2014; Al-Yahya et al., 2016). In other studies, DT-related increase in PFC activation has been shown in healthy elderly (Holtzer et al., 2015) and in people with PD (Maidan et al., 2016; Nieuwhof et al., 2016). Although healthy young adults responded to additional cognitive load with increased PFC activation (Meester et al., 2014), this was not associated with altered gait parameters. Whereas, a greater increase in PFC activation observed from ST to DT walking was related to a greater change in motor performance in stroke survivors (Al-Yahya et al., 2016). Similarly, a negative association between PFC activation and gait performance was observed in healthy elderly (Holtzer et al., 2016) and in people with PD (Maidan et al., 2016). In contrast, walking at different steady state speeds did not considerably affect PFC activation (Suzuki et al., 2004; Meester et al., 2014), which is similar to what we have found in this study. This is presumably due to the ability of brain stem and spinal circuits within the direct pathway to automatically adjust gait pattern without a substantial need for executive control (Clark, 2015). Taken together, these findings alongside ours are in line with a recently suggested model of gait control (Clark, 2015; Gramigna et al., 2017). This model proposes that when the automatic execution of gait is compromised, such that by normal aging, pathology of the CNS, or episodic cognitive load, individuals may compensate by switching to cognitive control, in particular executive control in the PFC.

Performing complex motor tasks, as opposed to simple ones, require additional activations in subcortical and cortical regions other than the PFC (Godde and Voelcker-Rehage, 2010). For example, consistent findings from NIRS imaging studies show gait related changes in motor and somatosensory regions (Suzuki et al., 2004; Kurz et al., 2012; Koenraadt et al., 2014). In the present study, we observed DT related increase in M1 activation in both groups during walking at different speeds.

Successful and adaptive control of motor performance requires not only excitatory, but also inhibitory functioning of neural circuits within motor area (Beck et al., 2008; Beck and Hallett, 2011). Recent TMS studies show that older adults exhibited decreased ability to inhibitory function within motor areas as compared to younger adults (Fujiyama et al., 2009), and suggest a significant relationship between motor performance under DT conditions and reduction in inhibitory control within

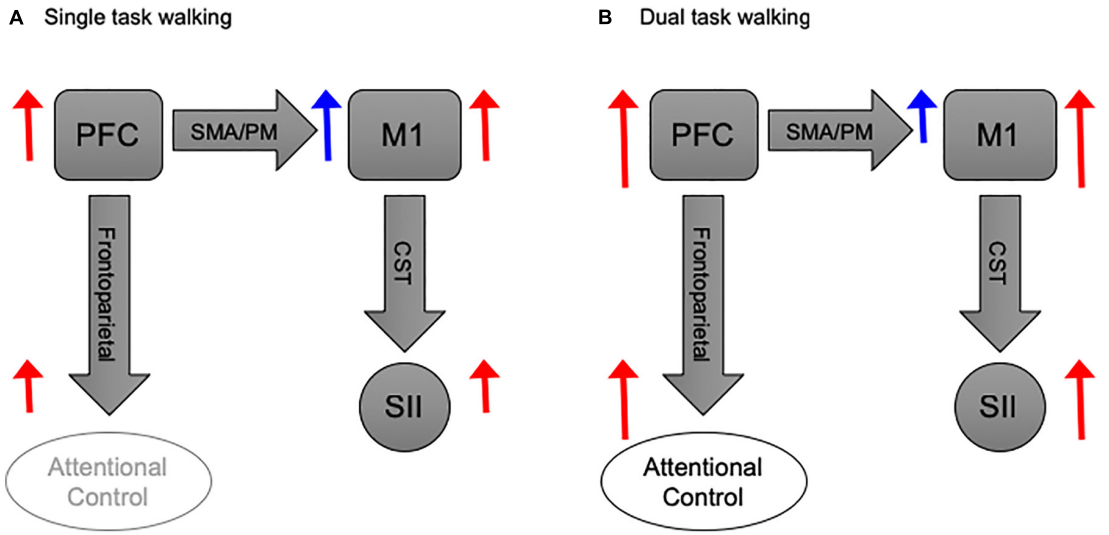

FIGURE 5 | Basic schematic illustration of the functional coupling between PFC and M1 during walking. **(A)** PFC activation during ST walking is devoted to inhibitory modulation of M1 activity via SMA/PM pathways. While PFC involvement in attentional control is tentative, M1 exerts excitatory modulation over SII via CST. **(B)** PFC activation during DT walking, albeit increased, is primarily devoted to attentional control. Thus, its inhibitory effect on M1 becomes less, and the later exerts a more substantial excitatory modulation over SII. Block arrows represent anatomical pathways. Red and blue arrows donate excitatory and inhibitory modulations, respectively. Sizes of blue and red arrows are relative to the proposed activation level. PFC, prefrontal cortex; M1, motor cortex; SMA, sensorimotor area; PM, premotor area; SII, spinal inhibitory interneurons; CST, corticospinal tract.

motor areas (Fujiyama et al., 2012a,b). It is likely that the additional task under DT conditions results in under activation of inhibitory circuits within motor areas (Corp et al., 2013), rather than increased activation of the excitatory circuits. Therefore, the observed DT related increase in M1 activation could be attributed to disinhibition, rather than excitation, of motor area.

Furthermore, we observed a considerable level of PFC activation during ST walking relative to baseline (i.e., standing). This may reflect a successful mechanism to compensate for loss of automaticity in PD and HO adults (Seidler et al., 2010), by exerting efficient executive control of gait (Clark, 2015). However, under challenging conditions this compensatory mechanism becomes less efficient, and overloading emerges leading to failure in gait adaptation (Maidan et al., 2017). In fact, the PFC modulates neuronal activity in cortical and subcortical motor structures (Fuster, 2015). Therefore, we propose that during DT walking the PFC becomes otherwise occupied with the executive control of concurrent tasks; thus, rendered less able to modulate its inhibitory control over motor area (**Figure 5**). However, this last notion requires further investigation.

Previous studies show that the Soleus H-reflex decreases with increased postural task difficulty (Stein and Capaday, 1988; Koceja et al., 1993; Tokuno et al., 2009), such as walking under DT conditions (Weaver et al., 2012). This reduction might reflect a strategy to prevent redundant stretch reflex from causing further postural instability yet permitting proprioceptive signals to reach supraspinal structures (Capaday and Stein, 1987; Llewellyn et al., 1990). Therefore, task-dependent modulation of H-reflex reflects adaptive control of stretch reflex according to task demands (Capaday, 2002). In agreement with this notion, we observed that the Soleus H-reflex gain decreased with the additional cognitive load relative to ST walking.

However, other studies report no modulation of the Soleus H-reflex under DT conditions (Baudry and Gaillard, 2014; Meester et al., 2014). It is worth noting that while participants in Baudry and Gaillard study (Baudry and Gaillard, 2014) were young and elderly adults, and participants in Meester et al's (2014) study were healthy young adults, neither of the studies measured the Soleus H-reflex gain.

Whilst ascending and descending neural signals can potentially modulate H-reflex (Misiaszek, 2003), available evidence suggests that task-dependent modulation of H-reflex is mediated by descending signals from supraspinal structures (Pijnappels et al., 1998; Haridas et al., 2005), in particular sensory-motor cortical activity (Wolpaw, 2007; Thompson and Wolpaw, 2014, 2015). The observed reduction in H-reflex gain, together with the increased activation of M1 under DT conditions, suggests a cortical origin of H-reflex modulation.

Finally, our observation that H-reflex gain at SSWS was more prominent in HO adults suggests that at steady state walking speed HO adults retain the ability to utilize these adaptive features of spinal circuits, while people with PD do not. However, the additional cognitive load at FWS not only changed the task-demands but also challenged recurrent sensory feedback, thereby rendering such input unreliable affecting stability during gait and potentially stopping normal propulsory peripheral gait inputs (Zehr and Duysens, 2004).

Methodological Considerations

The interpretation of our results should be considered in light of the following methodological concerns, however. Firstly, due

to unforeseen technical reasons, the NIRS signals from the right PFC showed very low gain for almost all participants, which limited our ability to assess brain activation in the right side of PFC. Considering that PFC hemispheric asymmetry has recently been advocated (Eggenberger et al., 2016), we could not rule out whether task-related increased activation was exclusive to the left PFC, or whether PFC asymmetry while walking would be affected by task complexity or individual's capability. In addition, while NIRS imaging is increasingly advocated to study cortical activations in gait control (Perrey, 2014; Hamacher et al., 2015; Gramigna et al., 2017; Herold et al., 2017), it has modest spatial resolution relative to fMRI. In the present study, our aim was to measure M1 relative activation, yet the recorded signals might reflect activities in M1 alongside adjacent sensorimotor areas. We did not use short separation channels for NIRS so as to control for the effect of superficial hemodynamic from skin (Gagnon et al., 2012; Kirilina et al., 2012). Therefore, we cannot utterly rule out the potential effect of this superficial contamination.

Another limitation concerns treadmill usage. Whilst gait kinematics have been shown to be similar between treadmill and overground walking in healthy adults (Lee and Hidler, 2008; Parvataneni et al., 2009), treadmill use might have posed a constraint, as it did not allow for proper adaptive mechanisms of gait adaptation, by forcing individuals not to adjust walking velocity between ST and DT conditions. However, treadmill use may explain why, counter intuitively, in previous reports PD showed increased PFC during usual over ground walking compared to healthy older adults (Maidan et al., 2016). Treadmill might have been utilized by PD patients as a cue that provided basic rhythm of walking, bypassing the defective basal ganglia in PD. This is supported by the increasing utilization of cues in rehabilitations of Parkinson's gait (Lohnes and Earhart, 2011; Luessi et al., 2012). An external regulator of gait might have decreased the load on attentional resources (Peterson and Smulders, 2015) that are otherwise used in over-ground walking and rather freed cortical resources to deal with the DT leaving treadmill to guide motion.

Other potential explanations for the lack of between group differences in brain activation might be that HO walked on the treadmill faster than PD at both speeds. Second, PD patients were mostly at initial stages of PD with no obvious or minimal unilateral physical impairments and intact balance. Thirdly, patients were tested "on medication", that is when the symptoms associated with PD are at the minimal.

Finally, we have not measured the counting task performance under control conditions, which might have changed relative to DT ones. Therefore, this study cannot infer any absolute amount of attention or a mechanism (Fraizer and Mitra, 2008). We rather utilized the serial subtraction task as an attentional distraction to load the system as it has been suggested to do so more effectively than other secondary tasks (Al-Yahya et al., 2011). Presumably by taxing higher-level executive functioning more than low-level divided attention processes (Walshe et al., 2015).

CONCLUSION

All in all, our findings provide direct evidence, for the first time, for the integration of central and peripheral control mechanisms during treadmill walking in HO adults and in people with PD. They suggest that the sensorimotor system utilizes different strategies to retain dynamic stability while walking, which could be achieved through adaptive regulation of spinal reflex circuits. This essential adaptive regulation entails a delicate balance between supraspinal, spinal, and peripheral input to spinal circuits, and it is dependent on task demands and individual's capabilities.

DATA AVAILABILITY

Data supporting authors' conclusions will be available by the authors upon request without undue reservation to interested researchers.

AUTHOR CONTRIBUTIONS

EA-Y conceived the project, designed the protocol, analyzed the data, performed the statistical analysis, prepared the **Figures 3**–**5**, and wrote the manuscript. WM collected that data, analyzed the data, performed the statistical analysis, and reviewed the manuscript. DM designed the protocol, prepared the **Figure 1**, and reviewed the manuscript. PE supervised the data collection, prepared the **Figure 2**, and reviewed the manuscript. HD conceived, supervised, and designed the protocol, acted as sponsor of the study, and reviewed the manuscript. EA-Y and HD had full access to all the data in the study and take responsibility for the integrity of the data and the accuracy of the data analysis. All authors gave final approval for submission.

FUNDING

EA-Y was supported by funds from The University of Jordan. WM was supported by Said Foundation, United Kingdom. HD receives support from the Elizabeth Casson Trust and the NIHR Oxford Biomedical Research Centre.

ACKNOWLEDGMENTS

We would like to thank the participants who took part in this study. We acknowledge the support of members of the Movement Science Group.

REFERENCES

Al-Yahya, E., Dawes, H., Collett, J., Howells, K., Izadi, H., Wade, D., et al. (2009). Gait adaptations to simultaneous cognitive and mechanical constraints. *Exp. Brain Res.* 199, 39–48. doi: 10.1007/s00221-009-1968-1

Al-Yahya, E., Dawes, H., Smith, L., Dennis, A., Howells, K., and Cockburn, J. (2011). Cognitive motor interference while walking: a systematic review and meta-analysis. *Neurosci. Biobehav. Rev.* 35, 715–728. doi: 10.1016/j.neubiorev.2010.08.008

Al-Yahya, E., Johansen-Berg, H., Kischka, U., Zarei, M., Cockburn, J., and Dawes, H. (2016). Prefrontal cortex activation while walking under dual-task conditions in stroke: a multimodal imaging study. *Neurorehabil. Neural Repair* 30, 591–599. doi: 10.1177/1545968315613864

Amano, S., Roemmich, R. T., Skinner, J. W., and Hass, C. J. (2013). Ambulation and parkinson disease. *Phys. Med. Rehabil. Clin. N. Am.* 24, 371–392. doi: 10.1016/j.pmr.2012.11.003

Axer, H., Axer, M., Sauer, H., Witte, O. W., and Hagemann, G. (2010). Falls and gait disorders in geriatric neurology. *Clin. Neurol. Neurosurg.* 112, 265–274. doi: 10.1016/j.clineuro.2009.12.015

Baudry, S., and Gaillard, V. (2014). Cognitive demand does not influence the responsiveness of homonymous Ia afferents pathway during postural dual task in young and elderly adults. *Eur. J. Appl. Physiol.* 114, 295–303. doi: 10.1007/s00421-013-2775-8

Beck, S., and Hallett, M. (2011). Surround inhibition in the motor system. *Exp. Brain Res.* 210, 165–172. doi: 10.1007/s00221-011-2610-6

Beck, S., Richardson, S. P., Shamim, E. A., Dang, N., Schubert, M., and Hallett, M. (2008). Short intracortical and surround inhibition are selectively reduced during movement initiation in focal hand dystonia. *J. Neurosci.* 28, 10363–10369. doi: 10.1523/JNEUROSCI.3564-08.2008

Capaday, C. (2002). The special nature of human walking and its neural control. *Trends Neurosci.* 25, 370–376. doi: 10.1016/S0166-2236(02)02173-2

Capaday, C., and Stein, R. B. (1987). Difference in the amplitude of the human soleus H reflex during walking and running. *J. Physiol.* 392, 513–522. doi: 10.1113/jphysiol.1987.sp016794

Chalmers, G. R., and Knutzen, K. M. (2000). Soleus Hoffmann-reflex modulation during walking in healthy elderly and young adults. *J. Gerontol. A Biol. Sci. Med. Sci.* 55, B570–B579. doi: 10.1093/gerona/55.12.B570

Clark, D. J. (2015). Automaticity of walking: functional significance, mechanisms, measurement and rehabilitation strategies. *Front. Hum. Neurosci.* 9:246. doi: 10.3389/fnhum.2015.00246

Corp, D. T., Drury, H. G., Young, K., Do, M., Perkins, T., and Pearce, A. J. (2013). Corticomotor responses to attentionally demanding motor performance: a mini-review. *Front. Psychol.* 4:165. doi: 10.3389/fpsyg.2013.00165

Delpy, D., Cope, M., Zee, P., Van Der, Arridge, S., Wray, S., et al. (1988). Estimation of optical pathlength through tissue from direct time of flight measurement. *Phys. Med. Biol.* 33, 1433–1442. doi: 10.1088/0031-9155/33/12/008

Dietz, V. (2002). Proprioception and locomotor disorders. *Nat. Rev. Neurosci.* 3, 781–790. doi: 10.1038/nrn939

Drew, T., and Marigold, D. S. (2015). Taking the next step: cortical contributions to the control of locomotion. *Curr. Opin. Neurobiol.* 33, 25–33. doi: 10.1016/j.conb.2015.01.011

Edamura, M., Yang, J. F., and Stein, R. B. (1991). Factors that determine the magnitude and time course of human H-reflexes in locomotion. *J. Neurosci.* 11, 420–427. doi: 10.1523/JNEUROSCI.11-02-00420.1991

Eggenberger, P., Wolf, M., Schumann, M., and De Bruin, E. D. (2016). Exergame and balance training modulate prefrontal brain activity during walking and enhance executive function in older adults. *Front. Aging Neurosci.* 8:66. doi: 10.3389/fnagi.2016.00066

Esser, P., Dawes, H., Collett, J., Feltham, M. G., and Howells, K. (2012). Validity and inter-rater reliability of inertial gait measurements in Parkinson's disease: a pilot study. *J. Neurosci. Methods* 205, 177–181. doi: 10.1016/j.jneumeth.2012.01.005

Esser, P., Dawes, H., Collett, J., and Howells, K. (2009). IMU: inertial sensing of vertical CoM movement. *J. Biomech.* 42, 1578–1581. doi: 10.1016/j.jbiomech.2009.03.049

Ferris, D. P., Aagaard, P., Simonsen, E. B., Farley, C. T., and Dyhre-Poulsen, P. (2001). Soleus H-reflex gain in humans walking and running under simulated reduced gravity. *J. Physiol.* 530, 167–180. doi: 10.1111/j.1469-7793.2001.0167m.x

Fraizer, E. V., and Mitra, S. (2008). Methodological and interpretive issues in posture-cognition dual-tasking in upright stance. *Gait Posture* 27, 271–279. doi: 10.1016/j.gaitpost.2007.04.002

Fujiyama, H., Garry, M. I., Levin, O., Swinnen, S. P., and Summers, J. J. (2009). Age-related differences in inhibitory processes during interlimb coordination. *Brain Res.* 1262, 38–47. doi: 10.1016/j.brainres.2009.01.023

Fujiyama, H., Hinder, M. R., Schmidt, M. W., Garry, M. I., and Summers, J. J. (2012a). Age-related differences in corticospinal excitability and inhibition during coordination of upper and lower limbs. *Neurobiol. Aging* 33, 1484.e1–1484.e14. doi: 10.1016/j.neurobiolaging.2011.12.019

Fujiyama, H., Hinder, M. R., Schmidt, M. W., Tandonnet, C., Garry, M. I., and Summers, J. J. (2012b). Age-related differences in corticomotor excitability and inhibitory processes during a visuomotor RT task. *J. Cogn. Neurosci.* 24, 1253–1263. doi: 10.1162/jocn_a_00201

Fujiyama, H., Van Soom, J., Rens, G., Gooijers, J., Leunissen, I., Levin, O., et al. (2016). Age-related changes in frontal network structural and functional connectivity in relation to bimanual movement control. *J. Neurosci.* 36, 1808–1822. doi: 10.1523/JNEUROSCI.3355-15.2016

Fuster, J. (2015). *The Prefrontal Cortex*. Cambridge, MA: Academic Press. doi: 10.1016/B978-0-12-407815-4.00002-7

Gagnon, L., Yucel, M. A., Dehaes, M., Cooper, R. J., Perdue, K. L., Selb, J., et al. (2012). Quantification of the cortical contribution to the NIRS signal over the motor cortex using concurrent NIRS-fMRI measurements. *Neuroimage* 59, 3933–3940. doi: 10.1016/j.neuroimage.2011.10.054

Garrett, M., Kerr, T., and Caulfield, B. (1999). Phase-dependent inhibition of H-reflexes during walking in humans is independent of reduction in knee angular velocity. *J. Neurophysiol.* 82, 747–753. doi: 10.1152/jn.1999.82.2.747

Godde, B., and Voelcker-Rehage, C. (2010). More automation and less cognitive control of imagined walking movements in high- versus low-fit older adults. *Front. Aging Neurosci.* 2:139. doi: 10.3389/fnagi.2010.00139

Goetz, C. G., Tilley, B. C., Shaftman, S. R., Stebbins, G. T., Fahn, S., Martinez-Martin, P., et al. (2008). Movement disorder society-sponsored revision of the unified parkinson's disease rating scale (MDS-UPDRS): scale presentation and clinimetric testing results. *Mov. Disord.* 23, 2129–2170. doi: 10.1002/mds.22340

Gramigna, V., Pellegrino, G., Cerasa, A., Cutini, S., Vasta, R., Olivadese, G., et al. (2017). Near-infrared spectroscopy in gait disorders: is it time to begin? *Neurorehabil. Neural Repair* 31, 402–412. doi: 10.1177/1545968317693304

Hamacher, D., Herold, F., Wiegel, P., Hamacher, D., and Schega, L. (2015). Brain activity during walking: a systematic review. *Neurosci. Biobehav. Rev.* 57, 310–327. doi: 10.1016/j.neubiorev.2015.08.002

Haridas, C., Zehr, E. P., and Misiaszek, J. E. (2005). Postural uncertainty leads to dynamic control of cutaneous reflexes from the foot during human walking. *Brain Res.* 1062, 48–62. doi: 10.1016/j.brainres.2005.09.003

Hayashi, R., Tako, K., Tokuda, T., and Yanagisawa, N. (1992). Comparison of amplitude of human soleus H-reflex during sitting and standing. *Neurosci. Res.* 13, 227–233. doi: 10.1016/0168-0102(92)90062-H

Hayashi, R., Tokuda, T., Tako, K., and Yanagisawa, N. (1997). Impaired modulation of tonic muscle activities and H-reflexes in the soleus muscle during standing in patients with Parkinson's disease. *J. Neurol. Sci.* 153, 61–67. doi: 10.1016/S0022-510X(97)00175-5

Herold, F., Wiegel, P., Scholkmann, F., Thiers, A., Hamacher, D., and Schega, L. (2017). Functional near-infrared spectroscopy in movement science: a systematic review on cortical activity in postural and walking tasks. *Neurophotonics* 4:041403. doi: 10.1117/1.NPh.4.4.041403

Hiraoka, K., Matsuo, Y., and Abe, K. (2005). Soleus H-reflex inhibition during gait initiation in Parkinson's disease. *Mov. Disord.* 20, 858–864. doi: 10.1002/mds.20448

Hoehn, M. M., and Yahr, M. D. (1967). Parkinsonism: onset, progression and mortality. *Neurology* 17, 427–442. doi: 10.1212/WNL.17.5.427

Holtzer, R., Mahoney, J. R., Izzetoglu, M., Wang, C., England, S., and Verghese, J. (2015). Online fronto-cortical control of simple and attention-demanding locomotion in humans. *Neuroimage* 112, 152–159. doi: 10.1016/j.neuroimage.2015.03.002

Holtzer, R., Verghese, J., Allali, G., Izzetoglu, M., Wang, C., and Mahoney, J. R. (2016). Neurological gait abnormalities moderate the functional brain signature

of the posture first hypothesis. *Brain Topogr.* 29, 334–343. doi: 10.1007/s10548-015-0465-z

Hughes, J., and Jacobs, N. (1979). Normal human locomotion. *Prosthet. Orthot. Int.* 3, 4–12.

Jeon, H.-S., Kukulka, C. G., Brunt, D., Behrman, A. L., and Thompson, F. J. (2007). Soleus h-reflex modulation and paired reflex depression from prone to standing and from standing to walking. *Int. J. Neurosci.* 117, 1661–1675. doi: 10.1080/00207450601067158

Kirilina, E., Jelzow, A., Heine, A., Niessing, M., Wabnitz, H., Bruhl, R., et al. (2012). The physiological origin of task-evoked systemic artefacts in functional near infrared spectroscopy. *Neuroimage* 61, 70–81. doi: 10.1016/j.neuroimage.2012.02.074

Knikou, M. (2008). The H-reflex as a probe: pathways and pitfalls. *J. Neurosci. Methods* 171, 1–12. doi: 10.1016/j.jneumeth.2008.02.012

Knikou, M. (2010). Neural control of locomotion and training-induced plasticity after spinal and cerebral lesions. *Clin. Neurophysiol.* 121, 1655–1668. doi: 10.1016/j.clinph.2010.01.039

Knikou, M., and Taglianetti, C. (2006). On the methods employed to record and measure the human soleus H-reflex. *Somatosens. Mot. Res.* 23, 55–62. doi: 10.1080/08990220600702715

Koceja, D. M., Markus, C. A., and Trimble, M. H. (1995). Postural modulation of the soleus H reflex in young and old subjects. *Electroencephalogr. Clin. Neurophysiol.* 97, 387–393.

Koceja, D. M., Trimble, M. H., and Earles, D. R. (1993). Inhibition of the soleus H-reflex in standing man. *Brain Res.* 629, 155–158. doi: 10.1016/0006-8993(93)90495-9

Koenraadt, K. L. M., Roelofsen, E. G. J., Duysens, J., and Keijsers, N. L. W. (2014). Cortical control of normal gait and precision stepping: An fNIRS study. *Neuroimage* 85, (Part 1), 415–422. doi: 10.1016/j.neuroimage.2013.04.070

Konrad, P. (2005). *The ABC of EMG*. Scottsdale, AZ: Noraxon Inc.

Kurz, M. J., Wilson, T. W., and Arpin, D. J. (2012). Stride-time variability and sensorimotor cortical activation during walking. *Neuroimage* 59, 1602–1607. doi: 10.1016/j.neuroimage.2011.08.084

la Fougère, C., Zwergal, A., Rominger, A., Förster, S., Fesl, G., Dieterich, M., et al. (2010). Real versus imagined locomotion: a [18F]-FDG PET-fMRI comparison. *Neuroimage* 50, 1589–1598. doi: 10.1016/j.neuroimage.2009.12.060

Lee, S. J., and Hidler, J. (2008). Biomechanics of overground vs. treadmill walking in healthy individuals. *J. Appl. Physiol.* 104, 747–755. doi: 10.1152/japplphysiol.01380.2006

Leff, D. R., Elwell, C. E., Orihuela-Espina, F., Atallah, L., Delpy, D. T., Darzi, A. W., et al. (2008). Changes in prefrontal cortical behaviour depend upon familiarity on a bimanual co-ordination task: an fNIRS study. *Neuroimage* 39, 805–813. doi: 10.1016/j.neuroimage.2007.09.032

Llewellyn, M., Yang, J. F., and Prochazka, A. (1990). Human H-reflexes are smaller in difficult beam walking than in normal treadmill walking. *Exp. Brain Res.* 83, 22–28. doi: 10.1007/BF00232189

Lohnes, C. A., and Earhart, G. M. (2011). The impact of attentional, auditory, and combined cues on walking during single and cognitive dual tasks in Parkinson disease. *Gait Posture* 33, 478–483. doi: 10.1016/j.gaitpost.2010.12.029

Luessi, F., Mueller, L. K., Breimhorst, M., and Vogt, T. (2012). Influence of visual cues on gait in Parkinson's disease during treadmill walking at multiple velocities. *J. Neurol. Sci.* 314, 78–82. doi: 10.1016/j.jns.2011.10.027

Mahoney, F. I., and Barthel, D. W. (1965). Functional evaluation: the barthel index. *Md. State Med. J.* 14, 61–65.

Maidan, I., Bernad-Elazari, H., Giladi, N., Hausdorff, J. M., and Mirelman, A. (2017). When is higher level cognitive control needed for locomotor tasks among patients with Parkinson's Disease? *Brain Topogr.* 30, 531–538. doi: 10.1007/s10548-017-0564-0

Maidan, I., Nieuwhof, F., Bernad-Elazari, H., Reelick, M. F., Bloem, B. R., Giladi, N., et al. (2016). The role of the frontal lobe in complex walking among patients with Parkinson's disease and healthy older adults: an FNIRS study. *Neurorehabil. Neural Repair* 30, 963–971. doi: 10.1177/1545968316650426

McCulloch, K. (2007). Attention and dual-task conditions: physical therapy implications for individuals with acquired brain injury. *J. Neurol. Phys. Ther.* 31, 104–118. doi: 10.1097/NPT.0b013e31814a6493

Meester, D., Al-Yahya, E., Dawes, H., Martin-Fagg, P., and Piñon, C. (2014). Associations between prefrontal cortex activation and H-reflex modulation during dual task gait. *Front. Hum. Neurosci.* 8:78. doi: 10.3389/fnhum.2014.00078

Minassian, K., Hofstoetter, U. S., Danner, S. M., Mayr, W., Bruce, J. A., Mckay, W. B., et al. (2015). Spinal rhythm generation by step-induced feedback and transcutaneous posterior root stimulation in complete spinal cord–injured individuals. *Neurorehabil. Neural Repair* 30, 233–243. doi: 10.1177/1545968315591706

Misiaszek, J. E. (2003). The H-reflex as a tool in neurophysiology: its limitations and uses in understanding nervous system function. *Muscle Nerve* 28, 144–160. doi: 10.1002/mus.10372

Mullie, Y., and Duclos, C. (2014). Role of proprioceptive information to control balance during gait in healthy and hemiparetic individuals. *Gait Posture* 40, 610–615. doi: 10.1016/j.gaitpost.2014.07.008

Nielsen, J. B. (2003). How we walk: central control of muscle activity during human walking. *Neuroscientist* 9, 195–204. doi: 10.1177/1073858403009003012

Nieuwhof, F., Reelick, M. F., Maidan, I., Mirelman, A., Hausdorff, J. M., Olde Rikkert, M. G., et al. (2016). Measuring prefrontal cortical activity during dual task walking in patients with Parkinson's disease: feasibility of using a new portable fNIRS device. *Pilot Feasibility Stud.* 2:59. doi: 10.1186/s40814-016-0099-2

Okamoto, M., Dan, H., Shimizu, K., Takeo, K., Amita, T., Oda, I., et al. (2004). Multimodal assessment of cortical activation during apple peeling by NIRS and fMRI. *Neuroimage* 21, 1275–1288. doi: 10.1016/j.neuroimage.2003.12.003

Parvataneni, K., Ploeg, L., Olney, S. J., and Brouwer, B. (2009). Kinematic, kinetic and metabolic parameters of treadmill versus overground walking in healthy older adults. *Clin. Biomech.* 24, 95–100. doi: 10.1016/j.clinbiomech.2008.07.002

Perrey, S. (2014). Possibilities for examining the neural control of gait in humans with fNIRS. *Front. Physiol.* 5:204. doi: 10.3389/fphys.2014.00204

Petersen, N. T., Butler, J. E., Marchand-Pauvert, V., Fisher, R., Ledebt, A., Pyndt, H. S., et al. (2001). Suppression of EMG activity by transcranial magnetic stimulation in human subjects during walking. *J. Physiol.* 537, 651–656. doi: 10.1111/j.1469-7793.2001.00651.x

Peterson, D. S., and Horak, F. B. (2016). Neural control of walking in people with Parkinsonism. *Physiology* 31, 95–107. doi: 10.1152/physiol.00034.2015

Peterson, D. S., and Smulders, K. (2015). Cues and attention in parkinsonian gait: potential mechanisms and future directions. *Front. Neurol.* 6:255. doi: 10.3389/fneur.2015.00255

Phadke, C. P., Klimstra, M., Zehr, E. P., Thompson, F. J., and Behrman, A. L. (2010). Soleus h-reflex modulation during stance phase of walking with altered arm swing patterns. *Motor Control* 14, 116–125. doi: 10.1123/mcj.14.1.116

Pijnappels, M., Van Wezel, B. M., Colombo, G., Dietz, V., and Duysens, J. (1998). Cortical facilitation of cutaneous reflexes in leg muscles during human gait. *Brain Res.* 787, 149–153. doi: 10.1016/S0006-8993(97)01557-6

Seidler, R. D., Bernard, J. A., Burutolu, T. B., Fling, B. W., Gordon, M. T., Gwin, J. T., et al. (2010). Motor control and aging: links to age-related brain structural, functional, and biochemical effects. *Neurosci. Biobehav. Rev.* 34, 721–733. doi: 10.1016/j.neubiorev.2009.10.005

Simonsen, E. B., and Dyhre-Poulsen, P. (1999). Amplitude of the human soleus H reflex during walking and running. *J. Physiol.* 515(Pt 3), 929–939. doi: 10.1111/j.1469-7793.1999.929ab.x

Stein, R. B., and Capaday, C. (1988). The modulation of human reflexes during functional motor tasks. *Trends Neurosci.* 11, 328–332. doi: 10.1016/0166-2236(88)90097-5

Suzuki, M., Miyai, I., Ono, T., and Kubota, K. (2008). Activities in the frontal cortex and gait performance are modulated by preparation. An fNIRS study. *Neuroimage* 39, 600–607. doi: 10.1016/j.neuroimage.2007.08.044

Suzuki, M., Miyai, I., Ono, T., Oda, I., Konishi, I., Kochiyama, T., et al. (2004). Prefrontal and premotor cortices are involved in adapting walking and running speed on the treadmill: an optical imaging study. *Neuroimage* 23, 1020–1026. doi: 10.1016/j.neuroimage.2004.07.002

Takakusaki, K. (2017). Functional neuroanatomy for posture and gait control. *J. Mov. Disord.* 10, 1–17. doi: 10.14802/jmd.16062

Thompson, A. K., and Wolpaw, J. R. (2014). Operant conditioning of spinal reflexes: from basic science to clinical therapy. *Front. Integr. Neurosci.* 8:25. doi: 10.3389/fnint.2014.00025

Thompson, A. K., and Wolpaw, J. R. (2015). Restoring walking after spinal cord injury: operant conditioning of spinal reflexes can help. *Neuroscientist* 21, 203–215. doi: 10.1177/1073858414527541

Tokuno, C. D., Carpenter, M. G., Thorstensson, A., Garland, S. J., and Cresswell, A. G. (2007). Control of the triceps surae during the postural sway of quiet standing. *Acta Physiol.* 191, 229–236. doi: 10.1111/j.1748-1716.2007.01727.x

Tokuno, C. D., Taube, W., and Cresswell, A. G. (2009). An enhanced level of motor cortical excitability during the control of human standing. *Acta Physiol.* 195, 385–395. doi: 10.1111/j.1748-1716.2008.01898.x

Voloshin, A. (2000). The influence of walking speed on dynamic loading on the human musculoskeletal system. *Med. Sci. Sports Exerc.* 32, 1156–1159. doi: 10.1097/00005768-200006000-00019

Walshe, E. A., Patterson, M. R., Commins, S., and Roche, R. A. (2015). Dual-task and electrophysiological markers of executive cognitive processing in older adult gait and fall-risk. *Front. Hum. Neurosci.* 9:200. doi: 10.3389/fnhum.2015.00200

Weaver, T. B., Janzen, M. R., Adkin, A. L., and Tokuno, C. D. (2012). Changes in spinal excitability during dual task performance. *J. Motor Behav.* 44, 289–294. doi: 10.1080/00222895.2012.702142

Wolpaw, J. R. (2007). Brain-computer interfaces as new brain output pathways. *J. Physiol.* 579, 613–619. doi: 10.1113/jphysiol.2006.125948

Yang, J. F., and Gorassini, M. (2006). Spinal and brain control of human walking: implications for retraining of walking. *Neuroscientist* 12, 379–389. doi: 10.1177/1073858406292151

Zehr, E. P. (2002). Considerations for use of the Hoffmann reflex in exercise studies. *Eur. J. Appl. Physiol.* 86, 455–468. doi: 10.1007/s00421-002-0577-5

Zehr, E. P., and Duysens, J. (2004). Regulation of arm and leg movement during human locomotion. *Neuroscientist* 10, 347–361. doi: 10.1177/1073858404264680

Zwergal, A., La Fougere, C., Lorenzl, S., Rominger, A., Xiong, G., Deutschenbaur, L., et al. (2013). Functional disturbance of the locomotor network in progressive supranuclear palsy. *Neurology* 80, 634–641. doi: 10.1212/WNL.0b013e318281cc43

Zwergal, A., Linn, J., Xiong, G., Brandt, T., Strupp, M., and Jahn, K. (2012). Aging of human supraspinal locomotor and postural control in fMRI. *Neurobiol. Aging* 33, 1073–1084. doi: 10.1016/j.neurobiolaging.2010.09.022

Conflict of Interest Statement: The authors declare that the research was conducted in the absence of any commercial or financial relationships that could be construed as a potential conflict of interest.

frontiers in Human Neuroscience

REVIEW
published: 20 March 2019
doi: 10.3389/fnhum.2019.00100

Corticomuscular Coherence and Its Applications: A Review

*Jinbiao Liu, Yixuan Sheng and Honghai Liu**

State Key Laboratory of Mechanical System and Vibration, School of Mechanical Engineering, Shanghai Jiao Tong University, Shanghai, China

Corticomuscular coherence (CMC) is an index utilized to indicate coherence between brain motor cortex and associated body muscles, conventionally. As an index of functional connections between the cortex and muscles, CMC research is the focus of neurophysiology in recent years. Although CMC has been extensively studied in healthy subjects and sports disorders, the purpose of its applications is still ambiguous, and the magnitude of CMC varies among individuals. Here, we aim to investigate factors that modulate the variation of CMC amplitude and compare significant CMC between these factors to find a well-developed research prospect. In the present review, we discuss the mechanism of CMC and propose a general definition of CMC. Factors affecting CMC are also summarized as follows: experimental design, band frequencies and force levels, age correlation, and difference between healthy controls and patients. In addition, we provide a detailed overview of the current CMC applications for various motor disorders. Further recognition of the factors affecting CMC amplitude can clarify the physiological mechanism and is beneficial to the implementation of CMC clinical methods.

OPEN ACCESS

Edited by:
Camillo Porcaro, Istituto di Scienze e Tecnologie della Cognizione (ISTC), Italy

Reviewed by:
Giovanni Assenza, Campus Bio-Medico University, Italy
Rohan Galgalikar, Corning Inc., United States

***Correspondence:**
Honghai Liu
honghai.liu@icloud.com

Received: *13 December 2018*
Accepted: *04 March 2019*
Published: *20 March 2019*

Citation:
Liu J, Sheng Y and Liu H (2019) Corticomuscular Coherence and Its Applications: A Review. Front. Hum. Neurosci. 13:100. doi: 10.3389/fnhum.2019.00100

Keywords: corticomuscular coherence, magnetoencephalography, electroencephalogram, surface electromyogram, stroke

INTRODUCTION

Preview human studies used positron emission tomography (PET), functional magnetic resonance imaging (fMRI), transcranial magnetic stimulation (TMS) or electroencephalogram (EEG) to suggest the underlying mechanisms of motor cortex in patients with strokes (Mima et al., 2001; Zheng et al., 2017). However, the exact role of how ipsilateral motor cortex or secondary motor areas control the muscle activity is still to be fully discovered. One approach to overcome this issue is to measure EEG signals and corresponding EMG signals simultaneously. This method is known as corticomuscular coherence, which is considered to be a classic and commonly used approach to assess the synchrony between neural signals and associated body muscles. Corticomuscular coherence (CMC) was initially reported between magnetoencephalography (MEG) and electromyography (EMG) (Kilner et al., 2000; Tecchio et al., 2006, 2008; Porcaro et al., 2008) and is widely detected by techniques such as EEG, electrocorticography (ECoG), surface electromyography (sEMG), and has thus been validated across methods and species (Gerloff et al., 2006).

Corticomuscular coherence is a common and useful method to study the mechanism of cerebral cortex's control of muscle activity. It reveals functional connection between the cortex and muscles

during continuous muscle contractions. The origin of CMC is the communication in corticospinal pathways between primary motor cortex and muscles. Normally, cortical events propagate to the periphery and motor cortex also receives input from the periphery (Salenius et al., 1997; Gross et al., 2000; Riddle and Baker, 2005). Horak's motion control theory emphasizes "Normal motion control refers to the central nervous system by using existing and past information to transform neural energy into kinetic energy and enable it to perform effectively functional activities" (Horak, 1991). In this process, the interaction between the two systems of central nervous system and motor muscle tissue is included. Utilizing hand grip as an example, the command which is issued by the motor cortex will be carried down along the motor conduction pathway and dominates upper body's peripheral nerves and muscles when motion occurs (Claudio et al., 2008). The sense of proprioception is simultaneously conducted along the sensory conduction pathway to the spinal cord, the brain stem and the cerebellum, and partly to the cerebral hemisphere. Most of the proprioceptive information are transmitted to the sensory regions of the brain for comprehensive analysis and regulate motion commands (Witham et al., 2011). The study of the cortical-muscle function coupling can reflect the interaction between the cerebral cortex and the muscle tissue which represents the flow of information within the motion system and is associated with the cerebral cortex sending commands to the muscle tissue and the afferent feedback of muscle contraction. Thus, it serves to understand how the brain controls muscle tissue, the effects of muscle movement on brain function and the explanations of the rooted causes of specific physiological conditions such as fatigue. More recent studies using directional coherence analysis have emphasized that CMC reflects both the corticoefferent descending locomote from motor cortex to muscles as well as ascending corticoafferent locomote from muscles to motor cortex in producing the CMC (Hellwig et al., 2001; Fang et al., 2009; Airaksinen et al., 2015a). **Figure 1** indicates the pathway of signal transmission between cortex and muscle.

Since Conway et al. (1995) reported increased coherence between MEG signals in the contralateral motor areas and the surface EMG (sEMG) signal during muscle contractions, CMC has been extensively studied for the continuous contraction of limb muscles (Kilner et al., 2000; Krause et al., 2013; Rossiter et al., 2013; Maezawa, 2016; Matsuya et al., 2017). Based on previous studies, it can be suggested that the magnitude of CMC reflects the indicator of human neurophysiology in both healthy subjects and sport disorders. However, neural system is extremely complex and diverse among individuals, which causes the CMC amplitude would be emerged different correlation results under different research conditions. Hellwig et al. (2001) applied EEG to reveal tremor-correlated cortical activity in tremor patients. EMG signals of wrist extensor and flexor muscles were recorded from tremor side of patients. With EEG recording, CMC was estimated and found that there was a highly significant coherence at the tremor frequency. Raethjen et al. (2002) discovered that CMC had a significant coherence in the 6–15 Hz range in four out of the six tremor patients. That because corticomuscular transmission of the oscillation was in progress between cortex and muscles rather than peripheral feedback to the cortex. This research pointed out that the band frequency was an important factor which may impact CMC. To compare CMC between young and older adults, Johnson and Shinohara (2012) discussed CMC and fine motor performance during the unilateral fine motor task and concurrent motor and cognitive tasks which asked participants to increase the force from zero to maximum using the index finger. From this study, results revealed that older adults had lower CMC in beta-band and higher alpha-band than young adults during dual tasks and young controls, rather than older adults, with greater beta-band CMC exhibited accurately motor output. Previous researches have confirmed that CMC magnitude often varies greatly due to different experimental designs, magnitude of exerted force, or individual differences. However, there are no relevant studies to make a detailed investigation of the factors affecting the amplitude of CMC.

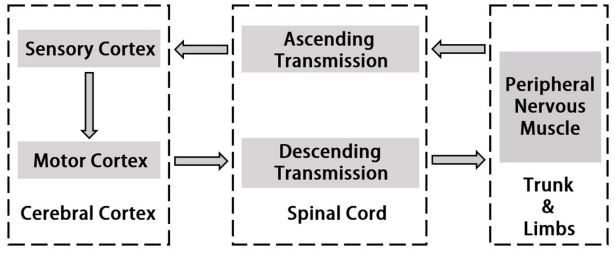

FIGURE 1 | Schematic diagram of signal transmission in cerebral cortex and peripheral nerve.

Compare with the coherence between all coupling degrees, the classifications which have significant coherence could be observed. These can serve as the research emphasis in the future. The remaining of this review is organized as follows: section *CMC DEFINITION AND FORMULAE* proposes a generalized definition of CMC; section *FACTORS AFFECTING CMC* provides a detailed overview of the factors affecting the corticomuscular coordination, including experimental design (von Carlowitz-Ghori et al., 2015), band frequencies (Schulz et al., 2014; Maezawa et al., 2016) and force levels (Dal Maso et al., 2017), age correlation (Kamp et al., 2013) and difference between healthy controls and patients (Krause et al., 2013; Rossiter et al., 2013); the applications of CMC for patients with various motor disorders are further presented in section *CMC APPLICATIONS*; section *DISCUSSION* proposes a discussion of CMC modulation and future directions; the paper is concluded in section *CONCLUSION*.

CMC DEFINITION AND FORMULAE

Coherence is an indicator of the linear connection between two signals (Grosse et al., 2003) and is an extension of Pearson correlation coefficient in the frequency domain

(Mima and Hallett, 1999). Coherence was obtained from the normalization of the cross-spectrum (Fang et al., 2009):

$$Coh_{S1,S2}(f) = \frac{|P_{S1,S2}(f)|^2}{|P_{S1}(f)| \times |P_{S2}(f)|} \quad (1)$$

$$P_{S1,S2}(f) = \frac{1}{n}\sum_{i=1}^{n} S1_i(f)\, S2^*{}_i(f) \quad (2)$$

Where $P_{S1,S2}(f)$ is the cross-spectrum density of the signal, $P_{S1}(f)$ and $P_{S2}(f)$ are the auto-spectrum densities of signals *S*1 and *S*2, respectively, at frequency f. Values of coherence is normalized and will always satisfy 0 to 1 where 1 indicates an ideal correlation between two signals and 0 indicates a total absence of association.

Corticomuscular coherence is an implement to understand how cortical activities control the muscle movements and examines the functional coupling between brain motor cortex and associated muscles. Ascending and descending corticomuscular pathways are two diverse directions which could both generate coherence, however, descending pathway are more clearly and certainly than ascending pathway. Hence, the common definition of CMC indicates the cortex-muscle coherence underlying descending pathway.

As the variety of signal collection techniques, CMC shows a widely research space to analyze different types of signals collecting from different approaches. From the recent studies, the most familiar techniques to collect brain activity signals are EEG, MEG, and ECoG and muscle activity signals are sEMG and ultrasound. In the researches of CMC, EEG-EMG, MEG-EMG, and ECoG-EMG are the most three commonly used methods to analyze the functional coupling between brain cortex and muscle activities and these three sets of signals are used to calculate the coherence parameter. Therefore, in the equations (1) and (2), two signals *S*1 and *S*2 could represent these three types of signal combinations. At the same time, ultrasound is an unusual signal format to use in CMC analysis, which could be regarded as a future research field.

Equation (1) and equation (2) offer a basic and intuitive technique to display the synchronous values. On this basis, wavelet-based coherence is proposed to enhance the relative level of the motor cortex and muscle and observes the coherence in time-frequency domain which estimates the signal spectral characteristics according to the function of time (Xu et al., 2015). To overcome the problems of non-stationary signals like sEMG signal, wavelet analysis is a rational method to analyze signals with fast-changing spectra (Lachaux et al., 2002). One primary advantage of wavelet analysis is to observe the significant coherence in different time for different tasks intuitively and expediently. Compare to traditional CMC analysis result, wavelet coherence increases precision when analyzing temporary activities between two oscillatory neural signals and is good at dynamic neural interactions.

Morlet wavelet family is a simple and suitable wavelet for spectral estimations although there are still many wavelets could be chosen. The signal $x(u)$ is decomposed along Morlet wavelet and under the frequency f and time τ, it could be calculated by the following formulae:

$$\psi_{\tau,f}(u) = \sqrt{f} \cdot \exp\left(i2\pi f\,(u-\tau)\right) \cdot \exp\left(-\frac{(u-\tau)^2}{\sigma^2}\right) \quad (3)$$

Where $\psi_{\tau,f}(u)$ is the product of a sinusoidal wave at frequency f, with a Gaussian function centered at time τ with a standard deviation σ proportional to the inverse of frequency f. The wavelet transform function $W_X(\tau, f)$ of a signal $x(u)$ is a function given by the convolution of x with Morlet wavelet family:

$$W_X(\tau, f) = \int_{(-\infty)}^{(+\infty)} x(u) \cdot \Psi_{\tau,f}{}^*(u)\, du \quad (4)$$

From the wavelet transform function, the wavelet cross-spectrum of two signals between brain cortex and muscle is as follow:

$$SW_{S1,S2}(t, f) = \int_{t-\delta/2}^{t+\delta/2} W_{S1}(\tau, f) \cdot W_{S2}{}^*(\tau, f)\, d\tau \quad (5)$$

Where δ is a scalar that can depend on frequency. Therefore, the wavelet coherence $\mathrm{W}Coh_{S1,S2}(f)$ could be defined as follow:

$$\mathrm{W}Coh_{S1,S2}(f) = \frac{|SW_{S1,S2}(f)|^2}{|SW_{S1,S1}(f)| \times |SW_{S2,S2}(f)|} \quad (6)$$

Besides the above two methods to analyze CMC, Fourier coherence and partial directed coherence are also reported in some researches (Lachaux et al., 2002; Porcaro et al., 2009; Mcmanus et al., 2013). Compare Fourier coherence with Wavelet coherence, these two methods both study non-stationary signals, however, the window size of wavelet analysis is fixed and it is more adapted to the frequency of the oscillatory signals. As a result, wavelet coherence has a more accurate consequence than Fourier coherence. For partial directed coherence, this technique could evaluate the flowing direction of neural information and indicate how cortical signals and muscular signals are functionally connected compared with ordinary CMC analysis. And this is a potential technique because the current researches are most focus on the synchrony between two signals or the descending corticospinal pathway.

With the intensive study of CMC, related analytical methods also evolve gradually. Researchers are not satisfied with commonly CMC analysis method; thus, Wavelet coherence has become a widely used technology in the recent years. Wavelet coherence could show CMC magnitude during the entire task time series. Since the strong coherence under specific movements could be observed, the discovery of the factors affecting CMC will be easier to achieve.

FACTORS AFFECTING CMC

Research shows strong correlated area of CMC has been confirmed by direct electrical stimulation in monkeys and human

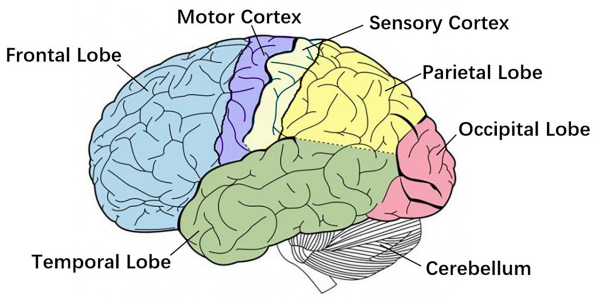

FIGURE 2 | Primary brain regions. Motor cortex is the region in charge of planning, control and execution of voluntary movements. Sensory cortex arranges tactile representation from the toe to mouth. Cerebellum is mainly responsible for motion control. These three regions are more related to Corticomuscular coherence (CMC).

surgery, including the anterior motor area, the primary motor area, the primary somatosensory area, the thalamus, the nucleus of the hypothalamus, and the cerebellum (Salenius and Hari, 2003), **Figure 2** shows primary brain regions which related to CMC. However, several studies suggest that the magnitude of CMC is not only related to the corresponding regions of the cerebral cortex, but also directly related to the CMC band (Cottone et al., 2017; Porcaro et al., 2018). Chakarov et al. (2009) found that the CMC value of the 15–45 Hz frequency band increased linearly with the rise of the dynamic force level, that is, the CMC value was a high-level dynamic synchronization process. Survey also shows that the CMC value of the beta band (13–30 Hz) is related to the output of the static force, and the coherence of the gamma band (31–45 Hz) is related to the output of the dynamic force (Gwin and Ferris, 2012). The CMC magnitude is significantly lower in the case of unpredictable low-level force frequency (Mendez-Balbuena et al., 2013). The unpredictability of the force frequency could lead to the decrease of the corticospinal tract synchronism, the increase of cortical and muscle activation, and the decrease of motor performance. Several studies have demonstrated that beta-band CMC value is modulated by afferent information (Fisher et al., 2002; Pohja et al., 2002; Kilner et al., 2004; Riddle and Baker, 2005; Baker et al., 2006), and visuomotor tasks (Perez et al., 2006).

Moreover, the CMC value of healthy subjects is generally higher than that of sport disorders. Stroke patients have a significantly lower corticomuscular coherence compare with healthy controls at both the beta (20–30 Hz) and lower gamma (30–40 Hz) bands during the movement (Fang et al., 2009). During light voluntary muscular contraction, beta-band CMC is markedly reduced in Amyotrophic Lateral Sclerosis patients compare with healthy controls (Proudfoot et al., 2018). However, research also indicates that stroke survivors manifest a more distributed range of cortical locations for peak CMC than healthy controls, in keeping with plastic reorganization of sensorimotor functionality (Farmer et al., 1993; Rossiter et al., 2013). In addition, with the rehabilitation of motor function, the value of CMC will increase gradually on sport disorder patients. Motor deficits secondary to acute stroke are accompanied by a unilateral reduction in CMC, which then normalizes with good functional recovery (von Carlowitz-Ghori et al., 2014).

Although the factors that affect the result of CMC amplitude have not been specifically counted, the classification and comparison of the current research focus on CMC can provide a more specific understanding of the mechanism of CMC. The factors affecting the corticomuscular coordination are summarized as follows: experimental design, band frequencies and force levels, age correlation and difference between healthy controls and patients.

Experimental Design

The magnitude of CMC is closely related to the paradigm design. Different experimental paradigms may result in separate CMC magnitude. **Table 1** displays different CMC experimental design. Force is one of the most significant indices in CMC experiment generally which is relevant to the form of muscle contraction during the experimental design, such as isometric contraction, isokinetic contraction, isotonic contraction, etc. Most studies used isometric contraction as a form of muscle contraction in CMC experiments. Dal Maso et al. (2017) investigated that whether CMC magnitude differed with torque levels during isometric knee contractions tasks. The net joint torque, muscles co-activation and CMC values were comparable when participants performed complete isometric elbow flexion exercise with three force output levels (Cremoux et al., 2017). Similarly, in order to explore whether oscillatory activity could contribute more to the stability of isometric muscle contraction, the subjects were required to perform steady isometric contractions, using two different finger muscles (Lim et al., 2014). Current studies on isokinetic and isotonic contractions are relatively limited. Intramuscular Tibialis Anterior (TA) coherence estimation was investigated within a specific frequency range during 120° isokinetic movement (Bravo-Esteban et al., 2014), and Yang et al. (2016) proposed a measure for evaluating non-linear corticomuscular coupling during isotonic wrist flexion.

Muscle fatigue is an unavoidable problem in the CMC experiment, therefore the time design of the experiment is an essential part, including the duration of the continuous force, the rest time, etc. For example, when subjects performed two specific tasks according to the prompts on the monitor, they needed to rest for 10 min between each trial to prevent muscle fatigue (Rong et al., 2014). Besides, a study of whether CMC magnitude in beta-band differed with torque levels required subjects to perform three 4s knee isometric MVC (maximum voluntary contraction) and 6s rMVC (relative maximum voluntary contraction) in both directions of contraction (Dal Maso et al., 2017). For experimental design with patient's participation, such as a stroke patient's experiment, the design of time interval between two experiments are required to ensure that the patient's affected side has achieved significant motor function recovery (Zheng et al., 2017).

Localization of muscle position by EMG electrodes is the underlying cause of CMC amplitude variation. From previous studies, normally, the acquisition of muscle signals derives from the limbs and hands. For instance, Lou et al. (2013) executed

TABLE 1 | Different experimental design of CMC.

Reference	Contraction form	Muscle position	Sample	CMC results
Dal Maso et al., 2017	Isometric	Agonist Antagonist	21 right-footed men	CMC magnitude decreased more in antagonist than in agonist muscles as torque level increased.
Cremoux et al., 2017	Isometric	Antagonist	8 SCI patients 10 healthy participants	Magnitude of CMC and muscle co-activation decreased with the increase in the force level.
Lim et al., 2014	Isometric	FPB FDMB	15 healthy subjects	Greater β-band DTF was associated with high EMG stability levels and greater β-band CMC strength.
Matsuya et al., 2017	Isometric	FDI SOL	16 healthy young adults	A significant, positive correlation between recurrent inhibition and peak CMC across individuals.
Rossiter et al., 2013	Isometric	Forearm flexors and extensors	25 stroke patients 23 healthy controls	Peak CMC in the contralesional hemisphere was found not only in some highly impaired patients, but also in some patients with good functional recovery.
Rong et al., 2014	Isometric	Right EDC	27 healthy subjects	CMC might represent a general marker of aging increased coherence amplitude might denote a compensatory mechanism to maintain isometric contraction.
Bravo-Esteban et al., 2014	Isokinetic	TA	14 SCI subjects 15 healthy controls	Analysis of intramuscular TA coherence during isometric activation is related to muscle strength and gait function following incomplete SCI.
Yang et al., 2016	Isotonic	FCR	11 healthy subjects	The corticospinal tracks mainly mediate linear corticomuscular coupling, while non-linear coupling might relate to sensory feedback pathways.

SCI, spinal cord injury; FPB, flexor pollicis brevis, FDMB, flexor digiti minimi brevis; FDI, first dorsal interosseous; SOL, soleus; EDC, extensor digitorum communis; TA, tibialis anterior; FCR, flexor carpi radialis.

4 hand movement tasks to investigate CMC. Rong et al. (2014) proved sensorimotor cortex enhanced communication with the measured muscle in right hand. EMG of biceps brachii muscle had also been studied to analyze the effects of mechanically amplified tremor on CMC (Budini et al., 2014). Otherwise, some studies have evaluated the influence of stance width, vision, and surface compliance on beta CMC during human stance. The results showed that under the condition of wide-stance, CMC amplitude is obviously larger than that under the condition of narrow-stance (Jacobs et al., 2015). However, no study placed electrodes in human trunk, the reason for this result is probably that the muscle contraction degree in human trunk is considerably lower than that in the limbs, and the EMG signal obtained is not enough to achieve obvious CMC amplitude.

Moreover, some comparative studies have demonstrated the effects of different forms of tasks in CMC. For example, study found that functional coupling between cortex activity and muscles was less in position-control task than in force-control task (Poortvliet et al., 2015). Similarly, research indicated that motor control strategies differed between force and position control tasks (Maluf and Enoka, 2005). Comparing to the position control task, EEG power of beta-range in the force control task showed greater activity desynchronization (Pfurtscheller and Lopes da Silva, 1999). For patients, the comparison of the CMC task between the affected side and the unaffected side is usually adopted. The study found that the frequency of CMC on the affected side reduced and the magnitude of CMC on the unaffected side increased in acute stroke (von Carlowitz-Ghori et al., 2014).

Experimental design is the initial step of studying CMC. Only a scientific and reasonable paradigm is possible to achieve satisfactory results. Future research on CMC experimental design should be transferred to isokinetic contraction and isotonic contraction since isokinetic movement excludes the muscle force is different during dynamic muscle contraction among individual which is superior to isometric contraction. Time design requires full consideration of the characteristics of muscle fatigue of diverse subjects and more reasonable allocation. Meanwhile, changes of muscle activity in human trunk are also the direction of future CMC research.

Band Frequencies and Force Levels

The corticomuscular coherence at a certain frequency is a function of power spectral density (PSD) and cross-spectral density (CSD), which indicates that frequency bands affect the CMC amplitude. Oscillations in the beta-range (14–30 Hz) are explicitly observed in recording EEG from the cerebral motor cortex (Budini et al., 2014). Significant coherence of beta-range between sensorimotor cortex and contraction muscles has been reported for the first time. Significant beta band coherent activities between the sensorimotor cortex and contracting muscle were proposed in both monkeys (Baker et al., 1997) and humans (Conway et al., 1995) around 20 years ago. Similar oscillations can also be observed in the EMG of forearm and medial muscles of hand during sustained contraction (Conway et al., 1995; Baker et al., 2003). More prominent beta-range rhythmic EMG burst accompanies with higher CMC. Ushiyama et al. (2011a) described that the amplitude of CMC was positively correlated with the beta-range oscillation of EMG signal. Besides, the experimental data also showed that there was a significant correlation

between the CMC amplitude and the beta-range intensity of EMG. CMC was noteworthy in both 13–21 and 21–31 Hz frequency bands in flexors and extensors regardless of subject group, torque level or direction of contraction (Dal Maso et al., 2017). In addition, research on alpha-band (8–13 Hz) and gamma (30–80 Hz) was also being undertaken. Alpha-range coherence showed advanced EMG reflecting ascending or feedback interactions and gamma-range coherence revealed delayed EMG activity indicated descending or feedforward interactions (Mehrkanoon et al., 2014).

Studies in participants with Parkinson's disease and essential tremor, however, have observed significant coherence between cerebral cortex and peripheral EMG activities in the alpha-range and the frequency range of pathological tremor (4–6 Hz) (Hellwig et al., 2000; Timmermann et al., 2003; Raethjen et al., 2007). In addition, significant peak CMC has been revealed at 8–12 Hz when healthy subjects imitated Parkinsonian resting tremor at 3–6 Hz (Pollok et al., 2004). From the present study, it has been proved that beta band is the focus of CMC research. CMC has stronger volatility and more obvious amplitude in this frequency band. However, the CMC amplitude of sport disorder patients at lower frequencies are easy to be observed.

In current CMC researches, diverse force levels are normally studied along with different band frequencies. **Table 2** shows some researches concerning force and bands. The muscular force level and the movement type can affect the CMC amplitude (Lattari et al., 2010). It has been further shown that the level of CMC increases with the strengthen EMG in healthy individuals (Kilner et al., 2000), which indicates that muscle output is dependent on CMC intensity. For example, to investigate the correlation of CMC in different MVC (maximum voluntary contraction) levels in both static and dynamic task of hand movement, the participants should reach 4, 8, and 16% MVC and the result showed that the amplitude of CMC tended to increase with the force increasing in static task and dynamic finger moving task and the CMC mainly concentrated in beta band (Fu et al., 2014). In the same way, Witte et al. (2007) also demonstrated a significant increase in CMC values of beta-range from 4 to 16% MVC which was associated with better performance. Thus, it could be seen that the force input level is closely related to the CMC frequency band, and prior studies have indicated that steady force is accompanied by beta-range CMC (Pfurtscheller and Neuper, 1992; Baker et al., 1997; Halliday et al., 1998; Kilner et al., 1999; Feige et al., 2000; Mima et al., 2000; Fu et al., 2014). Besides, studies demonstrated that CMC within the gamma band can be observed (Brown et al., 1998) during slow movements (Mima et al., 1999) and phasic movements for Previous studies also observed that gamma-range CMC has been related with isometric compensation of low dynamic force (4% MVC) and a markedly broad-band CMC (15–45 Hz) which composed of beta- and gamma- range was associated with the force level (Chakarov et al., 2009). These results show that the function of beta-range CMC is not limited to low-level steady forces. In addition, the sensorimotor system may resort to higher and also extended frequency range of CMC would generate stable corticospinal interaction during rising force standard (Lattari et al., 2010).

Furthermore, Lattari et al. (2010) also showed that greater corrective movements in the 4% MVC condition might reduce CMC. In line with that, the findings of Andrykiewicz et al. (2007) demonstrated that the amplitude of dynamic force did not modulate the gamma-range CMC, which suggested that changes in proprioceptive input during dynamic forces in the range from 1.6 to 4% MVC were insufficient for this modulation. In view of this, there is an explanation that weakening of cortical-muscular coupling may be the main neural mechanism induce to muscle fatigue and associate with performance impairment (Yang et al., 2009). Rong et al. (2014) found that when grip force increased, the sensorimotor cortex reduced communication in gamma band to keep stabilization. Besides, there are also studies consider that with force increasing, the CMC tends to shift to gamma-range (Omlor et al., 2007). For patients with different force levels, CMC is also significant in a certain frequency band. For example, in humans with cervical spinal cord injury, participants had an increased muscle co-activation associated with a decreased magnitude of the CMC in 10 Hz with antagonist muscles (Cremoux et al., 2017). Some authors proposed that lower limbs CMC was significantly reduced in SCA2 (spinocerebellar ataxia type 2) patients compared to healthy participants during repeated simultaneous flexion movements of fingers and wrist at a constant contraction level of 30% MVC (Velázquez-Pérez et al., 2017a).

Corticomuscular coherence is a key measurement to clarify the neural mechanism which is associated with an individual

TABLE 2 | Diverse force level and bands of CMC.

Reference	Force level	Bands	Sample	Significant CMC
Hori et al., 2013	1.96 N–3.92 N	Alpha/Theta	9 healthy subjects	Yes
Budini et al., 2014	20% MVC	Alpha	13 healthy subjects	Partially
Lim et al., 2014	20% MVC	Beta	15 healthy subjects	Yes
Ushiyama et al., 2017	30% MVC	Beta	22 healthy subjects	Yes
Mehrkanoon et al., 2014	target 1: 0.5–0.9 N target 2: 1.1–1.5 N	Alpha/Gamma	12 healthy subjects	No
Dal Maso et al., 2017	20,40, 60, and 80% of rMVC	Beta	10 ST subjects 11 ET subjects	CMC decreased
Rong et al., 2014	25 % MGF and 75 % MGF	Alpha/Beta/Gamma	14 healthy subjects	Alpha/Beta increased Gamma decreased
Fu et al., 2014	4, 8, and 16% MVC	Beta	8 healthy subjects	Yes

MVC, maximum voluntary contractions; ST, strength-trained; ET, endurance-trained subjects; rMVC, relative MVC; MGF, maximum grip force.

ability to stabilize muscle force output. CMC comparison between individuals with different force input level may provide a deeper understanding of the mechanisms. To sum up, no matter whether it is healthy subjects or patients, classification of force levels is one of the critical factors affecting CMC amplitude.

Age Correlation

Aging is also associated with neuromuscular changes that can impair corticomuscular communication (Yoshida et al., 2017). These changes include decreasing in the recruited motor neurons (Kawamura et al., 1977a,b; Tomlinson and Irving, 1977) and the white matter volume of the posterior limbs of the internal capsule that contain the corticospinal tracts (Good et al., 2001; Salat et al., 2005). To be exact, previous studies have proposed age-related reduction in the amplitude of motor evoked potentials (i.e., corticospinal excitability) (Eisen et al., 1996) and CMC during sustained contractions of upper limb muscles (Graziadio et al., 2010; Bayram et al., 2015).

Age as one of the factors affects corticomuscular communication during movements should not be ignored. There was evidence for CMC in all age groups and lager, more distributed cortical networks in the children and elderly compared with young adults (Graziadio et al., 2010). James et al. (2008) compared the CMC among subjects in ages from infancy to elderly and showed prominent CMC differences during motor development in children compared to adults. CMC changed in functional connection with increasing force output helps to explain muscle weakness in elderly subjects. It has been reported that there was a strong link between cortical-muscular coherence and force output in the elderly individuals during abnormal walking (Clark et al., 2013). Bayram et al. (2015) investigated the functional CMC values in the elderly participants by calculating CMC during voluntary motor performance. The result showed that the CMC was significantly lower in older compared with young participants at different levels of elbow flexion force. Johnson and Shinohara (2012) investigated the differences of CMC between young and older adults during unilateral fine motor task, concurrent motor and cognitive tasks. They found that CMC was increasing in older adults with a significant influence of an additional cognitive task in alpha-range and young adults with greater beta-range CMC may exhibit more accurate motor than elderly adults. Besides, beta-range CMC in the motor cognitive task was negatively correlated with motor output error across young but not elderly adults. CMC changed in functional connection with increasing force output could help explain muscle weakness in elderly subjects.

Task dependency is a critical insight into the effects of aging on neural activity and motor performance. From previous studies (James et al., 2008; Graziadio et al., 2010), elderly subjects usually used simple unilateral tasks that required less awareness of attention. Beta-range CMC was suggested to be attenuated with reduced attention to a motor task (Kristeva-Feige et al., 2002; Johnson et al., 2011). The current research intends to examine the CMC in elderly adults in view of the importance of attention to tasks. For example, the alpha-band CMC on aging was increased with awareness on the task. That is because significant CMC was observed only during attention focusing or cognitive processing (Kristeva-Feige et al., 2002). Tasks that require distracting tasks reduce performance and are more common in elderly adults (Beauchet et al., 2005; Zijdewind et al., 2006; Voelcker-Rehage and Alberts, 2007; Hiraga et al., 2009). However, study also found a significant negative correlation between beta-range CMC and EMG variability across multiple trials which were observed within young adults rather than elderly adults (Graziadio et al., 2010).

The current research is mainly comparing CMC between young people and the elderly which employed unilateral tasks and relatively simple dual tasks. For instance, during unilateral task, beta-range CMC increased with aging from childhood (0 years old) to middle age (35 and 59 years old), but not to senior age (55–80 years old) (Graziadio et al., 2010). Alpha-band CMC during unilateral task was observed in elderly adults (55–80 years old) in more cases than in young people (21–35 years old) (Graziadio et al., 2010). By summarizing the significance of age in CMC on elderly people, we found that age has been gradually valued as a factor which could affect the magnitude of CMC. However, for functional significance of CMC, future study requires more awareness of attention to the comparison of CMC between young adults and elderly under the condition of bilateral complex tasks.

Healthy Controls and Patients

To research the effects of corticomuscular coupling on motor injury and the possibility of clinical practice of CMC, some studies compare CMC between healthy subjects and patients with dyskinesia (i.e., stroke, Parkinson). **Table 3** displays the comparison of healthy controls and patients of CMC. In terms of significant areas, the evaluation of CMC strength of healthy controls and patients provides evidence that corticomuscular coupling could apply in the rehabilitative evaluation of dyskinesia (Gao et al., 2017). CMC was implemented early in the Parkinson's disease course which subsequent symptomatic relief with L-Dopa by CMC modulation (Salenius et al., 2002; Mckeown et al., 2006; Pollok et al., 2012). Usually, the CMC amplitude of patients on the affected side is lower than that of healthy subjects. For example, beta-range CMC was reduced dramatically in Amyotrophic Lateral Sclerosis (ALS) patients compared with healthy subjects during light voluntary muscular contraction (Proudfoot et al., 2018). Similarly, CMC was significantly lower in stroke patients compared with healthy participants for the anterior deltoid and brachii muscles at both beta (20–30 Hz) and lower gamma (30–40 Hz) ranges during the movement (Fang et al., 2009). Mima et al. (2001) and Fang et al. (2009) pointed that the functional coupling between cortex commands and corresponding muscular activities of stroke subjects was weaker than healthy subjects. Riquelme et al. (2014) investigated CMC during planning and execution of isotonic contractions in cerebral palsy (CP) patients and healthy subjects. The result showed that CP patients group displayed longer EMG onset latency and duration than healthy group and CMC in beta band of EEG was overall greater in CP than that in healthy controls. CMC in gamma-range was lower in CP group than healthy group, and brain functioning during movement initiation was altered in CP only at the beginning of muscular contraction. CMC is normally restored in patients with motor function

TABLE 3 | Health controls and patients of CMC.

Reference	Type	Sample	CMC result
Gao et al., 2017	EEG-EMG EMG-EEG	7 healthy controls 5 stroke patients	Patients had lower CMC than healthy subjects
Velázquez-Pérez et al., 2017a	EEG-EMG	24 healthy controls 19 SCA2 patients	Lower limbs CMC was significantly reduced in SCA2 patients as compared to healthy participants.
Sharifi et al., 2017	EEG-EMG	18 healthy controls 18 essential tremor patients	CMC remained a relatively high level in healthy subjects. CMC level frequently dropped below the confidence level in patients.
Riquelme et al., 2014	EEG-EMG	15 healthy controls 14 CP patients	CMC in gamma-band was lower in CP than in healthy controls
Proudfoot et al., 2018	EEG-EMG	17 healthy controls 17 ALS patients	Beta-band CMC was significantly reduced in ALS patients compared to healthy controls.
Fang et al., 2009	EEG-EMG	8 healthy subjects 21 stroke patients	Stroke patients had significantly lower CMC compared with healthy subjects for the anterior deltoid and brachii muscles.

EMG, electromyography; EEG, electroencephalogram; SCA2, spinocerebellar ataxia type 2; CP, cerebral palsy; ALS, amyotrophic lateral sclerosis.

recovery. One study reported that motor deficits secondary to acute stroke were attendant by a unilateral reduction in CMC (Nielsen et al., 2008), but the CMC magnitude was normalized with favorable functional recovery (Proudfoot et al., 2018). Research also demonstrated that the CMC strength was increasing with the restoration of motor function of the paretic limb. The measurement of CMC can reflect the recovery of motor function after stroke through quantifying interactions between the motor cortex and controlled muscle activities (Zheng et al., 2017).

Although relatively obvious differences on CMC analysis between patients and healthy individuals could be displayed in some studies, the consequences of CMC magnitude are varying. For instance, the significant CMC was only reported in a selection of patients (Hellwig et al., 2001), which indicated that the participation of the cortex in patients was not robust (Raethjen et al., 2007). Stroke patients manifest much more dispersive extent of cortical locations for peak CMC than healthy subjects, which purpose to keep with plastic reorganization of sensorimotor function (Rossiter et al., 2013; Farmer et al., 1993). In addition, it has been proved that CMC strength is modified in healthy subjects after immobilization (Lundbye-Jensen and Nielsen, 2008) or in neurological conditions such as essential (Muthuraman et al., 2010), neuropathic tremor (Weiss et al., 2010) and Parkinson disease (Weiss et al., 2012). Different choice of patients, analysis techniques and recording methods, types of sport duties, and possibly cognitive state (e.g., awareness of tremor) might be explained the reasons for inconsistent results (Sharifi et al., 2017). Through the comparative study of CMC between healthy controls and patients, we can find the potential clinical application of CMC, and the most direct application is motor rehabilitation. However, most of the current comparative studies could not give a quantitative index of CMC. There is only a simple comparison of CMC values between healthy controls and patients. If the CMC is to be clinically applied in the future, a more detailed classification of the affected CMC in patients with different movement disorders must be discussed and using CMC as a characteristic value to achieve a unified clinical measurement standard should also be studied.

CMC APPLICATIONS

As mentioned in the section of factors affecting CMC, the application and development trend of CMC should be the clinic rehabilitation of patients with sports disorders, even though most of the current CMC studies are still limited to the laboratory. The latest CMC studies focus on the types of patients, including stroke, Parkinson, tremor, etc. In the present review, a detailed overview of the current applications of CMC for patients with various motor disorders was provided.

CMC Applications for Stroke Patients

For stroke patients at different stages, the performance of muscle contraction can be approximated as an indicator of stroke rehabilitation level. Therefore, it is extremely common to try CMC experiments in stroke patients. **Table 4** shows the correlations of CMC and stroke. Normally, muscle atrophy in stroke patients cause a decrease in CMC. Some studies have also confirmed that stroke patients had dramatically lower CMC compared with healthy subjects for the anterior deltoid and brachii muscles (Fang et al., 2009). Similar result of restored CMC was also reported with well recovered patients with both Transcranial Magnetic Stimulation (TMS) and Magnetoencephalography (MEG) investigation (Braun et al., 2007). Rossiter et al. (2013) discovered that peak CMC in the contralesional hemisphere was found both in highly impaired patients and stroke patients with good functional recovery. This discovery provides evidence directly that brain regions in the contralesional hemisphere are participated in activities with the affected muscles in stroke patients. Zheng et al. (2017) demonstrated that the recovery level of motor function after stroke could be reflected by the measurement of CMC by quantifying interactions between the motor cortex and controlled muscle activities. Graziadio et al. (2012) proposed that the degree of global recovery after unilateral stroke in the chronic phase correlated with the degree symmetry achieved between the interdependent lesioned and non-lesioned corticospinal systems at CMC level. In addition to evaluation as rehabilitation indicator during the recovery of the stroke, CMC was also applied to distinguished types of stroke patients. Study investigated CMC in

TABLE 4 | Correlations of CMC and Stroke.

Reference	Number of Patients	Stroke Type	CMC value (Patients vs Controls)
Zheng et al., 2017	1	Hemorrhage	Peak CMC in Beta Band (only patients)
Fang et al., 2009	21	17/21 Ischemia 4/21 Hemorrhage	Patients < Controls
Gao et al., 2017	5	1/5 Ischemia 4/5 Hemorrhage	Patients > Controls
Rossiter et al., 2013	25		Patients < Controls
von Carlowitz-Ghori et al., 2014	11	Ischemia	Patients < Controls
Mima et al., 2001	6		Patients < Controls
Larsen et al., 2017	19	Ischemia	Patients < Controls
Pan et al., 2018	12		ES CMC > sham ES CMC (only patients)
Chen et al., 2018	8	5/8 Ischemia 3/8 Hemorrhage	Patients < Controls
Belardinelli et al., 2017	8	3/8 Ischemia 5/8 Hemorrhage	Peak CMC in Beta Band (only patients)

ES, electrical stimulation.

the chronic and acute stroke through following up the recovery courses, the results indicated CMC amplitude was increased on the unaffected side and CMC frequency was decreased on the affected side in acute stroke, however, there was no inter-hemispheric difference in CMC parameters of the chronic stroke. The dynamical changes of interaction between cortical cortex and muscle both at acute and chronic stage of stroke may be a characteristic parameter for clinical application of CMC.

CMC Applications for Parkinson Patients

Parkinson's disease (PD) is related to pathologically alter oscillatory activity (Krause et al., 2013). **Table 5** shows the correlations of CMC and Parkinson disease. CMC as a neuro-physiological indicator of functional coupling between the primary motor cortex (M1) and peripheral muscles (Hari and Salenius, 1999; Krause et al., 2013) was applied as an index for PD symptoms variation early. Airaksinen et al. (2015b) found CMC decreased when they investigated defective cortical drive to muscle in PD. Similarly, CMC is a therapeutic indicator, PD patients had anomalously weak CMC after levodopa treatment during isometric contraction (Krause et al., 2013). In the recent Parkinson study, deep brain stimulation (DBS) of the subthalamic nucleus (STN) has the effects of improving motor symptoms and normalizing pathologically altered oscillations and applied to trace the rehabilitation of Parkinson patients with CMC. For example, STN-DBS was increasing the CMC amplitude of 10–30 Hz range for the tremorous hand because of the improvement of tremor by DBS (Park et al., 2009). Similar to this result, a slight increase of CMC during DBS was observed in eight patients on the average of 8 days studied after DBS implantation (Weiss et al., 2012). In addition, Airaksinen et al. (2015b) also showed DBS improved the CMC in advanced PD with large interindividual variability. Despite the differences in research results, it can be considered that CMC may be associated with the therapeutic effects of DBS. Similar to DBS, transcranial alternating current stimulation (tACS) can modulate cortical brain activity, some researchers were combined with tACS to study the CMC of PD patients. Study showed that decreased beta-range CMC and variability of fast lateral movements were due to motor cortex tACS at 20 Hz in PD patients (Krause et al., 2013).

CMC Applications for Tremor and Other Patients

In addition to stroke and Parkinson diseases, CMC may be possible regarded as an index to value some other movement disorders. **Table 6** shows the correlations of CMC and other diseases. Tremor is one of the most common disorders. To confirm the motor cortex involved in essential tremor and factors that affect CMC strength, Sharifi et al. (2017) collected 18 essential tremor patients and the result showed that essential tremor CMC is desultory and subject to different functional duties. This result may serve to standardize tremor classification and the explanation of the analysis in clinical research. Proudfoot et al. (2018) aimed to measure pathological alteration to CMC resulting from ALC during steady force production. During light voluntary muscular contraction, beta-range CMC was dramatically reduced in ALS patients and propagation of motoric rhythms across the cortical cortex was also impaired. Velázquez-Pérez et al. (2017b) purposed to assess dysfunction of the corticospinal tract in spinocerebellar ataxia type 2 (SCA2) using CMC. Significant reductions of CMC in SCA2 patients showed an evidence of corticospinal tract dysfunction. The abnormal CMC

TABLE 5 | Correlations of CMC and Parkinson.

Reference	Number of Patients	Stimulation	CMC value (Patients vs Controls)
Airaksinen et al., 2015b	19	yes	DBS modifies patients' CMC (only patients)
Krause et al., 2013	10	yes	Patients < Controls
Yoshida et al., 2017	10	no	Patients < Controls
Pollok et al., 2012	20	no	Patients < Controls

DBS, deep brain stimulation.

TABLE 6 | Correlations of CMC and other diseases.

Reference	Number of Patients	Disease Type	CMC value (Patients vs Controls)
Sharifi et al., 2017	18	ET	Patients < Controls
Raethjen et al., 2013	37	ET	Patients > Controls
Hellwig et al., 2001	10	7/10 ET 3/10 EPT	Significant CMC at the tremor frequency in ET patients (only patients)
Velázquez-Pérez et al., 2017b	19	SCA2	Patients < Controls
Velázquez-Pérez et al., 2017a	15	SCA2	Patients < Controls
Proudfoot et al., 2018	17	ALS	Patients < Controls
Cremoux et al., 2017	8	SCI	Patients < Controls
Bravo-Esteban et al., 2014	14	SCI	Patients < Controls

ET, essential tremor; EPT, enhanced physiological tremor; SCA2, spinocerebellar ataxia type 2; ALS, amyotrophic lateral sclerosis; SCI, spinal cord injury.

could only be detected in lower limbs experiments rather than upper limbs experiments may result from the corticospinal tract length on the chrono dispersion of action potential conduction. Cerebral palsy (CP) is a motor impairment which could affect the muscular contractions and neural connections between motor cortex and relative muscle. Many researches indicated CP influenced the normal muscular activities such as reduced voluntary-contraction force (Barber et al., 2012; Braendvik and Roeleveld, 2012; De et al., 2012). Riquelme et al. (2014) compared CMC during planning and execution of hand movements in CP patients and healthy subjects. From the results, CP patients were characterized by an altered functional coupling through CMC analysis and CMC may consider as a tool for exploring deficits during early brain damage.

Current literatures show that the applications of CMC in patients are simply regarded as a pathological indicator and are not clearly defined as clinically reliable parameters. The statistical comparison of different disorders use for the CMC study was collected form the published CMC papers as **Figure 3** shown. This reflects that Stroke, Parkinson and Tremor are the top three diseases that be used to study CMC and explore the physiological variations during patients' rehabilitation process. Rehabilitation diagnosis and treatment system based on CMC is the direction of future research. In addition, the design of CMC paradigm for patients with different diseases needs careful consideration.

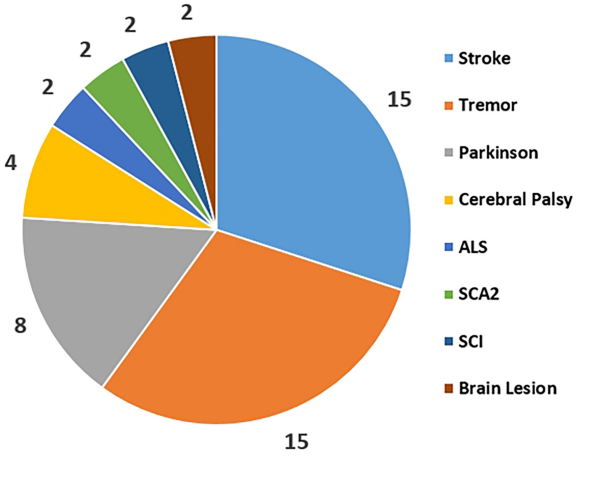

FIGURE 3 | Corticomuscular coherence application areas distribution for the disorders.

DISCUSSION

The aim of this study is to explore the impacts of corticomuscular coherence and how these impacts affect the cortex-muscle coherence. The experimental paradigms almost include all parts of human body to study whether the coupling strength between the relevant cortex and muscles would provide potential values and contributions. In this research, the findings appropriately display the CMC in diverse parts have the effects on recovery monitoring, motion changing and otherwise. Experimental protocol is a significant cause to influence the results of CMC. Muscle contraction forms and muscle fatigue are the most important limit conditions during experiments (Siemionow et al., 2010; Ushiyama et al., 2010, 2011b; Bayraktaroglu et al., 2011). At the same time, similar oscillations may be detected from adjacent muscles result in motion decoding confusion, thus discrimination of body parts in CMC has a potential research significance. Oscillatory activities in both cortex and muscles are commonly appeared in different band frequencies (alpha-band, beta-band and gamma-band) (Muthukumaraswamy, 2011; Schoffelen et al., 2011). Alpha-band and beta-band CMC contribute more to actual motor function, while the peak CMC is usually observed within beta-band in healthy subjects and within alpha-band in functional disorder patients (Caviness et al., 2006). Furthermore, in some findings, alpha-band CMC is related to precise control of movements like finger movements and for steady isometric or isotonic contractions, beta-band normally associates with these kind of movements (Omlor et al., 2011). In general, diverse band frequencies in CMC represent different modes of neural communication between cerebral cortex and spinal cord. Muscle activation is modulated by cortical activity which may result in voluntary contractions. Underlying the co-activation of antagonist and agonist muscles, reducing cortical influences on inhibiting antagonist muscles is supposed to increase the muscles co-activation. Maximum voluntary contractions (MVC) is a standard to limit force level during the experiments in common use. With the force level increasing, the magnitude of corticomuscular coherence seems to enhance and muscles co-activation would decrease and these

situations commonly appear in beta-band frequency rather than other band frequencies. The law of aging in CMC is also found. As age increases, the CMC would decrease gradually. However, the studies of aging are less than other factors correspondingly. To compare the CMC between healthy subjects and patients, healthy subjects have a higher CMC level than patients on account of nervous transmission damage (Patino et al., 2008; Meng et al., 2009). Meanwhile, peak CMC for healthy subjects emerges in beta-band while for patients, that shows in alpha-band.

In the present study, researchers are inclined to emphasize variance of corticomuscular coherence underlying distinct force levels and frequency bands (alpha, beta and gamma bands). Basically, a majority of researches of CMC would be able to consider band effects especially beta band and the effects of different bands in CMC have been studied thoroughly. CMC researches currently aim to seek a relationship or a correlation between CMC and other responsible factors which may modulate the amplitude of CMC. The challenges in the future focus on a greater depth of understanding the relationship between cortical and muscular activities and the applications in rehabilitation field and clinical field. The motion information decoding underlying the in-depth study of functional mechanism and CMC is possible to detect voluntary hand movements and more accurate than EEG only classification (Lou et al., 2013). If CMC is able to become a standard of motion decoding, it will eventually help exploit a new rehabilitation protocol. In general, the variance in CMC possible is related to communication issue between motor cortex and relative muscles. For instance, patients of cerebral lesion commonly have lower and intermittent CMC compare to healthy subjects, so they could not present a desirable movement since the motor impairment affects muscular contractions. Therefore, the further study, such as force controls or task complexity in both upper and lower limbs, would provide a precise CMC modulation protocols and a large number of experimental data basis for neuromuscular disorders. Furthermore, in rehabilitation field, experimental data basis might be benefit to establish a more reasonable and advanced rehabilitation programs for paralyzed patients and the improvement of CMC analysis could also provide a monitoring during the rehabilitation process. On the contrast, CMC monitoring could not only be used in patients' rehabilitation processing but also be applied in healthy inspection for the healthy person. If CMC has an abnormal change during a period, there may be a risk of corticospinal tract degeneration and a timely diagnosis is helpful in the prevention of such diseases.

Comparing with CMC as a physiological index, many other metrics have been used for disorder detection. EMG amplitude and EMG median power frequency are usually good indicators of fatigue in multiple sclerosis (Tomasevic et al., 2013). Functional neuroimaging techniques such as fMRI, TMS and PET have been used to assess neural correlates of motor impairment and recovery over the past decades. Rehme et al. (2012) discovered that patients with stroke showed more task-related brain activation in both the affected and the unaffected hemisphere from PET and fMRI assessments. Volz et al. (2015) combined TMS, MRI, and connectivity analyses to investigate corticospinal tract (CST) injury in patients. Cortical excitability and motor network were effective connectivity for hand function recovery in chronic stroke patients.

Bourguignon et al. (2015) proposed that corticokinematic coherence (CKC) to reflect coupling between magnetoencephalographic (MEG) signals and hand kinematics. It provided a reliable tool to monitor proprioceptive input to the cortex (Bourguignon et al., 2015). Intermuscular coherence (IMC) could quantify the strength of the coupling between cortex and the muscles. It was related to CMC in the beta band (Kilner et al., 1999) and reduced in the acute phase after stroke (Larsen et al., 2017). Dal Maso et al. (2018) explored correlations between event-related desynchronization (ERD), functional connectivity (FC) and CMC and skill retention, and suggested that cardiovascular exercise initiates significant changes in FC and CMC during motor memory consolidation (van Wijk et al., 2012). These metrics could be used as indicators of physiological activities through various forms of measurement, more or less relevant to the CMC.

Functional coupling between the motor cortex and muscle activity usually occurs with a time delay, which reflects signal propagation time between the brain and the muscle and information interaction (Xu et al., 2017). Perfect coherence (without temporal lags) does not exist which is only an ideal hypothesis in theory since multiple features influence the delays estimated using corticomuscular coherence, such as extra delays caused by the motor unit action potential, the duration of the corticomotoneuronal excitatory postsynaptic potential (EPSP), and a phase advance produced by motoneuron properties (Williams and Baker, 2008). The variety of temporal lags is the limitation of CMC as a physiological index. Some authors improved CMC by estimating the delay time. Govindan et al. (2005) used the method of maximizing coherence to obtain the time delay between two signals that were suitable for time delay estimation of narrow band coherence signals. Xu et al. (2017) proposed a CMC with time lag (CMCTL) function, which was the coherence displaced from a central observation point between segments of motor cortex EEG and EMG signals, and showed that it enhanced the CMC level and provided a more depth information on the temporal structure of CMC interaction than traditional CMC.

In summary, CMC research is still in a relatively early stage. Further exploration is needed in application, not only in rehabilitation and clinic for patients, but also in development of physical mechanism for healthy subjects.

CONCLUSION

Corticomuscular coherence is a method to evaluate the coherence ability between motor cortex and muscles. For a more comprehensive understanding of the mechanism of CMC, the comparison between related factors shows that the peak CMC amplitude has a great probability to emerge under relatively high force level, beta frequency band. As age increases, CMC decreases under various degrees, which is also in line with the natural trend of muscle aging. The amplitude of CMC in healthy subjects is

higher than that in patients in most cases. However, with the recovery of motor function of patients, CMC levels usually return to normal condition.

Current applications of CMC in patients is simply regarded as a pathological indicator and is not clearly defined as clinically reliable parameters. Further investigation is needed for a more complete understanding of enhancing CMC. Considering the use of different forms of muscle contraction to achieve superior results, scientific and reasonable paradigms are arranged to realize the target. Meanwhile, accurate classification of CMC on the affected side is needed to make CMC as an indicator in clinical application.

AUTHOR CONTRIBUTIONS

JL and YS wrote the body content and reviewed the whole article. HL reviewed the whole article and decided the final version.

FUNDING

This work was supported by the National Natural Science Foundation of China (Nos. 51575338, 51575407, 51475427, and 61733011) and the Fundamental Research Funds for the Central Universities (17JCYB03).

REFERENCES

Airaksinen, K., Lehti, T., Nurminen, J., Luoma, J., Helle, L., Taulu, S., et al. (2015a). Cortico-muscular coherence parallels coherence of postural tremor and MEG during static muscle contraction. *Neurosci. Lett.* 602, 22–26. doi: 10.1016/j.neulet.2015.06.034

Airaksinen, K., Mäkelä, J. P., Nurminen, J., Luoma, J., Taulu, S., Ahonen, A., et al. (2015b). Cortico-muscular coherence in advanced Parkinson's disease with deep brain stimulation. *Clin. Neurophysiol.* 126, 748–755. doi: 10.1016/j.clinph.2014.07.025

Andrykiewicz, A., Patino, L., Naranjo, J. R., Witte, M., Hepp-Reymond, M. C., and Kristeva, R. (2007). Corticomuscular synchronization with small and large dynamic force output. *BMC Neurosci.* 8:101. doi: 10.1186/1471-2202-8-101

Baker, S. N., Matthew, C., and Fetz, E. E. (2006). Afferent encoding of central oscillations in the monkey arm. *J. Neurophysiol.* 95, 3904–3910. doi: 10.1152/jn.01106.2005

Baker, S. N., Olivier, E., and Lemon, R. N. (1997). Coherent oscillations in monkey motor cortex and hand muscle EMG show task-dependent modulation. *J. Physiol.* 501, 225–241. doi: 10.1111/j.1469-7793.1997.225bo.x

Baker, S. N., Pinches, E. M., and Lemon, R. N. (2003). Synchronization in monkey motor cortex during a precision grip task. II. effect of oscillatory activity on corticospinal output. *J. Neurophysiol.* 89, 1941–1953. doi: 10.1152/jn.00832.2002

Barber, L., Barrett, R., and Lichtwark, G. (2012). Medial gastrocnemius muscle fascicle active torque-length and Achilles tendon properties in young adults with spastic cerebral palsy. *J. Biomech.* 45, 2526–2530. doi: 10.1016/j.jbiomech.2012.07.018

Bayraktaroglu, Z., Carlowitz-Ghori, K. V., Losch, F., Nolte, G., Curio, G., and Nikulin, V. V. (2011). Optimal imaging of cortico-muscular coherence through a novel regression technique based on multi-channel EEG and un-rectified EMG. *J. Neuroimage* 57, 1059–1067. doi: 10.1016/j.neuroimage.2011.04.071

Bayram, M., Siemionow, V., and Yue, G. (2015). Weakening of corticomuscular signal coupling during voluntary motor action in aging. *J. Gerontol. A Biol. Sci. Med. Sci.* 70, 1037–1043. doi: 10.1093/gerona/glv014

Beauchet, O., Dubost, V., Herrmann, F. R., and Kressig, R. W. (2005). Stride-to-stride variability while backward counting among healthy young adults. *J. Neuroeng. Rehabil.* 2:26. doi: 10.1186/1743-0003-2-26

Belardinelli, P., Laer, L., Ortiz, E., Braun, C., and Gharabaghi, A. (2017). Plasticity of premotor cortico-muscular coherence in severely impaired stroke patients with hand paralysis. *Neuroimage Clin.* 14, 726–733. doi: 10.1016/j.nicl.2017.03.005

Bourguignon, M., Piitulainen, H., Tiège, X. D., Jousmäki, V., and Hari, R. (2015). Corticokinematic coherence mainly reflects movement-induced proprioceptive feedback. *Neuroimage* 106, 382–390. doi: 10.1016/j.neuroimage.2014.11.026

Braendvik, S. M., and Roeleveld, K. (2012). The role of co-activation in strength and force modulation in the elbow of children with unilateral cerebral palsy. *J. Electromyogr. Kines* 22, 137–144. doi: 10.1016/j.jelekin.2011.10.002

Braun, C., Staudt, M., Schmitt, C., Preissl, H., Birbaumer, N., Gerloff, C., et al. (2007). Crossed cortico-spinal motor control after capsular stroke. *Eur. J. Neurosci.* 25, 2935–2945. doi: 10.1111/j.1460-9568.2007.05526.x

Bravo-Esteban, E., Taylor, J., Aleixandre, M., Simon-Martínez, C., Torricelli, D., Pons, J. L., et al. (2014). Tibialis Anterior muscle coherence during controlled voluntary activation in patients with spinal cord injury: diagnostic potential for muscle strength, gait and spasticity. *J. Neuroeng. Rehabil.* 11:23. doi: 10.1186/1743-0003-11-23

Brown, P., Salenius, S., Rothwell, J. C., and Hari, R. (1998). Cortical correlate of the Piper rhythm in humans. *J. Neurophysiol.* 80, 2911–2917. doi: 10.1007/s002329900465

Budini, F., Mcmanus, L. M., Berchicci, M., Menotti, F., Macaluso, A., Di Russo, F., et al. (2014). Alpha band cortico-muscular coherence occurs in healthy individuals during mechanically-induced tremor. *PLoS One* 9:e115012. doi: 10.1371/journal.pone.0115012

Caviness, J. N., Shill, H. A., Sabbagh, M. N., Evidente, V. G. H., Hernandez, J. L., and Adler, C. H. (2006). Corticomuscular coherence is increased in the small postural tremor of Parkinson's disease. *Mov. Disord.* 21, 492–499. doi: 10.1002/mds.20743

Chakarov, V., Naranjo, J. R., Schulte-Monting, J., Omlor, W., Huethe, F., and Kristeva, R. (2009). Beta-range EEG-EMG coherence with isometric compensation for increasing modulated low-level forces. *J. Neurophysiol.* 102, 1115–1120. doi: 10.1152/jn.91095.2008

Chen, X., Xie, P., Zhang, Y., Chen, Y., Yang, F., Zhang, L., et al. (2018). Multiscale information transfer in functional corticomuscular coupling estimation following stroke: a pilot study. *Front. Neurol.* 9:287. doi: 10.3389/fneur.2018.00287

Clark, D. J., Kautz, S. A., Bauer, A. R., Yen-Ting, C., and Christou, E. A. (2013). Synchronous EMG activity in the piper frequency band reveals the corticospinal demand of walking tasks. *Ann. Biomed. Eng.* 41, 1778–1786. doi: 10.1007/s10439-013-0832-4

Claudio, B., Fabrizio, V., Martin, B., Milan, B., Igor, N., Fabrizio, E., et al. (2008). Functional coupling between anterior prefrontal cortex (BA10) and hand muscle contraction during intentional and imitative motor acts. *Neuroimage* 39, 1314–1323. doi: 10.1016/j.neuroimage.2007.09.043

Conway, B. A., Halliday, D. M., Farmer, S. F., Shahani, U., Maas, P., Weir, A. I., et al. (1995). Synchronization between motor cortex and spinal motoneuronal pool during the performance of a maintained motor task in man. *J. Physiol.* 489, 917–924. doi: 10.1113/jphysiol.1995.sp021104

Cottone, C., Porcaro, C., Cancelli, A., Olejarczyk, E., Salustri, C., and Tecchio, F. (2017). Neuronal electrical ongoing activity as a signature of cortical areas. *Brain Struct. Funct.* 222, 1–12. doi: 10.1007/s00429-016-1328-4

Cremoux, S., Tallet, J., Dal, M. F., Berton, E., and Amarantini, D. (2017). Impaired corticomuscular coherence during isometric elbow flexion contractions in human with cervical Spinal Cord Injury. *Eur. J. Neurosci.* 46, 1991–2000. doi: 10.1111/ejn.13641

Dal Maso, F., Desormeau, B., Boudrias, M. H., and Roig, M. (2018). Acute cardiovascular exercise promotes functional changes in cortico-motor networks during the early stages of motor memory consolidation. *Neuroimage* 174, 380–392. doi: 10.1016/j.neuroimage.2018.03.029

Dal Maso, F., Longcamp, M., Cremoux, S., and Amarantini, D. (2017). Effect of training status on beta-range corticomuscular coherence in agonist vs. antagonist muscles during isometric knee contractions. *Exp. Brain Res.* 235, 1–9. doi: 10.1007/s00221-017-5035-z

De, G. S., Dallmeijer, A. J., Bessems, P. J., Lamberts, M. L., Lh, V. D. W., and Janssen, T. W. (2012). Comparison of muscle strength, sprint power and aerobic

capacity in adults with and without cerebral palsy. *J. Rehabil. Med.* 44, 932–938. doi: 10.2340/16501977-1037

Eisen, A., Entezari-Taher, M., and Stewart, H. (1996). Cortical projections to spinal motoneurons: changes with aging and amyotrophic lateral sclerosis. *Neurology* 46, 1396–1404. doi: 10.1212/WNL.46.5.1396

Fang, Y., Daly, J. J., Sun, J., Hvorat, K., Fredrickson, E., Pundik, S., et al. (2009). Functional corticomuscular connection during reaching is weakened following stroke. *Clin. Neurophysiol.* 120, 994–1002. doi: 10.1016/j.clinph.2009.02.173

Farmer, S. F., Swash, M., Ingram, D. A., and Stephens, J. A. (1993). Changes in motor unit synchronization following central nervous lesions in man. *J. Physiol.* 463, 83–105. doi: 10.1113/jphysiol.1993.sp019585

Feige, B., Aertsen, A., and Kristeva-Feige, R. (2000). Dynamic synchronization between multiple cortical motor areas and muscle activity in phasic voluntary movements. *J. Neurophysiol.* 84, 2622–2629. doi: 10.1016/S0165-5728(00)00367-2

Fisher, R. J., Galea, M., Brown, P., and Lemon, R. N. (2002). Digital nerve anaesthesia decreases EMG-EMG coherence in a human precision grip task. *Exp. Brain Res.* 145, 207–214. doi: 10.1007/s00221-002-1113-x

Fu, A., Rui, X., Feng, H., Qi, H., Zhang, L., Dong, M., et al. (2014). "Corticomuscular coherence analysis on the static and dynamic tasks of hand movement," in *Proceedings of the 19 the International Conference on Digital Signal Processing*, (Hong Kong: IEEE), doi: 10.1109/ICDSP.2014.6900757

Gao, Y., Ren, L., Li, R., and Zhang, Y. (2017). Electroencephalogram–electromyography coupling analysis in stroke based on symbolic transfer entropy. *Front. Neurol.* 8:716. doi: 10.3389/fneur.2017.00716

Gerloff, C., Braun, C., Staudt, M., Hegner, Y. L., Dichgans, J., and Krägeloh-Mann, I. (2006). Coherent corticomuscular oscillations originate from primary motor cortex: evidence from patients with early brain lesions. *Hum. Brain Mapp.* 27, 789–798. doi: 10.1002/hbm.20220

Good, C. D., Johnsrude, I. S., Ashburner, J., Henson, R. N. A., Friston, K. J., and Frackowiak, R. S. J. (2001). A voxel-based morphometric study of ageing in 465 normal adult human brains. *Neuroimage* 14, 21–36. doi: 10.1109/SSBI.2002.1233974

Govindan, R. B., Raethjen, J., Kopper, F., Claussen, J. C., and Deuschl, G. (2005). Estimation of time delay by coherence analysis. *Phys. A* 350, 277–295. doi: 10.1016/j.physa.2004.11.043

Graziadio, S., Basu, A. P., Zappasodi, F., Tecchio, F., and Eyre, J. A. (2010). Developmental tuning and decay in senescence of oscillations linking the corticomotoneuronal system. *J. Neurosci.* 30, 3363–3374. doi: 10.1523/JNEUROSCI.5621-09.2010

Graziadio, S., Tomasevic, L., Assenza, G., Tecchio, F., and Eyre, J. A. (2012). The myth of the 'unaffected' side after unilateral stroke: is reorganisation of the non-infarcted corticospinal system to re-establish balance the price for recovery? *Exp. Neurol.* 238, 168–175. doi: 10.1016/j.expneurol.2012.08.031

Gross, J., Tass, P. A., Salenius, S., Hari, R., Freund, H. J., and Schnitzler, A. (2000). Cortico-muscular synchronization during isometric muscle contraction in humans as revealed by magnetoencephalography. *J. Physiol.* 527, 623–631. doi: 10.1111/j.1469-7793.2000.00623.x

Grosse, P., Guerrini, R., Parmeggiani, L., Bonanni, P., Pogosyan, A., and Brown, P. (2003). Abnormal corticomuscular and intermuscular coupling in high-frequency rhythmic myoclonus. *Brain* 126, 326–342. doi: 10.1093/brain/awg043

Gwin, J. T., and Ferris, D. P. (2012). Beta- and gamma-range human lower limb corticomuscular coherence. *Front. Hum. Neurosci.* 6:258. doi: 10.3389/fnhum.2012.00258

Halliday, D., Conwayb, B., Farmerc, S., and Rosenberg, J. R. (1998). Using electroencephalography to study functional coupling between cortical activity and electromyograms during voluntary contractions in humans. *Neurosci. Lett.* 241, 5–8. doi: 10.1016/S0304-3940(97)00964-6

Hari, R., and Salenius, S. (1999). Rhythmical corticomotor communication. *Neuroreport* 10, 1–10. doi: 10.1016/S1388-2457(00)00248-0

Hellwig, B., Häussler, S., Lauk, M., Guschlbauer, B., Köster, B., Kristeva-Feige, R., et al. (2000). Tremor-correlated cortical activity detected by electroencephalography. *Clin. Neurophysiol.* 111, 806–809. doi: 10.1016/S1388-2457(00)00248-0

Hellwig, B., Häußler, S., Schelter, B., Lauk, M., Guschlbauer, B., Timmer, J., et al. (2001). Tremor-correlated cortical activity in essential tremor. *Lancet* 357, 519–523. doi: 10.1016/s0140-6736(00)04044-7

Hiraga, C. Y., Garry, M. I., Carson, R. G., and Summers, J. J. (2009). Dual-task interference: attentional and neurophysiological influences. *Behav. Brain Res.* 205, 10–18. doi: 10.1016/j.bbr.2009.07.019

Horak, F. B. (1991). "Assumptions underlying motor control for neurologic rehabilitation," in *Foundation for Physical Therapy*, ed. M. J. Lister (Alexandria, VA: Bookcrafters), 11–28. doi: 10.1016/j.neuroscience.2015.04.009

Hori, S., Matsumoto, J., Hori, E., Kuwayama, N., Ono, T., Kuroda, S., et al. (2013). Alpha- and theta-range cortical synchronization and corticomuscular coherence during joystick manipulation in a virtual navigation task. *Brain Topogr.* 26, 591–605. doi: 10.1007/s10548-013-0304-z

Jacobs, J. V., Wu, G., and Kelly, K. M. (2015). Evidence for beta corticomuscular coherence during human standing balance: effects of stance width, vision, and support surface. *Neuroscience* 298, 1–11. doi: 10.1016/j.neuroscience.2015.04.009

James, L., Halliday, D., Stephens, J. A., and Farmer, S. (2008). On the development of human corticospinal oscillations: age-related changes in EEG-EMG coherence and cumulant. *Eur. J. Neurosci.* 27, 3369–3379. doi: 10.1111/j.1460-9568.2008.06277.x

Johnson, A. N., and Shinohara, M. (2012). Corticomuscular coherence with and without additional task in the elderly. *J. Appl. Physiol.* 112, 970–981. doi: 10.1152/japplphysiol.01079.2011

Johnson, A. N., Wheaton, L. A., and Minoru, S. (2011). Attenuation of corticomuscular coherence with additional motor or non-motor task. *Clin. Neurophysiol.* 122, 356–363. doi: 10.1016/j.clinph.2010.06.021

Kamp, D., Krause, V., Butz, M., Schnitzler, A., and Pollok, B. (2013). Changes of cortico-muscular coherence: an early marker of healthy aging? *AGE* 35, 49–58. doi: 10.1007/s11357-011-9329-y

Kawamura, Y., O'brien, P., Okazaki, H., and Dyck, P. J. (1977a). Lumbar motoneurons of man II: the number and diameter distribution of large- and intermediate-diameter cytons in "motoneuron columns" of spinal cord of man. *J. Neuropathol. Exp. Neurol.* 36, 861–870. doi: 10.1097/00005072-197709000-00010

Kawamura, Y., Okazaki, H., O'brien, P. C., and Dyck, P. J. (1977b). Lumbar motoneurons of man: (I) number and diameter histogram of alpha and gamma axons of ventral root. *J. Neuropathol. Exp. Neurol.* 36, 853–860. doi: 10.1097/00005072-197709000-00009

Kilner, J. M., Baker, S. N., Salenius, S., Hari, R., and Lemon, R. N. (2000). Human cortical muscle coherence is directly related to specific motor parameters. *J. Neurosci.* 20, 8838–8845. doi: 10.1016/S0736-5748(99)00069-6

Kilner, J. M., Baker, S. N., Salenius, S., Jousmäki, V., Hari, R., and Lemon, R. N. (1999). Task-dependent modulation of 15-30 Hz coherence between rectified EMGs from human hand and forearm muscles. *J. Physiol.* 516, 559–570. doi: 10.1111/j.1469-7793.1999.0559v.x

Kilner, J. M., Fisher, R. J., and Lemon, R. N. (2004). Coupling of oscillatory activity between muscles is strikingly reduced in a deafferented subject compared with normal controls. *J. Neurophysiol.* 92, 790–796. doi: 10.1152/jn.01247.2003

Krause, V., Wach, C., Südmeyer, M., Ferrea, S., Schnitzler, A., and Pollok, B. (2013). Cortico-muscular coupling and motor performance are modulated by 20 Hz transcranial alternating current stimulation (tACS) in Parkinson's disease. *Front. Hum. Neurosci.* 7:928. doi: 10.3389/fnhum.2013.00928

Kristeva-Feige, R., Fritsch, C., Timmer, J., and Lucking, C. (2002). Effects of attention and precision of exerted force on beta range EEG-EMG synchronization during a maintained motor contraction task. *Clin. Neurophysiol.* 113, 124–131. doi: 10.1016/s1388-2457(01)00722-2

Lachaux, J. P., Lutz, A., Rudrauf, D., Cosmelli, D., Le Van Quyen, M., Martinerie, J., et al. (2002). Estimating the time-course of coherence between single-trial brain signals: an introduction to wavelet coherence. *Neurophysiol. Clin.* 32, 157–174. doi: 10.1016/s0987-7053(02)00301-5

Larsen, L. H., Zibrandtsen, I. C., Wienecke, T., Kjaer, T. W., Christensen, M. S., Nielsen, J. B., et al. (2017). Corticomuscular coherence in the acute and subacute phase after stroke. *Clin. Neurophysiol.* 128, 2217–2226. doi: 10.1016/j.clinph.2017.08.033

Lattari, E., Velasques, B., Paes, F., Cunha, M., Budde, H., Basile, L., et al. (2010). Corticomuscular coherence behavior in fine motor control of force: a critical review. *Rev. Neurol.* 51, 610–623. doi: 10.1212/WNL.0b013e3181fd636a

Lim, M., Kim, J. S., Kim, M., and Chung, C. K. (2014). Ascending beta oscillation from finger muscle to sensorimotor cortex contributes to enhanced steady-state isometric contraction in humans. *Clin. Neurophysiol.* 125, 2036–2045. doi: 10.1016/j.clinph.2014.02.006

Lou, X., Xiao, S., Qi, Y., Hu, X., Wang, Y., and Zheng, X. (2013). Corticomuscular coherence analysis on hand movement distinction for active rehabilitation. *Comput. Math. Methods Med.* 2013:908591. doi: 10.1155/2013/908591

Lundbye-Jensen, J., and Nielsen, J. (2008). Immobilization induces changes in presynaptic control of group Ia afferents in healthy humans. *J. Physiol.* 586, 4121–4135. doi: 10.1113/jphysiol.2008.156547

Maezawa, H. (2016). Cortico-muscular communication for motor control of the tongue in humans: a review. *J. Oral Biosci.* 58, 69–72. doi: 10.1016/j.job.2016.03.001

Maezawa, H., Mima, T., Yazawa, S., Matsuhashi, M., Shiraishi, H., and Funahashi, M. (2016). Cortico-muscular synchronization by proprioceptive afferents from the tongue muscles during isometric tongue protrusion. *Neuroimage* 128, 284–292. doi: 10.1016/j.neuroimage.2015.12.058

Maluf, K. S., and Enoka, R. M. (2005). Task failure during fatiguing contractions performed by humans. *J. Appl. Physiol.* 99, 389–396. doi: 10.1152/japplphysiol.00207.2005

Matsuya, R., Ushiyama, J., and Ushiba, J. (2017). Inhibitory interneuron circuits at cortical and spinal levels are associated with individual differences in corticomuscular coherence during isometric voluntary contraction. *Sci. Rep.* 7:44417. doi: 10.1038/srep44417

Mckeown, M. J., Palmer, S. J., Au, W., Mccaig, R., Saab, R., and Abu-Gharbieh, R. (2006). Cortical muscle coupling in Parkinson's disease (PD) bradykinesia. *J. Neura Transm. Suppl.* 70, 31–40. doi: 10.1007/978-3-211-45295-0_7

Mcmanus, L. M., Budini, F., Russo, F. D., Berchicci, M., and Lowery, M. M. (2013). "Analysis of the effects of mechanically induced tremor on EEG-EMG coherence using wavelet and partial directed coherence," in *Proceedings of the International IEEE/EMBS Conference on Neural Engineering*, (San Diego, CA: IEEE), 561–564. doi: 10.1109/NER.2013.6695996

Mehrkanoon, S., Breakspear, M., and Boonstra, T. (2014). The reorganization of corticomuscular coherence during a transition between sensorimotor states. *Neuroimage* 100, 692–702. doi: 10.1016/j.neuroimage.2014.06.050

Mendez-Balbuena, I., Naranjo, J. R., Wang, X., Andrykiewicz, A., Huethe, F., Schulte Monting, J., et al. (2013). The strength of the corticospinal coherence depends on the predictability of modulated isometric forces. *J. Neurophysiol.* 109, 1579–1588. doi: 10.1152/jn.00187.2012

Meng, F., Tong, K., Chan, S., Wong, W., Lui, K., Tang, K., et al. (2009). Cerebral plasticity after subcortical stroke as revealed by cortico-muscular coherence. *IEEE Trans. Neural Syst. Rehabil. Eng.* 17, 234–243. doi: 10.1109/TNSRE.2008.2006209

Mima, T., and Hallett, M. (1999). Corticomuscular coherence: a review. *J. Clin. Neurophysiol.* 16, 501–511. doi: 10.1097/00004691-199911000-00002

Mima, T., Simpkins, N., Oluwatimilehin, T., and Hallett, M. (1999). Force level modulates human cortical oscillatory activities. *Neurosci. Lett.* 275, 77–80. doi: 10.1016/S0304-3940(99)00734-X

Mima, T., Steger, J., Schulman, A. E., Gerloff, C., and Hallett, M. (2000). Electroencephalographic measurement of motor cortex control of muscle activity in humans. *Clin. Neurophysiol.* 111, 326–337. doi: 10.1016/S1388-2457(99)00229-1

Mima, T., Toma, K., Koshy, B., and Hallett, M. (2001). Coherence between cortical and muscular activities after subcortical stroke. *Stroke* 32, 2597–2601. doi: 10.1161/hs1101.098764

Muthukumaraswamy, S. D. (2011). Temporal dynamics of primary motor cortex γ oscillation amplitude and piper corticomuscular coherence changes during motor control. *Exp. Brain Res.* 212, 623–633. doi: 10.1007/s00221-011-2775-z

Muthuraman, M., Heute, U., Deuschl, G., and Raethjen, J. (2010). "The central oscillatory network of essential tremor," in *Proceedings of the International Conference of the IEEE Engineering in Medicine and Biology Society*, (Buenos Aires, AR: IEEE), 154–157. doi: 10.1109/IEMBS.2010.5627211

Nielsen, J., Brittain, J., Halliday, D., Marchand-Pauvert, V., Mazevet, D., and Conway, B. (2008). Reduction of common motoneuronal drive on the affected side during walking in hemiplegic stroke patients. *Clin. Neurophysiol.* 119, 2813–2818. doi: 10.1016/j.clinph.2008.07.283

Omlor, W., Patino, L., Hepp-Reymond, M. C., and Kristeva, R. (2007). Gamma-range corticomuscular coherence during dynamic force output. *Neuroimage* 34, 1191–1198. doi: 10.1016/j.neuroimage.2006.10.018

Omlor, W., Patino, L., Mendez Balbuena, I., Schulte Monting, J., and Kristeva, R. (2011). Corticospinal beta-range coherence is highly dependent on the pre-stationary motor state. *J. Neurosci.* 31, 8037–8045. doi: 10.1523/JNEUROSCI.4153-10.2011

Pan, L.-L. H., Yang, W.-W., Kao, C.-L., Tsai, M.-W., Wei, S.-H., Fregni, F., et al. (2018). Effects of 8-week sensory electrical stimulation combined with motor training on EEG-EMG coherence and motor function in individuals with stroke. *Sci. Rep.* 8:9217. doi: 10.1038/s41598-018-27553-4

Park, H., Kim, J. S., Paek, S. H., Jeon, B. S., Lee, J. Y., and Chung, C. K. (2009). Cortico-muscular coherence increases with tremor improvement after deep brain stimulation in Parkinson's disease. *Neuroreport* 20, 1444–1449. doi: 10.1097/WNR.0b013e328331a51a

Patino, L., Omlor, W., Chakarov, V., Hepp Reymond, M.-C., and Kristeva, R. (2008). Absence of gamma-range corticomuscular coherence during dynamic force in a deafferented patient. *J. Neurophysiol.* 99, 1906–1916. doi: 10.1152/jn.00390.2007

Perez, M. A., Lundbye Jensen, J., and Nielsen, J. B. (2006). Changes in corticospinal drive to spinal motoneurones following visuo-motor skill learning in humans. *J. Physiol.* 573, 843–855. doi: 10.1113/jphysiol.2006.105361

Pfurtscheller, G., and Lopes da Silva, F. H. (eds). (1999). "Functional meaning of event-related desynchronization (ERD) and synchronization (ERS)," in *Handbook of Electroencephalography and Clinical Neurophysiology*, vol 6, (Amsterdam: Elsevier), 51–65.

Pfurtscheller, G., and Neuper, C. (1992). Simultaneous EEG 10 Hz desynchronization and 40 Hz synchronization during finger movements. *Neuroreport* 3, 1057–1060. doi: 10.1097/00001756-199212000-00006

Pohja, M., Salenius, S., and Hari, R. (2002). Cortico-muscular coupling in a human subject with mirror movements - A magnetoencephalographic study. *Neurosci. Lett.* 327, 185–188. doi: 10.1016/s0304-3940(02)00426-3

Pollok, B., Gross, J., Dirks, M., Timmermann, L., and Schnitzler, A. (2004). The cerebral oscillatory network of voluntary tremor. *J. Physiol.* 554, 871–878. doi: 10.1113/jphysiol.2003.051235

Pollok, B., Krause, V., Martsch, W., Wach, C., Schnitzler, A., and Südmeyer, M. (2012). Motor-cortical oscillations in early stages of Parkinson's disease. *J. Physiol.* 590, 3203–3212. doi: 10.1113/jphysiol.2012.231316

Poortvliet, P. C., Tucker, K. J., Finnigan, S., Scott, D., Sowman, P., and Hodges, P. W. (2015). Cortical activity differs between position- and force-control knee extension tasks. *Exp. Brain Res.* 233, 3447–3457. doi: 10.1007/s00221-015-4404-8

Porcaro, C., Barbati, G., Zappasodi, F., Rossini, P. M., and Tecchio, F. (2008). Hand sensory-motor cortical network assessed by Functional Source Separation. *Hum. Brain Mapp.* 29, 70–81. doi: 10.1002/hbm.20367

Porcaro, C., Cottone, C., Cancelli, A., Salustri, C., and Tecchio, F. (2018). Functional semi-blind source separation identifies primary motor area without active motor execution. *Int. J. Neural Syst.* 28:1750047. doi: 10.1142/s0129065717500472

Porcaro, C., Zappasodi, F., Rossini, P. M., and Tecchio, F. (2009). Choice of multivariate autoregressive model order affecting real network functional connectivity estimate. *Clin. Neurophysiol.* 120, 436–448. doi: 10.1016/j.clinph.2008.11.011

Proudfoot, M., Ede, F. V., Quinn, A., Colclough, G. L., Wuu, J., Talbot, K., et al. (2018). Impaired corticomuscular and interhemispheric cortical beta oscillation coupling in amyotrophic lateral sclerosis. *Clin. Neurophysiol.* 129, 1479–1489. doi: 10.1016/j.clinph.2018.03.019

Raethjen, J., Govindan, R., Kopper, F., Muthuraman, M., and Deuschl, G. (2007). Cortical involvement in the generation of essential tremor. *J. Neurophysiol.* 97, 3219–3228. doi: 10.1152/jn.00477.2006

Raethjen, J., Lindemann, M., Dümpelmann, M., Wenzelburger, R., Stolze, H., Pfister, G., et al. (2002). Corticomuscular coherence in the 6–15 Hz band: Is the cortex involved in the generation of physiologic tremor? *Exp. Brain Res.* 142, 32–40. doi: 10.1007/s00221-001-0914-7

Raethjen, J., Muthuraman, M., Kostka, A., Nahrwold, M., Hellriegel, H., Lorenz, D., et al. (2013). Corticomuscular coherence in asymptomatic first-degree relatives of patients with essential tremor. *Mov. Disord.* 28, 679–682. doi: 10.1016/j.neuroimage.2011.10.023

Rehme, A. K., Eickhoff, S. B., Rottschy, C., Fink, G. R., and Grefkes, C. (2012). Activation likelihood estimation meta-analysis of motor-related neural activity after stroke. *Neuroimage* 59, 2771–2782. doi: 10.1016/j.neuroimage.2011.10.023

Riddle, C. N., and Baker, S. N. (2005). Manipulation of peripheral neural feedback loops alters human corticomuscular coherence. *J. Physiol.* 566, 625–639. doi: 10.1113/jphysiol.2005.089607

Riquelme, I., Cifre, I., Muñoz, M. A., and Pedro, M. (2014). Altered corticomuscular coherence elicited by paced isotonic contractions in individuals with cerebral palsy: a case-control study. *J. Electromyogr. Kines* 24, 928–933. doi: 10.1016/j.jelekin.2014.07.004

Rong, Y., Han, X., Hao, D., Cao, L., Wang, Q., Li, M., et al. (2014). Applying support vector regression analysis on grip force level-related corticomuscular coherence. *J. Comput. Neurosci.* 37, 281–291. doi: 10.1007/s10827-014-0501-0

Rossiter, H. E., Eaves, C., Davis, E., Boudrias, M. H., Park, C. H., Farmer, S., et al. (2013). Changes in the location of cortico-muscular coherence following stroke. *Neuroimage Clin.* 2, 50–55. doi: 10.1016/j.nicl.2012.11.002

Salat, D., Tuch, D., Greve, D., van der Kouwe, A., Hevelone, N., Zaleta, A., et al. (2005). Age-related alterations in white matter microstructure measured by diffusion tensor imaging. *Neurobiol. Aging* 26, 1215–1227. doi: 10.1016/j.neurobiolaging.2004.09.017

Salenius, S., Avikainen, S., Kaakkola, S., Hari, R., and Brown, P. (2002). Defective cortical drive to muscle in Parkinson's disease and its improvement with levodopa. *Brain* 125, 491–500. doi: 10.1093/brain/awf042

Salenius, S., and Hari, R. (2003). Synchronous cortical oscillatory activity during motor action. *Curr. Opin. Neurobiol.* 13, 678–684. doi: 10.1016/j.conb.2003.10.008

Salenius, S., Portin, K., Kajola, M., Salmelin, R., and Hari, R. (1997). Cortical control of human motoneuron firing during isometric contraction. *J. Neurophysiol.* 77, 3401–3405. doi: 10.1007/s002329900238

Schoffelen, J., Poort, J., Oostenveld, R., and Fries, P. (2011). Selective movement preparation is subserved by selective increases in corticomuscular gamma-band coherence. *J. Neurosci.* 31, 6750–6758. doi: 10.1523/jneurosci.4882-10.2011

Schulz, H., Ubelacker, T., Keil, J., Müller, N., and Weisz, N. (2014). Now I am ready-now i am not: the influence of pre-TMS oscillations and corticomuscular coherence on motor-evoked potentials. *Cereb. Cortex* 24, 1708–1719. doi: 10.1093/cercor/bht024

Sharifi, S., Luft, F., Verhagen, R., Heida, T., Speelman, J., Bour, L., et al. (2017). Intermittent cortical involvement in the preservation of tremor in essential tremor. *J. Neurophysiol.* 118, 2628–2635. doi: 10.1152/jn.00848.2016

Siemionow, V., Sahgal, V., and Yue, G. H. (2010). Single-Trial EEG-EMG coherence analysis reveals muscle fatigue-related progressive alterations in corticomuscular coupling. *IEEE Trans. Neural Syst. Rehabil. Eng.* 18, 97–106. doi: 10.1109/TNSRE.2010.2047173

Tecchio, F., Melgari, J., Zappasodi, F., Porcaro, C., Milazzo, D., Cassetta, E., et al. (2008). Sensorimotor integration in focal task-specific hand dystonia: a magnetoencephalographic assessment. *Neuroscience* 154, 563–571. doi: 10.1016/j.neuroscience.2008.03.045

Tecchio, F., Zappasodi, F., Melgari, J., Porcaro, C., Cassetta, E., and Rossini, P. M. (2006). Sensory-motor interaction in primary hand cortical areas: a magnetoencephalography assessment. *Neuroscience* 141, 533–542. doi: 10.1016/j.neuroscience.2006.03.059

Timmermann, L., Gross, J., Dirks, M., Volkmann, J., Freund, H.-J., and Schnitzler, A. (2003). The cerebral oscillatory network of parkinsonian resting tremor. *Brain* 126, 199–212. doi: 10.1093/brain/awg022

Tomasevic, L., Zito, G., Pasqualetti, P., Mm, F., Landi, D., Ghazaryan, A., et al. (2013). Cortico-muscular coherence as an index of fatigue in multiple sclerosis. *Mult. Scler.* 19, 334–343. doi: 10.1177/1352458512452921

Tomlinson, B., and Irving, D. (1977). The numbers of limb motor neurons in the human lumbosacral cord throughout life. *J. Neurol. Sci.* 34, 213–219. doi: 10.1016/0022-510X(77)90069-7

Ushiyama, J., Katsu, M., Masakado, Y., Kimura, A., Liu, M., and Ushiba, J. (2011a). Muscle fatigue-induced enhancement of corticomuscular coherence following sustained submaximal isometric contraction of the tibialis anterior muscle. *J. Appl. Physiol.* 110, 1233–1240. doi: 10.1152/japplphysiol.01194.2010

Ushiyama, J., Suzuki, T., Masakado, Y., Hase, K., Kimura, A., Liu, M., et al. (2011b). Between-subject variance in the magnitude of corticomuscular coherence during tonic isometric contraction of the tibialis anterior muscle in healthy young adults. *J. Neurophysiol.* 106, 1379–1388. doi: 10.1152/jn.00193.2011

Ushiyama, J., Takahashi, Y., and Ushiba, J. (2010). Muscle dependency of corticomuscular coherence in upper and lower limb muscles and training-related alterations in ballet dancers and weightlifters. *J. Appl. Physiol.* 109, 1086–1095. doi: 10.1152/japplphysiol.01194.2010

Ushiyama, J., Yamada, J., Liu, M., and Ushiba, J. (2017). Individual difference in β-band corticomuscular coherence and its relation to force steadiness during isometric voluntary ankle dorsiflexion in healthy humans. *Clin. Neurophysiol.* 128, 303–311. doi: 10.1016/j.clinph.2016.11.025

van Wijk, B. C. M., Beek, P. J., and Daffertshofer, A. (2012). Neural synchrony within the motor system: What have we learned so far? *Front. Hum. Neurosci.* 6:252. doi: 10.3389/fnhum.2012.00252

Velázquez-Pérez, L., Tünnerhoff, J., Rodríguez-Labrada, R., Torres-Vega, R., Belardinelli, P., Medrano-Montero, J., et al. (2017a). Corticomuscular coherence: a novel tool to assess the pyramidal tract dysfunction in spinocerebellar ataxia type 2. *Cerebellum* 16, 1–5. doi: 10.1007/s12311-016-0827-4

Velázquez-Pérez, L., Tünnerhoff, J., Rodríguez-Labrada, R., Torres-Vega, R., Ruiz-Gonzalez, Y., Belardinelli, P., et al. (2017b). Early corticospinal tract damage in prodromal SCA2 revealed by EEG-EMG and EMG-EMG coherence. *Clin. Neurophysiol.* 128, 2493–2502. doi: 10.1016/j.clinph.2017.10.009

Voelcker-Rehage, C., and Alberts, J. L. (2007). Effect of motor practice on dual-task performance in older adults. *J. Gerontol. B Psychol. Sci. Soc. Sci.* 62, 141–148. doi: 10.1093/geronb/62.3.P141

Volz, L. J., Sarfeld, A. S., Diekhoff, S., Rehme, A. K., Pool, E. M., Eickhoff, S. B., et al. (2015). Motor cortex excitability and connectivity in chronic stroke: a multimodal model of functional reorganization. *Brain Struct. Funct.* 220, 1093–1107. doi: 10.1007/s00429-013-0702-8

von Carlowitz-Ghori, K., Bayraktaroglu, Z., Hohlefeld, F. U., Florian, L., Gabriel, C., and Nikulin, V. V. (2014). Corticomuscular coherence in acute and chronic stroke. *Clin. Neurophysiol.* 125, 1182–1191. doi: 10.1016/j.clinph.2013.11.006

von Carlowitz-Ghori, K., Bayraktaroglu, Z., Waterstraat, G., Curio, G., and Nikulin, V. V. (2015). Voluntary control of corticomuscular coherence through neurofeedback: a proof-of-principle study in healthy subjects. *Neuroscience* 290, 243–254. doi: 10.1016/j.neuroscience.2015.01.013

Weiss, D., Breit, S., Hoppe, J., Hauser, A., Freudenstein, D., Krüger, R., et al. (2012). Subthalamic nucleus stimulation restores the efferent cortical drive to muscle in parallel to functional motor improvement. *Eur. J. Neurosci.* 35, 896–908. doi: 10.1111/j.1460-9568.2012.08014.x

Weiss, D., Govindan, R. B., Rilk, A., Wächter, T., Breit, S., Zizlsperger, L., et al. (2010). Central oscillators in a patient with neuropathic tremor: evidence from intraoperative local field potential recordings. *Mov. Disord.* 26, 323–327. doi: 10.1002/mds.23374

Williams, E. R., and Baker, S. N. (2008). Circuits generating corticomuscular coherence investigated using a biophysically based computational model. I. Descending systems. *J. Neurophysiol.* 101, 31–41.

Witham, C. L., Riddle, C. N., Baker, M. R., and Baker, S. N. (2011). Contributions of descending and ascending pathways to corticomuscular coherence in humans. *J. Physiol.* 589, 3789–3800. doi: 10.1113/jphysiol.2011.211045

Witte, M., Patino, L., Andrykiewicz, A., Hepp Reymond, M.-C., and Kristeva, R. (2007). Modulation of human corticomuscular beta-range coherence with low-level static forces. *Eur. J. Neurosci.* 26, 3564–3570. doi: 10.1111/j.1460-9568.2007.05942.x

Xu, R., He, F., Qiu, S., Chen, L., Liu, S., Zhao, X., et al. (2015). Corticomuscular coherence based on wavelet transform during imagination, execution and stimulation tasks. *J. Med. Imag. Health Inform.* 5, 335–341. doi: 10.1166/jmihi.2015.1397

Xu, Y., Mcclelland, V., Cvetkovic, Z., and Mills, K. (2017). Cortico-muscular coherence with time lag with application to delay estimation. *IEEE Trans. Biomed. Eng.* 64, 588–600. doi: 10.1109/TBME.2016.2569492

Yang, Q., Fang, Y., Sun, C. K., Siemionow, V., Ranganathan, V. K., Khoshknabi, D., et al. (2009). Weakening of functional corticomuscular coupling during muscle fatigue. *Brain Res.* 1250, 101–112. doi: 10.1016/j.brainres.2008.10.074

Yang, Y., Solis-Escalante, T., van de Ruit, M., van der Helm, F. C., and Schouten, A. C. (2016). Nonlinear coupling between cortical oscillations and muscle activity during isotonic wrist flexion. *Front. Comput. Neurosci.* 10:126. doi: 10.3389/fncom.2016.00126

Yoshida, T., Masani, K., Zabjek, K., Chen, R., and Popovic, M. (2017). Dynamic cortical participation during bilateral, cyclical ankle movements: effects of aging. *Sci. Rep*. 7:44658. doi: 10.1038/srep44658

Zheng, Y., Peng, Y., Xu, G., Li, L., and Wang, J. (2017). Using corticomuscular coherence to reflect function recovery of paretic upper limb after stroke: a case study. *Front. Neurol.* 8:728. doi: 10.3389/fneur.2017.00728

Zijdewind, I., Van Duinen, H., Zielman, R., and Monicque, M. L. (2006). Interaction between force production and cognitive performance in humans. *Clin. Neurophysiol.* 117, 660–667. doi: 10.1016/j.clinph.2005.11.016

Conflict of Interest Statement: The authors declare that the research was conducted in the absence of any commercial or financial relationships that could be construed as a potential conflict of interest.

frontiers in Human Neuroscience

ORIGINAL RESEARCH
published: 18 June 2019
doi: 10.3389/fnhum.2019.00194

Interpreting Prefrontal Recruitment During Walking After Stroke: Influence of Individual Differences in Mobility and Cognitive Function

*Sudeshna A. Chatterjee[1,2], Emily J. Fox[2,3], Janis J. Daly[1,4], Dorian K. Rose[1,2], Samuel S. Wu[5], Evangelos A. Christou[6], Kelly A. Hawkins[2], Dana M. Otzel[1,7], Katie A. Butera[1,2], Jared W. Skinner[8] and David J. Clark[1,7]**

[1]Brain Rehabilitation Research Center (BRRC), Malcom Randall VA Medical Center, Gainesville, FL, United States, [2]Department of Physical Therapy, University of Florida, Gainesville, FL, United States, [3]Brooks Rehabilitation, Jacksonville, FL, United States, [4]Department of Neurology, University of Florida, Gainesville, FL, United States, [5]Department of Biostatistics, University of Florida, Gainesville, FL, United States, [6]Department of Applied Physiology and Kinesiology, University of Florida, Gainesville, FL, United States, [7]Department of Aging and Geriatric Research, University of Florida, Gainesville, FL, United States, [8]Geriatric Research, Education and Clinical Center, Malcom Randall VA Medical Center, Gainesville, FL, United States

OPEN ACCESS

Edited by:
Stephane Perrey,
Université de Montpellier, France

Reviewed by:
Valentina Quaresima,
University of L'Aquila, Italy
Atsuhiro Tsubaki,
Niigata University of Health and Welfare, Japan

***Correspondence:**
David J. Clark
davidclark@ufl.edu

Received: 13 March 2019
Accepted: 23 May 2019
Published: 18 June 2019

Citation:
Chatterjee SA, Fox EJ, Daly JJ, Rose DK, Wu SS, Christou EA, Hawkins KA, Otzel DM, Butera KA, Skinner JW and Clark DJ (2019) Interpreting Prefrontal Recruitment During Walking After Stroke: Influence of Individual Differences in Mobility and Cognitive Function. Front. Hum. Neurosci. 13:194. doi: 10.3389/fnhum.2019.00194

Background: Functional near-infrared spectroscopy (fNIRS) is a valuable neuroimaging approach for studying cortical contributions to walking function. Recruitment of prefrontal cortex during walking has been a particular area of focus in the literature. The present study investigated whether task-related change in prefrontal recruitment measured by fNIRS is affected by individual differences in people post-stroke. The primary hypotheses were that poor mobility function would contribute to prefrontal over-recruitment during typical walking, and that poor cognitive function would contribute to a ceiling in prefrontal recruitment during dual-task walking (i.e., walking with a cognitive task).

Methods: Thirty-three adults with chronic post-stroke hemiparesis performed three tasks: typical walking at preferred speed (*Walk*), serial-7 subtraction (*Serial7*), and walking combined with serial-7 subtraction (*Dual-Task*). Prefrontal recruitment was measured with fNIRS and quantified as the change in oxygenated hemoglobin concentration (ΔO_2Hb) between resting and active periods for each task. Spatiotemporal gait parameters were measured on an electronic walkway. Stepwise regression was used to assess how prefrontal recruitment was affected by individual differences including age, sex, stroke region, injured hemisphere, stroke chronicity, 10-meter walking speed, balance confidence measured by Activities-specific Balance Confidence (ABC) Scale, sensorimotor impairment measured by Fugl-Meyer Assessment, and cognitive function measured by Mini-Mental State Examination (MMSE).

Results: For *Walk*, poor balance confidence (ABC Scale score) significantly predicted greater prefrontal recruitment (ΔO_2Hb; $R^2 = 0.25$, $p = 0.003$). For *Dual-Task*, poor cognitive function (MMSE score) significantly predicted lower prefrontal recruitment (ΔO_2Hb; $R^2 = 0.25$, $p = 0.002$).

Conclusions: Poor mobility function predicted higher prefrontal recruitment during typical walking, consistent with compensatory over-recruitment. Poor cognitive function predicted lower prefrontal recruitment during dual-task walking, consistent with a recruitment ceiling effect. These findings indicate that interpretation of prefrontal recruitment should carefully consider the characteristics of the person and demands of the task.

Keywords: dual-task walking, near-infrared spectroscopy, prefrontal cortex, stroke, walking

INTRODUCTION

Functional near-infrared spectroscopy (fNIRS) has emerged as a valuable measure for assessing the cortical contributions to locomotor control in both healthy and neurologically impaired populations (Mihara et al., 2007; Holtzer et al., 2011; Clark et al., 2014; Lu et al., 2015; Al-Yahya et al., 2016; Maidan et al., 2016b; Chen et al., 2017; Mirelman et al., 2017; Hawkins et al., 2018; Herold et al., 2018; Mori et al., 2018). The prefrontal cortex is an important region that has been examined extensively with fNIRS during walking. Task-related recruitment of prefrontal cortex infers a demand for cognitive/executive control resources, which support attention, working memory, motor planning, and task switching (Yogev-Seligmann et al., 2008; Al-Yahya et al., 2009; Amboni et al., 2013). These cognitive domains play an important role during every day walking in the home and community, especially in challenging environments or under distracted conditions (Suzuki et al., 2004; Yogev-Seligmann et al., 2008; Caliandro et al., 2012; Amboni et al., 2013).

An important challenge for studies investigating brain activation during walking is that increased recruitment could be interpreted as either an appropriate or an atypical neural control strategy. Therefore, it is important to carefully consider the demands of the task(s) as well as the characteristics of the study participants when interpreting brain recruitment.

When Is Higher Prefrontal Recruitment Appropriate?

Greater brain recruitment is beneficial when it enables the individual to meet the demands of high complexity tasks (Cabeza, 2002; Cabeza et al., 2002, 2004; Reuter-Lorenz and Cappell, 2008). In this context, higher recruitment of prefrontal cortex conveys robust availability and utilization of executive resources. In contrast, deficient cognitive function can impose a lower "ceiling" of brain resource recruitment and thereby limit performance on tasks that require those resources (Reuter-Lorenz and Cappell, 2008). For instance, Cabeza et al. (2002) reported that compared to lower performing older adults, higher performing older adults exhibited greater prefrontal recruitment during cognitive tasks (recall and source memory of words) and better task performance. They posited that higher performing older adults were able to counter age-related decline in neural networks by recruiting bilateral neurocognitive networks. Likewise, Reuter-Lorenz et al. (2000) have also reported that older adults who exhibited greater prefrontal recruitment (i.e., bilateral recruitment) also exhibited faster performance on a verbal working memory task. In agreement, similar findings have also been reported in the context of walking. Compared to older adults, younger adults exhibit a more effective utilization of prefrontal resources (achieved by higher recruitment) and better task performance during dual-task walking (Holtzer et al., 2011). This finding may be consistent with reports of age-related atrophy in the sensorimotor and frontoparietal areas (Rosano et al., 2008) and associated decline in attention, psychomotor processing speed and problem solving, and increased fall risk during walking in the elderly population (Gauchard et al., 2006; Alexander and Hausdorff, 2008; Herman et al., 2010; Fasano et al., 2012; Liu et al., 2014). Furthermore, older adults who exhibit a greater increase in prefrontal recruitment during complex walking tasks demonstrate better task performance, including a smaller reduction in walking speed and lower step length variability relative to typical walking (Clark et al., 2014). Likewise, increased recruitment in the frontal cortex is associated with improved walking performance (i.e., reduced gait variability) in older adults following rhythmic auditory cueing during walking (Vitorio et al., 2018).

When Is Higher Prefrontal Recruitment Atypical?

It is important to consider that major contributors to neural control of walking reside at lower levels of the neuraxis. These include brainstem regions, spinal pattern generating circuits, and cerebellar circuits that use both descending and afferent (e.g., somatosensory) inputs to generate patterns of intermuscular and interlimb coordination (Nielsen, 2003; Grillner, 2011). These mechanisms promote automaticity of walking, such that demand for executive control resources is minimized (Clark, 2015). Any impairment that disrupts these circuits of automaticity may give rise to compensatory recruitment of prefrontal resources to augment control (Clark et al., 2014; Maidan et al., 2016b; Hawkins et al., 2018).

Compensatory prefrontal recruitment for control of walking might be further exacerbated by impairments within the brain. Prior investigations from the cognitive literature suggest that neural mechanisms contributing to brain over-recruitment include: (1) inefficient processing, such that greater amounts of brain recruitment are required to achieve a given level of task performance; (2) poor specificity of recruiting specialized networks, thereby leading to widespread recruitment; (3) reactive recruitment to poor task performance in an attempt to improve performance; and (4) compensatory recruitment that is elicited

proactively to support task performance when primary brain regions/network recruitment is deficient (Cabeza et al., 2004, 2002; Cabeza, 2002; Reuter-Lorenz and Cappell, 2008; Goh and Park, 2009). Regardless of the specific causes of prefrontal over-recruitment, this phenomenon encumbers resources and hastens reaching the recruitment ceiling, particularly under conditions of increased task complexity (Reuter-Lorenz and Cappell, 2008). Since walking is a complex task that utilizes cognitive resources, the aforementioned cognitive control scenarios of over-recruitment and ceiling effect might also influence walking function.

Prefrontal Recruitment During Walking in Adults Post-stroke

Stroke is a leading cause of long-term physical disability, with devastating consequences that often include loss of independence, restricted participation in life roles, and a decline in quality of life (Lord et al., 2004; D'Alisa et al., 2005; Rosen et al., 2005; Robinson et al., 2011; Schmid et al., 2012). Since the ability to walk safely in the community is critical for preservation of independence, social integration, and participation in life-roles, recovery of walking function is often the most emphasized rehabilitation goal after stroke (Bohannon et al., 1988; Lord et al., 2004; Pang et al., 2007). Stronger improvements in rehabilitation outcomes might be possible if mechanistic targets can be more accurately identified and understood. One such target is the high demand for executive/prefrontal control resources during walking in adults post-stroke (Hawkins et al., 2018).

The objective of this study was to investigate whether task-related changes in prefrontal recruitment measured by fNIRS are affected by individual differences in people post-stroke. The first hypothesis was that during typical walking, people with poor mobility/motor function would exhibit higher prefrontal recruitment, consistent with compensatory over-recruitment. The second hypothesis was that during dual-task walking (with an added cognitive task), people with poor cognitive function would exhibit a lack of task-appropriate prefrontal recruitment (i.e., ceiling effect) and worse dual-task performance. Exploratory analyses were also conducted to examine the extent to which task-related differences in prefrontal recruitment explained task performance.

MATERIALS AND METHODS

Participants

Thirty-three adults with chronic post-stroke hemiparesis and moderate to severe walking deficits were enrolled. The inclusion criteria for the study included age >21 years; at least 6 months post-stroke; medically stable; able to follow 3-stage commands; ability to walk without support from another person; 10-meter walking speed $\leq$0.8 m/s (Perry et al., 1995) and Fugl-Meyer lower extremity (FMA-LE) score <30 to ensure that the participants had substantial motor deficits (Fugl-Meyer et al., 1975). These clinical evaluations were conducted by a licensed physical therapist who also confirmed the presence of a hemiparetic walking deficit. Some participants used an ankle/foot orthosis and/or a cane if needed to safely complete the walking assessments (see **Table 1**). Stroke side and lesion location for each participant was determined from medical records, and the location was broadly categorized as: anterior cerebral artery (ACA) territory, middle cerebral artery (MCA) territory, basal ganglia (BG), and/or pons (see **Table 1**).

TABLE 1 | Mean demographic and clinical data.

Age (years)	59.6 ± 9.7
Gender (Male/Female)	22/11
Affected Hemisphere (Left/Right)	16/17
Chronicity (months)	19.2 ± 10.4
10MWT (m/s)	0.6 ± 0.2
Fugl-Meyer LE score (out of 34)	24.7 ± 4.4
DGI (out of 24)	13.6 ± 3.5
MMSE (out of 30)	26.6 ± 3.1
ABC Scale (%)	59.2 ± 19.6
Lesion Location (ACA/MCA/BG&IC/Pons)	4/10/14/5
Assistive Device (AD) only	2
Ankle-foot Orthosis (AFO) only	6
AD + AFO	4

Abbreviations: ABC, Activities-Specific Balance Confidence Scale; DGI, Dynamic Gait Index; Fugl-Meyer LE, Fugl-Meyer Lower Extremity Score; MMSE, Mini-Mental State Examination; 10MWT, 10-Meter Walk Test; ACA, Anterior Cerebral Artery Territory; MCA, Middle Cerebral Artery Territory; BG, Basal Ganglia; IC, Internal Capsule; AD, Assistive Device; AFO, Ankle-Foot Orthosis. The errors denote standard deviation.

Exclusion criteria included Mini-Mental State Examination (MMSE) score <21 to exclude individuals with moderate to severe cognitive impairments from the study (Folstein et al., 1975); uncontrolled hypertension; lower extremity pain that would interfere with walking; severe obesity (body mass index >40); cardiovascular disease such as congestive heart failure, significant valvular disease, history of cardiac arrest, presence of an implantable defibrillator, uncontrolled angina; history of myocardial infarction or heart surgery in the prior year; lung disease requiring use of corticosteroids or supplemental oxygen; renal disease requiring dialysis; significant visual and/or vestibular impairment impacting safe mobility; lower motor neuron injury; bone fracture or joint replacement in the prior 6 months; diagnosis of a terminal illness. The study procedures were approved by the local Institutional Review Board and all participants provided written informed consent at the time of enrollment.

Protocol and Equipment

All assessments were conducted at a research laboratory located in an outpatient hospital setting. Three tasks were assessed for this study: typical walking (*Walk*), serial-7 subtraction (*Serial7*), and combined typical walking plus serial-7 subtraction (*Dual-Task*). The *Serial7* task was performed in a seated position. This facilitated consistency across participants when assessing single task cognitive performance and related prefrontal activity, since even standing balance can be cognitively demanding for some people after stroke. For both *Walk* and *Dual-Task*, participants walked at their preferred self-selected speed for 2–3 consecutive laps on an 18-m oval-shaped walking path. An instrumented walkway (GAITRite, CIR Systems, PA, USA) was located on one side of the path to measure spatiotemporal gait data. For both *Serial7* and *Dual-Task*, participants were asked to continuously subtract by seven beginning from a

randomly assigned number between 91 and 99 (Hayman, 1942; Williams et al., 1996). If the participant reached zero a new number was immediately assigned. The order of tasks was randomized. Participants were not given any special instructions pertaining to prioritization during *Dual-Task*. A small number of participants had expressive aphasia with consequent difficulty verbalizing their responses. These individuals were instructed to perform the serial-7 subtraction task silently to minimize the confounding effect.

fNIRS (Niro 200NX, Hamamatsu Photonics, Japan) was used to measure prefrontal recruitment from the anterior prefrontal cortex (Brodmann Area 10) during all tasks. fNIRS estimates neuronal activity in underlying tissue by calculating hemodynamic changes due to neurovascular coupling (Leff et al., 2011; Perrey, 2014). A diode emitted infrared light at continuous wavelengths of 735 nm and 810 nm. Changes in prefrontal oxygenated (O_2Hb) and deoxygenated (HHb) hemoglobin concentration were estimated with the modified Beer-Lambert Law. Change in O_2Hb concentration was used as the primary outcome measure of prefrontal recruitment because this measure has been consistently reported to be sensitive to walking-related changes in cortical activity (Miyai et al., 2001; Harada et al., 2009; Maidan et al., 2015).

For each channel (left and right side), a rubber probe holder was used to set optode spacing at 3 cm and to block ambient light. The optodes were secured to the forehead over the left and right anterior prefrontal cortices by double-sided adhesive. The optodes were placed high on the forehead to avoid the temporalis muscle and sufficiently lateral from the midline to avoid the superior sagittal sinus (Al-Rawi and Kirkpatrick, 2006; Tisdall et al., 2009). We have successfully implemented this procedure in our prior published work (Clark et al., 2014; Hawkins et al., 2018). To further minimize movement artifact in the signal, optodes and wires were secured by a fabric headband and the wires were also secured to the upper back. Prior to beginning each walking task, participants rested quietly in a standing position for approximately 1 min to provide a baseline level of prefrontal activity. Participants were not told exactly when the walking task would begin to prevent an anticipatory increase in prefrontal recruitment.

Clinical Assessments

Preferred walking speed was measured with the 10-Meter Walk Test (10MWT). Cognitive function was measured with Mini-Mental State Examination (MMSE; Folstein et al., 1975). Balance confidence was measured by self-report with the Activities-specific Balance Confidence (ABC) Scale (Powell and Myers, 1995). Gait and balance function were measured with the Dynamic Gait Index (DGI; Jonsdottir and Cattaneo, 2007). Lower extremity sensorimotor impairment was measured with the lower extremity Fugl-Meyer Assessment (FMA-LE; Fugl-Meyer et al., 1975).

DATA ANALYSIS

Prefrontal O_2Hb data were analyzed with custom programs created with Matlab version R2015a (Mathworks, Natick, MA, USA). Data were sampled at 2 Hz and saved directly to a memory card in the data acquisition unit, and later downloaded to a computer for analysis. All data were inspected for signal artifact using procedures that were based on the recommendations of Cooper et al. (2012). Artifacts in the O_2Hb signal were defined as amplitude offset exceeding 1 μM within a 2-s period, and/or a 2-s sliding window standard deviation that exceeded 3 standard deviations of the original full signal. All automatically detected artifacts were visually confirmed by a trained team member. The occurrence of artifacts was relatively infrequent (less than one per trial, on average) and transient. Artifacts were removed and replaced with linear interpolation to the surrounding data points.

Resting baseline prefrontal activity was quantified during the final 10 s of the rest period that preceded each task. For the active period, prefrontal activity was measured over a 30-s period that began 7 s after task onset in order to allow for cerebral blood flow changes to stabilize. This is based on prior work on neurovascular coupling, and is consistent with the recommendations for fNIRS measurement of peak task-related hemodynamic response which occurs approximately 6 s after the onset of neuronal activity (Cui et al., 2010; Tong and Frederick, 2010; Vitorio et al., 2017; Herold et al., 2018). The primary fNIRS outcome measure was the change in oxygenated hemoglobin concentration (ΔO_2Hb) between the resting baseline period and active period within each task, calculated using the following equation: Prefrontal ΔO_2Hb = Active O_2Hb − Resting O_2Hb.

Similarly, the change in deoxygenated hemoglobin concentration (ΔHHb) between the resting baseline period and active period within each task was calculated using the following equation: Prefrontal ΔHHb = Active HHb − Resting HHb.

STATISTICAL ANALYSIS

Statistical analysis was conducted using JMP software (JMP® 11. SAS Institute Inc., Cary, NC, USA). For all analyses, statistical significance level was set at alpha < 0.05. Paired *t*-tests were conducted to compare the magnitude of left and right prefrontal ΔO_2Hb to examine whether the data were affected by the laterality of the cortical recording site. Pearson's correlation coefficient was used to examine the consistency of prefrontal ΔO_2Hb measured from the left and right prefrontal cortical recording sites.

Confirmation of Dual-Task Cost

Paired *t*-tests were conducted to compare walking speed, stride length, and step width between *Walk* and *Dual-Task*, and to also compare cognitive performance between *Serial7* and *Dual-Task*. A one-way repeated measures analysis of variance (ANOVA) model was used to compare prefrontal ΔO_2Hb across the three tasks. The assumption of sphericity for the ANOVA model was tested by Mauchly's test ($\chi^2_{(2)} = 1.96$, $p = 0.37$). Paired *t*-tests were conducted *post hoc* to compare prefrontal ΔO_2Hb between *Dual-Task* and *Walk*, and between *Dual-Task* and *Serial7*. Separate paired *t*-tests were conducted to compare prefrontal ΔHHb between *Dual-Task* and *Walk*, and between *Dual-Task* and *Serial7*.

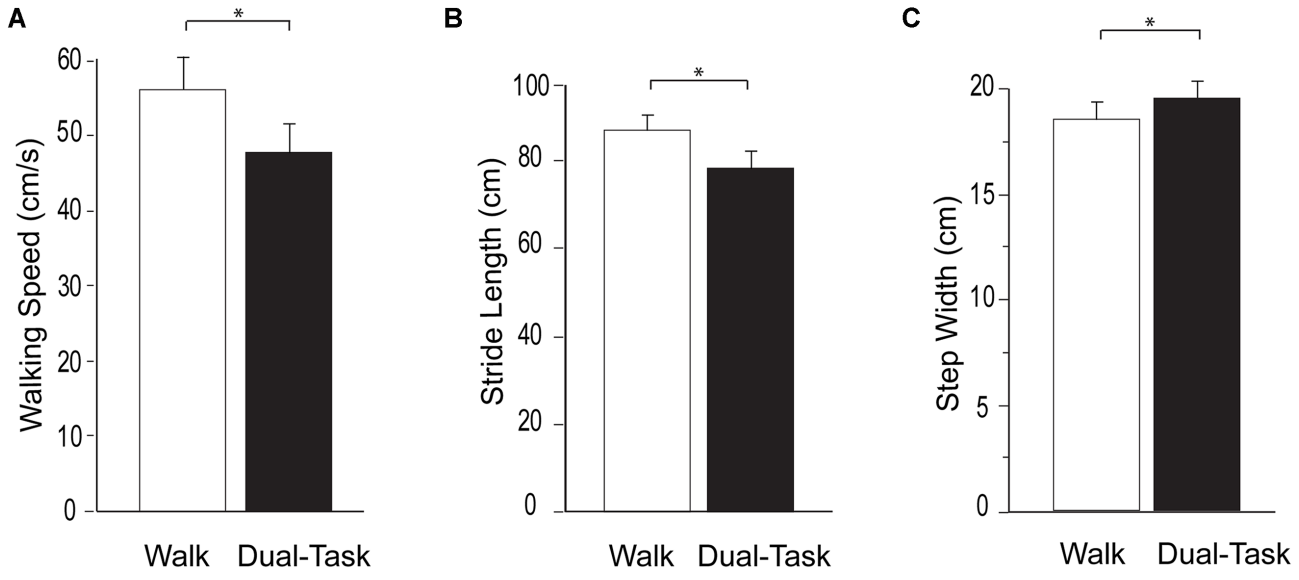

FIGURE 1 | Group average data for the measurements of walking performance during typical walking (Walk) shown in white and dual-task walking (Dual-Task) shown in black. From left to right the graphs show walking speed **(A)**, stride length **(B)**, and step width **(C)**. The error bars denote the standard error. *$p < 0.05$.

Predictors of Task-Related Prefrontal ΔO_2Hb and Task Performance

A stepwise mixed-model regression analysis was conducted to identify the variables that significantly predicted the magnitude of prefrontal ΔO_2Hb during each task. The variables entered in the model included age, sex, stroke region, injured hemisphere, stroke chronicity, and performance on clinical assessments including 10MWT, ABC Scale, DGI, FMA-LE, and MMSE. All assumptions for multiple regression models were met. For each task, the criteria for entering the predictor variable into the regression model was set at $p = 0.10$ and exiting the model was set at $p = 0.15$. Based on the identified predictor(s), subgroups were formed (lower and higher functioning) and *t*-test used to compare prefrontal ΔO_2Hb and task performance.

Association Between Prefrontal ΔO_2Hb and Task Performance

Pearson's correlation coefficient was used to explore the associations between dual-task cost of prefrontal recruitment denoted as ΔO_2Hb_{cost} (calculated as dual-task − single task) and dual-task cost of performance (calculated as dual-task − single task). Dual-task costs were calculated for both cognitive performance (serial-7 subtraction response rate) and walking performance (speed, stride length, and step width).

RESULTS

Group Characteristics and Confirmation of Dual-Task Cost

Demographic and clinical data for all participants are presented in **Table 1**.

Walking task performance is presented in **Figure 1**. Consistent with prior studies, a substantial dual-task cost was observed. Compared to *Walk, Dual-Task* walking speed was significantly slower ($p < 0.0001$), stride length was significantly shorter ($p < 0.0001$), and step width was significantly wider ($p < 0.001$). Likewise, compared to *Serial7*, cognitive performance deteriorated significantly during *Dual-Task* (0.13 ± 0.09 vs. 0.11 ± 0.08 responses/s; $p = 0.01$).

Consistent with prior reports, no effect of laterality on prefrontal ΔO_2Hb was observed for the single and dual-tasks (Mirelman et al., 2014; Nieuwhof et al., 2016). The group mean ΔO_2Hb was not significantly different between the left and right prefrontal cortex for *Serial7* ($p = 0.20$), *Walk* ($p = 0.56$), or *Dual-Task* ($p = 0.76$). Furthermore, ΔO_2Hb was strongly correlated for the left and right prefrontal cortex for *Serial7* ($r = 0.87$, $p < 0.0001$), *Walk* ($r = 0.79$, $p < 0.0001$), and *Dual-Task* ($r = 0.91$, $p < 0.0001$). Therefore, prefrontal ΔO_2Hb data from both hemispheres were averaged within each participant prior to all subsequent analyses. The magnitude of prefrontal ΔO_2Hb varied across tasks ($p < 0.01$; **Figure 2**). *Post hoc* analysis revealed that prefrontal ΔO_2Hb during *Dual-Task* was greater than *Walk* ($p = 0.001$; $d = 0.79$) and *Serial7* (trend with $p = 0.06$; $d = 0.44$). In agreement, prefrontal ΔHHb was more negative during *Dual-Task* than *Walk* ($p = 0.03$) and *Serial7* (trend with $p = 0.11$; **Figure 2**).

Predictors of Task-Related Prefrontal ΔO_2Hb and Task Performance

Examination of collinearity between the predictors revealed that DGI was significantly correlated with the 10MWT ($r = 0.64$, $p < 0.0001$), FMA-LE ($r = 0.45$, $p = 0.006$), and MMSE ($r = 0.46$, $p = 0.005$) scores. 10MWT was significantly correlated with ABC Scale ($r = 0.45$, $p = 0.006$), and FMA-LE ($r = 0.41$,

p = 0.01) scores. FMA-LE was significantly correlated with chronicity of stroke (r = 0.36, p = 0.04). DGI was excluded from the stepwise mixed-model regression analysis to ensure that collinearity between the predictor variables did not influence the study findings. The mean variance inflation factor (VIF) was 1.85 before and 1.41 after the removal of DGI which is well within the recommended limits (Hair et al., 1995; Kutner et al., 2005; Kennedy, 2008).

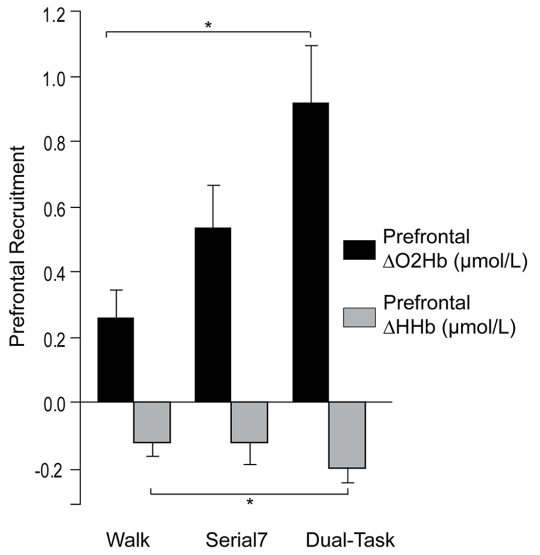

FIGURE 2 | Group average data for the change in prefrontal oxygenated (ΔO_2Hb) and deoxygenated (ΔHHb) hemoglobin concentration from resting period to the active period during single and dual-tasks. From left to right the graphs show ΔO_2Hb (in black) and ΔHHb (in light gray) during typical walking (Walk), serial-7 single task (Serial7), and dual-task walking (Dual-Task). The error bars denote the standard error. *$p < 0.05$.

Prefrontal ΔO_2Hb During *Walk*

For the stepwise regression model assessing predictors of prefrontal ΔO_2Hb during *Walk* (R^2 = 0.33; **Table 2**), lower self-reported balance confidence measured by the ABC Scale (p = 0.003) and lower FMA-LE score (trend with p = 0.09) were associated with greater prefrontal ΔO_2Hb. The bivariate correlation between balance confidence and prefrontal ΔO_2Hb was r = 0.48, p = 0.004 (**Figure 3A**). Based on this finding, further investigation was conducted by subdividing participants into Low and High Balance Confidence groups based on the median of the ABC Scale scores. Participants scoring ≤58.75% were placed in the Low Balance Confidence group. Demographic and clinical data for the balance confidence subgroups are presented in **Table 3**. ABC Scale scores were confirmed to be significantly lower in the Low Balance Confidence group (44.5% ± 13.3 vs. 75.0% ± 10.9, $p < 0.001$). The Low Balance Confidence group exhibited significantly higher prefrontal ΔO_2Hb (p = 0.002; **Figure 3B**), slower walking speed ($p < 0.001$), and shorter stride length (p = 0.008) during *Walk* (**Figure 3C**).

Prefrontal ΔO_2Hb During *Serial7* and *Dual-Task*

For the stepwise regression model assessing predictors of prefrontal ΔO_2Hb during *Serial7*, lower MMSE score was associated with greater prefrontal ΔO_2Hb (R^2 = 0.18, p = 0.02). For the stepwise regression model assessing predictors of ΔO_2Hb during the *Dual-Task* (R^2 = 0.36; **Table 2**), higher MMSE scores (p = 0.002) and lower FMA-LE scores (trend with p = 0.05) were associated with greater prefrontal ΔO_2Hb.

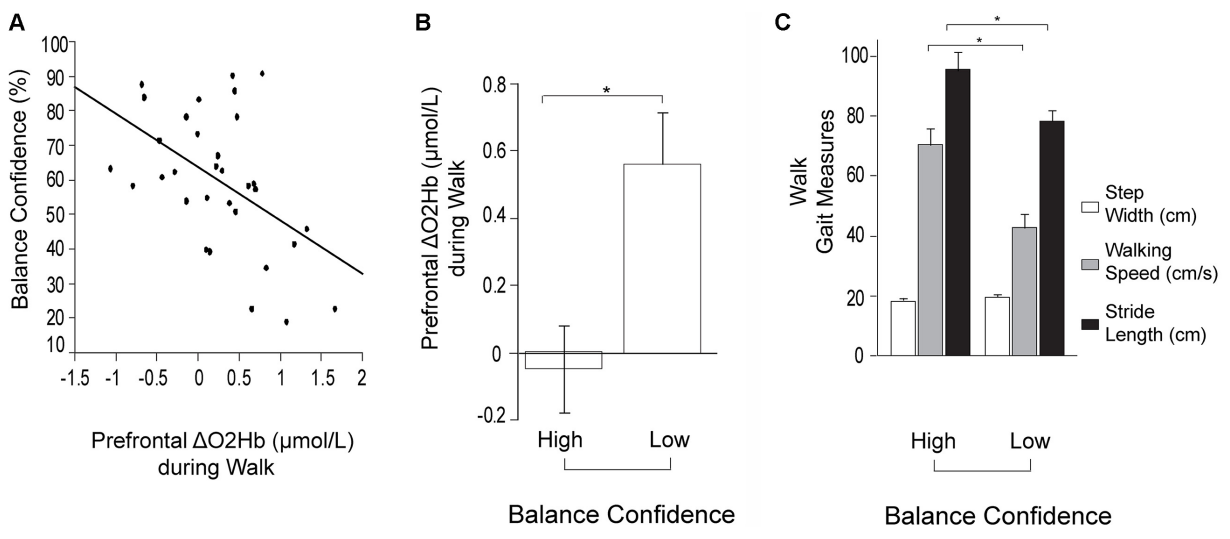

FIGURE 3 | Prefrontal oxygenated hemoglobin (ΔO_2Hb) concentration and the measurements of walking performance during typical walking (Walk). The error bars denote the standard error. *$p < 0.05$. **(A)** Association between prefrontal recruitment (ΔO_2Hb) during typical walking (Walk) and balance confidence (%) measured by the Activities-specific Balance Confidence (ABC) Scale. **(B)** Comparison of prefrontal recruitment (ΔO_2Hb) between the High (left) and Low (right) Balance Confidence groups during typical walking (Walk). **(C)** Comparison of walking performance between the High (left) and Low (right) Balance Confidence groups during typical walking (Walk). The graphs show step width in white, walking speed in light gray, and stride length in black.

TABLE 2 | Stepwise regression table showing the predictors of task-related prefrontal ΔO_2Hb.

Variables	Tasks								
	Walk			Serial7			Dual-Task		
	Estimate	R^2	*p*-value	Estimate	R^2	*p*-value	Estimate	R^2	*p*-value
Age	-	-	0.63	-	-	0.86	-	-	0.62
Sex	-	-	0.99	-	-	0.36	-	-	0.81
Stroke Region (BG-Pons and MCA and ACA)	-	-	0.30	-	-	0.14	-	-	0.59
Stroke Region (Pons-MCA and ACA)	-	-	0.68	-	-	0.87	-	-	0.59
Stroke Region (MCA)	-	-	0.92	-	-	0.59	-	-	0.89
Injured Hemisphere (Left/Right)	-	-	0.80	-	-	0.53	-	-	0.70
Chronicity	-	-	0.92	-	-	0.97	-	-	0.58
10-Meter Walking Speed	-	-	0.46	-	-	0.99	-	-	0.85
Balance Confidence (ABC Scale)	−0.016	0.25	**0.003***	-	-	0.31	-	-	0.26
Fugl-Meyer lower extremity score	−0.040	0.33	0.09	-	-	0.20	−0.069	0.36	0.05
Mini-Mental State Examination	-	-	0.62	−0.111	0.18	**0.02***	0.188	0.25	**0.002***

*Abbreviations: ABC, Activities-Specific Balance Confidence Scale; ACA, Anterior Cerebral Artery; BG, Basal Ganglia; MCA, Middle Cerebral Artery. Predictors of change in task-related prefrontal oxygenated hemoglobin (ΔO_2Hb) concentration based on the findings of the stepwise mixed-model regression analysis. *$p < 0.05$.*

TABLE 3 | Demographics and clinical assessments for balance confidence subgroups.

Clinical assessments	Balance confidence subgroups	
	Low (*n* = 17)	High (*n* = 16)
Age (years)	57.8 ± 10.6	61.6 ± 8.5
Chronicity (months)	19.6 ± 10.9	18.8 ± 10.1
*10MWT (m/s)	0.4 ± 0.2	0.7 ± 0.2
Fugl-Meyer LE score (out of 34)	23.9 ± 5.2	25.6 ± 3.1
DGI (out of 24)	12.9 ± 2.5	14.4 ± 4.3
MMSE (out of 30)	26.4 ± 3.2	26.8 ± 3.1
*ABC Scale (%)	44.4 ± 13.3	75.0 ± 10.8

*Abbreviations: ABC, Activities-Specific Balance Confidence Scale; DGI, Dynamic Gait Index; Fugl-Meyer LE, Fugl-Meyer Lower Extremity Score; MMSE, Mini-Mental State Examination; 10MWT, 10-Meter Walk Test. The errors denote standard deviation. *$p < 0.05$.*

TABLE 4 | Demographics and clinical assessments for cognitive function subgroups.

Clinical assessments	Cognitive function subgroups	
	Low (*n* = 19)	High (*n* = 14)
Age (years)	57.8 ± 8.8	62.1 ± 10.7
Chronicity (months)	20.0 ± 10.8	17.9 ± 10.0
10MWT (m/s)	0.5 ± 0.2	0.6 ± 0.2
Fugl-Meyer LE score (out of 34)	23.8 ± 4.2	25.9 ± 4.4
*DGI (out of 24)	12.4 ± 3.3	15.3 ± 3.2
*MMSE (out of 30)	24.7 ± 2.9	29.2 ± 0.8
ABC Scale (%)	59.5 ± 17.8	58.9 ± 22.4

*Abbreviations: ABC, Activities-Specific Balance Confidence Scale; DGI, Dynamic Gait Index; Fugl-Meyer LE, Fugl-Meyer Lower Extremity Score; MMSE, Mini-Mental State Examination; 10MWT, 10-Meter Walk Test. The errors denote standard deviation. *$p < 0.05$.*

Based on this finding, further investigation was conducted by subdividing participants into Low and High Cognitive Function groups based on the median of the MMSE scores. Participants scoring ≤27 were placed in the Low Cognitive Function group. Demographic and clinical data for the cognitive subgroups are presented in **Table 4**. MMSE scores were confirmed to be significantly lower in the Low Cognitive Function group (24.7 ± 3.0 vs. 29.2 ± 0.8, $p < 0.001$). Cognitive performance was also significantly worse in the Low Cognitive Function group compared to the High group for *Serial7* (0.08 ± 0.06 vs. 0.21 ± 0.09 responses/s, $p < 0.001$) and *Dual-Task* (0.07 ± 0.06 vs. 0.15 ± 0.09 responses/s, $p = 0.01$; **Figure 4B**). Similarly, walking performance during *Dual-Task* (**Figure 4C**) was worse in the Low Cognitive Function group, as exhibited by slower walking speed ($p = 0.03$), shorter stride length ($p = 0.02$), and a trend for wider step width ($p = 0.10$).

For *Dual-Task*, prefrontal ΔO_2Hb was significantly higher in the High Cognitive Function group compared to the Low Cognitive Function group ($p = 0.01$; **Figure 4A**). The High Cognitive Function group exhibited a task-appropriate increase in prefrontal recruitment during dual-tasking, as demonstrated by significantly higher prefrontal ΔO_2Hb during *Dual-Task* compared to both *Serial7* ($p = 0.006$) and *Walk* ($p = 0.0008$). In contrast, the Low Cognitive Function group exhibited similar prefrontal ΔO_2Hb during *Dual-Task* compared to *Serial7* ($p = 0.73$), and only a trend for higher prefrontal ΔO_2Hb during *Dual-Task* compared to *Walk* ($p = 0.10$).

Association Between Prefrontal ΔO_2Hb and Task Performance

Also examined was the extent to which dual-task costs of prefrontal recruitment were associated with dual-task costs of cognitive performance and walking performance. For cognitive performance (*Dual-Task—Serial7*), higher prefrontal ΔO_2Hb_{cost} was associated with worse serial-7 subtraction cost ($r = 0.43$, $p = 0.02$; **Figure 5**). For walking performance (*Dual-Task—Walk*), higher prefrontal ΔO_2Hb_{cost} showed a trend for an association with slowing of walking speed ($r = 0.28$, $p = 0.11$; **Figure 6A**), as well as with shorter stride length ($r = 0.33$, $p = 0.06$; **Figure 6B**).

DISCUSSION

The objective of this study was to investigate whether task-related changes in prefrontal cortical recruitment measured by fNIRS are affected by individual differences in people post-

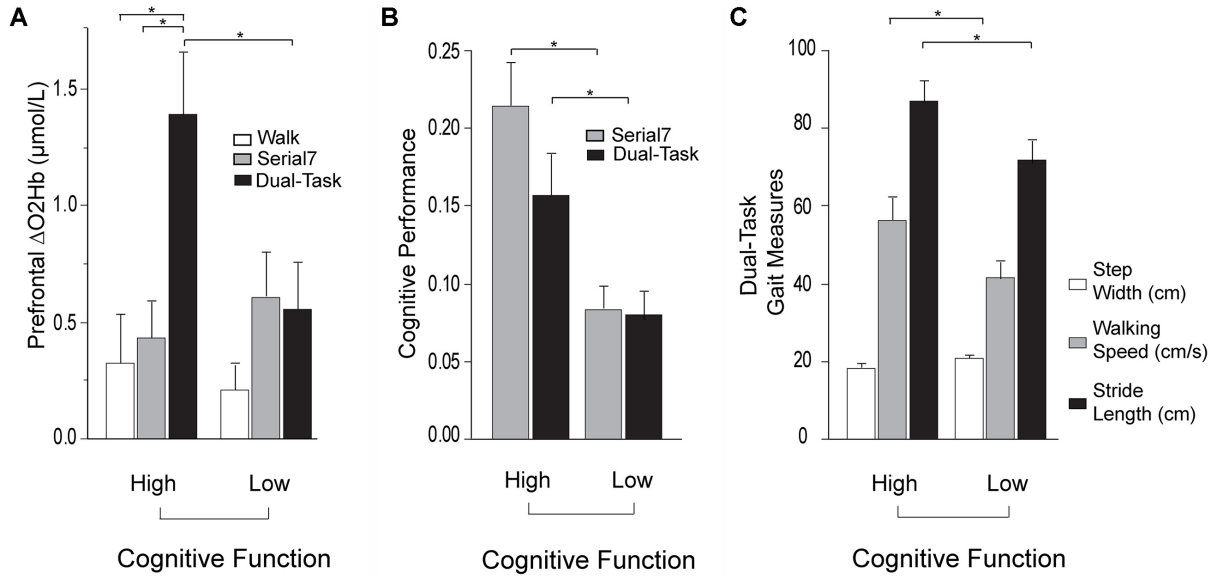

FIGURE 4 | Prefrontal oxygenated hemoglobin (ΔO_2Hb) concentration, cognitive performance, and the measurements of walking performance in High (left) and Low (right) Cognitive Function groups during single and dual-tasks. The error bars denote the standard error. $^*p < 0.05$. **(A)** Comparison of prefrontal recruitment (ΔO_2Hb) between the High (left) and Low (right) Cognitive Function groups during typical walking (Walk) in white, serial-7 single task (Serial7) in light gray, and dual-task walking (Dual-Task) in black. **(B)** Comparison of serial-7 response rate between the High (left) and Low (right) Cognitive Function groups for serial-7 single task (Serial7) in light gray and dual-task walking (Dual-Task) in black. **(C)** Comparison of walking performance between the High (left) and Low (right) Cognitive Function groups during dual-task walking (Dual-Task). The graphs show step width in white, walking speed in light gray, and stride length in black.

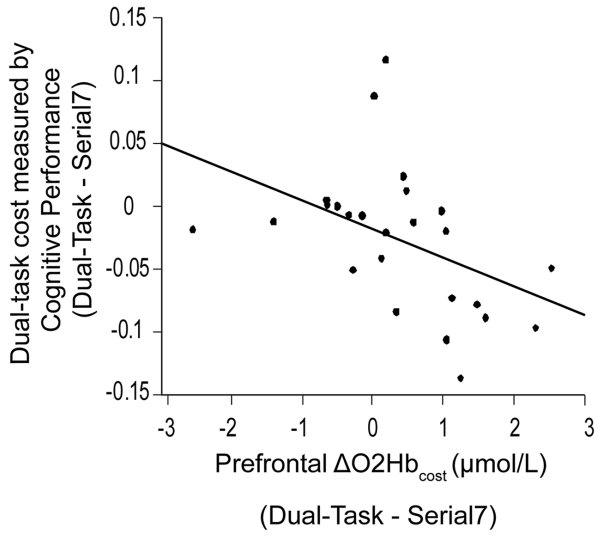

FIGURE 5 | Association between dual-task cost measured by cognitive performance, and the change in prefrontal oxygenated hemoglobin (ΔO_2Hb_{cost}) concentration from serial-7 single task (Serial7) to dual-task walking (Dual-Task). Higher task-based increase in prefrontal recruitment (dual-task minus single task) is associated with worse dual-task cost measured by cognitive performance (i.e., a greater drop in serial-7 response rate).

stroke. The primary hypotheses were that people with poor mobility function would exhibit higher prefrontal recruitment (i.e., compensatory over-recruitment) during typical walking, and people with poor cognitive function would exhibit lower prefrontal recruitment (i.e., recruitment ceiling effect) during dual-task walking.

Typical Walking (*Walk*): Prefrontal Recruitment and Task Performance

Based on the results from the stepwise regression model, greater prefrontal recruitment during *Walk* was strongly associated with lower self-reported balance confidence, as measured with the ABC Scale (**Table 2**). There is strong evidence from prior work that supports the important role of balance confidence (and related measures of mobility self-efficacy) as an independent predictor of walking-related activity and participation, even after accounting for deficits in physical function (Robinson et al., 2011; Danks et al., 2016). Paretic leg motor dysfunction (i.e., poorer FMA-LE scores) also showed a trend for predicting higher levels of prefrontal recruitment during *Walk*, as previously reported (Hawkins et al., 2018). One explanation for this finding is that individuals with more severe mobility/motor deficits after stroke exhibit compensatory recruitment of executive control resources to counter the loss of automatic/healthy control mechanisms. Indeed the "cautious" gait behaviors (slower walking speed and shorter stride length; **Figure 3C**) in the subgroup with lower balance confidence is consistent with a more cognitively demanding control strategy. These findings also build upon prior evidence from people post-stroke and other mobility compromised populations. For instance, prefrontal over-recruitment during walking has previously been reported in people post-stroke compared to

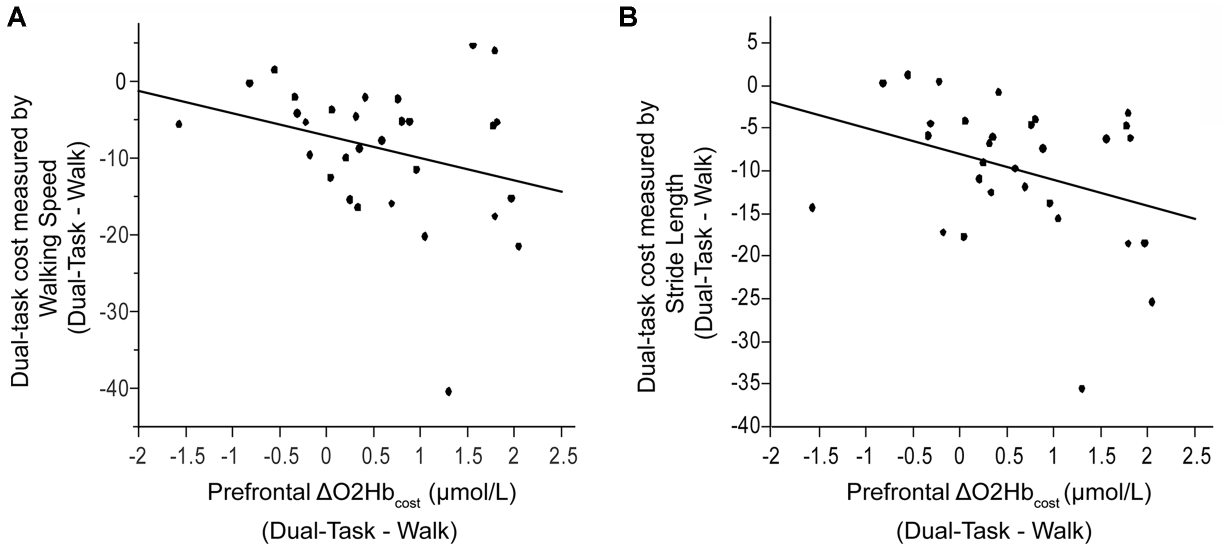

FIGURE 6 | Association between dual-task cost measured by walking speed (Panel **A**) and stride length (Panel **B**), and the change in prefrontal oxygenated hemoglobin (ΔO_2Hb_{cost}) concentration from typical walking (Walk) to dual-task walking (Dual-Task). Higher task-based increase in prefrontal recruitment (dual-task minus single task) is associated with worse dual-task cost measured by walking speed and stride length.

healthy adults without neurologic deficits (Mihara et al., 2007; Hawkins et al., 2018), as well as in other clinical populations including people with ataxia (Caliandro et al., 2012), Parkinson's disease (Maidan et al., 2016a,b), and Multiple Sclerosis (Hernandez et al., 2016).

Serial7 and *Dual-Task*: Prefrontal Recruitment and Task Performance

Prefrontal recruitment during *Dual-Task* was higher than either of the single tasks (i.e., *Walk* and *Serial7*), which is consistent with the greater cognitive demands of dual-tasking (**Figure 2**). For *Serial7*, higher MMSE score was found to be a predictor of lower prefrontal recruitment. This finding suggests that when people perform a relatively low-demand task (e.g., single task compared to a dual-tasking condition), those with better cognitive function exhibit more efficient prefrontal recruitment. That is, fewer resources are needed to accomplish the task. This is generally consistent with the aforementioned result from typical walking (people with better mobility function exhibited less prefrontal recruitment), although the mechanistic reasoning might differ as explained in the "*Introduction*" section.

For *Dual-Task*, better MMSE score and worse FMA-LE score were associated with greater prefrontal recruitment (**Table 2**). Notably, the direction of the MMSE association is reversed from what was observed in *Serial7*. As discussed above, neural efficiency (where less recruitment is "better") may have been the dominant factor driving the association in the relatively less demanding *Serial7* task. In contrast, the more demanding *Dual-Task* condition may cause some individuals to reach a ceiling of resource recruitment. In this case, higher recruitment can be considered "better" if due to greater availability of cognitive resource reserves. The recruitment ceiling might be the dominant factor driving the association for *Dual-Task*. To further investigate these data, participants were divided into two subgroups based on the median of MMSE scores. Within each subgroup, prefrontal recruitment was compared for the *Serial7* vs. *Dual-Task* condition. The Low Cognitive Function subgroup did not exhibit a significant change in prefrontal recruitment between the conditions (**Figure 4A**), which further suggests a ceiling effect such that both tasks were performed at or near the maximal prefrontal recruitment capability. This apparent ceiling effect might indicate that the Low Cognitive Function group did not have available resources to recruit for optimal performance of either *Serial7* or *Dual-Task*, which would help to explain the poor performance of this group on both tasks. In marked contrast, the High Cognitive Function group exhibited a substantial increase in prefrontal recruitment during *Dual-Task* relative to *Serial7*, which suggests that *Serial7* prefrontal recruitment was well below the recruitment ceiling (**Figure 4A**). This is consistent with more efficient brain processing and relative ease of performance during *Serial7* and is in agreement with the much better cognitive performance demonstrated by this group (**Figure 4B**). Cumulatively, these data are consistent with the hypothesis that during *Dual-Task*, people with poor cognitive function exhibit a lack of task-appropriate prefrontal recruitment that might be due to a recruitment ceiling effect.

It is unclear whether the greatly increased recruitment during *Dual-Task* compared to either of the single task conditions in the High Cognitive Function group is an indicator of good or poor neural control. As noted in prior studies, increased brain recruitment might support better performance, or a lack of performance ability might elicit increased brain recruitment as a compensation (Cabeza, 2002; Cabeza et al., 2002; Reuter-

Lorenz and Cappell, 2008; Schneider-Garces et al., 2010; Holtzer et al., 2011; Clark et al., 2014; Hawkins et al., 2018). For the single task conditions, better performance was accompanied by lower levels of prefrontal recruitment consistent with efficient processing and/or absence of compensatory recruitment. A large increase in brain recruitment for *Dual-Task* might reflect poor efficiency of neural circuits and/or difficulty performing the task, which leads to additional recruitment. Indeed, further analysis shows that individuals with a greater increase in prefrontal recruitment (for *Dual-Task* relative to *Serial7*) also exhibit a greater decrement in serial-7 response rate (i.e., greater dual-task cost; **Figure 5**). Likewise, a trend between higher prefrontal recruitment and greater dual-task cost during walking was observed. The increased prefrontal recruitment during dual-tasking in the High Cognitive Function group might instead reflect the positive use of available resources to support task performance. While the notion of a higher ceiling in this subgroup is certainly supported, there is a lack of support that this higher ceiling led to benefits in task performance. Within the High Cognitive Function group, serial-7 performance (**Figure 4B**) and walking speed (**Figure 4C**) dropped significantly from single to dual-task despite the large increase in prefrontal recruitment. While it is possible that the heightened prefrontal recruitment prevented an even more precipitous performance decline, this assertion cannot be fully tested with the present data. Furthermore, the Low Cognitive Function group had no drop in serial-7 performance from single to dual-task (**Figure 4B**). This was despite also lacking the potential compensatory benefit of additional prefrontal recruitment. However, it should be acknowledged that the Low Cognitive Function group already had extremely low response rates for *Serial7* (less than one correct response per 10 s; approximately 70% lower than the High Cognitive Function group). They also walked at a slower walking speed during *Walk*, which slowed even more for *Dual-Task*. Therefore, the performance of this group was already very poor and there was little room to drop further. Furthermore, the absolute task demand for this group was lower, given that walking speed, stride length, and rate of serial-7subtraction response were significantly lower. These factors would have made the task easier compared to if walking speed and rate of serial-7 computation rate was matched between the Low and High Cognitive Function subgroups. More detailed insights could be gained by standardizing dual-task difficulty such as by asking individuals to walk at a predetermined walking speed (e.g., controlled by a treadmill) and standardizing the rate of computational items (e.g., a fixed number of serial-7 subtractions per minute).

The findings of this study have important implications for real-world mobility function and participation. These findings build upon existing evidence showing that adults with neurologic impairments have a poorer capability for multitasking and appear to reach a ceiling in resource recruitment more easily than healthy adults (O'Shea et al., 2002). Consequently, individuals with neurologic impairments may experience a greater decline in performance when performing concurrent cognitive and motor tasks, such as more severe gait deficits and postural instability during walking (Morris et al., 1996; Hollman et al., 2006). This may increase the susceptibility to falls (Lundin-Olsson et al., 1997; Hyndman and Ashburn, 2004; Weerdesteyn et al., 2008; Nordin et al., 2010). Additionally, a broader implication of the reduced capacity to dual-task could be the inability to continue living independently (Oppewal and Hilgenkamp, 2017), and restricted participation in societal roles (Lord et al., 2004; D'Alisa et al., 2005; Rosen et al., 2005).

LIMITATIONS AND FUTURE DIRECTIONS

A methodological limitation of this study is that cortical activity was recorded from only a small region of cerebral cortex. Several other cerebral regions are also involved in the executive control of walking and should be examined by future studies (Hamacher et al., 2015; Metzger et al., 2017).

The findings of this study demonstrate that the interaction between task demands and individual characteristics play an important role in how prefrontal recruitment may be interpreted during walking tasks. This, in turn, can motivate the selection of intervention approaches to improve walking function. People with higher prefrontal recruitment during typical walking, interpreted as over-recruitment, may benefit from intervention approaches that aim to reduce the demand for executive control of walking. The present data suggests two potential targets; improving balance confidence and/or addressing impaired lower limb voluntary control. People with lower prefrontal recruitment during dual-task walking, interpreted as a recruitment ceiling, may benefit from intervention approaches that attempt to increase resource capacity. Possible approaches might include cognitive or dual-task training, perhaps with neuromodulatory adjuvants (e.g., pharmacological or non-invasive brain stimulation). Enhancing recovery of walking function by optimizing brain recruitment is an important area for future research investigations.

DATA AVAILABILITY

The datasets generated for this study are available on request to the corresponding author.

ETHICS STATEMENT

This study was carried out in accordance with the recommendations of the University of Florida Institutional Review Board with written informed consent from all subjects. All subjects gave written informed consent in accordance with the Declaration of Helsinki. The protocol was approved by the University of Florida Institutional Review Board and the North Florida/South Georgia Veterans Affairs Human Research Protection Program.

AUTHOR CONTRIBUTIONS

DC and EF designed the study. DC, SC, KH, DO and JS did the data collection. SC, DC, KH and JS did the data analysis. DC, EF,

SC, KH, DO, JS, JD, DR, SW, EC and KB contributed towards the interpretation and preparation of the manuscript.

FUNDING

This work was supported by Merit Review B1149R from the U.S. Department of Veterans Affairs Rehabilitation Research and Development (RR&D) Service (to DC); National Institutes of Health T-32 Neuromuscular Plasticity Training Pre-Doctoral Fellowship (NIH T32 HD 043730; to KB and KH); and the Foundation for Physical Therapy's Promotion of Doctoral Studies (PODS) program (KH and KB).

ACKNOWLEDGMENTS

Resources for this study were provided by the North Florida/South Georgia Veterans Health System, the VA Brain Rehabilitation Research Center, and Brooks Rehabilitation Clinical Research Center. The contents of this article do not represent the views of the U.S. Department of Veterans Affairs or the United States Government.

REFERENCES

Alexander, N. B., and Hausdorff, J. M. (2008). Guest editorial: linking thinking, walking, and falling. *J. Gerontol. A Biol. Sci. Med. Sci.* 63, 1325–1328. doi: 10.1093/gerona/63.12.1325

Al-Rawi, P. G., and Kirkpatrick, P. J. (2006). Tissue oxygen index: thresholds for cerebral ischemia using near-infrared spectroscopy. *Stroke* 37, 2720–2725. doi: 10.1161/01.STR.0000244807.99073.ae

Al-Yahya, E., Dawes, H., Collett, J., Howells, K., Izadi, H., Wade, D. T., et al. (2009). Gait adaptations to simultaneous cognitive and mechanical constraints. *Exp. Brain Res.* 199, 39–48. doi: 10.1007/s00221-009-1968-1

Al-Yahya, E., Johansen-Berg, H., Kischka, U., Zarei, M., Cockburn, J., and Dawes, H. (2016). Prefrontal cortex activation while walking under dual-task conditions in stroke: a multimodal imaging study. *Neurorehabil. Neural Repair* 30, 591–599. doi: 10.1177/1545968315613864

Amboni, M., Barone, P., and Hausdorff, J. M. (2013). Cognitive contributions to gait and falls: evidence and implications. *Mov. Disord.* 28, 1520–1533. doi: 10.1002/mds.25674

Bohannon, R. W., Andrews, A. W., and Smith, M. B. (1988). Rehabilitation goals of patients with hemiplegia. *Int. J. Rehabil. Res.* 11, 181–184. doi: 10.1097/00004356-198806000-00012

Cabeza, R. (2002). Hemispheric asymmetry reduction in older adults: the HAROLD model. *Psychol. Aging* 17, 85–100. doi: 10.1037/0882-7974.17.1.85

Cabeza, R., Anderson, N. D., Locantore, J. K., and McIntosh, A. R. (2002). Aging gracefully: compensatory brain activity in high-performing older adults. *Neuroimage* 17, 1394–1402. doi: 10.1006/nimg.2002.1280

Cabeza, R., Daselaar, S. M., Dolcos, F., Prince, S. E., Budde, M., and Nyberg, L. (2004). Task-independent and task-specific age effects on brain activity during working memory, visual attention and episodic retrieval. *Cereb. Cortex* 14, 364–375. doi: 10.1093/cercor/bhg133

Caliandro, P., Masciullo, M., Padua, L., Simbolotti, C., Di Sante, G., Russo, G., et al. (2012). Prefrontal cortex controls human balance during overground ataxic gait. *Restor. Neurol. Neurosci.* 30, 397–405. doi: 10.3233/RNN-2012-120239

Chen, M., Pillemer, S., England, S., Izzetoglu, M., Mahoney, J. R., and Holtzer, R. (2017). Neural correlates of obstacle negotiation in older adults: an fNIRS study. *Gait Posture* 58, 130–135. doi: 10.1016/j.gaitpost.2017.07.043

Clark, D. J. (2015). Automaticity of walking: functional significance, mechanisms, measurement and rehabilitation strategies. *Front. Hum. Neurosci.* 9:246. doi: 10.3389/fnhum.2015.00246

Clark, D. J., Rose, D. K., Ring, S. A., and Porges, E. C. (2014). Utilization of central nervous system resources for preparation and performance of complex walking tasks in older adults. *Front. Aging Neurosci.* 6:217. doi: 10.3389/fnagi.2014.00217

Cooper, R. J., Selb, J., Gagnon, L., Phillip, D., Schytz, H. W., Iversen, H. K., et al. (2012). A systematic comparison of motion artifact correction techniques for functional near-infrared spectroscopy. *Front. Neurosci.* 6:147. doi: 10.3389/fnins.2012.00147

Cui, X., Bray, S., and Reiss, A. L. (2010). Speeded near infrared spectroscopy (NIRS) response detection. *PLoS One* 5:e15474. doi: 10.1371/journal.pone.0015474

D'Alisa, S., Baudo, S., Mauro, A., and Miscio, G. (2005). How does stroke restrict participation in long-term post-stroke survivors? *Acta Neurol. Scand.* 112, 157–162. doi: 10.1111/j.1600-0404.2005.00466.x

Danks, K. A., Pohlig, R. T., Roos, M., Wright, T. R., and Reisman, D. S. (2016). Relationship between walking capacity, biopsychosocial factors, self-efficacy, and walking activity in persons poststroke. *J. Neurol. Phys. Ther.* 40, 232–238. doi: 10.1097/npt.0000000000000143

Fasano, A., Plotnik, M., Bove, F., and Berardelli, A. (2012). The neurobiology of falls. *Neurol. Sci.* 33, 1215–1223. doi: 10.1007/s10072-012-1126-6

Folstein, M. F., Folstein, S. E., and McHugh, P. R. (1975). "Mini-mental state". A practical method for grading the cognitive state of patients for the clinician. *J. Psychiatr. Res.* 12, 189–198. doi: 10.1016/0022-3956(75)90026-6

Fugl-Meyer, A. R., Jääskö, L., Leyman, I., Olsson, S., and Steglind, S. (1975). The post-stroke hemiplegic patient: 1. A method for evaluation of physical performance. *Scand. J. Rehabil. Med.* 7, 13–31.

Gauchard, G. C., Deviterne, D., Guillemin, F., Sanchez, J., Perrin, P. P., Mur, J.-M., et al. (2006). Prevalence of sensory and cognitive disabilities and falls and their relationships: a community-based study. *Neuroepidemiology* 26, 108–118. doi: 10.1159/000090445

Goh, J. O., and Park, D. C. (2009). Neuroplasticity and cognitive aging: the scaffolding theory of aging and cognition. *Restor. Neurol. Neurosci.* 27, 391–403. doi: 10.3233/RNN-2009-0493

Grillner, S. (2011). "Control of locomotion in bipeds, tetrapods, and fish," in *Comprehensive Physiology*, ed. R. Terjung (Hoboken, NJ: John Wiley and Sons, Inc.), 1179–1236.

Hair, J. F., Anderson, R. E., Tatham, R. L., and Black, W. C. (1995). *Multivariate Data Analysis with Readings*. Englewood Cliffs, NJ: Prentice Hall. Available online at: https://dl.acm.org/citation.cfm?id=207590. Accessed April 26, 2019.

Hamacher, D., Herold, F., Wiegel, P., Hamacher, D., and Schega, L. (2015). Brain activity during walking: a systematic review. *Neurosci. Biobehav. Rev.* 57, 310–327. doi: 10.1016/j.neubiorev.2015.08.002

Harada, T., Miyai, I., Suzuki, M., and Kubota, K. (2009). Gait capacity affects cortical activation patterns related to speed control in the elderly. *Exp. Brain Res.* 193, 445–454. doi: 10.1007/s00221-008-1643-y

Hawkins, K. A., Fox, E. J., Daly, J. J., Rose, D. K., Christou, E. A., McGuirk, T. E., et al. (2018). Prefrontal over-activation during walking in people with mobility deficits: interpretation and functional implications. *Hum. Mov. Sci.* 59, 46–55. doi: 10.1016/j.humov.2018.03.010

Hayman, M. (1942). Two minute clinical test for measurement of intellectual impairment in psychiatric disorders. *Arch. Neurol. Psychiatry* 47:454. doi: 10.1001/archneurpsyc.1942.02290030112010

Herman, T., Mirelman, A., Giladi, N., Schweiger, A., and Hausdorff, J. M. (2010). Executive control deficits as a prodrome to falls in healthy older adults: a prospective study linking thinking, walking and falling. *J. Gerontol. A Biol. Sci. Med. Sci.* 65, 1086–1092. doi: 10.1093/gerona/glq077

Hernandez, M. E., Holtzer, R., Chaparro, G., Jean, K., Balto, J. M., Sandroff, B. M., et al. (2016). Brain activation changes during locomotion in middle-aged to older adults with multiple sclerosis. *J. Neurol. Sci.* 370, 277–283. doi: 10.1016/j.jns.2016.10.002

Herold, F., Wiegel, P., Scholkmann, F., Müller, N., Herold, F., Wiegel, P., et al. (2018). Applications of functional near-infrared spectroscopy (fNIRS) neuroimaging in exercise-cognition science: a systematic, methodology-focused review. *J. Clin. Med.* 7:E466. doi: 10.3390/jcm7120466

Hollman, J. H., Kovash, F. M., Kubik, J. J., and Linbo, R. A. (2006). Age-related differences in spatiotemporal markers of gait stability during dual task walking. *J. Geriatr. Phys. Ther.* 29, 113–119. doi: 10.1016/j.gaitpost.2006.08.005

Holtzer, R., Mahoney, J. R., Izzetoglu, M., Izzetoglu, K., Onaral, B., and Verghese, J. (2011). fNIRS study of walking and walking while talking in young and old individuals. *J. Gerontol. A Biol. Sci. Med. Sci.* 66, 879–887. doi: 10.1093/gerona/glr068

Hyndman, D., and Ashburn, A. (2004). Stops walking when talking as a predictor of falls in people with stroke living in the community. *J. Neurol. Neurosurg. Psychiatry* 75, 994–997. doi: 10.1136/jnnp.2003.016014

Jonsdottir, J., and Cattaneo, D. (2007). Reliability and validity of the dynamic gait index in persons with chronic stroke. *Arch. Phys. Med. Rehabil.* 88, 1410–1415. doi: 10.1016/j.apmr.2007.08.109

Kennedy, P. (2008). *A Guide To Econometrics.* Malden, MA: Blackwell.

Kutner, M. H., Nachtsheim, C., Neter, J., and Li, W. (2005). *Applied Linear Statistical Models. 5th Edn.* Boston, MA: McGraw-Hill Irwin.

Leff, D. R., Orihuela-Espina, F., Elwell, C. E., Athanasiou, T., Delpy, D. T., Darzi, A. W., et al. (2011). Assessment of the cerebral cortex during motor task behaviours in adults: a systematic review of functional near infrared spectroscopy (fNIRS) studies. *Neuroimage* 54, 2922–2936. doi: 10.1016/j.neuroimage.2010.10.058

Liu, Y., Chan, J. S. Y., and Yan, J. H. (2014). Neuropsychological mechanisms of falls in older adults. *Front. Aging Neurosci.* 6:64. doi: 10.3389/fnagi.2014.00064

Lord, S. E., McPherson, K., McNaughton, H. K., Rochester, L., and Weatherall, M. (2004). Community ambulation after stroke: how important and obtainable is it and what measures appear predictive? *Arch. Phys. Med. Rehabil.* 85, 234–239. doi: 10.1016/j.apmr.2003.05.002

Lu, C.-F., Liu, Y.-C., Yang, Y.-R., Wu, Y.-T., and Wang, R.-Y. (2015). Maintaining gait performance by cortical activation during dual-task interference: a functional near-infrared spectroscopy study. *PLoS One* 10:e0129390. doi: 10.1371/journal.pone.0129390

Lundin-Olsson, L., Nyberg, L., and Gustafson, Y. (1997). "Stops walking when talking" as a predictor of falls in elderly people. *Lancet* 349:617. doi: 10.1016/S0140-6736(97)24009-2

Maidan, I., Bernad-Elazari, H., Gazit, E., Giladi, N., Hausdorff, J. M., and Mirelman, A. (2015). Changes in oxygenated hemoglobin link freezing of gait to frontal activation in patients with Parkinson disease: an fNIRS study of transient motor-cognitive failures. *J. Neurol.* 262, 899–908. doi: 10.1007/s00415-015-7650-6

Maidan, I., Nieuwhof, F., Bernad-Elazari, H., Reelick, M. F., Bloem, B. R., Giladi, N., et al. (2016a). The role of the frontal lobe in complex walking among patients with Parkinson's disease and healthy older adults. *Neurorehabil. Neural Repair* 30, 963–971. doi: 10.1177/1545968316650426

Maidan, I., Rosenberg-Katz, K., Jacob, Y., Giladi, N., Deutsch, J. E., Hausdorff, J. M., et al. (2016b). Altered brain activation in complex walking conditions in patients with Parkinson's disease. *Parkinsonism Relat. Disord.* 25, 91–96. doi: 10.1016/j.parkreldis.2016.01.025

Metzger, F. G., Ehlis, A. C., Haeussinger, F. B., Schneeweiss, P., Hudak, J., Fallgatter, A. J., et al. (2017). Functional brain imaging of walking while talking—an fNIRS study. *Neuroscience* 343, 85–93. doi: 10.1016/j.neuroscience.2016.11.032

Mihara, M., Miyai, I., Hatakenaka, M., Kubota, K., and Sakoda, S. (2007). Sustained prefrontal activation during ataxic gait: a compensatory mechanism for ataxic stroke? *Neuroimage* 37, 1338–1345. doi: 10.1016/j.neuroimage.2007.06.014

Mirelman, A., Maidan, I., Bernad-Elazari, H., Nieuwhof, F., Reelick, M., Giladi, N., et al. (2014). Increased frontal brain activation during walking while dual tasking: an fNIRS study in healthy young adults. *J. Neuroeng. Rehabil.* 11:85. doi: 10.1186/1743-0003-11-85

Mirelman, A., Maidan, I., Bernad-Elazari, H., Shustack, S., Giladi, N., and Hausdorff, J. M. (2017). Effects of aging on prefrontal brain activation during challenging walking conditions. *Brain Cogn.* 115, 41–46. doi: 10.1016/j.bandc.2017.04.002

Miyai, I., Tanabe, H. C., Sase, I., Eda, H., Oda, I., Konishi, I., et al. (2001). Cortical mapping of gait in humans: a near-infrared spectroscopic topography study. *Neuroimage* 14, 1186–1192. doi: 10.1006/nimg.2001.0905

Mori, T., Takeuchi, N., and Izumi, S. I. (2018). Prefrontal cortex activation during a dual task in patients with stroke. *Gait Posture* 59, 193–198. doi: 10.1016/j.gaitpost.2017.09.032

Morris, M. E., Iansek, R., Matyas, T. A., and Summers, J. J. (1996). Stride length regulation in Parkinson's disease. Normalization strategies and underlying mechanisms. *Brain* 119, 551–568. doi: 10.1093/brain/119.2.551

Nielsen, J. B. (2003). How we walk: central control of muscle activity during human walking. *Neuroscientist* 9, 195–204. doi: 10.1177/1073858403009003012

Nieuwhof, F., Reelick, M. F., Maidan, I., Mirelman, A., Hausdorff, J. M., Olde Rikkert, M. G. M., et al. (2016). Measuring prefrontal cortical activity during dual task walking in patients with Parkinson's disease: feasibility of using a new portable fNIRS device. *Pilot Feasibility Stud.* 2:59. doi: 10.1186/s40814-016-0099-2

Nordin, E., Moe-Nilssen, R., Ramnemark, A., and Lundin-Olsson, L. (2010). Changes in step-width during dual-task walking predicts falls. *Gait Posture* 32, 92–97. doi: 10.1016/j.gaitpost.2010.03.012

O'Shea, S., Morris, M. E., and Iansek, R. (2002). Dual task interference during gait in people with Parkinson disease: effects of motor versus cognitive secondary tasks. *Phys. Ther.* 82, 888–897. doi: 10.1093/ptj/82.9.888

Oppewal, A., and Hilgenkamp, T. I. M. (2017). The dual task effect on gait in adults with intellectual disabilities: is it predictive for falls? *Disabil. Rehabil.* 41, 26–32. doi: 10.1080/09638288.2017.1370730

Pang, M. Y., Eng, J. J., and Miller, W. C. (2007). Determinants of satisfaction with community reintegration in older adults with chronic stroke: role of balance self-efficacy. *Phys. Ther.* 87, 282–291. doi: 10.2522/ptj.20060142

Perrey, S. (2014). Possibilities for examining the neural control of gait in humans with fNIRS. *Front. Physiol.* 5:204. doi: 10.3389/fphys.2014.00204

Perry, J., Garrett, M., Gronley, J. K., and Mulroy, S. J. (1995). Classification of walking handicap in the stroke population. *Stroke* 26, 982–989. doi: 10.1161/01.str.26.6.982

Powell, L. E., and Myers, A. M. (1995). The activities-specific balance confidence (ABC) scale. *J. Gerontol. A Biol. Sci. Med. Sci.* 1, M28–M34. doi: 10.1093/gerona/50a.1.m28

Reuter-Lorenz, P. A., and Cappell, K. A. (2008). Neurocognitive aging and the compensation hypothesis. *Curr. Dir. Psychol. Sci.* 17, 177–182. doi: 10.1111/j.1467-8721.2008.00570.x

Reuter-Lorenz, P. A., Jonides, J., Smith, E. E., Hartley, A., Miller, A., Marshuetz, C., et al. (2000). Age differences in the frontal lateralization of verbal and spatial working memory revealed by PET. *J. Cogn. Neurosci.* 12, 174–187. doi: 10.1162/089892900561814

Robinson, C. A., Shumway-Cook, A., Ciol, M. A., and Kartin, D. (2011). Participation in community walking following stroke: subjective versus objective measures and the impact of personal factors. *Phys. Ther.* 91, 1865–1876. doi: 10.2522/ptj.20100216

Rosano, C., Aizenstein, H., Brach, J., Longenberger, A., Studenski, S., and Newman, A. B. (2008). Special article: gait measures indicate underlying focal gray matter atrophy in the brain of older adults. *J. Gerontol. A Biol. Sci. Med. Sci.* 63, 1380–1388. doi: 10.1093/gerona/63.12.1380

Rosen, E., Sunnerhagen, K. S., and Kreuter, M. (2005). Fear of falling, balance, and gait velocity in patients with stroke. *Physiother Theory Pract.* 21, 113–120. doi: 10.1080/09593980590922299

Schmid, A. A., Van Puymbroeck, M., Altenburger, P. A., Dierks, T. A., Miller, K. K., Damush, T. M., et al. (2012). Balance and balance self-efficacy are associated with activity and participation after stroke: a cross-sectional study in people with chronic stroke. *Arch. Phys. Med. Rehabil.* 93, 1101–1107. doi: 10.1016/j.apmr.2012.01.020

Schneider-Garces, N. J., Gordon, B. A., Brumback-Peltz, C. R., Shin, E., Lee, Y., Sutton, B. P., et al. (2010). Span, CRUNCH, and beyond: working memory capacity and the aging brain. *J. Cogn. Neurosci.* 22, 655–669. doi: 10.1162/jocn.2009.21230

Suzuki, M., Miyai, I., Ono, T., Oda, I., Konishi, I., Kochiyama, T., et al. (2004). Prefrontal and premotor cortices are involved in adapting walking and running speed on the treadmill: an optical imaging study. *Neuroimage* 23, 1020–1026. doi: 10.1016/j.neuroimage.2004.07.002

Tisdall, M. M., Taylor, C., Tachtsidis, I., Leung, T. S., Elwell, C. E., and Smith, M. (2009). The effect on cerebral tissue oxygenation index of changes

in the concentrations of inspired oxygen and end-tidal carbon-dioxide in healthy adult volunteers. *Anesth. Analg.* 109, 906–913. doi: 10.1213/ane.0b013e3181aedcdc

Tong, Y., and Frederick, B. D. (2010). Time lag dependent multimodal processing of concurrent fMRI and near-infrared spectroscopy (NIRS) data suggests a global circulatory origin for low-frequency oscillation signals in human brain. *Neuroimage* 53, 553–564. doi: 10.1016/j.neuroimage.2010.06.049

Vitorio, R., Stuart, S., Gobbi, L. T. B., Rochester, L., Alcock, L., and Pantall, A. (2018). Reduced gait variability and enhanced brain activity in older adults with auditory cues: a functional near-infrared spectroscopy study. *Neurorehabil. Neural Repair* 32, 976–987. doi: 10.1177/1545968318805159

Vitorio, R., Stuart, S., Rochester, L., Alcock, L., and Pantall, A. (2017). fNIRS response during walking—artefact or cortical activity? A systematic review. *Front. Neurosci.* 83, 160–172. doi: 10.1016/j.neubiorev.2017.10.002

Weerdesteyn, V., de Niet, M., van Duijnhoven, H. J., and Geurts, A. C. (2008). Falls in individuals with stroke. *J. Rehabil. Res. Dev.* 45, 1195–1213. doi: 10.1682/JRRD.2007.09.0145

Williams, M. A., LaMarche, J. A., Alexander, R. W., Stanford, L. D., Fielstein, E. M., and Boll, T. J. (1996). Serial 7s and Alphabet Backwards as brief measures of information processing speed. *Arch. Clin. Neuropsychol.* 11, 651–659. doi: 10.1016/s0887-6177(96)80002-3

Yogev-Seligmann, G., Hausdorff, J. M., and Giladi, N. (2008). The role of executive function and attention in gait. *Mov. Disord.* 23, 329–342. doi: 10.1002/mds.21720

Conflict of Interest Statement: The authors declare that the research was conducted in the absence of any commercial or financial relationships that could be construed as a potential conflict of interest.

frontiers in Human Neuroscience

REVIEW
published: 04 September 2019
doi: 10.3389/fnhum.2019.00306

G2019S Variation in LRRK2: An Ideal Model for the Study of Parkinson's Disease?

Chao Ren[1,2,3†], Yu Ding[3,4†], Shizhuang Wei[3†], Lina Guan[5], Caiyi Zhang[6], Yongqiang Ji[7], Fen Wang[3], Shaohua Yin[8*] and Peiyuan Yin[9*]*

[1] Department of Neurology, The Affiliated Yantai Yuhuangding Hospital of Qingdao University, Yantai, China, [2] Department of Neurology, The Second Affiliated Hospital of Soochow University, Suzhou, China, [3] Institute of Neuroscience, Soochow University, Suzhou, China, [4] Department of Orthopedic Surgery, The First Affiliated Hospital of Soochow University, Suzhou, China, [5] Department of Neurosurgical Intensive Care Unit, The Affiliated Yantai Yuhuangding Hospital of Qingdao University, Yantai, China, [6] Department of Emergency and Rescue Medicine, Xuzhou Medical University, Xuzhou, China, [7] Department of Nephrology, The Affiliated Yantai Yuhuangding Hospital of Qingdao University, Yantai, China, [8] Department of Nursing, The Affiliated Yantai Yuhuangding Hospital of Qingdao University, Yantai, China, [9] Department of Blood Supply, Yantai Center Blood Station, Yantai, China

OPEN ACCESS

Edited by:
Filippo Brighina, University of Palermo, Italy

Reviewed by:
Suzanne Lesage, Institut National de la Santé et de la Recherche Médicale (INSERM), France
Jan O. Aasly, Norwegian University of Science and Technology, Norway

***Correspondence:**
Fen Wang
wangfen_1982@126.com
Shaohua Yin
Yhdysh@126.com
Peiyuan Yin
yinpeiyuan2010@163.com

[†]*These authors are co-first authors*

Specialty section:
This article was submitted to Motor Neuroscience, a section of the journal Frontiers in Human Neuroscience

Received: *15 April 2019*
Accepted: *19 August 2019*
Published: *04 September 2019*

Citation:
Ren C, Ding Y, Wei S, Guan L, Zhang C, Ji Y, Wang F, Yin S and Yin P (2019) G2019S Variation in LRRK2: An Ideal Model for the Study of Parkinson's Disease? Front. Hum. Neurosci. 13:306. doi: 10.3389/fnhum.2019.00306

Parkinson's disease (PD) is the second most common neurodegenerative disorder and has plagued humans for more than 200 years. The etiology and detailed pathogenesis of PD is unclear, but is currently believed to be the result of the interaction between genetic and environmental factors. Studies have found that PD patients with the LRRK2:G2019S variation have the typical clinical manifestations of PD, which may be familial or sporadic, and have age-dependent pathogenic characteristics. Therefore, the LRRK2:G2019S variation may be an ideal model to study the interaction of multiple factors such as genetic, environmental and natural aging factors in PD in the future. This article reviewed the progress of LRRK2:G2019S studies in PD research in order to provide new research ideas and directions for the pathogenesis and treatment of PD.

Keywords: LRRK2, G2019S mutation, Parkinson's disease, disease model, pathogenesis

BACKGROUND

Parkinson's disease (PD) is the second most common neurodegenerative disorder after Alzheimer's disease, and has plagued humans for more than 200 years. According to statistics, the prevalence of PD is approximately 0.3% in developed countries and is 1% in individuals over 60 years old. The main pathological changes in PD are the formation of Lewy corpuscles and a decrease in dopaminergic neurons (DANs) in the substantia nigra-striatum system, which leads to a decrease in dopamine (DA) content in the related nerve endings and an imbalance between DA and acetylcholine. It is generally believed that when DANs in the substantia nigra are reduced by more than 50% and DA content is reduced by more than 70%, PD patients will exhibit typical motor symptoms such as movement retardation, static tremor, myotonia and abnormal posture and gait (Rogers et al., 2017). Of course, prior to that, other non-motor symptoms may also occur in some PD patients such as sensory disturbance and sleep disorders[1]. Clinically, PD can be divided into sporadic PD and familial PD. The etiology of sporadic PD is unclear. Familial PD may be caused by gene mutation. The age at onset, the rate of progression and the severity of PD vary, which

[1] www.nice.org.uk/guidance/ng71

may be the result of the interaction between genetic and environmental factors (Pan-Montojo and Reichmann, 2014). However, the true real etiology and full pathogenesis of PD are still unclear. At present, the incidence of PD increases with the aging of the population and an increased life span, and the prevalence of PD is also rising worldwide. Because of the large population in China, the increasing number of PD patients has resulted in heavy economic and psychological burdens to society and families. Although scientists continue to make efforts to study the diagnosis and treatment of PD, few novel and significant breakthroughs have been reported. Therefore, there is an urgent need for more in-depth innovative research on the pathogenesis of PD to obtain more effective and updated intervention and prevention methods.

With the identification and cloning of disease-related genes, such as the *leucine-rich repeat kinase 2* (LRRK2), α-*synuclein* (αSyn), SNCA, Parkin, PINK1, and GBA, the role of genetic factors in PD has attracted more attention (Lee and Liu, 2008). At present, of the 23 known pathogenic genes of PD, only LRRK2 is associated with both sporadic and familial PD. In addition, PD patients with the LRRK2 variation often present all the major clinical manifestations of typical non-carrier PD patients. Therefore, it is of great significance to carry out relevant research on PD patients with the LRRK2 variation (Di Maio et al., 2018). Among LRRK2 variations, G2019S mutation is the most common, as seen in familial and sporadic PD. In addition, the penetrance of LRRK2:G2019S mutation in PD is age-dependent, which suggests the important involvement of age and environmental factors (Goldwurm et al., 2007). This is consistent with the hypothesis that PD is attributed to the interaction of genetic, environmental, natural aging and other factors. Therefore, the LRRK2:G2019S mutation may be an ideal disease model and one potential breakthrough in PD research to determine the mechanisms of PD and to develop new treatment methods by studying PD patients with LRRK2:G2019S variation.

INTRODUCTION OF LRRK2

The coding gene of LRRK2 is located on chromosome 12q12, spans 7,584 bp, and contains 51 exons. The LRRK2 protein weighs 280 kD, has 2,527 amino acids, and consists of ankyrin-like repeats (ALRs), leucine-rich repeats (LRRs), the Ras of complex (Roc) GTPase domain, carboxy-terminal of Roc (COR), kinase domain, and the WD40 domain from the N-terminal to C-terminal (Mata et al., 2006). LRRK2 is expressed in brain tissues such as the brain stem (midbrain), striatum, olfactory bulb, cortex, hippocampus, and cerebellum. LRRK2 is mainly involved in the regulation of protein translation, axon growth and aging in the nervous system, and its mutation was discovered in 2004 (Zimprich et al., 2004). At present, the functions of the major domains of LRRK2 have not been fully defined. It is generally believed that the WD40 domain, LRR sequence and ALR sequence are involved in protein-protein interactions (**Figure 1**; Gloeckner et al., 2006; Ito et al., 2007). In addition, the WD40 domain may be involved in protein-lipid interactions, suggesting a possible interplay between LRRK2 and membrane structures. The tandem COR domain and Roc domain are unique to and prevalent in the ROCO superfamily of proteins. The interaction between COR and Roc domains facilitates the formation of dimers among ROCO proteins. Normally, LRRK2 proteins act as dimers, the formation of which is dependent on the COR domain. Sequence homology analysis and functional characterization demonstrated high sequence similarity between LRRK2 and mixed-lineage kinases (MLK). However, MLK possess serine/threonine and tyrosine kinase activity, while LRRK2 has no tyrosine kinase activity. MLK belongs to the mitogen-activated protein kinase (MAPK) family, exerting the function of a MAPK kinase kinase (MAPKKK). Despite the high similarity between LRRK2 and MLK, whether LRRK2 is also a MAPKKK and how its role as a MAPKKK is played are still unclear, as the activation pathway of LRRK2 and its downstream kinase effectors are currently unknown. Proteomics and random peptide analysis have suggested that LRRK2 is a serine/threonine protein kinase that preferentially phosphorylates threonine.

Relevant studies (Di Fonzo et al., 2005; Gilks et al., 2005; Mata et al., 2005; Nichols et al., 2005) have found that there are many mutation sites in the *LRRK2* gene, resulting in approximately 100 LRRK2 variants, many of which are related to PD, and the G2019S, R1441G, R1441C, R1441H, Y1699C, I2020T, and N1437H variants were confirmed to be pathogenic. Among these variants, for R1441G, R1441C, and R1441H the mutation is located within the Roc GTPase domain, while for Y1699C the mutation is within the COR domain, which also reduces the Roc GTPase activity. In addition, the newly discovered N1437H mutation within the Roc GTPase domain is also pathogenic. However, it is not clear which specific effects it has on GTPase activity. Finally, the remaining I2020T and G2019S mutations are located in the kinase domain, which increases the kinase activity of LRRK2. Recently, new mutations such as G2385R, A1441G and R1628P have also attracted considerable attention.

LRRK2:G2019S AND PD

Among the variations of LRRK2, G2019S is the most common. It not only comprises a high proportion (approximately 4–5%) in familial PD, but is also a common mutation (approximately 1%) in sporadic PD. Furthermore, it is markedly increased in specific populations and is up to 40% in North Africans and 30% in Ashkenazi Jews (Trinh et al., 2016). It is the first example of a Mendelian form of PD[2]. This variation originated from a G > A substitution at position 6055 of exon 41 of LRRK2 gene that results in the change of a glycine to serine at codon 2019 of LRRK2. It was previously believed that the LRRK2:G2019S variation mainly occurred in Caucasians and no correlation was found between G2019S and PD in Asians until one such case was reported in Japan (Pirkevi et al., 2009). Fundamental studies (Xiao et al., 2015, Karuppagounder et al., 2016; Howlett et al., 2017; Kim et al., 2017, 2018; Litteljohn et al., 2018; Vermilyea and Emborg, 2018) revealed that the LRRK2:G2019S variation can

[2]http://www.intechopen.com/books/etiology-and-pathophysiology-of-parkinson-s-disease/genetics-of-parkinsondisease

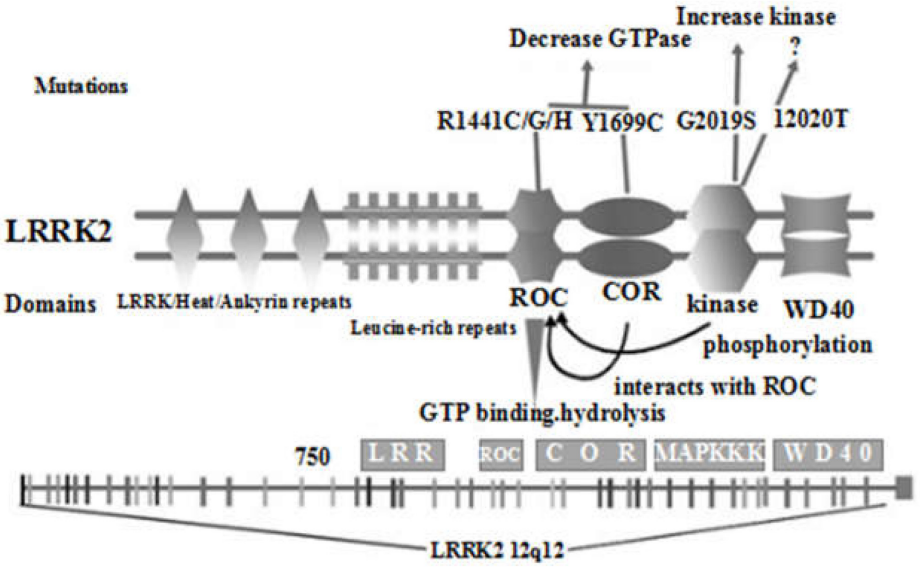

FIGURE 1 | Schematic diagram of the distribution of the main domains of LRRK2 protein and the location of current important mutations (Re-creation based on Cookson, 2010 and Mata et al., 2005).

lead to elevated levels of αSyn and tau proteins, mitochondrial dysfunction, synaptic vesicle transport disorder, and can induce abnormal Erk, c-Jun and Akt signaling pathways, leading to apoptotic regulation disorder and hyperautophagy, reduce neurite growth, increase abnormal growth and differentiation of DANs cells, and induce cellular degeneration. However, the specific structural and functional changes in DANs and their related influencing factors and mechanisms in LRRK2:G2019S-bearing PD patients are still unclear.

Similar to many other LRRK2-associated PD patients, PD patients with G2019S mutations have a heterogeneous pathology. However, the pathology has been reported in patients with a G2019S mutation, and it not only conforms to the typical α-synuclein Lewy-body type of PD, but also include diffuse Lewy-body disease, nigral degeneration without distinctive histopathology and, rarely, even aggregates of the microtubule-associated protein tau, suggestive of progressive supranuclear palsy or frontotemporal dementia. To date, it is still not fully understood how LRRK2 may affect the biology/pathobiology of α-Syn. One possibility is that the effect of LRRK2 on α-Syn may take place via the modulation of other key proteins, such as Rab GTPases or other kinases, which affect pathways involved in the degradation of α-Syn, and the propagation of pathology as well, resulting in PD-associated features, for example the appearance of typical α-synuclein Lewy-bodies (Outeiro et al., 2019). Accordingly, a question is raised: "Is LRRK2 detection in human biofluids a potential Parkinson's disease biomarker?" (Taymans et al., 2017). The answer is no. Although LRRK2 cannot be used as a biomarker for PD, West (2017) suggested that recommendations should be given for a biomarker-guided initial entry of LRRK2 kinase inhibitors in PD patients. Of course, this also includes those patients with a G2019S mutation. Interestingly, the total neopterin levels in the cerebrospinal fluid (CSF) of the LRRK2-PD patients may be one of the candidate biomarkers, which might be useful for understanding the pathophysiology of patients with a G2019S mutation (Ichinose et al., 2018).

Studies have found (Belarbi et al., 2010; Alcalay et al., 2013; Gatto et al., 2013; Sierra et al., 2017; Gunzler et al., 2018; Mestre et al., 2018) that the clinical features of PD patients with the LRRK2:G2019S variation included a high average age at onset, more female patients, long disease course, starting mainly in the lower limbs, abnormal posture and gait disorders, and more depression, hallucinations, sleep disorders and cognitive disorders. The remaining core clinical features of PD patients carrying the variation are similar to those of PD patients not carrying the variation. Moreover, the penetrance in LRRK2:G2019S carriers increases from only 28% at 59 years of age to 51% at 69 years, suggesting that it is age-dependent. It has been reported that dynamin 3 (DNM3) may be a potential genetic modifier in the relationship between LRRK2 and age-dependent penetrance in LRRK2-associated PD in Arab-Berber patients (Trinh et al., 2016). However, recent studies in Spain (Fernández-Santiago et al., 2018), Asia (Foo et al., 2019) and China (Yang et al., 2019) have not yielded similar results. An incidental finding showed that SNCA but not DNM3, modifies the age at onset of LRRK2-related PD, and the studies in Spain (Fernández-Santiago et al., 2018) and China (Yang et al., 2019) were noteworthy.

The information mentioned above is in accordance with the current hypothesis that PD is caused by the interaction of genetic factors, environmental factors and natural aging factors. Therefore, this will promote the future study of PD if a PD model with the LRRK2:G2019S variation can be established.

The development of induced pluripotent stem cells (iPSCs) and related techniques has provided new ideas for resolving the above issues (Park et al., 2008; Bumpei et al., 2016). iPSCs are generated by introducing pluripotency-related factors such as Oct4, Sox2, Klf, and c-Myc into mature somatic cells, so that they can be reprogrammed and restored to the cell state with embryonic stem cell characteristics. These cells can differentiate into cell types of multiple lineages (Chari and Mao, 2016).

With maturation of the iPSCs technology, the establishment of an iPSCs cell model from a LRRK2:G2019S PD patient was reported in 2011 (Nguyen et al., 2011), and related publications have gradually increased (Liu et al., 2012; Mak et al., 2012; Reinhardt et al., 2013; Schwab and Ebert, 2015). However, up to now, there has been no report on the iPSCs cell model derived from the LRRK2:G2019S mutant lineage with the same genetic background. Therefore, it will be of great significance to obtain the LRRK2:G2019S mutant lineage with the same genetic background and to use iPSCs and related technologies to study the pathogenesis of PD in patients with LRRK2:G2019S mutation. This can then be used to develop relevant prevention and treatment strategies, especially when there are PD patients and non-onset carriers present in the family.

CONCLUSION: QUESTIONS AND PROSPECTS

The onset of PD caused by the LRRK2:G2019S variation is the outcome of interactions between multiple genes and molecular mechanisms. On the one hand, this involves the intersection of familial and sporadic PD, and on the other hand the embodiment of PD gene-environment-aging factor interactions. Therefore, more attention should be paid to the study of LRRK2:G2019S variation. It has been suggested that individuals with a family history of PD caused by LRRK2:G2019S variation should be screened. Early dopamine transporter imaging with single photon emission computed tomography (DAT-SPECT) evaluation (Artzi et al., 2017) or measurement of Lamp2 concentration in the cerebrospinal fluid has been proposed (Klaver et al., 2018). However, further investigations are necessary to determine whether these procedures are applicable to areas with a low incidence and a low LRRK2:G2019S mutation rate, as a LRRK2:G2019S mutation carrier who was neurologically healthy at the age of 80 has been reported (Kay et al., 2005). Of course, the study of LRRK2:G2019S-related PD is not only about disease screening and diagnosis, but also about its clinical application in the future. It was found that the effect of deep brain stimulation (DBS) in patients with LRRK2 gene was better than that in non-mutation carriers (Sayad et al., 2016).

In addition, research on the genetic correction of LRRK2: G2019S has also been carried out (Sanders et al., 2014). At present, most of the targeted drugs are LRRK2 kinase inhibitors (Deng et al., 2011). Other drugs include coenzyme Q10, rapamycin and lovastatin (Cooper et al., 2012; Lin et al., 2016). Finally, we believe that the LRRK2:G2019S mutation will not only open a novel era in PD genetics, as proposed by Bonifati (2006), but will also bring about a new prospect, as the latest research showed that normal *LRRK2* gene also promotes PD (Di Maio et al., 2018).

AUTHOR CONTRIBUTIONS

CR, YD, and SW found references and drafted the manuscript. YD and SW readed literature. LG and CZ summarized information. YJ helped to draft the manuscript. FW, SY, and PY designed literature retrieval strategy. CR, FW, SW, and SY modified and revised the manuscript. YD and PY drew figure. CR obtained fundings. All authors read and approved the final manuscript.

FUNDING

This work was supported by Postgraduate Research & Practice Innovation Program of Jiangsu Province (KYCX19_1984).

ACKNOWLEDGMENTS

Thanks a lot to Professor Chun-feng Liu of Soochow University for his support and help in this article.

REFERENCES

Alcalay, R. N., Mirelman, A., Saunders-Pullman, R., Tang, M. X., Mejia Santana, H., Raymond, D., et al. (2013). Parkinson disease phenotype in ashkenazi jews with and without LRRK2 G2019S mutations. *Mov. Disord.* 28, 1966–1971. doi: 10.1002/mds.25647

Artzi, M., Evensapir, E., Lerman, S. H., Thaler, A., Urterger, A. O., Bressman, S., et al. (2017). DaT-SPECT assessment depicts dopamine depletion among asymptomatic G2019S LRRK2 mutation carriers. *PLoS One* 12:e0175424. doi: 10.1371/journal.pone.0175424

Belarbi, S., Hecham, N., Lesage, S., Kediha, M. I., Smail, N., Benhassine, T., et al. (2010). LRRK2 G2019S mutation in Parkinson's disease:a neuropsychological and neuropsychiatric study in a large algerian cohort. *Parkinsonism Relat. Disord.* 16, 676–679. doi: 10.1016/j.parkreldis.2010.09.003

Bonifati, V. (2006). Parkinson's disease: the LRRK2-G2019S mutation: opening a novel era in Parkinson's disease genetics. *Eur. J. Hum. Genet.* 14, 1061–1062. doi: 10.1038/sj.ejhg.5201695

Bumpei, S., Daisuke, D., Kaneyasu, N., Kikuchi, T., Watanabe, A., Sakamoto, Y., et al. (2016). Purification of functional human ES and iPSC-derived midbrain dopaminergic progenitors using LRTM1. *Nat. Commun.* 7:13097. doi: 10.1038/ncomms13097

Chari, S., and Mao, S. (2016). Timeline: IPSCS-the first decade. *Cell Stem Cell* 164:580. doi: 10.1016/j.cell.2016.01.023

Cookson, M. R. (2010). The role of leucine-rich repeat kinase 2 (*LRRK2*) in Parkinson's disease. *Nat. Rev. Neurosci.* 11, 791–797. doi: 10.1038/nrn2935

Cooper, O., Seo, H., Andrabi, S., Guardia-Laguarta, C., Graziotto, J., Sundberg, M., et al. (2012). Pharmacological rescue of mitochondrial deficits in IPSC-derived neural cells from patients with familial Parkinson's disease. *Sci. Transl. Med.* 4, 979–980. doi: 10.1126/scitranslmed.3003985

Deng, X., Dzamko, N., Prescott, A., Davies, P., Liu, Q., Yang, Q., et al. (2011). Characterization of a selective inhibitor of the Parkinson's disease kinase LRRK2. *Nat. Chem. Biol.* 7, 203–205. doi: 10.1038/nchembio.538

Di Fonzo, A., Rohe, C. F., Ferreira, J., Chien, H. F., Vacca, L., Stocchi, F., et al. (2005). A frequent LRRK2 gene mutation associated with autosomal dominant Parkinson's disease. *Lancet* 365, 412–415. doi: 10.1016/S0140-6736(05)17829-17825

Di Maio, R., Hoffman, E. K., Rocha, E. M., Keeney, M. T., Sanders, L. H., De Miranda, B. R., et al. (2018). LRRK2 activation in idiopathic Parkinson's disease. *Sci. Transl. Med.* 10:eaar5429. doi: 10.1126/scitranslmed.aar5429

Fernández-Santiago, R., Garrido, A., Infante, J., González-Aramburu, I., Sierra, M., Fernández, M., et al. (2018). α-synuclein (SNCA) but not dynamin 3 (DNM3) influences age at onset of leucine-rich repeat kinase 2 (LRRK2) Parkinson's disease in Spain. *Mov. Disord.* 33, 637–641. doi: 10.1002/mds.27295

Foo, J. N., Tan, L. C., Au, W. L., Prakash, K. M., Liu, J., and Tan, E. K. (2019). No association of DNM3 with age of onset in Asian Parkinson's disease. *Eur. J. Neurol.* 26, 827–829. doi: 10.1111/ene.13785

Gatto, E. M., Parisi, V., Converso, D. P., Poderoso, J. J., Carreras, M. C., Marti-Masso, J. F., et al. (2013). The LRRK2 G2019S mutation in a series of argentinean patients with Parkinson's disease clinical and demographic characteristics. *Neurosci. Lett.* 537, 1–5. doi: 10.1016/j.neulet.2013.01.011

Gilks, W. P., Abou-Sleiman, P. M., Gandhi, S., Jain, S., Singleton, A., Lees, A. J., et al. (2005). A common LRRK2 mutation in idiopathic Parkinson's disease. *Lancet* 365, 415–416. doi: 10.1016/S0140-6736(05)17830-17831

Gloeckner, C. J., Kinkl, N., Schumacher, A., Braun, R. J., O'Neill, E., Meitinger, T., et al. (2006). The Parkinson disease causing LRRK2 mutation I2020T is associated with increased kinase activity. *Hum. Mol. Genet.* 15, 223–232. doi: 10.1093/hmg/ddi439

Goldwurm, S., Zini, M., Mariani, L., Tesei, S., Miceli, R., Sironi, F., et al. (2007). Evaluation of LRRK2 G2019S penetrance: relevance for genetic counseling in Parkinson disease. *Neurology* 68, 1141–1143. doi: 10.1212/01.wnl.0000254483.19854.ef

Gunzler, S. A., Riley, D. E., Chen, S. G., Tatsuoka, C. M., Johnson, W. M., Mieyal, J. J., et al. (2018). Motor and non-motor features of Parkinson's disease in LRRK2 G2019S carriers versus matched controls. *J. Neurol. Sci.* 388, 203–207. doi: 10.1016/j.jns.2018.03.025

Howlett, E. H., Jensen, N., Belmonte, F., Zafar, F., Hu, X., Kluss, J., et al. (2017). LRRK2 G2019S-induced mitochondrial DNA damage is LRRK2 kinase dependent and inhibition restores mtDNA integrity in Parkinson's disease. *Hum. Mol. Genet.* 26, 4340–4351. doi: 10.1093/hmg/ddx320

Ichinose, H., Inoue, K. I., Arakawa, S., Watanabe, Y., Kurosaki, H., Koshiba, S., et al. (2018). Alterations in the reduced pteridine contents in the cerebrospinal fluids of LRRK2 mutation carriers and patients with Parkinson's disease. *J. Neural Transm.* 125, 45–52. doi: 10.1007/s00702-017-1784-x

Ito, G., Okai, T., Fujino, G., Takeda, K., Ichijo, H., Katada, T., et al. (2007). GTP binding is essential to the protein kinase activity of LRRK2, a causative gene product for familial Parkinson's disease. *Biochemistry* 46, 1380–1388. doi: 10.1021/bi061960m

Karuppagounder, S. S., Xiong, Y., Lee, Y., Lawless, M. C., Kim, D., Nordquist, E., et al. (2016). LRRK2 G2019S transgenic mice display increased susceptibility to 1-methyl-4-phenyl-1,2,3,6-tetrahydropyridine (MPTP)-mediated neurotoxicity. *J. Chem. Neuroanat.* 76, 90–97. doi: 10.1016/j.jchemneu.2016.01.007

Kay, D. M., Kramer, P., Higgins, D., Zabetian, C. P., and Payami, H. (2005). Escaping Parkinson's disease: a neurologically healthy octogenarian with the LRRK2 G2019S mutation. *Mov. Disord.* 20, 1077–1078. doi: 10.1002/mds.20618

Kim, J., Jeong, Y. H., Lee, E. J., Park, J. S., Seo, H., and Kim, H. S. (2017). Suppression of neuroinflammation by matrix metalloproteinase-8 inhibitor in aged normal and LRRK2 G2019S Parkinson's disease model mice challenged with lipopolysaccharide. *Biochem. Biophys. Res. Commun.* 493, 879–886. doi: 10.1016/j.bbrc.2017.09.129

Kim, K. S., Marcogliese, P. C., Yang, J., Callaghan, S. M., Resende, V., Abdel-Messih, E., et al. (2018). Regulation of myeloid cell phagocytosis by LRRK2 via WAVE2 complex stabilization is altered in Parkinson's disease. *PNAS.* 115, E5164–E5173. doi: 10.1073/pnas.1718946115

Klaver, A. C., Coffey, M. P., Aasly, J. O., and Loeffler, D. A. (2018). CSF lamp2 concentrations are decreased in female Parkinson's disease patients with LRRK2 mutations. *Brain Res.* 1683, 12–16. doi: 10.1016/j.brainres.2018.01.016

Lee, F. J., and Liu, F. (2008). Genetic factors involved in the pathogenesis of Parkinson's disease. *Brain Res. Rev.* 58, 354–364. doi: 10.1016/j.brainresrev.2008.02.001

Lin, C. H., Lin, H. I., Chen, M. L., Lai, T. T., Cao, L. P., Farrer, M. J., et al. (2016). Lovastatin protects neurite degeneration in LRRK2-G2019S parkinsonism through activating the Akt/Nrf pathway and inhibiting GSK3β activity. *Hum. Mol. Genet.* 25, 1965–1978. doi: 10.1093/hmg/ddw068

Litteljohn, D., Rudyk, C., Dwyer, Z., Farmer, K., Fortin, T., Hayley, S., et al. (2018). The impact of murine LRRK2 G2019S transgene overexpression on acute responses to inflammatory challenge. *Brain Behav. Immun.* 67, 246–256. doi: 10.1016/j.bbi.2017.09.002

Liu, G. H., Qu, J., Suzuki, K., Nivet, E., Li, M., Montserrat, N., et al. (2012). Progressive degeneration of human neural stem cells caused by pathogenic LRRK2. *Nature* 491, 603–607. doi: 10.1038/nature11557

Mak, S. K., Huang, Y. A., Iranmanesh, S., Vangipuram, M., Sundararajan, R., Nguyen, L., et al. (2012). Small molecules greatly improve conversion of human-induced pluripotent stem cells to the neuronal lineage. *Stem Cells Int.* 2012, 140427. doi: 10.1155/2012/140427

Mata, I. F., Kachergus, J. M., Taylor, J. P., Lincoln, S., Aasly, J., Lynch, T., et al. (2005). Lrrk2 pathogenic substitutions in Parkinson's disease. *Neurogenetics* 6, 171–177. doi: 10.1007/s10048-005-0005-1

Mata, I. F., Wedemeyer, W. J., Farrer, M. J., Taylor, J. P., and Gallo, K. A. (2006). LRRK2 in Parkinson's disease: protein domains and functional insights. *Trends Neurosci.* 29, 286–293. doi: 10.1016/j.tins.2006.03.006

Mestre, T. A., Pont-Sunyer, C., Kausar, F., Visanji, N. P., Ghate, T., Connolly, B. S., et al. (2018). Clustering of motor and nonmotor traits in leucine-rich repeat kinase 2 G2019S Parkinson's disease nonparkinsonian relatives: a multicenter family study. *Mov. Disord.* 33, 960–965. doi: 10.1002/mds.27272

Nguyen, H. N., Byers, B., Cord, B., Shcheglovitov, A., Byrne, J., Gujar, P., et al. (2011). LRRK2 mutant iPSC-Derived DA Neurons Demonstrate Increased Susceptibility to Oxidative Stress. *Cell Stem Cell* 8, 267–280. doi: 10.1016/j.stem.2011.01.013

Nichols, W. C., Pankratz, N., Hernandez, D., Paisan-Ruiz, C., Jain, S., Halter, C. A., et al. (2005). Genetic screening for a single common LRRK2 mutation in familial Parkinson's disease. *Lancet* 365, 410–412. doi: 10.1016/s0140-6736(05)17828-3

Outeiro, T. F., Harvey, K., Dominguez-Meijide, A., and Gerhardt, E. (2019). LRRK2, alpha-synuclein, and tau: partners in crime or unfortunate bystanders? *Biochem. Soc. Trans.* 47, 827–838. doi: 10.1042/BST20180466

Pan-Montojo, F., and Reichmann, H. (2014). Considerations on the role of environmental toxins in idiopathic Parkinson's disease pathophysiology. *Transl. Neurodegener.* 3, 1–13. doi: 10.1186/2047-9158-3-10

Park, I. H., Arora, N., Huo, H., Maherali, N., Ahfeldt, T., Shimamura, A., et al. (2008). Disease-specific induced pluripotent stem cells. *Cell* 134, 877–886. doi: 10.1016/j.cell.2008.07.041

Pirkevi, C., Lesage, S., Condroyer, C., Tomiyama, H., Hattori, N., Ertan, S., et al. (2009). A LRRK2 G2019S mutation carrier from Turkey shares the Japanese haplotype. *Neurogenetics* 10, 271–273. doi: 10.1007/s10048-009-0173-175

Reinhardt, P., Schmid, B., Burbulla, L., Schondorf, D. C., Wagner, L., Glatza, M., et al. (2013). Genetic correction of a LRRK2 mutation in human IPSCS links parkinsonian neurodegeneration to ERK-dependent changes in gene expression. *Cell Stem Cell* 12, 354–367. doi: 10.1016/j.stem.2013.01.008

Rogers, G., Davies, D., Pink, J., and Cooper, P. (2017). Parkinson's disease: summary of updated NICE guidance. *BMJ* 358:j1951. doi: 10.1136/bmj.l961

Sanders, L. H., Laganière, J., Cooper, O., Mak, S. K., Vu, B. J., Huang, Y. A., et al. (2014). LRRK2, mutations cause mitochondrial DNA damage in IPSC-derived neural cells from Parkinson's disease patients: reversal by gene correction. *Neurobiol. Dis.* 62, 381–386. doi: 10.1016/j.nbd.2013.10.013

Sayad, M., Zouambia, M., Chaouch, M., Ferrat, F., Nebbal, M., Bendini, M., et al. (2016). Greater improvement in LRRK2 G2019S patients undergoing subthalamic nucleus deep brain stimulation compared to non-mutation carriers. *BMC Neurosci.* 17:6. doi: 10.1186/s12868-016-0240-244

Schwab, A. J., and Ebert, A. D. (2015). Neurite aggregation and calcium dysfunction in IPSC-derived sensory neurons with Parkinson's Disease-RELATEDLRRK2G2019S mutation. *Stem Cell Rep.* 5, 1039–1052. doi: 10.1016/j.stemcr.2015.11.004

Sierra, M., Martínezrodríguez, I., Sánchezjuan, P., Gonzalez-Aramburu, I., Jimenez-Alonso, M., Sanchez-Rodriguez, A., et al. (2017). Prospective clinical

and DaT-SPECT imaging in premotor LRRK2 G2019S-associated Parkinson disease. *Neurology* 89, 439–444. doi: 10.1212/WNL.0000000000004185

Taymans, J. M., Mutez, E., Drouyer, M., Sibran, W., and Chartier-Harlin, M. C. (2017). LRRK2 detection in human biofluids: potential use as a Parkinson's disease biomarker? *Biochem. Soc. Trans.* 45, 207–212. doi: 10.1042/BST20160334

Trinh, J., Gustavsson, E. K., Vilarino-Guell, C., Bortnick, S., Latourelle, J., McKenzie, M. B., et al. (2016). DNM3 and genetic modifiers of age of onset in LRRK2 Gly2019Ser parkinsonism: a genome-wide linkage and association study. *Lancet Neurol.* 15, 1248–1256. doi: 10.1016/S1474-4422(16)30203-30204

Vermilyea, S. C., and Emborg, M. (2018). In vitro modeling of leucine-rich repeat kinase 2 (LRRK2) G2019S-mediated Parkinson's disease pathology. *Stem Cells Dev.* 23, 5499–5507. doi: 10.1089/scd.2017.0286

West, A. B. (2017). Achieving neuroprotection with LRRK2 kinase inhibitors in Parkinson disease. *Exp. Neurol.* 45, 207–212. doi: 10.1016/j.expneurol.2017.07.019

Xiao, Q., Yang, S., and Le, W. (2015). G2019S LRRK2 and aging confer susceptibility to proteasome inhibitor-induced neurotoxicity in nigrostriatal dopaminergic system. *J. Neural. Transm.* 122, 1645–1657. doi: 10.1007/s00702-015-1438-1439

Yang, Z. H., Li, Y. S., Shi, M. M., Yang, J., Liu, Y. T., Mao, C. Y., et al. (2019). SNCA but not DNM3 and GAK modifies age at onset of LRRK2-related Parkinson's disease in Chinese population. *J. Neurol.* 266, 1796–1800. doi: 10.1007/s00415-019-09336-9337

Zimprich, A., Biskup, S., Leitner, P., Lichtner, P., Farrer, M., Lincoln, S., et al. (2004). Mutations in LRRK2 cause autosomal-dominant parkinsonism with pleomorphic pathology. *Neuron* 44, 601–607. doi: 10.1016/j.neuron.2004.11.005

Conflict of Interest Statement: The authors declare that the research was conducted in the absence of any commercial or financial relationships that could be construed as a potential conflict of interest.

frontiers in Human Neuroscience

SYSTEMATIC REVIEW
published: 04 October 2019
doi: 10.3389/fnhum.2019.00328

The Effect of Cerebellar Transcranial Direct Current Stimulation on Motor Learning: A Systematic Review of Randomized Controlled Trials

Nitika Kumari, Denise Taylor and Nada Signal*

Health and Rehabilitation Research Institute, Auckland University of Technology, Auckland, New Zealand

Background: Cerebellar transcranial direct current stimulation (ctDCS) appears to modulate motor performance in both adaptation and motor skill tasks; however, whether the gains are long-lasting is unclear.

Objectives: This systematic review aims to evaluate the effect of ctDCS with respect to different time scales of motor learning.

Methods: Ten electronic databases (CINAHL, MEDLINE, SPORT Discus, Scopus, Web of Science, Cochrane via OVID, Evidence-Based Reviews (EBM) via OVID, AMED: Allied and Complementary Medicine, PsycINFO, and PEDro) were systematically searched. Studies evaluating the effect of ctDCS compared to sham ctDCS on motor learning in healthy individuals were selected and reviewed. Two authors independently reviewed the quality of the included studies using the revised Cochrane's risk-of-bias tool. The results were extracted with respect to the time scale in which changes in motor performance were evaluated.

Results: Seventeen randomized controlled trials met the eligibility criteria of which 65% of the studies had a "high" risk-of-bias, and 35% had "some concerns." These studies included data from 629 healthy participants. Of the studies that evaluated the effect of anodal ctDCS during and immediately after the stimulation, four found enhanced, three found impaired, and ten found no effect on gains in motor performance. Of the studies that evaluated the effect of anodal ctDCS after a break of 24 h or more, seven found enhanced, two found impaired, and one found no effect on gains in motor performance. Of the studies that evaluated the effect of cathodal ctDCS across a range of time scales, five found impaired, one found enhanced, and five found no effect on gains in motor performance.

Conclusions: In healthy individuals, anodal ctDCS appears to improve short to longer-term motor skill learning, whereas it appears to have no effect on gains in motor performance during and immediate after the stimulation. ctDCS may have potential to improve motor performance beyond the training period. The challenge of the motor task and its characteristics, and the stimulation parameters are likely to influence the effect of ctDCS on motor learning.

Keywords: transcranial direct current stimulation, tDCS, cerebellum, motor learning, motor adaptation, skill learning

OPEN ACCESS

Edited by:
Ferdinand Binkofski,
RWTH Aachen University, Germany

Reviewed by:
Wei-Peng Teo,
Nanyang Technological University, Singapore
Timmann Dagmar,
Essen University Hospital, Germany

****Correspondence:***
Nitika Kumari
nitika.kumari@aut.ac.nz

Specialty section:
This article was submitted to Motor Neuroscience, a section of the journal Frontiers in Human Neuroscience

Received: *19 June 2019*
Accepted: *06 September 2019*
Published: *04 October 2019*

Citation:
Kumari N, Taylor D and Signal N (2019) The Effect of Cerebellar Transcranial Direct Current Stimulation on Motor Learning: A Systematic Review of Randomized Controlled Trials. Front. Hum. Neurosci. 13:328. doi: 10.3389/fnhum.2019.00328

INTRODUCTION

Motor learning is the set of processes associated with practice or experience, which lead to a relatively permanent change in skilled motor performance (Schmidt and Lee, 2011). This is fundamental for acquiring new motor skills, responding to dynamic environmental conditions and for re-learning lost motor skills after injury (Kitago and Krakauer, 2013). Repeated training or practice is required to acquire complex motor skills and achieve peak performance. Therefore, strategies which maximize performance and enhance the acquisition of motor skills have received considerable attention in motor learning and rehabilitation literature (Winstein et al., 2014).

Recently, the modulation of cortical and sub-cortical excitability through external means such as non-invasive brain stimulation has received increasing attention as a means to enhance performance during training (Banissy and Muggleton, 2013; Okano et al., 2015; Edwards et al., 2017). One such application is transcranial direct current stimulation (tDCS). tDCS involves the delivery of continuous, weak electric currents to the brain to alter the resting membrane potentials of neurons to influence excitability (Bolognini et al., 2009). There is growing consumer interest in the ability of tDCS to modulate brain activity. Halo Sport (2019) and Caputron (2019) are two examples of commercially available tDCS devices being marketed to sporting populations. The manufacturers make reference to research evidence which illustrates the efficacy of tDCS to enhance motor performance (Waters-Metenier et al., 2014; Ciechanski et al., 2017), including in sporting populations (Huang et al., 2019). Much of the tDCS research has focused on the primary motor cortex and pre-motor areas (Ammann et al., 2016); however, researchers are increasingly considering the cerebellum as a target (Block H. J. and Celnik, 2012; Ferrucci et al., 2016, 2019; Grimaldi et al., 2016). The cerebellum contributes to the control of both motor and non-motor behaviors, including learning, posture and balance, coordination, cognition, emotion, and language (Timmann and Daum, 2007; Manto et al., 2012; Perciavalle et al., 2013; Koziol et al., 2014; Mariën et al., 2014; Caligiore et al., 2017; Lang et al., 2017). The cerebellum has a particular role in error-based learning (Miall and Wolpert, 1996; Diedrichsen et al., 2005; Tseng et al., 2007). In error-based learning, sensory prediction errors; the difference between predicted sensory consequences of a movement command, and the resultant sensory feedback, are used to adjust the subsequent motor output (Miall and Wolpert, 1996; Wolpert and Flanagan, 2001; Izawa and Shadmehr, 2011). Furthermore, evidence from neurophysiological, neuroimaging and behavioral studies in animals and humans suggest that cerebellar activation varies with the type of motor task performed and the stage of motor learning (Doyon and Benali, 2005; Dayan and Cohen, 2011; Lohse et al., 2014). Given the importance of the cerebellum in error-based motor learning (Ito, 2000; De Zeeuw and Ten Brinke, 2015) and re-learning of motor skills after central nervous system injury (Small et al., 2002; Ward et al., 2003; Sokolov et al., 2017), transcranial direct current stimulation over the cerebellum (ctDCS) has been advocated as an alternative tDCS stimulation site to promote motor learning (Grimaldi et al., 2014; Celnik, 2015; Oldrati and Schutter, 2018).

In a laboratory setting, motor learning is often evaluated using two paradigms: motor adaptation or skill learning. Motor adaptation consists of a perturbation applied during the performance of a well-learnt motor skill, for example, perturbing limb trajectories during reaching. The learner adapts to the error induced by the perturbation rapidly over minutes to hours (adaptation). When the perturbation is removed, the adaptation is retained for a period of time (after-effects) and gradually wanes over time (de-adaptation) (Martin et al., 1996). However, with repeated exposure to the perturbation, learning is observed through rapid reductions in errors (Martin et al., 1996) and faster rates of adaptation on subsequent exposures (Kojima et al., 2004). In motor skill learning paradigms, learning is evaluated through exposure to a novel motor task. Motor learning is observed through the reduction of errors and performance improvement beyond baseline levels (Reis et al., 2009).

Motor learning occurs over distinct phases. There is the early (fast) learning in which improvements in performance are seen rapidly within a single training session (Doyon and Benali, 2005). In the later slow stage, further performance gains are seen across several sessions of practice (Dayan and Cohen, 2011). Progression from fast to slow learning depends on appropriate rest periods and subsequent sleep (Diekelmann et al., 2009), where gains in performance can be observed without the additional practice of the task (Dayan and Cohen, 2011). Changes in performance are initially transient in nature, but with extended practice, the performance of skilled behavior becomes less attention-demanding and skilled performance is possible even after long breaks (Doyon and Benali, 2005). For the purposes of this paper, the time scales of learning are represented as (1) long-term changes in performance measured after a break of 24 h or more; (2) short-term change in performance after a break of $<$24 h; (3) change in performance measured immediately after training; and (4) change in performance during training.

There is ample evidence indicating that ctDCS can modulate cerebellar activity at a neurophysiological level (Galea et al., 2009), less is known about its effect on behavioral outcomes (Block H. and Celnik, 2012). To date, the evidence for the efficacy of ctDCS has been limited to its ability to modulate motor performance (Oldrati and Schutter, 2018). A recent meta-analysis reported the effectiveness of anodal and cathodal ctDCS in modulating motor performance in healthy individuals in both motor adaptation and motor skills tasks (Oldrati and Schutter, 2018), however, a systematic understanding of how ctDCS contributes to different timescales of motor learning is still lacking (Grimaldi et al., 2014; van Dun et al., 2016). Therefore, the present systematic review aims to elucidate the effects of ctDCS on motor learning across different time scales in healthy individuals to determine if the documented gains in performance persist for a substantial period after training. This understanding will be useful in ascertaining the prospects of using ctDCS as a neuro-modulatory tool to augment motor learning in both elite performance in healthy individuals and following brain lesions in clinical populations.

METHODS

Study Design

A systematic search and review of the literature were undertaken based on an *a priori* plan.

Inclusion and Exclusion Criteria

Studies were included if they met all the following criteria: involved healthy individuals above the age of 18 years, delivered real or sham tDCS over the cerebellum, random assignment to groups, measured behavioral outcomes of change in motor performance, and appeared in peer-reviewed English-language journals. Studies that compared different stimulation areas in the brain were included if data from cerebellar stimulation could be extracted and viewed separately.

Studies were excluded if they were reviews, books, theses, conference papers, commentaries, letters; if the sample consisted of animals; if the motor skill learning task did not involve the use of upper and lower limb; or if ctDCS was applied in combination with another intervention.

Information Sources

A search (July 2019) of the following databases was undertaken: CINAHL, MEDLINE, SPORT Discus, Scopus, Web of Science, Cochrane via OVID, Evidence-Based Reviews (EBM) via OVID, AMED: Allied and Complementary Medicine, PsycINFO, and PEDro. No limit was placed on the publication date. The search strategy (**Supplementary File 1**) included following key search terms: acquisition, motor performance, motor control, learning, adapt*, ctDCS, cerebellar stimulation, tDCS, transcranial direct current stimulation, non-invasive brain stimulation, noninvasive brain stimulation, direct current stimulation, cerebell*. The reference list of included studies, recent systematic reviews, and meta-analyses were also searched.

Study Selection

Following duplicate removal, the first author (N.K.) reviewed the titles and abstracts of all remaining studies. If a decision to include an article could not be made based on the title and abstract review, the full text was reviewed. A second reviewer (N.S.) was consulted if eligibility was unclear and a consensus reached.

Data Extraction

Data was extracted using a form developed from the Cochrane data extraction and assessment template (Higgins and Green, 2011). Extracted information included the study characteristics, ctDCS stimulation parameters, motor learning task description, outcome measures, and key findings.

Assessment of Study Quality

The quality of the included studies was critically appraised using the revised Cochrane's risk-of-bias tool for randomized trials (RoB 2) (Sterne et al., 2019). Two reviewers (N.K. and N.S.) independently rated the studies with any disagreements being discussed until consensus was reached. The revised Cochrane's risk-of-bias tool evaluates the methodological quality of the studies in relation to trial design, conduct, and reporting. Based on the answers to a series of signaling questions within five domains (randomization process, deviations from the intended interventions, missing outcome data, measurement of the outcome, and selection of the reported results), the studies were considered to have "low" or "high" risk-of-bias or "some concerns." For randomized crossover trials signaling questions on carryover effect were additionally assessed. The overall risk-of-bias judgment for each study was categorized according to the revised Cochrane's risk-of-bias guidelines (Sterne et al., 2019).

RESULTS

Search Results

The electronic search retrieved 633 studies, which was reduced to 281 following duplicate removal. Title and abstract review excluded 237 studies which did not meet the eligibility criteria. On full-text review, a further 31 studies were excluded for reasons outlined in **Figure 1**.

Seventeen RCTs met the criteria for inclusion in this systematic review. No additional studies met the inclusion criteria upon searching the reference list of the included studies. The included studies constituted a total of 629 participants with a mean age between 18 and 69 years. Only two studies had participants above the age of 40 years (Panouillères et al., 2015; Samaei et al., 2017). Random allocation of participants was in either a parallel ($n = 14$) (Jayaram et al., 2012; Dutta et al., 2014; Panouillères et al., 2015; Ehsani et al., 2016; Panico et al., 2016; Taubert et al., 2016; Yavari et al., 2016; Samaei et al., 2017; Liew et al., 2018; Poortvliet et al., 2018; Summers et al., 2018; Jackson et al., 2019; Jongkees et al., 2019; Mamlins et al., 2019) or crossover design ($n = 3$) (Shah et al., 2013; Fernandez et al., 2017; Foerster et al., 2017), with 349 participants receiving real ctDCS. Refer to **Table 1** (study characteristics).

One of the seventeen studies, six had "some concerns" (Shah et al., 2013; Ehsani et al., 2016; Fernandez et al., 2017; Samaei et al., 2017; Poortvliet et al., 2018; Jackson et al., 2019), and eleven had "high" risk-of-bias (Jayaram et al., 2012; Dutta et al., 2014; Panouillères et al., 2015; Panico et al., 2016; Taubert et al., 2016; Yavari et al., 2016; Foerster et al., 2017; Liew et al., 2018; Jongkees et al., 2019; Mamlins et al., 2019). Studies having "some concerns" were due to failure to explicitly report on the randomization process and trial registration or pre-specified statistical analysis plan. Studies having a "high" risk-of-bias was due to differences in baseline characteristics between the intervention groups suggesting issues with the randomization process, lack of information on blinding of the outcome assessor, the bias in the selection of reported results, and insufficient time for washout of carry-over effects. Refer to **Figure 2**, **Supplementary File 2**.

ctDCS Intervention

The type of ctDCS stimulation varied across the studies. Eight studies applied anodal ctDCS (Dutta et al., 2014; Panouillères et al., 2015; Ehsani et al., 2016; Samaei et al., 2017; Liew et al., 2018; Poortvliet et al., 2018; Summers et al., 2018; Jackson et al., 2019), two cathodal ctDCS (Panico et al., 2016; Fernandez et al., 2017), and the remaining seven applied both anodal and cathodal

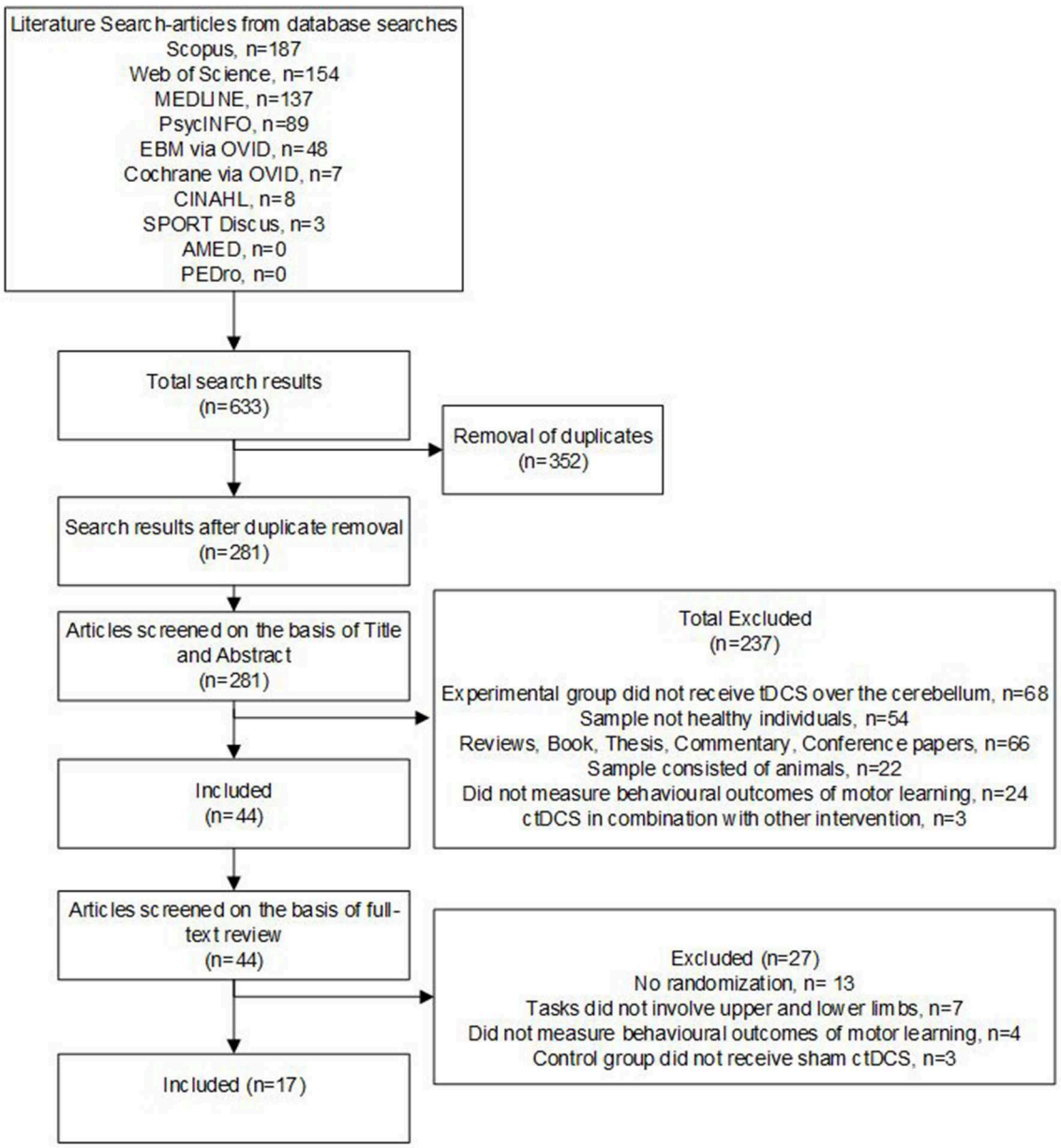

FIGURE 1 | Flow chart showing the study selection process and results.

stimulation (Jayaram et al., 2012; Shah et al., 2013; Taubert et al., 2016; Yavari et al., 2016; Foerster et al., 2017; Jongkees et al., 2019; Mamlins et al., 2019).

All studies investigated the effects of a single session of ctDCS. In the majority of studies ($n = 9$) stimulation was delivered *during* the training of a motor task (Jayaram et al., 2012; Shah et al., 2013; Dutta et al., 2014; Ehsani et al., 2016; Taubert et al., 2016; Yavari et al., 2016; Samaei et al., 2017; Summers et al., 2018; Jongkees et al., 2019). In three studies stimulation was delivered *prior* to the training of the task (Fernandez et al., 2017; Foerster et al., 2017; Poortvliet et al., 2018) and in the remaining five studies ctDCS was delivered just *prior to in conjunction with task training* (Panouillères et al., 2015; Panico et al., 2016; Liew et al., 2018; Jackson et al., 2019; Mamlins et al., 2019). The stimulation duration ranged between 8 and 30 min.

In tasks involving the upper limb, the stimulation was predominantly applied to the lateral cerebellum ($n = 11$) with respect to the training limb, ipsilaterally ($n = 10$) (Shah et al., 2013; Panouillères et al., 2015; Ehsani et al., 2016; Panico et al., 2016; Taubert et al., 2016; Yavari et al., 2016; Samaei et al., 2017; Liew et al., 2018; Jackson et al., 2019; Mamlins et al., 2019), or contralaterally ($n = 1$) (Dutta et al., 2014). Two studies applied the stimulation to the bilateral cerebellar hemispheres (Summers et al., 2018; Jongkees et al., 2019). Four studies investigated the

TABLE 1 | Characteristics of included studies.

References	Sample size; mean age (years) ± SD	ctDCS stimulation type	Task	Training sessions	Outcome measure	Results			
						≥24 h	<24 h	IA	D
Jayaram et al., 2012	40 (A = 8, C = 8, A = 8, C = 8, S = 8); 27, 20–33	A, C, and S	Adaptation: split-belt treadmill walking task	Single	Step length symmetry: rate, amount	NT	NT	A: X C: X	A: + C: –
Shah et al., 2013	8 (A = 8, C = 8, S = 8); 18–26	A, C, and S	Skill: ankle tracking task	Single for each condition	Normalized accuracy index	NT	A: + C: +	NT	NT
Dutta et al., 2014	8 (A = 4, S = 4); 24–36	A and S	Skill: myoelectric visual pursuit task	Single	Normalized response latency; tracking accuracy: mean absolute error	NT	NT	NT	–
Panouillères et al., 2015	53 (A = 26, S = 27); Old: 63.2 ± 7.5 Young: 22.5 ± 3.1	A and S	Adaptation: visuomotor rotation task	Single	Angular error	NT	X	NT	X
Yavari et al., 2016	29 (A = 10, C = 10, S = 9); 24 ± 5	A, C, and S	Adaptation: visuomotor adaptation task	Single	Reach angles; perception of hand position; mean reach direction	NT	NT	NT	A: + C: –
Ehsani et al., 2016	39 (A = 20, S=19); 22.77 ± 1.32	A and S	Skill: serial response time task	Single	Response time (RT); number of errors (ER)	RT: + ER: +	RT: X ER: +	NT	RT: X ER: +
Taubert et al., 2016	41 (A = 14, C = 12, S = 15); 27 ± 3	A, C, and S	Adaptation: force field adaptation task	Single	Reaching error; set-break forgetting	A: – C: X	NT	NT	A: – C: X
Panico et al., 2016	26 (C =13, S = 13); 21.57 ± 2.33	C and S	Adaptation: visuomotor rotation task	Single	Error; Error rate; Time course of stimulation effect on error	NT	NT	NT	–
Fernandez et al., 2017	14 (C = 14, S = 14); 28.93 ± 4.59	C and S	Adaptation: spatio-temporal gait task	Single for each condition	SD of stride length and step time	NT	NT	–	NT
Samaei et al., 2017	30 (A = 15, S = 15); 68.70 ± 5.28	A and S	Skill: serial reaction time task	Single	Response time (RT); number of errors (ER)	RT: + ER: X	RT: + ER: X	NT	RT: X ER: X
Foerster et al., 2017	15 (A = 15, C = 15, S = 15); 21–24	A, C, and S	Adaptation: balance Control	Single for each condition	Overall stability index (OSI)	NT	NT	A: X C: –	NT
Poortvliet et al., 2018	28 (A = 14, S = 14); 25.64 ± 3.82	A and S	Adaptation: postural adaptation	Single	Postural steadiness: center of pressure displacement; SD; total path length	NT	NT	+	NT

(Continued)

TABLE 1 | Continued

References		Sample size; mean age (years) ± SD	ctDCS stimulation type	Task	Training sessions	Outcome measure	Results			
							≥24 h	<24 h	IA	D
Summers et al., 2018		14 (A = 7, S = 7); 28.8 ± 10.5	A and S	Skill: finger tracking task	Single	Tracking accuracy index	NT	NT	X	X
Liew et al., 2018		31 (A:16, S: 15), NG	A and S	Adaptation: visuomotor adaptation task	Single	Hand endpoint angle: target error (E); reaction time (RcT)	NT	NT	E: X RcT: X	E: X, RT:X
		19 (A:10, S:9), NG	A and S	Adaptation: visuomotor adaptation task	Single	Hand endpoint angle: target error	NT	NT	X	X
Jongkees et al., 2019		72 (A = 24, C = 24, S = 24); A: 19.8 ± 1.6, C: 19.5 ± 1.5, S: 19.3 ± 1.8	A, C, and S	Skill: serial reaction time task	Single	Percentage accuracy (ACC); reaction time (RcT)	A: ACC-X, RT- –; C: ACC-X, RT: X	NT	NT	A: ACC-X, RT- –; C: ACC-X, RT: X
Jackson et al., 2019		42 (A = 21, S = 21); 25 ± 3.9	A and S	Skill: overhand throwing task	Single	Endpoint error: total (T); online (On) and offline (Of) learning	T: +, Of: X	On: +	NT	NT
Mamlins et al., 2019	I	30 (A = 10, C = 10, S = 10); 24.1 ± 2.3	A, C, and S	Adaptation: force field adaptation task	Single	Maximum error (extent and rate of learning);	NT	NT	A:X, C:X	A:X, C:X
		30 (A = 10, C = 10, S = 10); 24.1 ± 2.3				Perpendicular velocity			A:X, C:X	A:X, C:X
	II	30 (A = 10, C = 10, S = 10); 22.3 ± 3.1	A, C and S	Adaptation: visuomotor adaptation task	Single	Angular end point error (extent and rate of learning)	NT	NT	A:X, C:X	A:X, C:X
		30 (A = 10, C = 10, S = 10); 22.3 ± 3.1							A:X, C:X	A:X, C:X
Summary total		*n* = 629	A = 15 C= 9	Adaptation =10 Skill = 7			A=5 C=2	A = 5 C = 1	A = 6 C = 3	A = 11 C = 5

I, experiment 1; II, experiment 2; IA, immediately after; D, during the intervention; A, anodal ctDCS; C, cathodal ctDCS; S, sham ctDCS; NT, not tested; +, enhanced; –, impaired; X, no effect; SD, standard deviation; NG, not given.

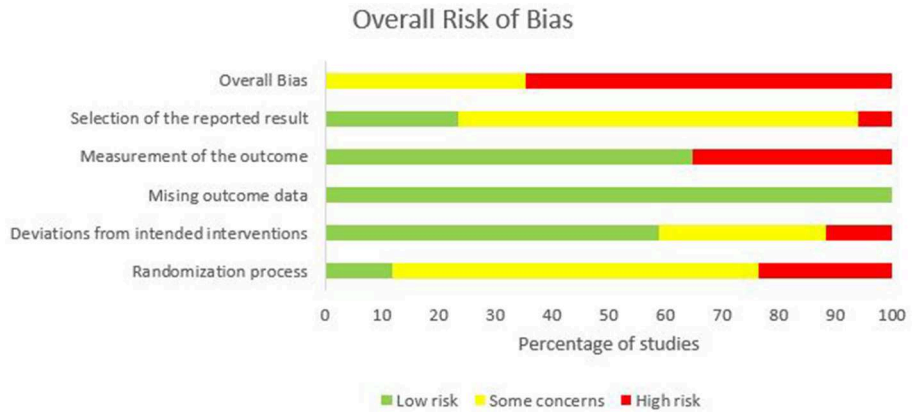

FIGURE 2 | Overall risk-of-bias judgments for each domain.

effect of ctDCS on a bilateral task by placing the target electrode centrally (Poortvliet et al., 2018) or with respect to the dominant limb (Jayaram et al., 2012; Fernandez et al., 2017; Foerster et al., 2017). The return electrode was placed on the forehead (Dutta et al., 2014; Poortvliet et al., 2018), buccinator muscle (Jayaram et al., 2012; Shah et al., 2013; Taubert et al., 2016; Yavari et al., 2016; Fernandez et al., 2017; Summers et al., 2018), or upper limb (Panouillères et al., 2015; Ehsani et al., 2016; Panico et al., 2016; Foerster et al., 2017; Samaei et al., 2017).

ctDCS was delivered at a current density of 0.13 mA/cm^2 ($n =$ 1) (Shah et al., 2013), 0.08 mA/cm^2 ($n = 10$) (Jayaram et al., 2012; Ehsani et al., 2016; Panico et al., 2016; Taubert et al., 2016; Yavari et al., 2016; Foerster et al., 2017; Samaei et al., 2017; Liew et al., 2018; Jackson et al., 2019; Mamlins et al., 2019), 0.06 mA/cm^2 ($n = 2$) (Panouillères et al., 2015; Fernandez et al., 2017), or 0.03 mA/cm^2 ($n = 4$) (Dutta et al., 2014; Poortvliet et al., 2018; Summers et al., 2018; Jongkees et al., 2019). Full details of the stimulation parameters are shown in **Table 2**.

Motor Learning Tasks

Ten studies evaluated a motor adaptation task, and seven studies evaluated a motor skill task. The motor adaptation tasks included perturbation during visuomotor (Panouillères et al., 2015; Panico et al., 2016; Yavari et al., 2016; Liew et al., 2018; Mamlins et al., 2019), locomotor (Jayaram et al., 2012; Fernandez et al., 2017), reaching (Taubert et al., 2016), or postural control (Foerster et al., 2017; Poortvliet et al., 2018) tasks. Skill learning paradigms used serial reaction time task (Ehsani et al., 2016; Samaei et al., 2017; Jongkees et al., 2019), tracking (Shah et al., 2013; Dutta et al., 2014; Summers et al., 2018), or a throwing task (Jackson et al., 2019).

Outcomes

Motor performance outcomes were measured based on error (n = 16) (Jayaram et al., 2012; Shah et al., 2013; Dutta et al., 2014; Panouillères et al., 2015; Ehsani et al., 2016; Panico et al., 2016; Taubert et al., 2016; Yavari et al., 2016; Foerster et al., 2017; Samaei et al., 2017; Liew et al., 2018; Poortvliet et al., 2018; Summers et al., 2018; Jackson et al., 2019; Jongkees et al., 2019; Mamlins et al., 2019), response latency ($n = 1$) (Dutta et al., 2014), response time ($n = 2$) (Ehsani et al., 2016; Samaei et al., 2017), reaction time ($n = 2$) (Liew et al., 2018; Jongkees et al., 2019), or movement variability ($n = 2$) (Fernandez et al., 2017; Poortvliet et al., 2018). Studies measured outcomes over a range of time scales including; after a break of 24 h or more post intervention ($n = 5$) (Ehsani et al., 2016; Taubert et al., 2016; Samaei et al., 2017; Jackson et al., 2019; Jongkees et al., 2019), after a break of <24 h post intervention ($n = 5$) (Shah et al., 2013; Panouillères et al., 2015; Ehsani et al., 2016; Samaei et al., 2017; Jackson et al., 2019), immediately after the intervention ($n = 7$) (Jayaram et al., 2012; Fernandez et al., 2017; Foerster et al., 2017; Liew et al., 2018; Poortvliet et al., 2018; Summers et al., 2018; Mamlins et al., 2019), or during the intervention ($n = 12$) (Jayaram et al., 2012; Dutta et al., 2014; Panouillères et al., 2015; Ehsani et al., 2016; Panico et al., 2016; Taubert et al., 2016; Yavari et al., 2016; Samaei et al., 2017; Liew et al., 2018; Summers et al., 2018; Jongkees et al., 2019; Mamlins et al., 2019).

Long-Term Motor Learning–Motor Performance After a Break of 24 h or More

Of the five studies which evaluated the effect of ctDCS after a break of 24 h or more, three reported enhanced (Ehsani et al., 2016; Samaei et al., 2017; Jackson et al., 2019), while two reported impaired (Taubert et al., 2016; Jongkees et al., 2019) gains in motor performance with anodal ctDCS. Compared to sham ctDCS, anodal ctDCS enhanced the gains in the performance of a motor skill tasks evaluated after a break of 24 (Jackson et al., 2019) and 48 h (Ehsani et al., 2016; Samaei et al., 2017). This was reflected by a greater reduction in the number of errors and/or faster response time in those aged <40 years (Ehsani et al., 2016; Jackson et al., 2019) and a greater reduction in response time, but not the number of errors, in individuals over 40 years (Samaei et al., 2017). Of the two studies that reported impaired gains in motor performance, one found impaired reaction time, but not the number of errors in a motor skill task after 24 h (Jongkees et al., 2019), and the other reported impaired early adaptation in a motor adaptation task when evaluated after 24 h (Taubert

TABLE 2 | Stimulation parameters.

References	ctDCS delivery	Electrode location		Electrode size (cm^2)		Intensity (mA)	Density (mA/cm^2)	ctDCS duration	
		Target	Return	Target	Return			Real (min.)	Sham (min.)
Jayaram et al., 2012	During the task	Lateral cerebellar hemisphere, I/L and C/L to DL	Buccinator, I/L and C/L to DL	25	25	2	0.08	15	0.5
Shah et al., 2013	During the task	Left cerebellar hemisphere, I/L to TL	Left buccinator, I/L to TL	8	35	1	0.13	15	0
Dutta et al., 2014	During the task	Left cerebellar hemisphere, C/L to TL	Forehead above the right supraorbital ridge, I/L to TL	35	35	1	0.03	15	0.17
Panouillères et al., 2015	Prior + during the task	Right cerebellar hemisphere, I/L to TL	Left trapezius, C/L to TL	35	35	2	0.06	17	0.5
Yavari et al., 2016	During the task	Right cerebellar hemisphere, I/L to TL	Right buccinator I/L, to TL	25	25	2	0.08	15	0.5
Ehsani et al., 2016	During the task	Right cerebellar hemisphere, I/L to TL	Right deltoid, I/L to TL	25	25	2	0.08	20	1
Taubert et al., 2016	During the task	Right cerebellar hemisphere, I/L to TL	Right buccinator, I/L to TL	25	25	2	0.08	20	0.5
Panico et al., 2016	Prior + during the task	Right cerebellar hemisphere, I/L to TL	Right deltoid, I/L to TL	25	25	2	0.08	21	0.5
Fernandez et al., 2017	Prior to the task	Right cerebellar hemisphere, I/L to DL	Right buccinator, I/L to DL	35	35	2	0.06	20	0
Samaei et al., 2017	During the task	Right cerebellar hemisphere, I/L to TL	Right deltoid, I/L to TL	25	25	2	0.08	20	0.5
Foerster et al., 2017	Prior to the task	Right cerebellar hemisphere, I/L to TL	Right deltoid, I/L to TL	25	25	2	0.08	A:13 C: 9	0.5
Poortvliet et al., 2018	Prior to the task	Ventral, dorsolateral aspects of the cerebellum and the cerebellar vermis	Centrally on the forehead	35	100	1	0.03	20	0.67
Summers et al., 2018	During the task	BL cerebellar hemisphere	Buccinator IL to TL	70	35	2	0.03	30	0.5
Liew et al., 2018	Prior + during the task	Right cerebellar hemisphere, I/L to TL	Buccinator IL to TL	25	25	2	0.08	>25	0.5
Jongkees et al., 2019	During the task	BL cerebellar hemisphere	BL mastoid	35	35	1	0.03	20	0.25
Jackson et al., 2019	Prior + during the task	Right cerebellar hemisphere, I/L to TL	Buccinator IL to TL	25	25	2	0.08	25	0.5
Mamlins et al., 2019	I: During, Prior + during	I: Right cerebellar hemisphere, I/L to TL	I: Buccinator IL to TL	I: 25	I: 25	I: 2	I: 0.08	I: 10.36 (0.12), 13.81 (0.19)	I: 1
	II: During, Prior + during	II: Right cerebellar hemisphere, I/L to TL	II: Buccinator IL to TL	II: 25	II: 25	II: 2	II: 0.08	II: 7.61 [0.17], 10.20 [0.16]	II: 1

A, anodal ctDCS; C, cathodal ctDCS; I/L, ipsilateral; C/L, contralateral; TL, training limb; DL, dominant limb; BL, bilateral.

et al., 2016). Two studies evaluated the effect of cathodal ctDCS and found no difference in motor performance 24 h after the intervention (Taubert et al., 2016; Jongkees et al., 2019). These studies applied anodal and cathodal ctDCS centered over the inion (Jongkees et al., 2019) or ipsilateral to the training limb during task training or prior to and in conjunction with task training (Jackson et al., 2019). The stimulation was delivered at a current density of 0.03 mA/cm^2 (Jongkees et al., 2019) or 0.08 mA/cm^2 for 20–25 min (Ehsani et al., 2016; Taubert et al., 2016; Samaei et al., 2017; Jackson et al., 2019; Jongkees et al., 2019).

Short-Term Motor Learning–Motor Performance After a Break of <24 h

Of the studies that evaluated the effect of anodal ctDCS after a break of <24 h, four found enhanced (Shah et al., 2013; Ehsani et al., 2016; Samaei et al., 2017; Jackson et al., 2019) and one found no effect (Panouillères et al., 2015) on gains in motor performance compared to sham ctDCS. Anodal ctDCS enhanced the performance of a motor skill task by reducing the number of errors but not response time in healthy young individuals (Ehsani et al., 2016) and reduced the response time but not the number of errors in healthy older individuals tested after a break of 35 min (Samaei et al., 2017). Anodal ctDCS also improved performance of motor skill task 5 (Jackson et al., 2019), 10, 30, and 60 min after intervention. All four studies stimulated the lateral cerebellum ipsilateral to the training limb for 15 (Shah et al., 2013), 20 (Ehsani et al., 2016; Samaei et al., 2017), or 25 (Jackson et al., 2019) min at a current density of 0.13 mA/cm^2 (Shah et al., 2013) or 0.08 mA/cm^2 (Ehsani et al., 2016; Samaei et al., 2017; Jackson et al., 2019). Whereas anodal ctDCS did not affect the number of errors in a motor adaptation task performed after a gap of 50 min when the stimulation was delivered ipsilateral to the training limb at a current density of 0.06 mA/cm^2 for 17 min (Panouillères et al., 2015).

One study evaluated the effect of cathodal ctDCS on motor performance after a break of <24 h and reported improvement in ankle tracking accuracy tested after 10, 30, and 60 min (Shah et al., 2013).

Immediate Motor Learning–Motor Performance Immediately After the Intervention

Of the studies that evaluated the effect of anodal ctDCS immediately after the intervention, one study reported enhanced (Poortvliet et al., 2018), and five found no effect on gains in motor performance as compared to a sham ctDCS group (Jayaram et al., 2012; Foerster et al., 2017; Liew et al., 2018; Summers et al., 2018; Mamlins et al., 2019). Anodal ctDCS at a current density of 0.03 mA/cm^2 for 20 min improved the performance by reducing the postural variability and increasing steadiness when the target electrode was placed centrally over the cerebellum (Poortvliet et al., 2018). While the same site of stimulation and current density delivered for 30 min had no effect on finger tracking accuracy (Summers et al., 2018). Anodal ctDCS delivered ipsilateral to the dominant limb at a current density of 0.08 mA/cm^2 for around 15 min had no effect on static and dynamic balance (Foerster et al., 2017), visuomotor adaptation (Liew et al., 2018; Mamlins et al., 2019), forcefield adaptation (Mamlins et al., 2019), or locomotor adaptation (Jayaram et al., 2012).

Application of cathodal ctDCS had no effect (Mamlins et al., 2019) or impaired (Fernandez et al., 2017; Foerster et al., 2017) gains in motor performance evaluated immediately after stimulation. As compared to sham ctDCS, cathodal ctDCS increased variability in a walking adaptation task (Fernandez et al., 2017) and impaired static but not dynamic balance in adaptation task (Foerster et al., 2017). These effects were seen when ctDCS was delivered ipsilateral to the dominant limb prior to motor task training at a current density of 0.06 mA/cm^2 (Fernandez et al., 2017) or 0.08 mA/cm^2 (Foerster et al., 2017) for 20 (Fernandez et al., 2017) or 9 (Foerster et al., 2017) min.

Simultaneous Motor Learning–Motor Performance During the Intervention

Application of ctDCS had a varied impact on motor performance during task training. Anodal ctDCS enhanced ($n = 3$) (Jayaram et al., 2012; Ehsani et al., 2016; Yavari et al., 2016), impaired ($n = 3$) (Dutta et al., 2014; Taubert et al., 2016; Jongkees et al., 2019), or had no effect on gains in motor performance during task training ($n = 5$) (Panouillères et al., 2015; Samaei et al., 2017; Liew et al., 2018; Summers et al., 2018; Mamlins et al., 2019). Compared to sham ctDCS, anodal ctDCS enhanced motor performance by improving the rate of adaptation (Jayaram et al., 2012; Yavari et al., 2016) and reduced the number of errors but not response time in a serial reaction time task (Ehsani et al., 2016). These effects were primarily observed when anodal ctDCS was delivered ipsilateral to the dominant limb (Jayaram et al., 2012) or training limb (Ehsani et al., 2016; Yavari et al., 2016) for 15 min (Jayaram et al., 2012; Yavari et al., 2016) or more (Ehsani et al., 2016) at a current density of 0.08 mA/cm^2. Anodal ctDCS impaired gains in motor performance during a perturbed reaching task (Taubert et al., 2016), visual pursuit task (Dutta et al., 2014), and serial reaction time task (Jongkees et al., 2019). In the serial reaction task, the impaired gains in motor performance occurred in reaction time but not in the number of errors. In the perturbed reaching task, ctDCS was delivered ipsilateral to the training limb for 20 min at a current density of 0.08 mA/cm^2 (Taubert et al., 2016). Whereas, impaired gains in performance of the serial reaction time task or visual pursuit task were seen when the current was delivered centrally (Jongkees et al., 2019) or on the lateral cerebellum contralateral to the training limb (Dutta et al., 2014) for up to 20 min at a current density of 0.03 mA/cm^2 (Dutta et al., 2014; Jongkees et al., 2019). Anodal ctDCS had no effect on response time in skill task (Samaei et al., 2017) and the number of errors in adaptation (Panouillères et al., 2015; Liew et al., 2018; Mamlins et al., 2019) or skill task (Summers et al., 2018) when the current density was 0.08, 0.06, and 0.03 mA/cm^2, respectively. The target electrode was placed either centrally over the cerebellum (Summers et al., 2018) or on the lateral cerebellum ipsilateral to the training limb (Panouillères et al., 2015; Samaei et al., 2017; Liew et al., 2018; Summers et al., 2018; Mamlins et al., 2019) which delivered the stimulation for up to 30 min.

Of the five studies that evaluated the effect of cathodal ctDCS during task training, three reported impaired (Jayaram et al., 2012; Panico et al., 2016; Yavari et al., 2016) and two reported

no effects (Jongkees et al., 2019; Mamlins et al., 2019) on gains in motor performance. As compared to sham ctDCS, cathodal ctDCS resulted in impaired adaptation (Jayaram et al., 2012; Panico et al., 2016; Yavari et al., 2016) and impaired rate of de-adaptation (Panico et al., 2016). These effects were seen when cathodal ctDCS was delivered ipsilateral to training limb (Jayaram et al., 2012; Panico et al., 2016; Yavari et al., 2016) for 15 min (Jayaram et al., 2012; Yavari et al., 2016) or more (Panico et al., 2016) at a current density of 0.08 mA/cm^2. Two studies found no effect of cathodal ctDCS on skill or adaptation task (Jongkees et al., 2019; Mamlins et al., 2019). These studies applied cathodal ctDCS centrally (Jongkees et al., 2019) or ipsilateral to the training limb (Mamlins et al., 2019) during task training alone (Jongkees et al., 2019) or prior to and in conjunction with task training (Mamlins et al., 2019) for up to 20 min at a current density of 0.03 mA/cm^2 (Jongkees et al., 2019) or 0.08 mA/cm^2 (Mamlins et al., 2019).

DISCUSSION

This review aimed to determine the effects of cerebellar transcranial direct current stimulation on motor learning. For the first time, this study provides a systematic review of RCTs to quantify the effects of ctDCS based on the time scale of motor learning. There is a modest body of research, with 17 studies including 629 participants. The body of evidence is subject to considerable risk-of-bias. The main findings of this systematic review are that anodal ctDCS appears to be effective at enhancing motor skill learning in the short (<24 h) and longer-term (≥24 h). Whereas, it appears to have no effect on motor learning immediately after or during stimulation. This review suggests that the type of motor task, the tDCS stimulation parameters and the interaction between task and stimulation parameters are likely to influence the efficacy of ctDCS.

When compared to sham ctDCS, anodal ctDCS appears to be effective at improving short and longer-term motor learning in healthy individuals when applied primarily during motor skill learning (Shah et al., 2013; Ehsani et al., 2016; Samaei et al., 2017; Jackson et al., 2019) but not motor adaptation paradigms (Panouillères et al., 2015; Taubert et al., 2016). Task characteristics and their interaction with the time scale of learning may explain this. Motor skill training paradigms use novel or complex motor skills, which may take weeks or months to master (Schmidt and Lee, 2011). In contrast, motor adaptation tasks involve modifying a well-learnt skill in response to error feedback. Often participants adapt to induced errors within minutes to hours in motor adaptation tasks (Bastian, 2008). It is possible that motor adaptation paradigms are subject to a ceiling effect in healthy individuals. Repeated exposure to the same adaptation task may not provide sufficient stimulus to induce learning (Bastian, 2008; Criscimagna-Hemminger et al., 2010). In addition, an interference task was undertaken between the intervention and testing sessions of one of the motor adaptation tasks, making interpretation of their results challenging (Taubert et al., 2016).

The reported gains in the performance of a motor skill task in response to anodal ctDCS may also depend on the measure of motor performance used and the age of the participants. In studies investigating healthy young individuals undertaking a unimanual serial reaction time task, ctDCS enhances accuracy but not response time after a break of <24 h and enhanced accuracy and response time after a break of 24 h or more (Ehsani et al., 2016). A previous non-randomized experimental study has also reported that ctDCS may have a greater effect on accuracy than response time within and after 24 h (Cantarero et al., 2015). In contrast, in a study investigating healthy older individuals undertaking the same task, a greater reduction in response time but not the number of errors was observed in response to ctDCS irrespective of the time scale of measurement (Samaei et al., 2017). These findings suggest that ctDCS may differentially influence short and longer-term motor learning of different parameters of movement performance. However, it is unclear whether the difference between older and younger individuals reflects differences in the mechanism of action of ctDCS or that older individuals have slower response time but not greater inaccuracy in these types of task (Voelcker-Rehage, 2008).

In studies which investigated the effects of ctDCS using serial reaction time tasks, conflicting results were observed. Improved response times were seen in a unimanual task (Ehsani et al., 2016; Samaei et al., 2017), whereas impaired reaction time was seen in a bimanual task (Jongkees et al., 2019). The performance measure used to reflect motor learning in the two tasks may evaluate different aspects of motor performance. Reaction time reflects the time between stimulus appearance and movement initiation. Whereas, response time is comprised of both reaction time and movement time (Pascual-Leone et al., 1995). However, it is notable that the studies also differed in the stimulation parameters used, where a current density of 0.03 mA/cm^2 centered over bilateral cerebellar hemisphere impaired gains, while a current density of 0.08 mA/cm^2 targeting the lateral cerebellum ipsilateral to the training limb enhanced gains in motor performance. The challenge of unpacking these conflicting results illustrates the importance of taking a systematic approach to investigating ctDCS; where the influence of motor task, performance metric, and stimulation parameters should be considered.

Anodal ctDCS appears to have no effect on gains in motor performance measured during and immediately after the intervention, where most of the studies demonstrated no effect (Jayaram et al., 2012; Panouillères et al., 2015; Foerster et al., 2017; Samaei et al., 2017; Liew et al., 2018; Summers et al., 2018; Mamlins et al., 2019) and some enhanced (Jayaram et al., 2012; Ehsani et al., 2016; Yavari et al., 2016; Poortvliet et al., 2018) or impaired (Dutta et al., 2014; Taubert et al., 2016; Jongkees et al., 2019) gains in motor performance. These results were observed irrespective of the type of task being studied (adaptation or skill) as has been noted in previous narrative reviews (Ferrucci et al., 2015; van Dun et al., 2016). It is therefore unclear whether ctDCS has any effect on motor learning during or immediately after task training. Motor learning research highlights the paradoxical relationship between learning and performance. That is, motor learning, as defined as a permanent change in motor performance, can occur without immediate changes in motor performance. In fact, immediate changes in

motor performance in response to an intervention are often not sustained after a break (Soderstrom and Bjork, 2015). This suggests that changes in motor performance during and immediately after anodal ctDCS are less relevant in determining the effectiveness of anodal ctDCS than changes observed after 24 h or more.

This systematic review highlights that the site of anodal ctDCS stimulation and current density are the critical stimulation parameters which appear to impact the effect produced, irrespective of time scale. Greater gains in motor performance were seen with the target electrode placed centrally on the cerebellum in a bilateral postural control task (Poortvliet et al., 2018) and ipsilateral to the training limb in unilateral tasks (Shah et al., 2013; Ehsani et al., 2016; Samaei et al., 2017). In addition, motor performance is enhanced during a bilateral task involving greater perturbation to one of the limbs with the placement of target electrode ipsilateral to that limb (Jayaram et al., 2012). This suggests that the parameters of the motor task may be an important consideration in determining an appropriate site for stimulation. Therefore, researchers should explicitly consider where in the cerebellum motor control and learning is occurring for a given task and select electrode configuration with this in mind (Hulst et al., 2017), acknowledging that current density and specificity is dependent on electrode size and position (Ferrucci et al., 2013). Positive effects were more likely to be observed when anodal ctDCS was delivered with a current density of 0.08 mA/cm^2 or more. This current density is greater than that recommended for cerebral ctDCS (Nitsche et al., 2003); however, modeling studies illustrate the need for higher current density to stimulate the cerebellum to overcome large shunting of current at the base of the skull (Rampersad et al., 2014). Other stimulation parameters such as stimulation duration and timing of stimulation delivery (at rest or during task training) had an equivocal effect. The total duration of stimulation was not hugely variable and ranged from 15 to 20 min. Contrary to previous literature (Monte-Silva et al., 2010), no relationship between stimulation duration and time scale of effect was observed. Further research is required to unpack the effect of stimulation duration on the permanence of ctDCS effects across time scales.

When compared to sham ctDCS, cathodal ctDCS has an equivocal effect on short and longer-term motor learning in healthy individuals. However, most of the studies found impaired gains in motor performance of adaptation tasks during and immediately after cathodal ctDCS (Jayaram et al., 2012; Panico et al., 2016; Yavari et al., 2016; Fernandez et al., 2017; Foerster et al., 2017) with few reporting no effect on gains in motor performance (Jongkees et al., 2019; Mamlins et al., 2019). Overall, there is insufficient evidence to infer the effect of cathodal ctDCS on motor learning.

Although most of the included studies employed randomized, blinded, sham-controlled designs, their methodological quality was globally considered to have "high" risk-of-bias. Potential sources of bias included failure to report the method of randomization used, allocation concealment and failure to explicitly state who was blinded: the participant, the person administering the intervention, and/or the outcome assessor. The majority of studies did not report trial registration details or a pre-specified statistical analysis plan. Further, some studies had baseline differences between intervention groups that suggested a problem with the randomization process. Whilst these judgments of research quality may not reflect what the researchers actually did during the protocol but rather a lack of explicit documentation; it is essential that adherence to, and reporting of, these standards of practice become commonplace in this body of literature. The potential for bias may contribute to the reporting of contradictory results and suggests that the interpretation of the research findings to date must be approached with some caution (Steiner et al., 2016; Hulst et al., 2017; Jalali et al., 2017).

Limitations, Implications and Future Research

The included studies had considerable variability in both measurement and data processing methods. Some studies measured the time course of change in error throughout the task training (Panouillères et al., 2015), some in specific epochs (early or late epochs) (Panico et al., 2016; Taubert et al., 2016), some fitted an exponential curve (Jayaram et al., 2012; Yavari et al., 2016), while other measured change scores (Shah et al., 2013; Ehsani et al., 2016; Samaei et al., 2017; Jackson et al., 2019). Furthermore, the method for calculating changes in motor performance was inconsistent across studies. For instance, the error was calculated as mean error (Jayaram et al., 2012), mean absolute error (Dutta et al., 2014), or normalized accuracy index using root mean square error (Shah et al., 2013) while others failed to describe how the error was calculated (Ehsani et al., 2016). The method by which error is calculated affects its accuracy; for example, a simple mean of errors may not reflect individual variability while a mean absolute error encompasses bias due to individual variability (Schmidt and Lee, 2011). This makes comparing results across studies challenging.

Despite these limitations, the review adds to our understanding of the potential of ctDCS to impact motor learning, with particular reference to the time scale of learning. It highlights the importance of task characteristics, movement parameter outcome measurement techniques, participant age, and stimulation parameters when interpreting the research body and designing future studies. Further research, which explores the time scales of >24 h are required. There are also many unanswered questions regarding the cumulative effects of ctDCS over multiple sessions and the long-term retention of performance after a delay of weeks and months. More studies evaluating the effect of ctDCS on motor adaptation tasks over longer time scales are needed to elucidate its effect on adaptive learning.

CONCLUSIONS

In conclusion, anodal ctDCS appears to be effective at improving short and long-term motor skill learning. However, these results are predicated upon just four modest-quality studies. While these findings illustrate the potential of targeting the cerebellum with tDCS to enhance learning in healthy and clinical populations, researchers need to take a methodologically robust

and systematic approach to future research. Factors including the challenge of the motor task and its characteristics, the ctDCS stimulation parameters, method of measuring motor performance, and participant age are likely to influence whether ctDCS will enhance or have no effect on motor learning.

DATA AVAILABILITY STATEMENT

The raw data supporting the conclusions of this manuscript will be made available by the authors, without undue reservation, to any qualified researcher.

AUTHOR CONTRIBUTIONS

All authors were involved in the conceptualization and designing of the study. NK was involved with the literature search and data extraction. NK and NS were involved with manuscript preparation. NS and DT were involved in supervision. All authors were involved in reviewing and editing the manuscript.

FUNDING

This research did not receive any specific grant from funding agencies in the public, commercial, or not-for-profit sectors.

SUPPLEMENTARY MATERIAL

The Supplementary Material for this article can be found online at: https://www.frontiersin.org/articles/10.3389/fnhum.2019.00328/full#supplementary-material

REFERENCES

Ammann, C., Spampinato, D., and Márquez-Ruiz, J. (2016). Modulating motor learning through transcranial direct-current stimulation: an integrative view. *Front. Psychol.* 7:1981. doi: 10.3389/fpsyg.2016.01981

Banissy, M. J., and Muggleton, N. G. (2013). Transcranial direct current stimulation in sports training: potential approaches. *Front. Hum. Neurosci.* 7:129. doi: 10.3389/fnhum.2013.00129

Bastian, A. J. (2008). Understanding sensorimotor adaptation and learning for rehabilitation. *Curr. Opin. Neurol.* 21, 628–633. doi: 10.1097/WCO.0b013e328315a293

Block, H., and Celnik, P. (2012). Stimulating the cerebellum affects visuomotor adaptation but not intermanual transfer of learning. *Cerebellum* 12, 781–793. doi: 10.1007/s12311-013-0486-7

Block, H. J., and Celnik, P. (2012). Can cerebellar transcranial direct current stimulation become a valuable neurorehabilitation intervention? *Expert Rev. Neurother.* 12, 1275–1277. doi: 10.1586/ern.12.121

Bolognini, N., Pascual-Leone, A., and Fregni, F. (2009). Using non-invasive brain stimulation to augment motor training-induced plasticity. *J. Neuroeng. Rehabil.* 6:8. doi: 10.1186/1743-0003-6-8

Caligiore, D., Pezzulo, G., Baldassarre, G., Bostan, A. C., Strick, P. L., Doya, K., et al. (2017). Consensus paper: towards a systems-level view of cerebellar function: the interplay between cerebellum, basal ganglia, and cortex. *Cerebellum* 16, 203–229. doi: 10.1007/s12311-016-0763-3

Cantarero, G., Spampinato, D., Reis, J., Ajagbe, L., Thompson, T., Kulkarni, K., et al. (2015). Cerebellar direct current stimulation enhances on-line motor skill acquisition through an effect on accuracy. *J. Neurosci.* 35, 3285–3290. doi: 10.1523/JNEUROSCI.2885-14.2015

Caputron (2019). *What is TDCS New York City*. Available online at: https://caputron.com/collections/research-and-clinical (accessed March 27, 2019).

Celnik, P. (2015). Understanding and modulating motor learning with cerebellar stimulation. *Cerebellum* 14, 171–174. doi: 10.1007/s12311-014-0607-y

Ciechanski, P., Cheng, A., Lopushinsky, S., Hecker, K., Gan, L. S., Lang, S., et al. (2017). Effects of transcranial direct-current stimulation on neurosurgical skill acquisition: a randomized controlled trial. *World Neurosurg.* 108, 876–84.e4. doi: 10.1016/j.wneu.2017.08.123

Criscimagna-Hemminger, S. E., Bastian, A. J., and Shadmehr, R. (2010). Size of error affects cerebellar contributions to motor learning. *J. Neurophysiol.* 103, 2275–2284. doi: 10.1152/jn.00822.2009

Dayan, E., and Cohen, L. G. (2011). Neuroplasticity subserving motor skill learning. *Neuron* 72, 443–454. doi: 10.1016/j.neuron.2011.10.008

De Zeeuw, C. I., and Ten Brinke, M. M. (2015). Motor learning and the cerebellum. *Cold Spring Harb. Perspect. Biol.* 7:a021683. doi: 10.1101/cshperspect.a021683

Diedrichsen, J., Hashambhoy, Y., Rane, T., and Shadmehr, R. (2005). Neural correlates of reach errors. *J Neurosci.* 25, 9919–9931. doi: 10.1523/JNEUROSCI.1874-05.2005

Diekelmann, S., Wilhelm, I., and Born, J. (2009). The whats and whens of sleep-dependent memory consolidation. *Sleep Med. Rev.* 13, 309–321. doi: 10.1016/j.smrv.2008.08.002

Doyon, J., and Benali, H. (2005). Reorganization and plasticity in the adult brain during learning of motor skills. *Curr. Opin. Neurobiol.* 15, 161–167. doi: 10.1016/j.conb.2005.03.004

Dutta, A., Paulus, W., and Nitsche, M. A. (2014). Facilitating myoelectric-control with transcranial direct current stimulation: a preliminary study in healthy humans. *J. Neuroeng. Rehabil.* 11:13. doi: 10.1186/1743-0003-11-13

Edwards, D. J., Cortes, M., Wortman-Jutt, S., Putrino, D., Bikson, M., Thickbroom, G., et al. (2017). Transcranial direct current stimulation and sports performance. *Front. Hum. Neurosci.* 11:243. doi: 10.3389/fnhum.2017.00243

Ehsani, F., Bakhtiary, A., Jaberzadeh, S., Talimkhani, A., and Hajihasani, A. (2016). Differential effects of primary motor cortex and cerebellar transcranial direct current stimulation on motor learning in healthy individuals: A randomized double-blind sham-controlled study. *Neurosci. Res.* 112, 10–19. doi: 10.1016/j.neures.2016.06.003

Fernandez, L., Albein-Urios, N., Kirkovski, M., McGinley, J. L., Murphy, A. T., Hyde, C., et al. (2017). Cathodal transcranial direct current stimulation (tDCS) to the right cerebellar hemisphere affects motor adaptation during gait. *Cerebellum* 16, 168–177. doi: 10.1007/s12311-016-0788-7

Ferrucci, R., Bocci, T., Cortese, F., Ruggiero, F., and Priori, A. (2016). Cerebellar transcranial direct current stimulation in neurological disease. *Cerebellum Ataxias* 3:16. doi: 10.1186/s40673-016-0054-2

Ferrucci, R., Bocci, T., Cortese, F., Ruggiero, F., and Priori, A. (2019). Noninvasive cerebellar stimulation as a complement tool to pharmacotherapy. *Curr. Neuropharmacol.* 17, 14–20. doi: 10.2174/1570159X15666171114142422

Ferrucci, R., Brunoni, A. R., Parazzini, M., Vergari, M., Rossi, E., Fumagalli, M., et al. (2013). Modulating human procedural learning by cerebellar transcranial direct current stimulation. *Cerebellum* 12, 485–492. doi: 10.1007/s12311-012-0436-9

Ferrucci, R., Cortese, F., and Priori, A. (2015). Cerebellar tDCS: how to do it. *Cerebellum* 14, 27–30. doi: 10.1007/s12311-014-0599-7

Foerster, Á., Melo, L., Mello, M., Castro, R., Shirahige, L., Rocha, S., et al. (2017). Cerebellar transcranial direct current stimulation (ctDCS) impairs balance control in healthy individuals. *Cerebellum* 16, 872–875. doi: 10.1007/s12311-017-0863-8

Galea, J. M., Jayaram, G., Ajagbe, L., and Celnik, P. (2009). Modulation of cerebellar excitability by polarity-specific noninvasive direct current stimulation. *J. Neurosci.* 29, 9115–9122. doi: 10.1523/JNEUROSCI.2184-09.2009

Grimaldi, G., Argyropoulos, G., Boehringer, A., Celnik, P., Edwards, M., Ferrucci, R., et al. (2014). Non-invasive cerebellar stimulation-a consensus paper. *Cerebellum* 13, 121–138. doi: 10.1007/s12311-013-0514-7

Grimaldi, G., Argyropoulos, G. P., Bastian, A., Cortes, M., Davis, N. J., Edwards, D. J., et al. (2016). Cerebellar transcranial direct current stimulation (ctDCS): a novel approach to understanding cerebellar function in health and disease. *Neuroscientist* 22, 83–97. doi: 10.1177/1073858414559409

Halo (2019). *Improve Your Game San Francisco*. Available online at: https://www.haloneuro.com/ (accessed March 14, 2019).

Higgins, J., Green, S (eds.). (2011). *Cochrane Handbook for Systematic Reviews of Interventions. Version 5.1.0*.

Huang, L., Deng, Y., Zheng, X., and Liu, Y. (2019). Transcranial direct current stimulation with halo sport enhances repeated sprint cycling and cognitive performance. *Front. Physiol.* 10:118. doi: 10.3389/fphys.2019.00118

Hulst, T., John, L., Kuper, M., van der Geest, J. N., Goricke, S. L., Donchin, O., et al. (2017). Cerebellar patients do not benefit from cerebellar or M1 transcranial direct current stimulation during force-field reaching adaptation. *J. Neurophysiol.* 118, 732–748. doi: 10.1152/jn.00808.2016

Ito, M. (2000). Mechanisms of motor learning in the cerebellum. *Brain Res.* 886, 237–245. doi: 10.1016/S0006-8993(00)03142-5

Izawa, J., and Shadmehr, R. (2011). Learning from sensory and reward prediction errors during motor adaptation. *PLoS Comput. Biol.* 7:e1002012. doi: 10.1371/journal.pcbi.1002012

Jackson, A. K., de Albuquerque, L. L., Pantovic, M., Fischer, K. M., Guadagnoli, M. A., Riley, Z. A., et al. (2019). Cerebellar transcranial direct current stimulation enhances motor learning in a complex overhand throwing task. *Cerebellum* 18, 813–816. doi: 10.1007/s12311-019-01040-6

Jalali, R., Miall, R., and Galea, J. M. (2017). No consistent effect of cerebellar transcranial direct current stimulation on visuomotor adaptation. *J. Neurophysiol.* 118, 655–665. doi: 10.1152/jn.00896.2016

Jayaram, G., Tang, B., Pallegadda, R., Vasudevan, E. V., Celnik, P., and Bastian, A. (2012). Modulating locomotor adaptation with cerebellar stimulation. *J. Neurophysiol.* 107, 2950–2957. doi: 10.1152/jn.00645.2011

Jongkees, B. J., Immink, M. A., Boer, O. D., Yavari, F., Nitsche, M. A., and Colzato, L. S. (2019). The effect of cerebellar tDCS on sequential motor response selection. *Cerebellum* 18, 738–749. doi: 10.1007/s12311-019-01029-1

Kitago, T., and Krakauer, J. W. (2013). "Chapter 8 - Motor learning principles for neurorehabilitation," in *Handbook of Clinical Neurology*, Vol. 110, eds M. P. Barnes and D. C. Good (New York, NY: Elsevier), 93–103. doi: 10.1016/B978-0-444-52901-5.00008-3

Kojima, Y., Iwamoto, Y., and Yoshida, K. (2004). Memory of learning facilitates saccadic adaptation in the monkey. *J. Neurosci.* 24, 7531–7539. doi: 10.1523/JNEUROSCI.1741-04.2004

Koziol, L. F., Budding, D., Andreasen, N., D'Arrigo, S., Bulgheroni, S., Imamizu, H., et al. (2014). Consensus paper: the cerebellum's role in movement and cognition. *Cerebellum* 13, 151–177. doi: 10.1007/s12311-013-0511-x

Lang, E. J., Apps, R., Bengtsson, F., Cerminara, N. L., De Zeeuw, C. I., Ebner, T. J., et al. (2017). The roles of the olivocerebellar pathway in motor learning and motor control. A consensus paper. *Cerebellum* 16, 230–252. doi: 10.1007/s12311-016-0787-8

Liew, S. L., Thompson, T., Ramirez, J., Butcher, P. A., Taylor, J. A., and Celnik, P. A. (2018). Variable neural contributions to explicit and implicit learning during visuomotor adaptation. *Front. Neurosci.* 12:610. doi: 10.3389/fnins.2018.00610

Lohse, K. R., Lang, C. E., and Boyd, L. A. (2014). Is more better? Using metadata to explore dose–response relationships in stroke rehabilitation. *Stroke* 45, 2053–2058. doi: 10.1161/STROKEAHA.114.004695

Mamlins, A., Hulst, T., Donchin, O., Timmann, D., and Claassen, J. (2019). No effects of cerebellar transcranial direct current stimulation on force field and visuomotor reach adaptation in young and healthy subjects. *J. Neurophysiol.* 121, 2112–2125. doi: 10.1152/jn.00352.2018

Manto, M., Bower, J. M., Conforto, A. B., Delgado-García, J. M., Da Guarda, S. N. F., Gerwig, M., et al. (2012). Consensus paper: roles of the cerebellum in motor control—the diversity of ideas on cerebellar involvement in movement. *Cerebellum* 11, 457–487. doi: 10.1007/s12311-011-0331-9

Mariën, P., Ackermann, H., Adamaszek, M., Barwood, C. H., Beaton, A., Desmond, J., et al. (2014). Consensus paper: language and the cerebellum: an ongoing enigma. *Cerebellum* 13, 386–410. doi: 10.1007/s12311-013-0540-5

Martin, T. A., Keating, J. G., Goodkin, H. P., Bastian, A. J., and Thach, W. T. (1996). Throwing while looking through prismsII. Specificity and storage of multiple gaze—throw calibrations. *Brain* 119, 1199–1211. doi: 10.1093/brain/119.4.1199

Miall, R. C., and Wolpert, D. M. (1996). Forward models for physiological motor control. *Neural netw.* 9, 1265–1279. doi: 10.1016/S0893-6080(96)00035-4

Monte-Silva, K., Kuo, M. F., Liebetanz, D., Paulus, W., and Nitsche, M. A. (2010). Shaping the optimal repetition interval for cathodal transcranial direct current stimulation (tDCS). *J. Neurophysiol.* 103, 1735–1740. doi: 10.1152/jn.00924.2009

Nitsche, M. A., Liebetanz, D., Lang, N., Antal, A., Tergau, F., and Paulus, W. (2003). Safety criteria for transcranial direct current stimulation (tDCS) in humans. *Clin. Neurophysiol.* 114, 2220–2222; author reply 2–3. doi: 10.1016/S1388-2457(03)00235-9

Okano, A. H., Fontes, E. B., Montenegro, R. A., Farinatti Pd,TV., Cyrino, E. S., Li, L. M., et al. (2015). Brain stimulation modulates the autonomic nervous system, rating of perceived exertion and performance during maximal exercise. *Br. J. Sports Med.* 49, 1213–1218. doi: 10.1136/bjsports-2012-091658

Oldrati, V., and Schutter, D. J. (2018). Targeting the human cerebellum with transcranial direct current stimulation to modulate behavior: a meta-analysis. *Cerebellum* 17, 228–236. doi: 10.1007/s12311-017-0877-2

Panico, F., Sagliano, L., Grossi, D., and Trojano, L. (2016). Cerebellar cathodal tDCS interferes with recalibration and spatial realignment during prism adaptation procedure in healthy subjects. *Brain Cogn.* 105, 1–8. doi: 10.1016/j.bandc.2016.03.002

Panouillères, M. T., Joundi, R. A., Brittain, J.-S., and Jenkinson, N. (2015). Reversing motor adaptation deficits in the ageing brain using non-invasive stimulation. *J. Physiol. (Lond).* 593, 3645–3655. doi: 10.1113/JP270484

Pascual-Leone, A., Nguyet, D., Cohen, L. G., Brasil-Neto, J. P., Cammarota, A., and Hallett, M. (1995). Modulation of muscle responses evoked by transcranial magnetic stimulation during the acquisition of new fine motor skills. *J. Neurophysiol.* 74, 1037–1045. doi: 10.1152/jn.1995.74.3.1037

Perciavalle, V., Apps, R., Bracha, V., Delgado-García, J. M., Gibson, A. R., Leggio, M., et al. (2013). Consensus paper: current views on the role of cerebellar interpositus nucleus in movement control and emotion. *Cerebellum* 12, 738–757. doi: 10.1007/s12311-013-0464-0

Poortvliet, P., Hsieh, B., Cresswell, A., Au, J., and Meinzer, M. (2018). Cerebellar transcranial direct current stimulation improves adaptive postural control. *Clin. Neurophysiol.* 129, 33–41. doi: 10.1016/j.clinph.2017.09.118

Rampersad, S. M., Janssen, A. M., Lucka, F., Aydin, Ü., Lanfer, B., Lew, S., et al. (2014). Simulating transcranial direct current stimulation with a detailed anisotropic human head model. *IEEE Trans. Neural Syst. Rehabil. Eng.* 22, 441–452. doi: 10.1109/TNSRE.2014.2308997

Reis, J., Schambra, H. M., Cohen, L. G., Buch, E. R., Fritsch, B., Zarahn, E., et al. (2009). Noninvasive cortical stimulation enhances motor skill acquisition over multiple days through an effect on consolidation. *Proc. Natl. Acad. Sci. U.S.A.* 106, 1590–1595. doi: 10.1073/pnas.0805413106

Samaei, A., Ehsani, F., Zoghi, M., Yosephi, M. H., and Jaberzadeh, S. (2017). Online and offline effects of cerebellar transcranial direct current stimulation on motor learning in healthy older adults: a randomized double-blind sham-controlled study. *Eur. J. Neurosci.* 45, 1177–1185. doi: 10.1111/ejn.13559

Schmidt, R. A., and Lee, T. D. (2011). *Motor Control and Learning: A Behavioral Emphasis, 5th Edn*. Champaign, IL: Human Kinetics.

Shah, B., Nguyen, T. T., and Madhavan, S. (2013). Polarity independent effects of cerebellar tDCS on short term ankle visuomotor learning. *Brain Stimul.* 6, 966–968. doi: 10.1016/j.brs.2013.04.008

Small, S., Hlustik, P., Noll, D., Genovese, C., and Solodkin, A. (2002). Cerebellar hemispheric activation ipsilateral to the paretic hand correlates with functional recovery after stroke. *Brain* 125, 1544–1557. doi: 10.1093/brain/awf148

Soderstrom, N. C., and Bjork, R. A. (2015). Learning versus performance: An integrative review. *Perspect. Psychol. Sci.* 10, 176–199. doi: 10.1177/1745691615569000

Sokolov, A. A., Miall, R. C., and Ivry, R. B. (2017). The cerebellum: adaptive prediction for movement and cognition. *Trends Cogn. Sci. (Regul. Ed).* 21, 313–332. doi: 10.1016/j.tics.2017.02.005

Steiner, K. M., Enders, A., Thier, W., Batsikadze, G., Ludolph, N., Ilg, W., et al. (2016). Cerebellar tDCS does not improve learning in a complex whole body

dynamic balance task in young healthy subjects. *PLoS ONE* 11:e0163598. doi: 10.1371/journal.pone.0163598

Sterne, J. A. C., Savović, J., Page, M. J., Elbers, R. G., Blencowe, N. S., Boutron, I., et al. (2019). RoB 2: a revised tool for assessing risk of bias in randomised trials. *BMJ* 366:l4898. doi: 10.1136/bmj.l4898

Summers, R. L. S., Chen, M., Hatch, A., and Kimberley, T. J. (2018). Cerebellar transcranial direct current stimulation modulates corticospinal excitability during motor training. *Front. Hum. Neurosci.* 12:118. doi: 10.3389/fnhum.2018.00118

Taubert, M., Stein, T., Kreutzberg, T., Stockinger, C., Hecker, L., Focke, A., et al. (2016). Remote effects of non-invasive cerebellar stimulation on error processing in motor re-learning. *Brain Stimul.* 9, 692–699. doi: 10.1016/j.brs.2016.04.007

Timmann, D., and Daum, I. (2007). *Cerebellar contributions to cognitive* functions: a progress report after two decades of research. *Cerebellum* 6:159. doi: 10.1080/14734220701496448

Tseng, Y. W., Diedrichsen, J., Krakauer, J. W., Shadmehr, R., and Bastian, A. J. (2007). Sensory prediction errors drive cerebellum-dependent adaptation of reaching. *J. Neurophysiol.* 98, 54–62. doi: 10.1152/jn.00266.2007

van Dun, K., Bodranghien, F., Mariën, P., and Manto, M. U. (2016). tDCS of the cerebellum: where do we stand in 2016? technical issues and critical review of the literature. *Front. Hum. Neurosci.* 10:199. doi: 10.3389/fnhum.2016.00199

Voelcker-Rehage, C. (2008). Motor-skill learning in older adults—a review of studies on age-related differences. *Euro. Rev. Aging Phys. Act*. 5, 5–16. doi: 10.1007/s11556-008-0030-9

Ward, N., Brown, M., Thompson, A., and Frackowiak, R. (2003). Neural correlates of motor recovery after stroke: a longitudinal fMRI study. *Brain* 126, 2476–2496. doi: 10.1093/brain/awg245

Waters-Metenier, S., Husain, M., Wiestler, T., and Diedrichsen, J. (2014). Bihemispheric transcranial direct current stimulation enhances effector-independent representations of motor synergy and sequence learning. *J. Neurosci.* 34, 1037–1050. doi: 10.1523/JNEUROSCI.2282-13.2014

Winstein, C., Lewthwaite, R., Blanton, S. R., Wolf, L. B., and Wishart, L. (2014). Infusing motor learning research into neurorehabilitation practice: a historical perspective with case exemplar from the accelerated skill acquisition program. *J. Neurol. Phys. Ther.* 38, 190–200. doi: 10.1097/NPT.0000000000000046

Wolpert, D. M., and Flanagan, J. R. (2001). Motor prediction. *Curr. Biol.* 11, R729–R32. doi: 10.1016/S0960-9822(01)00432-8

Yavari, F., Mahdavi, S., Towhidkhah, F., Ahmadi-Pajouh, M. A., Ekhtiari, H., and Darainy, M. (2016). Cerebellum as a forward but not inverse model in visuomotor adaptation task: a tDCS-based and modeling study. *Exp. Brain Res.* 234, 997–1012. doi: 10.1007/s00221-015-4523-2

Conflict of Interest: The authors declare that the research was conducted in the absence of any commercial or financial relationships that could be construed as a potential conflict of interest.

frontiers in Human Neuroscience

ORIGINAL RESEARCH
published: 01 November 2019
doi: 10.3389/fnhum.2019.00396

Coupling Robot-Aided Assessment and Surface Electromyography (sEMG) to Evaluate the Effect of Muscle Fatigue on Wrist Position Sense in the Flexion-Extension Plane

Maddalena Mugnosso[1,2], Jacopo Zenzeri[1], Charmayne M. L. Hughes[3] and Francesca Marini[1]*

[1] Motor Learning, Assistive and Rehabilitation Robotics Laboratory, Robotics, Brain and Cognitive Sciences Department, Istituto Italiano di Tecnologia, Genoa, Italy, [2] Department of Informatics, Bioengineering, Robotics and System Engineering, University of Genoa, Genoa, Italy, [3] NeuroTech Laboratory, Health Equity Institute, San Francisco State University, San Francisco, CA, United States

OPEN ACCESS

Edited by:
Sheng Li,
The University of Texas Health Science Center at Houston, United States

Reviewed by:
Fan Gao,
University of Kentucky, United States
Tomofumi Yamaguchi,
Yamagata Prefectural University of Health Sciences, Japan

***Correspondence:**
Maddalena Mugnosso
Maddalena.mugnosso@iit.it

Specialty section:
This article was submitted to Motor Neuroscience, a section of the journal Frontiers in Human Neuroscience

Received: 18 July 2019
Accepted: 22 October 2019
Published: 01 November 2019

Citation:
Mugnosso M, Zenzeri J, Hughes CML and Marini F (2019) Coupling Robot-Aided Assessment and Surface Electromyography (sEMG) to Evaluate the Effect of Muscle Fatigue on Wrist Position Sense in the Flexion-Extension Plane. Front. Hum. Neurosci. 13:396. doi: 10.3389/fnhum.2019.00396

Proprioception is a crucial sensory modality involved in the control and regulation of coordinated movements and in motor learning. However, the extent to which proprioceptive acuity is influenced by local muscle fatigue is obscured by methodological differences in proprioceptive and fatiguing protocols. In this study, we used high resolution kinematic measurements provided by a robotic device, as well as both frequency and time domain analysis of signals captured via surface electromyography (sEMG) to examine the effects of local muscle fatigue on wrist proprioceptive acuity in 16 physically and neurologically healthy young adults. To this end, participants performed a flexion/extension ipsilateral joint position matching test (JPM), after which a high-resistive robotic task was used to induce muscle fatigue of the flexor carpi radialis (FCR) muscle. The JPM test was then repeated in order to analyze potential changes in proprioceptive acuity. Results indicated that the fatigue protocol had a significant effect on movements performed in flexion direction, with participants exhibiting a tendency to undershoot the target before the fatigue protocol (−1.218°), but overshooting after the fatigue protocol (0.587°). In contrast, in the extension direction error bias values were similar before and after the fatigue protocol as expected (pre = −1.852°, post = −1.237°) and reflected a tendency to undershoot the target. Moreover, statistical analysis indicated that movement variability was not influenced by the fatigue protocol or movement direction. In sum, results of the present study demonstrate that an individual's estimation of wrist joint displacement (i.e., error bias), but not precision (i.e., variability), is affected by muscular fatigue in a sample of neurologically and physically healthy adults.

Keywords: proprioception, surface electromyography, wrist, robot-aided assessment, muscle fatigue

INTRODUCTION

Over the last half-century researchers have convincingly demonstrated the importance of proprioceptive acuity in the control and regulation of coordinated movements, motor learning, and error correction (Jeannerod, 1988; Schmidt and Lee, 2005). Proprioception[1] is commonly divided into two modalities: joint position sense (JPS) and kinesthesia, where the former refers to the ability of the subject to perceive a presented joint angle (Proske and Gandevia, 2009), while the latter refers to the ability to perceive movements of the body (Hiemstra et al., 2001). JPS is the most commonly examined among the two modalities, with research demonstrating that JPS acuity is impaired after physical injury (Hertel, 2008), as well as in elderly individuals and chronic post-stroke patients (Hughes et al., 2015). Deficits in upper extremity proprioceptive function are said to arise from changes in both the central and peripheral nervous systems (CNS and PNS, respectively) (Good et al., 2001; Resnick et al., 2003; Quiton et al., 2007). Specifically, CNS changes include decreased gray matter volume in the frontal (Good et al., 2001; Quiton et al., 2007) and parietal lobes (Good et al., 2001; Resnick et al., 2003), and reduced activity in proprioceptive regions of the basal ganglia (Goble et al., 2012), both of which may contribute to declines in position sense across adulthood. Changes in the PNS that account for declines in proprioceptive function include increases in capsular thickness (Swash and Fox, 1974), decreases in muscle spindle sensitivity (Burke et al., 1996; Kim et al., 2007) and diameter size (Kararizou et al., 2005), as well as decreases in the number of intrafusal fibers (Swash and Fox, 1974) and cutaneous mechanoreceptors (Aydoğ et al., 2006).

Previous research has examined the effects of exercise-induced local muscle fatigue on JPS (Kazutomo et al., 2004; Givoni et al., 2007; Ribeiro and Oliveira, 2007; Ju et al., 2010; Karagiannopoulos et al., 2019; Sadler and Cressman, 2019) with somewhat mixed results. A previous study investigated the changes in knee JPS due to exercise-induced muscle fatigue (i.e., 30 consecutive maximal concentric contractions of the knee extensors and flexors) and reported an increase in both absolute and relative angular error in the extension direction after fatigue (Ribeiro and Oliveira, 2007). In contrast, another research failed to find differences in internal and external shoulder proprioception after a fatigue protocol in which participants performed two bouts of maximal reciprocal concentric isokinetic contractions until force output decreased below 50% of the participant's maximum voluntary contraction (MVC) (Sterner et al., 1998).

One possible explanation for the divergent results lies in the different JPS protocols used in prior studies (Ager et al., 2017). For example, in previous protocols an experimenter passively moved the patient's limb to a target position and then back to the starting position, after which the participant actively moved the same limb to the remembered position (Sharpe and Miles, 1993; Sterner et al., 1998; Kazutomo et al., 2004). Given that it is nearly impossible for the experimenter to maintain movement velocity across trials and participants, and that JPS is influenced by the speed of movement (Goble and Brown, 2009), this approach is considered to be a coarse measure of proprioceptive acuity.

With respect to measurements of end-point error, researchers have used techniques such as 2D motion capture based on video analysis (Kazutomo et al., 2004; Ribeiro et al., 2007) which have been found to be less reliable than isokinetic dynamometer and continuous passive motion devices (Ager et al., 2017). Moreover, the conflicting findings in prior studies may arise from the specific fatiguing protocol used to induce local muscle fatigue, as well as the way that fatigue is quantified. For example, many researchers have defined local muscle fatigue as the exercise-induced decline of the peak torque (Sharpe and Miles, 1993; Sterner et al., 1998; Kazutomo et al., 2004; Ribeiro and Oliveira, 2007). However, these studies did not use surface electromyography (sEMG) to confirm whether their fatigue protocols resulted in a decrease in the frequency of motor unit discharge (Dideriksen et al., 2012) and muscle conduction velocity (Enoka and Duchateau, 2008).

The benefit of using sEMG to quantify the physiological responses accompanying local muscle fatigue is that frequency domain analyses [e.g., Fast Fourier Transform (FFT)] are capable of reliably measuring the spectrum shift to lower frequencies while temporal parameters [e.g., Root Mean Square (RMS)] measure the typical increase in signal amplitude (Merletti and Parker, 2004; Cifrek et al., 2009; González-Izal et al., 2010). A second benefit of using sEMG, rather than peak torque, to measure fatigue, is its application to clinical rehabilitation settings. Post-stroke upper limb hemiplegia alters the neural strategies underlying force regulation, resulting in decreased voluntary muscle activation (Bowden et al., 2014), altered motor unit (MU) firing rates (McNulty et al., 2014), a reduced ability to modulate MU firing (Mottram et al., 2014) and abnormal MU recruitment patterns (Hu et al., 2013). As such, fatigue protocols in which participants are required to generate muscle force levels during the performance of maximal voluntary torque movements are not appropriate for stroke patients.

In recent years, collaborative work by our laboratories has focused on developing and testing robotic devices for upper extremity neurorehabilitation in healthy (Mugnosso et al., 2018), and neurologically impaired populations (Squeri et al., 2011; De Santis et al., 2015; Marini et al., 2017b). The advantage of robotic devices is that they have better diagnostic and prognostic precision than current clinical evaluation measures, resulting in a greater sensitivity to subtle differences in neurological status (Rinderknecht et al., 2016). However, in order to understand sensorimotor functions in these populations, it is important that we have a clear understanding of normative function in neurologically and physically healthy individuals. Such data can enable the comparison of measurement values during initial clinical assessment and at later periods in the rehabilitation life cycle.

As such, the aim of this study was to examine the effects of local muscle fatigue on wrist proprioceptive acuity using a robotic device specifically designed for human neuromotor control and rehabilitation (Masia et al., 2009) and ensuring the rise of

[1]Although there is some debate over the concept of proprioception, we adopt the terminology used by Ribeiro et al. (2007) who defined proprioception as the cumulative neural input to the central nervous system from specialized mechanoreceptors located in the joint capsule, ligament, muscle, tendon, and skin.

muscle fatigue through frequency domain analyses captured via sEMG. To this end, sixteen participants first performed an ipsilateral wrist flexion/extension joint position matching (JPM) test, then a series of planar wrist flexion and extension movements while immersed in a viscoelastic force field that induced local muscle fatigue in the flexor carpi radialis (FCR) muscle, followed immediately by a second block of the JPM test. It is hypothesized that the fatigue protocol would lead to a decrease in JPS performance in the flexion direction. However, because the fatigue protocol targets the FCR, but not the extensor carpi radialis (ECR) muscles, it is hypothesized that there would be no change in proprioceptive acuity in the extension direction.

MATERIALS AND METHODS

Participants

Sixteen neurologically and physically healthy right-handed individuals (seven males and nine females, mean age 27.6 ± 2.9 years) participated in the current study. Videogame use habits was assessed by querying the amount of time participants spend playing games on weekdays and weekends, and by calculating the average daily amount of game playing time. Overall, participants spent 2.83 ± 0.80 h/day playing video games, with no significant difference between male and female participants (2.90 and 2.78, respectively). The study was carried out at the Motor Learning, Assistive and Rehabilitation Robotics Laboratory of the Istituto Italiano di Tecnologia (Genoa, Italy) in accordance with the Declaration of Helsinki and the local ethical committee (Liguria Region: n. 222REG2015).

Experimental Apparatus

The experiment involved the use of a haptic device [hereafter called Wristbot (Masia et al., 2009)] a 3 degrees of freedom (DoFs) fully backdrivable robotic manipulandum developed specifically for the study of human motor control and sensorimotor rehabilitation (**Figure 1A**). The Wristbot's range of motion (ROM) in the three DoFs approximates that of the human wrist [flexion/extension (FE): human = 65°/70°, robot = 62°/62°; radial/ulnar deviation (RUD): human = 15°/30°, robot = 45°/40°; pronation/supination (PS): human = 90°/90°, robot: 60°/60°]. The Wristbot is powered by four brushless motors that provide accurate haptic rendering, and compensate for the weight and inertia of the device. The motors can provide a maximum torque of 1.57 Nm in the FE DoF, 3.81 Nm in the RUD DoF, and 2.87 Nm in the PS DoF. Angular rotations on the three axes are acquired by means of high-resolution incremental encoders with a maximum error of ±0.17°. A virtual reality environment was integrated into the system and provided users with visual feedback during the fatigue task.

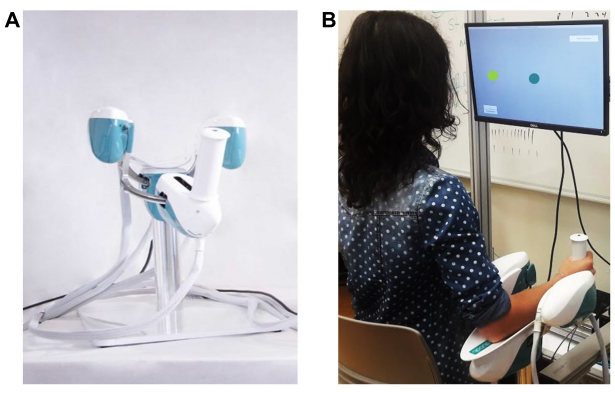

FIGURE 1 | Experimental setup depicting the Wristbot **(A)** and a subject performing the Joint Position Matching test **(B)**.

A multichannel surface electromyography (sEMG) system (OTBiolab EMG-USB2+) was used to quantify activity of right extensor carpi radialis and flexor carpi radialis muscles (ECR and FCR, respectively) during the experiment. The sEMG system was set to collect data at 2048 Hz, with a gain of 1000, and a hardware bandpass filter (10–900 Hz). Following standard electrode preparation (Hermens et al., 1999), Ag/AgCl electrodes were placed on the ECR and FCR with an interelectrode distance of 26 mm. At the beginning of the fatigue task, a trigger signal was sent from the Wristbot to the sEMG base unit to ensure that the sEMG and Wristbot kinematic signals were correctly segmented and analyzed.

Experimental Protocol

Prior to the experiment, participant provided written informed consent, after which his/her handedness was evaluated using the Edinburgh Handedness Inventory (Oldfield, 1971). Subsequently, the participant sat in front of the experimental setup, so that the participant's body midline was vertically arranged with the computer monitor (**Figure 1B**), and grasped the Wristbot handle with his/her right hand. Then the experimenter ensured that the participant's wrist axes were in correct alignment with the Wristbot, and used soft bands to strap the forearm to the mechanical support to ensure that the alignment would be maintained across the experimental protocol.

Participants first performed an ipsilateral Joint Position Matching (JPM) test (**Figure 2A**). Test instructions were explained to the participants, after which they performed 10 practice trials to familiarize themselves with the task and with the robot. Once the experimenter answered any of the participants' questions, the participants' vision was blocked with a pair of opaque glasses and the alignment of their wrist was rechecked. At the start of each trial, a high-frequency auditory cue sounded and the Wristbot moved the wrist from the start position (0°, neutral) to a determined angular position (passive reaching phase), and after 3 s brought the Wristbot handle back to the start position (passive return phase). A low-frequency auditory cue then sounded, and the participant moved actively the robot handle to the remembered target position and pressed the handheld response button when they believed they were in the correct position (active matching phase). The Wristbot then returned the robot handle to the start position (return phase). The targets were randomly presented at 48° of ROM in the FE DoF (with a random shift of ±0.5° to prevent learning effects). Participants performed 18 trials in the flexion DoF and 18 in the extension DoF, yielding a total of 36 initial JPM test trials.

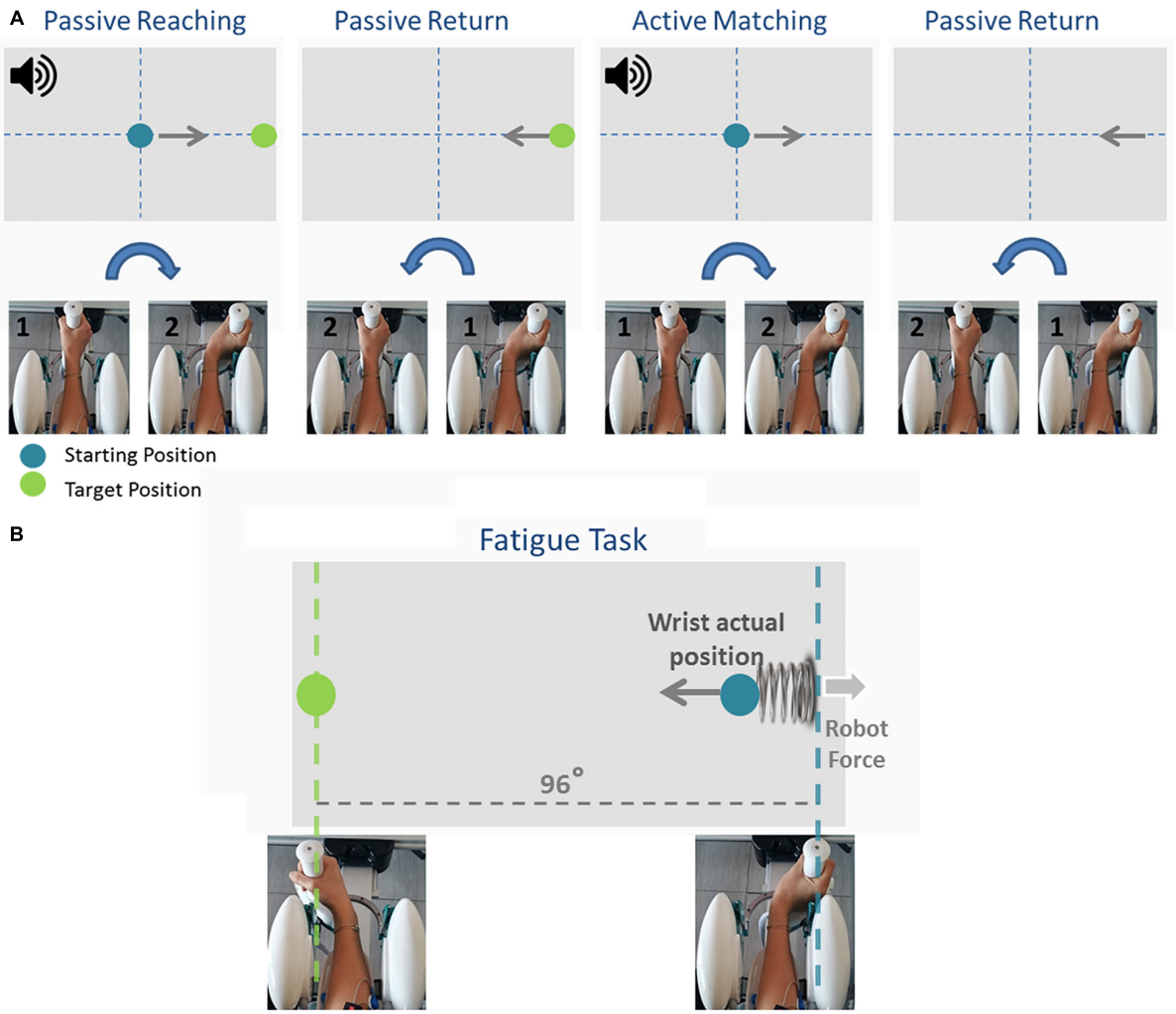

FIGURE 2 | The temporal sequence of the Joint Position Matching task and the Fatigue task. During the Joint Position Matching task **(A)**, the robot moved the participant's hand to a target location, held it there for 3 s, then brought the hand back to the start position. The participant then moved the robot handle to the remembered target position. During the fatigue task **(B)**, participants performed alternating flexion/extension movements, and the robotic device applied a viscoelastic force field that provided assistive forces to wrist extension movements and resistive forces during wrist flexion movements.

Participants subsequently performed a series of planar wrist flexion and extension movements while immersed in a viscoelastic force field that induced local muscle fatigue in the FCR muscles. The targets were presented at 48° of FE ROM in an alternating fashion, and participants moved the cursor to the target position using the visual feedback of the hand position provided on the computer screen (**Figure 2B**). A speed constraint prevented subjects resting between trials, and in the event that the participant did not reach the target within 1.5 s, the color of the cursor changed from green to yellow. The applied viscoelastic force field provided assistive forces to wrist extension movements and resistive forces during wrist flexion movements (see Eq. 1):

$$F = -k\left(\theta - \theta_{eq}\right) - b\dot{\theta} \quad (1)$$

where θ_{eq} = 48° is the virtual spring equilibrium angle, θ is the actual wrist position that moves at speed $\dot{\theta}$. k (= 22.2 N/rad for female and = 27.7 N/rad for male subjects, respectively) and b(= 1.77 Ns/rad) are the stiffness of the elastic force and the damping coefficient of the viscous contribution. The difference in the stiffness value between genders was based on the empirical literature demonstrating that female grip force values are 30% lower than male grip force values (Bäckman et al., 1995; Phillips et al., 2000), and enabled us to obtain comparable results for all participants. Participants were instructed to perform the fatigue task until the experienced forearm fatigue prevented them from flexing or extending the wrist. During the fatigue task, the experimenter verbally encouraged participants to sustain the task as long as possible to ensure the maximum level of subjective fatigue was reached (i.e., "completely fatigued" on the Borg CR-10 scale of perceived fatigue (Borg, 1990).

After the fatigue task, participants immediately completed a second block of the JPM test. The mean inter-task interval

between the fatiguing protocol and the second JPM task was 45 ± 12 s.

Data and Statistical Analysis

Robot encoders provided data at a 100 Hz sample rate which were used to extract angular displacements and angular velocities. The acquired data were processed with a sixth-order Savitzky–Golay low-pass filter (10 Hz cut-off frequency). Wrist proprioceptive acuity was evaluated using the metrics *Error Bias* and *Variability* (Schmidt, 1988; Dukelow et al., 2010; Marini et al., 2016a, 2018). *Error Bias* is defined as the average over the 18 trials, in each of the two directions (flexion and extension), of the difference between the reference joint angle (θ_T) and the participants matching position (θ_i) in the *i*-trial.

$$Error\ Bias = \frac{\sum_{tr=1:18}(\theta_i - \theta_T)}{18} \quad (2)$$

Error Bias provides information about participants' response bias: it is the directional distance evaluated as algebraic summation between the ideal proprioceptive target and the actual wrist position, indicating the subjects' tendency in undershooting (negative *Error Bias*) or overshooting (positive *Error Bias*) the target. *Variability* is defined as the standard deviation of matching position (θ_i) across the 18 repetitions in each of the two directions (flexion and extension).

$$Variability = \mathrm{StD}(\theta_{1:18}) \quad (3)$$

While the *Error Bias* indicates error amplitude and is a direct measure of proprioceptive acuity and accuracy, the *Variability* measures the consistency across the 18 repetitions of the same target, thus providing information about precision.

To ascertain the occurrence of muscular fatigue, we first filtered the sEMG signals, recorded during the fatigue task, with a band-pass filter (5–350 Hz). The trajectory data was then extracted from the robot, and allowed us to determine the concentric phase of each movement. The sEMG signal of the FCR was analyzed during flexion movements, while ECR muscle activity was analyzed during extension movements. Indeed, as can be seen in **Figure 3**, the wrist kinematics recorded by the robot enabled us to segment the sEMG signal of the flexor and extensor carpi radialis during flexion and extension movements, separately.

For each movement, we then computed a single value of the *Mean Frequency* of the sEMG spectrum (Cifrek et al., 2009) using the formula:

$$Mean\ Frequency = \frac{\int_0^{\frac{fs}{2}} fP(f)\,df}{\int_0^{\frac{fs}{2}} P(f)df} \quad (4)$$

where *fs* is the sampling frequency, and $P(f)$ is the power spectrum density (PSD) of the signal. A Fourier transform of the autocorrelation function of the signal was employed to obtain a representation of the sEMG signal into the frequency domain, while the PSD was computed using the periodogram. Therefore, *N Mean Frequency* values were obtained for each subject, with *N* reflecting the total number of movements performed by the subjects.

The obtained *Mean Frequency* values were then fitted using a second order polynomial function based on mean least square approximation. To compare data among participants, *Mean Frequency* curves were interpolated separately for each participant, were normalized respect to the value of the first trial, and then averaged among subjects.

In addition to spectral analysis, we ensured the occurrence of muscle fatigue by examining the sEMG signal amplitude. Following the same segmentation and fitting procedures as above, we calculated the Root Mean Square parameter (*RMS*) on the filtered and rectified sEMG signal using the formula:

$$RMS = \sqrt{\frac{1}{N}\sum_{i=1}^{N} x_i^2} \quad (5)$$

where x_i is the i^{th} sample of the sEMG signal, and *N* is the number of samples in the concentric phase of each movement.

Preliminary analysis did not reveal any systematic differences due to gender or video game experience. As such, potential differences effects of muscular fatigue on wrist proprioceptive acuity were examined using Repeated Measures Analysis of Variance (RM ANOVA) with Time (pre, post) and Direction (flexion, extension) as the within subjects factors, separately for the variables *Error Bias* and *Variability*.

RESULTS

Participants performed an average of 146 ± 19 movements, during which the *Mean Frequency* of the sEMG signals decreased (**Figure 4** depicts the normalized *Mean Frequency* curves for the flexor and extensor muscles (averaged across participants), with the corresponding goodness of the fit (r^2) and *rmse*). Overall, the *Mean Frequency* of the flexor muscles exhibited a consistent decrease than that of the extensor muscles. Indeed, the average decrease in flexor muscle *Mean Frequency* was 25% of the original value (average r^2 = 0.93), while extensor muscle *Mean Frequency* decreased by only 10% (average r^2 = 0.57). The shift toward lower frequencies was accompanied by an increase in the signal amplitude, as shown by the *RMS* curves in **Figure 5**. Similarly, the rise of the *RMS* values was greater for the flexor than in the extensor muscles. Indeed, *RMS* reached 154% of the initial value in the flexor muscle (average r^2 = 0.52), while *RMS* reached 98% in the extensor muscle (average r^2 = 0.17).

Individual results of the difference between the *Error Bias* after and before the fatigue task showed that 13 subjects out of 16 had a negative difference in the flexion direction (see **Figure 6A**) resulting from a greater overestimation of the reference position after the fatigue task. However, this trend was not present for targets located in the extension direction (**Figure 6B**).

Results of the mean *Error Bias* values prior to and after the fatigue protocol are displayed in **Figure 7A**. Analysis indicated that there was a significant main effect of Time, with participants exhibiting a greater tendency to undershoot

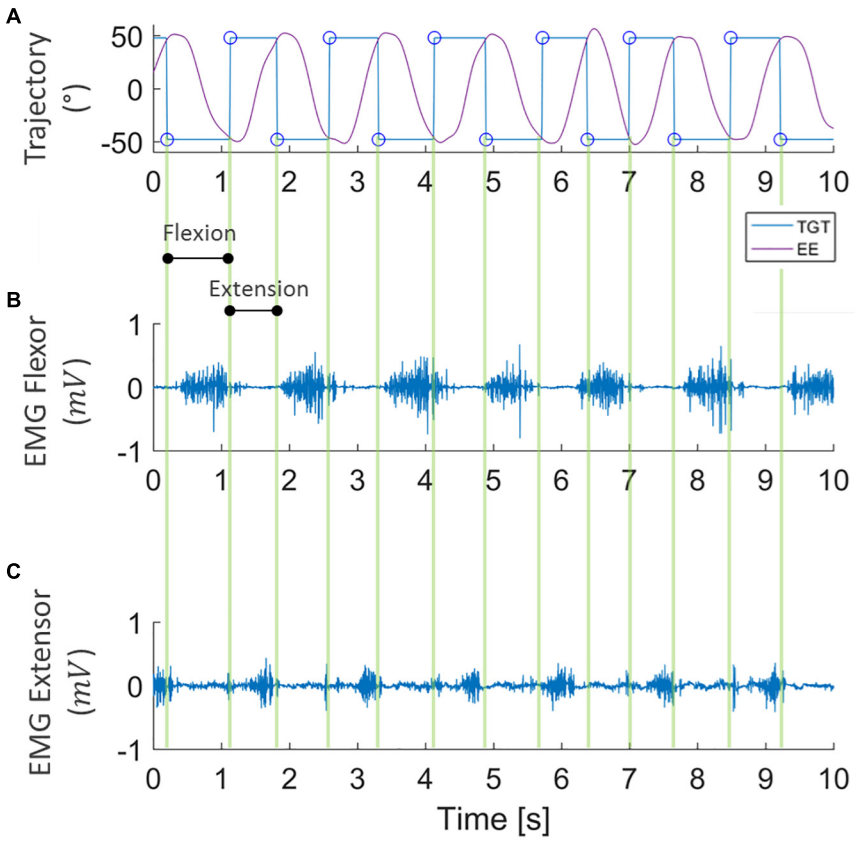

FIGURE 3 | Example of data segmentation. Kinematic data collected from robot encoders **(A)** where purple lines represent the end-effector trajectory (EE) along flexion-extension to reach the target (TGT) that moves between ±48° (blue line). sEMG signal of *flexor* and *extensor carpi radialis* (**B**,**C**, respectively) during the task, segmented into flexion and extension directions.

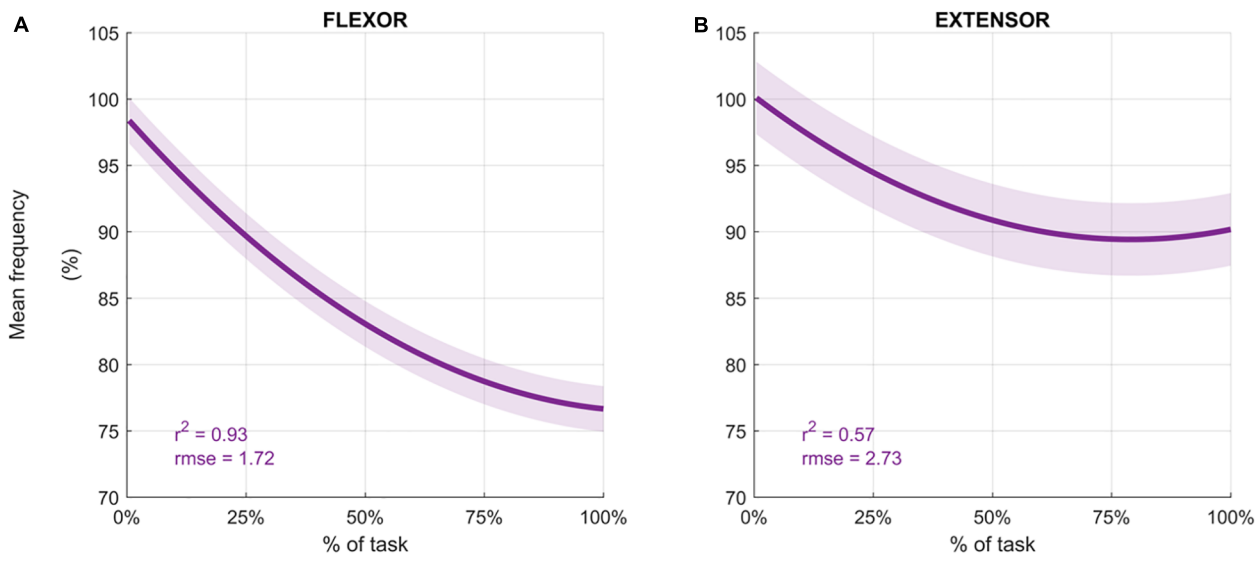

FIGURE 4 | Average mean frequency values (%) for the flexor carpi radialis **(A)** and extensor carpi radialis muscles **(B)** during the fatigue protocol. Mean frequency (Hz) was normalized to the initial frequency of each sequence and averaged across participants to obtain the percentage. Depicted data was fitted with a second order polynomial function (dark purple) and standard error (light purple).

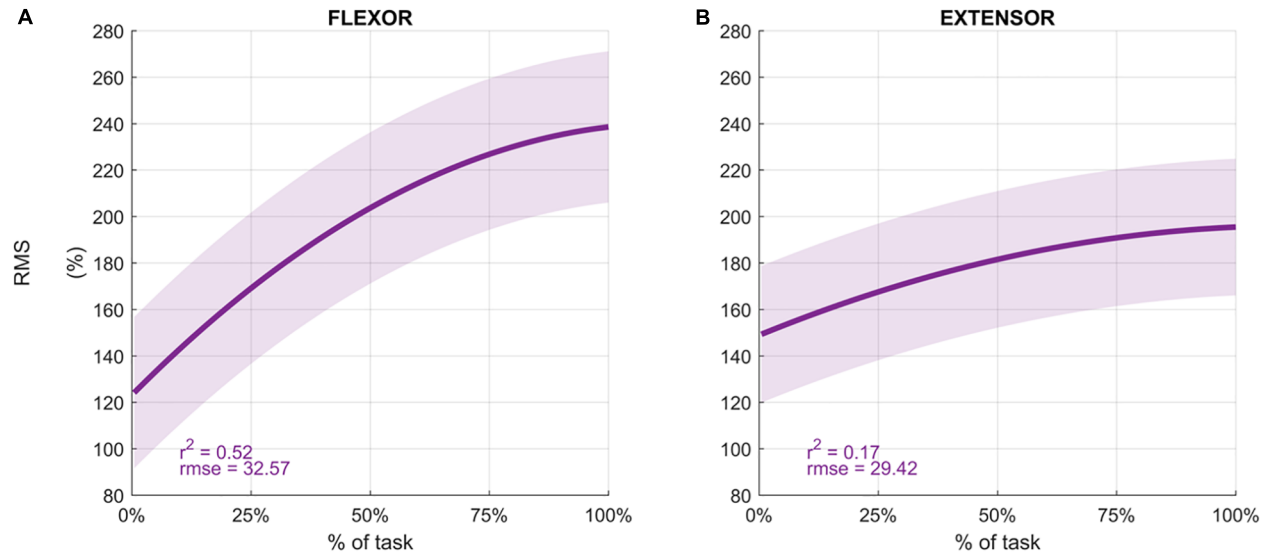

FIGURE 5 | Average Root Mean Square values (%) for the flexor carpi radialis **(A)** and extensor carpi radialis muscles **(B)** during the fatigue protocol. RMS was normalized to the initial value of each sequence and averaged across participants to obtain the percentage. Depicted data was fitted with a second order polynomial function (dark purple) and standard error (light purple).

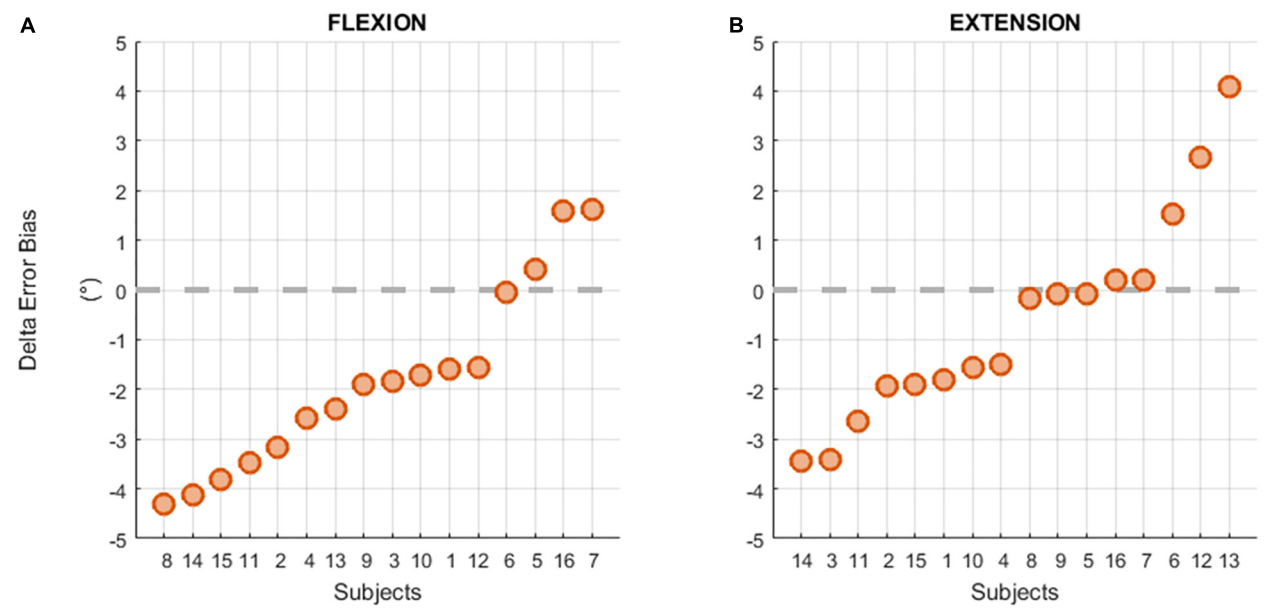

FIGURE 6 | Individual differences between the *Error Bias* before and after the fatigue task in flexion **(A)** and extension **(B)** movements.

the target prior to the fatigue protocol (−1.535°) compared to after the fatigue protocol (−0.325°) regardless from the direction, $F(1,15) = 8.607$, $p = 0.010$, $\eta^2_p = 0.365$. There was also a significant Time × Direction interaction, $F(1,15) = 4.574$, $p = 0.049$, $\eta^2_p = 0.234$. *Post hoc* analysis indicated that *Error Bias* values were similar before and after (pre = −1.852°, post = −1.237°) the fatigue protocol for the extension direction and reflected a tendency to undershoot the target. In contrast, the fatigue protocol had a significant effect on movements performed in flexion direction, with participants exhibiting a tendency to undershoot the target before the fatigue protocol (−1.218°), but overshooting after the fatigue protocol (0.587°).

Mean wrist proprioceptive acuity *Variability* is shown in **Figure 7B**. RM ANOVA revealed that mean *Variability* was similar regardless of direction [$F(1,15) = 2.942$, $p = 0.107$, $\eta^2_p = 0.164$] and time [$F(1,15) = 1.221$, $p = 0.287$, $\eta^2_p = 0.075$]. In addition, the interaction between Direction and Time was non-significant [$F(1,15) = 0.945$, $p = 0.347$, $\eta^2_p = 0.059$], indicating

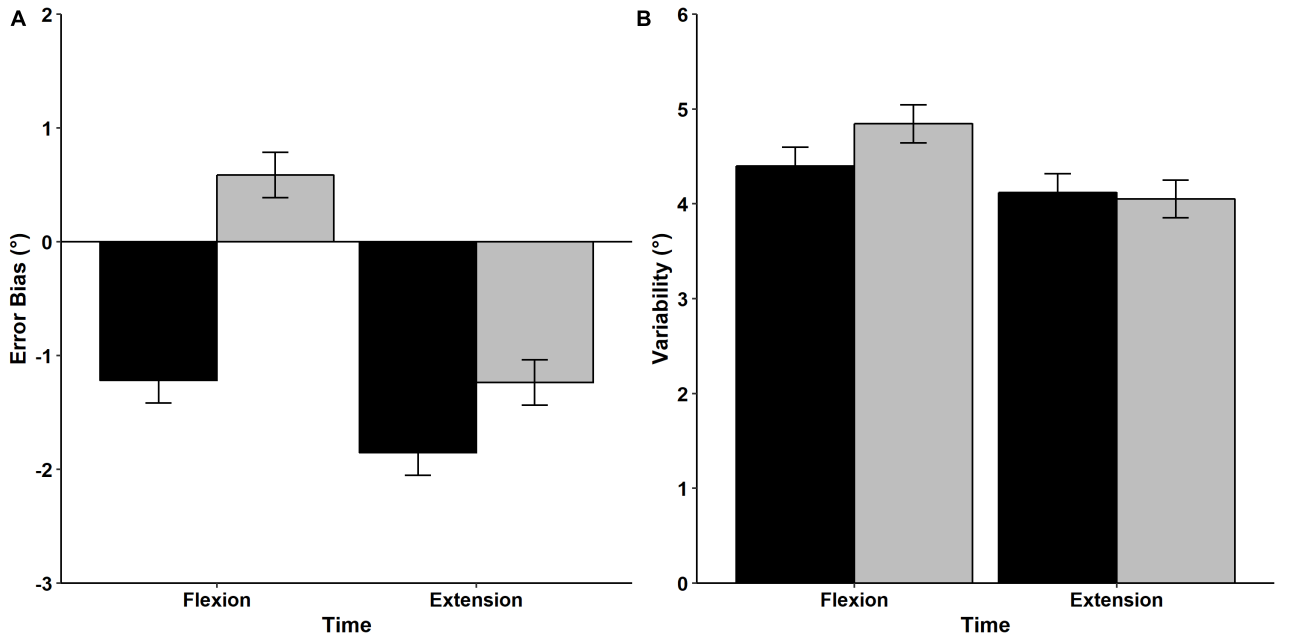

FIGURE 7 | Mean and standard error values of *Error Bias* **(A)** and *Variability* **(B)** for movements performed in the flexion and extension directions before (black bars) and after (gray bars) the fatigue task.

that movement *Variability* was not influenced by the fatigue protocol or movement direction.

DISCUSSION

This study utilized a high resolution robotic device and sEMG to examine the effects of local muscle fatigue on wrist proprioceptive acuity in healthy young adults. Congruent with prior research on the shoulder (Voight et al., 1996; Carpenter et al., 1998) and knee joints (Skinner et al., 1986; Lattanzio et al., 1997) we found that local muscle fatigue induces impairments in proprioceptive acuity. Prior research into this line of work used high-intensity isometric or isokinetic exercise protocols to elicit local muscle fatigue (Forestier et al., 2002; Lee et al., 2003; Walsh et al., 2004). However, we designed and implemented a fatigue task that involved concentric contractions restricted to the flexor muscles so that the impact of the fatigue task on the forearm extensor muscles could be minimized, and any potential damage to all forearm muscles could be avoided (Proske and Morgan, 2001). Utilizing this protocol, we were able to demonstrate that a high-resistive viscoelastic force field that targets only the FCR muscles is capable of eliciting a significant change in JPS response bias for the FCR, but not the ECR, muscle. Additionally, examining proprioceptive acuity in both flexion and extension muscles provided data regarding the repeatability of the measures. The lack of significant differences in proprioceptive acuity for the extension direction indicates that participants were equally focused on the task during the two repetitions of the test, thus ensuring that the changes in repositioning bias in flexion targets were entirely due to the fatigued FCR.

There is now a growing corpus of literature indicating that the muscle spindles are the primary receptor involved in the sense of position, whereas Golgi tendon organs, joint receptors, and skin receptors provide only limited information about joint movements throughout the normal range of motion (Proske and Gandevia, 2009). Muscle spindles are mechanoreceptors that are stretch-sensitive, and contribute to a person's ability to perceive joint positions based upon information regarding the length and velocity of muscle contraction. As the muscle lengthens, there is a proportional increase in the discharge of the muscle spindles. Thus, the CNS can approximate the position of the limb based on the spindle firing rate and muscle length. However, when the muscle is fatigued, the high concentration of metabolites and inflammatory products of muscular contraction (e.g., bradykinin, arachidonic acid, prostaglandin E2, potassium, and lactic acid) causes the activation of nociceptors, greater alpha-gamma co-activation, and an increase in the muscle spindle discharge rate (Pedersen et al., 1998).

In the context of the current experiment, we attribute the changes in proprioceptive accuracy and precision to the differential impact that muscle fatigue exerts on muscle spindle discharge (Pedersen et al., 1998). Specifically, we hypothesize that muscle spindle discharge was affected by muscle fatigue, which resulted in the significant reduction in flexion direction proprioceptive accuracy. However, although affected, the muscle spindle discharge rate did not vary throughout the execution of the test. Consequently, the altered muscle spindle discharge rate did not prevent subjects from repeating similar errors in repositioning during the whole session as indicated by the absence of significant differences in *Variability* values across time. Therefore, the precise methods used in the present study

not only clarifies conflicting findings from previous studies (Sterner et al., 1998; Kazutomo et al., 2004; Givoni et al., 2007), but also confirms that muscle fatigue decreases proprioception acuity by affecting the muscle spindles, but that muscle spindle discharge rate may not vary as long as the muscle is in a fatigued condition. The small but significant post-fatigue increase in *Error Bias* is congruent with prior studies that have reported a 1° difference in proprioceptive acuity, regardless of the examined joint [knee (Lattanzio et al., 1997) ankle (Forestier et al., 2001), elbow (Walsh et al., 2004)] and modality used to induce muscle fatigue (MVC or isokinetic movements). However, whether the magnitude of decrease in proprioceptive acuity is clinically relevant is still an open question (Refshaug, 2002), and the relationship between JPS acuity declines and alterations in motion or joint instability cannot be determined from the present work. The robotic device used in the present study was designed for use by both engineers and clinicians, and as such it is possible to adapt the task protocols to the needs of individual patients. In particular, the methodology of the present study may provide insights regarding proprioception sense in individuals that frequently experience muscle fatigue (e.g., individuals with neuromuscular disorders), as well as illuminate the extent to which symptoms of fatigue impact their motor control. In addition to the robotic systems relevance to populations with neuromotor dysfunction, the employed methodologies of the current study could add meaningful information regarding the prevention of injuries due to the fatiguing nature of manual work, or the maintenance of high level motor performance (i.e., in the case of athletes).

The efficacy of the fatiguing protocol used in the present study is supported by both the frequency and time domain analyses of the muscular signals captured via sEMG, in which a concurrent decrease in mean frequency and an increase in signal amplitude was observed. Time domain analysis indicated that a greater increase in *RMS* for the FCR muscle compared to the ECR muscle. Supporting this work, the frequency domain analysis revealed a 25% decrease in *Mean Frequency* for the FCR muscle, and 10% decrease in *Mean Frequency* for the ECR muscle, both of which are greater than the 8% decrease in *Mean Frequency* indicative of fatigue onset forwarded by prior research (Öberg et al., 1990). While at first glance (and according to the threshold proposed by Öberg et al., 1990) it may appear that the fatigue protocol elicited local muscle fatigue to both the wrist extensors and flexors, it is more likely that the muscle activation observed for the ECR is due to the co-activation of the FCR and ECR required to provide global stability to the wrist joint (Johansson et al., 1990; Myers and Lephart, 2000) and maintain smooth and even motions (Lieber and Lieber, 2002).

Another noteworthy point regards the locus of fatigue. It is well recognized that muscle fatigue can originate from central (e.g., insufficient drive from supraspinal sites, reflex inhibition, and disfacilitation) and/or peripheral mechanisms (e.g., decreased muscle fiber conduction velocity) (cf. Taylor et al., 2016). The observed decrease in EMG mean frequency, reflective of a decline in muscle fiber conduction velocity, indicates that the fatigue protocol resulted in peripheral muscle fatigue. However, we cannot conclusively state whether central muscle fatigue occurred in our study, as we did not employ the twitch interpolation technique or calculate the fractal dimension of the sEMG interference pattern (Beretta-Piccoli et al., 2015).

In evaluating the effects of local muscle fatigue on proprioceptive acuity, it is essential that the time interval between the execution of the fatiguing protocol and the following JPM test is minimized. Prior works used one device to test proprioceptive acuity and another one to implement the fatiguing protocol (Lattanzio et al., 1997; Walsh et al., 2004; Allen et al., 2007). For example proprioception of the knee joint has been measured using a JPM task where the participant sat on the end of a table with the knee at 90°, and the experimenter passively moved the participant's limb to a target position and then back to the start position (Kazutomo et al., 2004). However, the local muscle fatiguing protocol required the participant sit on a Cybex isokinetic dynamometer and perform 60 consecutive maximum concentric knee flexion and extension contractions. We postulate that the lack of significant results found in different studies (Sharpe and Miles, 1993; Sterner et al., 1998; Kazutomo et al., 2004) may result from the amount of time that elapsed between the fatigue protocol and second proprioceptive acuity test. As such, a further novelty of the present work is the use of a robotic device that can both evaluate proprioceptive acuity and deliver the fatiguing protocol. In contrast to prior studies that had reported large intervals between the fatiguing protocol and the second JPM task (e.g., 15 min in Allen et al., 2007, 3 min in Lee et al., 2003, 5 min in Lattanzio et al., 1997), we were able to minimize the time between the execution of the fatigue task and the following JPM test to 45 $\pm$ 12 s, and as such avoided any potential muscle fatigue recovery between the two tests which could jeopardize the reliability of the JPM results. Furthermore, the use of the robotic device ensures the repeatability of the test and its high-resolution encoders guarantee the precision of the measures. Such advantages have already been exploited in previous works allowing to investigate the codification of proprioceptive information both in terms of kinesthesia (Marini et al., 2018) and joint position sense (Marini et al., 2016b, 2017a).

Our interest lies in understanding the neuromotor control mechanisms surrounding proprioceptive function, especially given that sensorimotor impairment in older adults is associated with recurrence of falls (Rossat et al., 2010) and a decline in the ability to perform functional activities (Shaffer and Harrison, 2007). It is likely that these deficits occur, in large part, due to the numerous anatomical and physiological changes that happen in the muscle spindle apparatus as people age (e.g., an increase in muscle spindle thickness (Swash and Fox, 1972), a decrease in intrafusal fibers and nuclear chain fibers (Jennekens et al., 1972; Swash and Fox, 1972; Lexell, 1992; Liu et al., 2005), and an increased proportion of type I extrafusal muscle fibers (Jennekens et al., 1972; Lexell, 1992). Further compounding this issue are changes in motor unit size, number, properties, and morphology that render older adults more prone to muscular fatigability compared to their younger counterparts (Kent-Braun et al., 2014; Hepple and Rice, 2016). Future research will aim to examine how local muscle fatigue impacts JPS acuity in aging populations, as well as determining factors (e.g., physical activity) that influence proprioceptive acuity in the aging population.

CONCLUSION

In this study, we used a high resolution robotic device and frequency domain analyses of signals captured via surface electromyography (sEMG) to examine the effects of local muscle fatigue on wrist proprioceptive acuity in 16 healthy young adults. Utilizing a high-resistive robotic task to induce muscle fatigue of the flexor carpi radialis (FCR) muscle, we found that the fatigue protocol had a significant effect on movements performed in flexion direction, but not the extension direction. Thus, results of the present study indicate that an individual's estimation of wrist joint displacement (i.e., *Error Bias*), but not precision (i.e., *Variability*), is affected by muscular fatigue.

DATA AVAILABILITY STATEMENT

Raw data were generated at the Motor Learning, Assistive and Rehabilitation Robotics Laboratory of the Istituto Italiano di Tecnologia. Derived data supporting the findings of this study are available from the corresponding author, MM, on request.

ETHICS STATEMENT

The studies involving human participants were reviewed and approved by the local ethical committee (Liguria Region: n. 222REG2015). The patients/participants provided their written informed consent to participate in this study.

AUTHOR CONTRIBUTIONS

FM, MM, and JZ designed the experiment and formulated the experimental question. MM programed the robot and collected the data. FM, MM, and CH performed the data analysis and statistics and wrote the manuscript. JZ revised the final version of the manuscript.

FUNDING

This study was funded by the Istituto Italiano di Tecnologia, Genoa, Italy.

REFERENCES

Ager, A. L., Roy, J.-S., Roos, M., Belley, A. F., Cools, A., and Hébert, L. J. (2017). Shoulder proprioception: how is it measured and is it reliable? A systematic review. *J. Hand Ther.* 30, 221–231. doi: 10.1016/j.jht.2017.05.003

Allen, T. J., Ansems, G. E., and Proske, U. (2007). Effects of muscle conditioning on position sense at the human forearm during loading or fatigue of elbow flexors and the role of the sense of effort. *J. Physiol.* 580, 423–434. doi: 10.1113/jphysiol.2006.125161

Aydoğ, S. T., Korkusuz, P., Doral, M. N., Tetik, O., and Demirel, H. A. (2006). Decrease in the numbers of mechanoreceptors in rabbit ACL: the effects of ageing. *Knee Surg. Sports Traumatol. Arthrosc.* 14, 325–329. doi: 10.1007/s00167-005-0673-2

Bäckman, E., Johansson, V., Häger, B., Sjöblom, P., and Henriksson, K. G. (1995). Isometric muscle strength and muscular endurance in normal persons aged between 17 and 70 years. *Scand. J. Rehabil. Med.* 27, 109–117.

Beretta-Piccoli, M., D'Antona, G., Barbero, M., Fisher, B., Dieli-Conwright, C. M., Clijsen, R., et al. (2015). Evaluation of central and peripheral fatigue in the quadriceps using fractal dimension and conduction velocity in young females. *PLoS One* 10:e0123921. doi: 10.1371/journal.pone.0123921

Borg, G. (1990). Psychophysical scaling with applications in physical work and the perception of exertion. *Scand. J. Work. Environ. Health* 16, 55–58. doi: 10.2307/40965845

Bowden, J. L., Taylor, J. L., and McNulty, P. A. (2014). Voluntary activation is reduced in both the more- and less-affected upper limbs after unilateral stroke. *Front. Neurol.* 5:239. doi: 10.3389/fneur.2014.00239

Burke, J. R., Schutten, M. C., Koceja, D. M., and Kamen, G. (1996). Age-dependent effects of muscle vibration and the Jendrassik maneuver on the patellar tendon reflex response. *Arch. Phys. Med. Rehabil.* 77, 600–604. doi: 10.1016/s0003-9993(96)90302-0

Carpenter, J. E., Blasier, R. B., and Pellizzon, G. G. (1998). The effects of muscle fatigue on shoulder joint position sense. *Am. J. Sports Med.* 26, 262–265. doi: 10.1177/03635465980260021701

Cifrek, M., Medved, V., Tonković, S., and Ostojić, S. (2009). Surface EMG based muscle fatigue evaluation in biomechanics. *Clin. Biomech.* 24, 327–340. doi: 10.1016/j.clinbiomech.2009.01.010

De Santis, D., Zenzeri, J., Casadio, M., Masia, L., Riva, A., Morasso, P., et al. (2015). Robot-assisted training of the kinesthetic sense: enhancing proprioception after stroke. *Front. Hum. Neurosci.* 8:1037. doi: 10.3389/fnhum.2014.01037

Dideriksen, J. L., Negro, F., Enoka, R. M., and Farina, D. (2012). Motor unit recruitment strategies and muscle properties determine the influence of synaptic noise on force steadiness. *J. Neurophysiol.* 107, 3357–3369. doi: 10.1152/jn.00938.2011

Dukelow, S. P., Herter, T. M., Moore, K. D., Demers, M. J., Glasgow, J. I., Bagg, S. D., et al. (2010). Quantitative assessment of limb position sense following stroke. *Neurorehabil. Neural Repair* 24, 178–187. doi: 10.1177/1545968309345267

Enoka, R. M., and Duchateau, J. (2008). Muscle fatigue: what, why and how it influences muscle function. *J. Physiol.* 586, 11–23. doi: 10.1113/jphysiol.2007.139477

Forestier, N., Teasdale, N., and Nougier, V. (2001). *Alteration of the Position Sense at the Ankle Induced by Muscular Fatigue In Humans. Academia.edu*. Available at: http://www.academia.edu/download/43236853/Alteration_of_the_position_sense_at_the_20160301-13544-1opji3g.pdf (accessed September 13, 2018).

Forestier, N., Teasdale, N., and Nougier, V. (2002). *Alteration of the Position Sense at the Ankle Induced by Muscular Fatigue in Humans. Academia.edu*. Available at: http://www.academia.edu/download/43236853/Alteration_of_the_position_sense_at_the_20160301-13544-1opji3g.pdf (accessed September 13, 2018).

Givoni, N. J., Pham, T., Allen, T. J., and Proske, U. (2007). The effect of quadriceps muscle fatigue on position matching at the knee. *J. Physiol.* 584, 111–119. doi: 10.1113/jphysiol.2007.134411

Goble, D. J., and Brown, S. H. (2009). Dynamic proprioceptive target matching behavior in the upper limb: effects of speed, task difficulty and arm/hemisphere asymmetries. *Behav. Brain Res.* 200, 7–14. doi: 10.1016/j.bbr.2008.11.034

Goble, D. J., Coxon, J. P., Van Impe, A., Geurts, M., Van Hecke, W., Sunaert, S., et al. (2012). The neural basis of central proprioceptive processing in older versus younger adults: an important sensory role for right putamen. *Hum. Brain Mapp.* 33, 895–908. doi: 10.1002/hbm.21257

González-Izal, M., Malanda, A., Navarro-Amézqueta, I., Gorostiaga, E. M., Mallor, F., Ibañez, J., et al. (2010). EMG spectral indices and muscle power fatigue during dynamic contractions. *J. Electromyogr. Kinesiol.* 20, 233–240. doi: 10.1016/j.jelekin.2009.03.011

Good, C. D., Johnsrude, I. S., Ashburner, J., Henson, R. N. A., Friston, K. J., and Frackowiak, R. S. J. (2001). A voxel-based morphometric study of ageing in 465 normal adult human brains. *Neuroimage* 14, 21–36. doi: 10.1006/nimg.2001.0786

Hepple, R. T., and Rice, C. L. (2016). Innervation and neuromuscular control in ageing skeletal muscle. *J. Physiol.* 594, 1965–1978. doi: 10.1113/JP270561

Hermens, H. J., Freriks, B., Merletti, R., Stegeman, D., Blok, J., Rau, G., et al. (1999). *SENIAM - Deliverable 8 - European Recommendations for*

Surface ElectroMyoGraphy Chapter. Available at: http://www.seniam.org/pdf/contents8.PDF (accessed April 23, 2019).

Hertel, J. (2008). Sensorimotor deficits with ankle sprains and chronic ankle instability. *Clin. Sports Med.* 27, 353–370. doi: 10.1016/J.CSM.2008.03.006

Hiemstra, L. A., Lo, I. K. Y., and Fowler, P. J. (2001). Effect of fatigue on knee proprioception: implications for dynamic stabilization. *J. Orthop. Sport. Phys. Ther.* 31, 598–605. doi: 10.2519/jospt.2001.31.10.598

Hu, X., Rymer, W. Z., and Suresh, N. L. (2013). Motor unit pool organization examined via spike-triggered averaging of the surface electromyogram. *J. Neurophysiol.* 110, 1205–1220. doi: 10.1152/jn.00301.2012

Hughes, C. M. L., Tommasino, P., Budhota, A., and Campolo, D. (2015). Upper extremity proprioception in healthy aging and stroke populations, and the effects of therapist- and robot-based rehabilitation therapies on proprioceptive function. *Front. Hum. Neurosci.* 9:120. doi: 10.3389/fnhum.2015.00120

Jeannerod, M. (1988). *The Neural and Behavioural Organization of Goal-Directed Movements*. Oxford: Oxford University Press.

Jennekens, F. G., Tomlinson, B. E., and Walton, J. N. (1972). The extensor digitorum brevis: histological and histochemical aspects. *J. Neurol. Neurosurg. Psychiatry* 35, 124–132. doi: 10.1136/jnnp.35.1.124

Johansson, H., Sjölander, P., and Sojka, P. (1990). Activity in receptor afferents from the anterior cruciate ligament evokes reflex effects on fusimotor neurones. *Neurosci. Res.* 8, 54–59. doi: 10.1016/0168-0102(90)90057-l

Ju, Y.-Y., Wang, C.-W., and Cheng, H.-Y. K. (2010). Effects of active fatiguing movement versus passive repetitive movement on knee proprioception. *Clin. Biomech.* 25, 708–712. doi: 10.1016/J.CLINBIOMECH.2010.04.017

Karagiannopoulos, C., Watson, J., Kahan, S., and Lawler, D. (2019). The effect of muscle fatigue on wrist joint position sense in healthy adults. *J. Hand Ther.* doi: 10.1016/J.JHT.2019.03.004 [Epub ahead of print].

Kararizou, E., Manta, P., Kalfakis, N., and Vassilopoulos, D. (2005). Morphometric study of the human muscle spindle. *Anal. Quant. Cytol. Histol.* 27, 1–4.

Kazutomo, M., Yasuyuki, I., Eiichi, T., Yoshihisa, O., Hironori, O., and Satoshi, T. (2004). The effect of local and general fatigue on knee proprioception. *Arthrosc. J. Arthrosc. Relat. Surg.* 20, 414–418. doi: 10.1016/J.ARTHRO.2004.01.007

Kent-Braun, J. A., Callahan, D. M., Fay, J. L., Foulis, S. A., and Buonaccorsi, J. P. (2014). Muscle weakness, fatigue, and torque variability: effects of age and mobility status. *Muscle Nerve* 49, 209–217. doi: 10.1002/mus.23903

Kim, G. H., Suzuki, S., and Kanda, K. (2007). Age-related physiological and morphological changes of muscle spindles in rats. *J. Physiol.* 582, 525–538. doi: 10.1113/jphysiol.2007.130120

Lattanzio, P. J., Petrella, R. J., Sproule, J. R., and Fowler, P. J. (1997). Effects of fatigue on knee proprioception. *Clin. J. Sport Med.* 7, 22–27. doi: 10.1097/00042752-199701000-00005

Lee, H.-M., Liau, J.-J., Cheng, C.-K., Tan, C.-M., and Shih, J.-T. (2003). Evaluation of shoulder proprioception following muscle fatigue. *Clin. Biomech.* 18, 843–847. doi: 10.1016/S0268-0033(03)00151-7

Lexell, J. (1992). What is the effect of aging on type II muscle fibers? The Sports-related injuries and illnesses in paralympic sport study (SRIIPSS) view project. *Artic. J. Neurol. Sci.* 107, 250–251. doi: 10.1016/0022-510X(92)90297-X

Lieber, R. L., and Lieber, R. L. (2002). *Skeletal Muscle Structure, Function & Plasticity: The Physiological Basis of Rehabilitation*. Philadelphia, PA: Lippincott Williams & Wilkins.

Liu, J.-X., Eriksson, P.-O., Thornell, L.-E., and Pedrosa-Domellöf, F. (2005). Fiber Content and myosin heavy chain composition of muscle spindles in aged human biceps brachii. *J. Histochem. Cytochem.* 53, 445–454. doi: 10.1369/jhc.4A6257.2005

Marini, F., Contu, S., Hughes, C. M. L., Morasso, P., and Masia, L. (2016a). "Robotic assessment of manual asymmetries in unimanual and bimanual wrist joint position sense," in *Proceedings of the IEEE RAS and EMBS International Conference on Biomedical Robotics and Biomechatronics*, Singapore.

Marini, F., Squeri, V., Morasso, P., and Masia, L. (2016b). Wrist proprioception: amplitude or position coding? *Front. Neurorobot.* 10:13. doi: 10.3389/fnbot.2016.00013

Marini, F., Contu, S., Morasso, P., Masia, L., and Zenzeri, J. (2017a). "Codification mechanisms of wrist position sense," in *Proceedings of the 2017 International Conference on Rehabilitation Robotics (ICORR)*, London.

Marini, F., Hughes, C. M. L., Squeri, V., Doglio, L., Moretti, P., Morasso, P., et al. (2017b). Robotic wrist training after stroke: adaptive modulation of assistance in pediatric rehabilitation. *Rob. Auton. Syst.* 91, 169–178. doi: 10.1016/j.robot.2017.01.006

Marini, F., Ferrantino, M., and Zenzeri, J. (2018). Proprioceptive identification of joint position versus kinaesthetic movement reproduction. *Hum. Mov. Sci.* 62, 1–13. doi: 10.1016/J.HUMOV.2018.08.006

Masia, L., Casadio, M., Giannoni, P., Sandini, G., and Morasso, P. (2009). Performance adaptive training control strategy for recovering wrist movements in stroke patients: a preliminary, feasibility study. *J. Neuroeng. Rehabil.* 6:44. doi: 10.1186/1743-0003-6-44

McNulty, P. A., Lin, G., and Doust, C. G. (2014). Single motor unit firing rate after stroke is higher on the less-affected side during stable low-level voluntary contractions. *Front. Hum. Neurosci.* 8:518. doi: 10.3389/fnhum.2014.00518

Merletti, R., and Parker, P. (2004). *Electromyography: Physiology, Engineering, and Noninvasive Applications*. Piscataway, NJ: IEEE Press.

Mottram, C. J., Heckman, C. J., Powers, R. K., Rymer, W. Z., and Suresh, N. L. (2014). Disturbances of motor unit rate modulation are prevalent in muscles of spastic-paretic stroke survivors. *J. Neurophysiol.* 111, 2017–2028. doi: 10.1152/jn.00389.2013

Mugnosso, M., Marini, F., Holmes, M., Morasso, P., and Zenzeri, J. (2018). Muscle fatigue assessment during robot-mediated movements. *J. Neuroeng. Rehabil.* 15:119. doi: 10.1186/s12984-018-0463-y

Myers, J. B., and Lephart, S. M. (2000). The role of the sensorimotor system in the athletic shoulder. *J. Athl. Train.* 35, 351–363.

Öberg, T., Sandsjö, L., and Kadefors, R. (1990). Electromyogram mean power frequency in non-fatigued trapezius muscle. *Eur. J. Appl. Physiol.* 61, 362–369. doi: 10.1007/bf00236054

Oldfield, R. C. (1971). The assessment and analysis of handedness: the edinburgh inventory. *Neuropsychologia* 9, 97–113. doi: 10.1016/0028-3932(71)90067-4

Pedersen, J., Ljubisavljevic, M., Bergenheim, M., and Johansson, H. (1998). Alterations in information transmission in ensembles of primary muscle spindle afferents after muscle fatigue in heteronymous muscle. *Neuroscience* 84, 953–959. doi: 10.1016/s0306-4522(97)00403-x

Phillips, B. A., Lo, S. K., and Mastaglia, F. L. (2000). Muscle force measured using "break" testing with a hand-held myometer in normal subjects aged 20 to 69 years. *Arch. Phys. Med. Rehabil.* 81, 653–661. doi: 10.1016/S0003-9993(00)90050-9

Proske, U., and Gandevia, S. C. (2009). The kinaesthetic senses. *J. Physiol.* 587, 4139–4146. doi: 10.1113/jphysiol.2009.175372

Proske, U., and Morgan, D. L. (2001). Muscle damage from eccentric exercise: mechanism, mechanical signs, adaptation and clinical applications. *J. Physiol.* 537, 333–345. doi: 10.1111/j.1469-7793.2001.00333.x

Quiton, R. L., Roys, S. R., Zhuo, J., Keaser, M. L., Gullapalli, R. P., and Greenspan, J. D. (2007). Age-related changes in nociceptive processing in the human brain. *Ann. N. Y. Acad. Sci.* 1097, 175–178. doi: 10.1196/annals.1379.024

Refshaug, K. M. (2002). Proprioception and joint pathology. *Adv. Exp. Med. Biol.* 508, 95–101. doi: 10.1007/978-1-4615-0713-0_12

Resnick, S. M., Pham, D. L., Kraut, M. A., Zonderman, A. B., and Davatzikos, C. (2003). Longitudinal magnetic resonance imaging studies of older adults: a shrinking brain. *J. Neurosci.* 23, 3295–3301. doi: 10.1523/jneurosci.23-08-03295.2003

Ribeiro, F., Mota, J., and Oliveira, J. (2007). Effect of exercise-induced fatigue on position sense of the knee in the elderly. *Eur. J. Appl. Physiol.* 99, 379–385. doi: 10.1007/s00421-006-0357-8

Ribeiro, F., and Oliveira, J. (2007). Aging effects on joint proprioception: the role of physical activity in proprioception preservation. *Eur. Rev. Aging Phys. Act* 4, 71–76. doi: 10.1007/s11556-007-0026-x

Rinderknecht, M. D., Popp, W. L., Lambercy, O., and Gassert, R. (2016). Reliable and rapid robotic assessment of wrist proprioception using a gauge position matching paradigm. *Front. Hum. Neurosci.* 10:316. doi: 10.3389/fnhum.2016.00316

Rossat, A., Fantino, B., Nitenberg, C., Annweiler, C., Poujol, L., Herrmann, F. R., et al. (2010). Risk factors for falling in community-dwelling older adults: which of them are associated with the recurrence of falls? *J. Nutr. Health Aging* 14, 787–791. doi: 10.1007/s12603-010-0089-7

Sadler, C. M., and Cressman, E. K. (2019). Central fatigue mechanisms are responsible for decreases in hand proprioceptive acuity following shoulder muscle fatigue. *Hum. Mov. Sci.* 66, 220–230. doi: 10.1016/J.HUMOV.2019.04.016

Schmidt, R. A. (1988). *Motor Control and Learning: A Behavioral Emphasis*, 2nd Edn, Champaign, IL: Human Kinetics Publishers.

Schmidt, R. A., and Lee, T. D. (2005). *Motor Control and Learning: A Behavioral Emphasis*. Champaign, IL: Human Kinetics.

Shaffer, S. W., and Harrison, A. L. (2007). Aging of the somatosensory system: a translational perspective. *Phys. Ther.* 87, 193–207. doi: 10.2522/ptj.20060083

Sharpe, M., and Miles, T. (1993). Position sense at the elbow after fatiguing contractions. *Exp. Brain Res.* 94, 179–182. doi: 10.1007/BF00230480

Skinner, H. B., Wyatt, M. P., Hodgdon, J. A., Conard, D. W., and Barrack, R. L. (1986). Effect of fatigue on joint position sense of the knee. *J. Orthop. Res.* 4, 112–118. doi: 10.1002/jor.1100040115

Squeri, V., Zenzeri, J., Morasso, P., and Basteris, A. (2011). Integrating proprioceptive assessment with proprioceptive training of stroke patients. *IEEE Int. Conf. Rehabil. Robot.* 2011:5975500. doi: 10.1109/ICORR.2011.5975500

Sterner, R. L., Pincivero, D. M., and Lephart, S. M. (1998). The effects of muscular fatigue on shoulder proprioception. *Clin. J. Sport Med.* 8, 96–101. doi: 10.1097/00042752-199804000-00006

Swash, M., and Fox, K. P. (1972). The effect of age on human skeletal muscle studies of the morphology and innervation of muscle spindles. *J. Neurol. Sci.* 16, 417–432. doi: 10.1016/0022-510X(72)90048-2

Swash, M., and Fox, K. P. (1974). The pathology of the human muscle spindle: effect of denervation. *J. Neurol. Sci.* 22, 1–24. doi: 10.1016/0022-510x(74)90050-1

Taylor, J. L., Amann, M., Duchateau, J., Meeusen, R., and Rice, C. L. (2016). Neural contributions to muscle fatigue: from the brain to the muscle and back again. *Med. Sci. Sports Exerc.* 48, 2294–2306. doi: 10.1249/MSS.0000000000000923

Voight, M. I., Hardin, A., Blackburn, T. A., Steve Tippett, A., and Canner, G. C. (1996). The effects of muscle fatigue on and the relationship of Arm dominance to shoulder proprioception. *J. Orthop. Sports Phys. Ther.* 23, 348–352. doi: 10.2519/jospt.1996.23.6.348

Walsh, L. D., Hesse, C. W., Morgan, D. L., and Proske, U. (2004). Human forearm position sense after fatigue of elbow flexor muscles. *J. Physiol.* 558, 705–715. doi: 10.1113/jphysiol.2004.062703

Conflict of Interest: The authors declare that the research was conducted in the absence of any commercial or financial relationships that could be construed as a potential conflict of interest.

frontiers in Human Neuroscience

ORIGINAL RESEARCH
published: 26 June 2020
doi: 10.3389/fnhum.2020.00251

Anodal Transcranial Direct Current Stimulation Enhances Retention of Visuomotor Stepping Skills in Healthy Adults

Shih-Chiao Tseng[1]*, *Shuo-Hsiu Chang*[2], *Kristine M. Hoerth*[1], *Anh-Tu A. Nguyen*[1] *and Daniel Perales*[1]

[1]Neuroscience Laboratory, School of Physical Therapy, Texas Woman's University, Houston, TX, United States, [2]Motor Recovery Laboratory, Department of Physical Medicine and Rehabilitation, University of Texas Health Science Center at Houston, Houston, TX, United States

Transcranial direct current stimulation (tDCS) paired with exercise training can enhance learning and retention of hand tasks; however, there have been few investigations of the effects of tDCS on leg skill improvements. The purpose of this study was to investigate whether tDCS paired with visuomotor step training can promote skill learning and retention. We hypothesized that pairing step training with anodal tDCS would improve skill learning and retention, evidenced by decreased step reaction times (RTs), both immediately (online skill gains) and 30 min after training (offline skill gains). Twenty healthy adults were randomly assigned to one of two groups, in which 20-min anodal or sham tDCS was applied to the lower limb motor cortex and paired with visuomotor step training. Step RTs were determined across three time points: (1) before brain stimulation (baseline); (2) immediately after brain stimulation (P0); and (3) 30 min after brain stimulation (P3). A continuous decline in RT was observed in the anodal tDCS group at both P0 and P3, with a significant decrease in RT at P3; whereas there were no improvements in RT at P0 and P3 in the sham group. These findings do not support our hypothesis that anodal tDCS enhances online learning, as RT was not decreased significantly immediately after stimulation. Nevertheless, the results indicate that anodal tDCS enhances offline learning, as RT was significantly decreased 30 min after stimulation, likely because of tDCS-induced neural modulation of cortical and subcortical excitability, synaptic efficacy, and spinal neuronal activity.

Keywords: tDCS, motor learning, rehabilitation, stepping, gait

OPEN ACCESS

Edited by:
Giovanni Di Pino,
Campus Bio-Medico University, Italy

Reviewed by:
Patrick Ragert,
Leipzig University, Germany
Fabio Castro,
Brunel University London, United Kingdom
Irene Di Giulio,
King's College School, United Kingdom

***Correspondence:**
Shih-Chiao Tseng
stseng@twu.edu

Specialty section:
This article was submitted to Motor Neuroscience, a section of the journal Frontiers in Human Neuroscience

Received: *31 March 2020*
Accepted: *05 June 2020*
Published: *26 June 2020*

Citation:
Tseng S-C, Chang S-H, Hoerth KM, Nguyen A-TA and Perales D (2020) Anodal Transcranial Direct Current Stimulation Enhances Retention of Visuomotor Stepping Skills in Healthy Adults. Front. Hum. Neurosci. 14:251. doi: 10.3389/fnhum.2020.00251

INTRODUCTION

The ability to acquire new motor skills and subsequently retain "learned" motor skills are crucial in our daily lives. Motor skill acquisition refers to improvements in motor performance as a result of practice, whereby movements become automatic and precise (Dayan and Cohen, 2011). Skills such as speaking, writing, and walking are all acquired through repetitive practice/training. To remember and retain such learned skills throughout life, human brains must transform recently learned, fragile motor skills into durable, long-lasting motor memories, through a set of processes referred to

as "consolidation," whereby long-term memories become more stable with time (Krakauer and Shadmehr, 2006; King et al., 2017). Regardless of performance improvements directly resulting from repetitive practice (online skill gains), memory consolidation can result in a continuum of skill improvements between practice sessions, referred to as "offline" skill gains, and evidenced by time-dependent skill improvements that occur within a specific time window after training or following overnight sleep (Borich and Kimberley, 2011; Cantarero et al., 2013; Reis et al., 2015; King et al., 2017).

Transcranial direct current stimulation (tDCS) is a non-invasive, low-intensity brain stimulation technique used to modulate neural excitability and enhance motor performance and learning of hand tasks in humans (Reis et al., 2009, 2015; Reis and Fritsch, 2011; Stagg et al., 2011). The weak tDCS current induces persisting excitability changes in the human motor cortex, lasting up to approximately 90 min after the cessation of stimulation (Nitsche and Paulus, 2000, 2001). These plastic excitability changes are selectively controlled by the polarity, duration, and current strength of the stimulus (Nitsche and Paulus, 2000, 2001; Nitsche et al., 2005). Depending on the polarity of stimulation, tDCS can up- or down-regulate cortical excitability, thereby facilitating or impeding skill performance and learning. Hence, tDCS may be a promising tool to assist motor skill re-training for individuals with neurological disorders after brain injuries, such as stroke. Recent studies suggest that lesions to the primary motor cortex (i.e., M1) have a significant impact on skill re-learning, as a result of decreased cortical excitability post-injury (Dayan and Cohen, 2011; Zimerman et al., 2012). This indicates that the same brain area responsible for controlling motor activity is also involved in memorizing newly learned skills during the early stages of motor learning. The presence of persistent motor control deficits may be attributable to the fact that damage to the brain significantly impacts the ability to acquire motor skills and hence defers the improvement of motor function, including gait.

Visuomotor tasks involve the use of real-time visual feedback to direct a computer cursor toward a visual target while a cursor represents the real-time body motion in space, requiring complex sensorimotor integration through skill practice and learning (Borich and Kimberley, 2011; Dayan and Cohen, 2011; Sarlegna and Sainburg, 2009). In a healthy young population, evidence suggests that visuomotor task training can enhance motor skill performance as it provides real-time visual feedback for the correction of movement trajectory as well as the refinement of motor planning before movement start (Sarlegna and Sainburg, 2009; Shabbott and Sainburg, 2009). In motor learning, skill acquisition (online skill gains) and retention (offline skill gains) are enhanced in healthy adults when anodal tDCS is co-applied with visuomotor hand skill training (Reis et al., 2009, 2015; Reis and Fritsch, 2011; Stagg et al., 2011). Moreover, skill gains after training only occurred when tDCS was applied simultaneously with skill training. Offline skill improvements induced by tDCS are mostly time-dependent, requiring more than 15 min post-stimulation to materialize (Reis et al., 2015). The majority of research studies have examined the effects of tDCS on the recovery of upper limb function in healthy and patient populations (Reis et al., 2009, 2015; Zimerman et al., 2012). A recent study has investigated skill retention of a complex whole-body serial reaction time (RT) task (Mizuguchi et al., 2019); however, there has been a lack of investigations exploring the effects of tDCS on leg skill acquisition and retention (Devanathan and Madhavan, 2016; Seidel and Ragert, 2019). Specific effects of tDCS on visuomotor step training remain unclear. Stepping is an important motor skill for the elderly population, used in response to balance threats (Luchies et al., 1994; Maki and McIlroy, 1997, 2006). Impaired stepping control has been correlated with falls, gait balance deficits, gait dysfunction in the elderly population (Lord and Fitzpatrick, 2001; Cho et al., 2004; Maki and McIlroy, 2006; Melzer et al., 2007; Tisserand et al., 2016).

In this study, we implemented a novel visuomotor stepping task, in which we asked subjects to move their leg forward a pre-determined distance toward a virtual visual target *via* real-time visual feedback of foot trajectory, similar to stepping training used in the clinic to improve walking function. The purpose of this study was to determine whether anodal tDCS, paired with visuomotor step training, can enhance step control in healthy adults. Findings from this study will gude the development of effective multimodal interventions (i.e., brain stimulation with stepping training) to improve walking for people with neurological disorders. We believe that real-time visual feedback will enhance sensory awareness of the distance a leg moves, related to a target location, and ultimately help individuals to regain step control. We hypothesized that this visuomotor step training, in conjunction with anodal tDCS, would improve skill learning and retention, evidenced by decreased step RTs, both immediately (online skill gains) and 30 min after training (offline skill gains).

MATERIALS AND METHODS

Subjects

Twenty self-reported healthy adults [age (mean ± SD), 27.3 ± 4.1 years; 11 females and nine males] participated in the study (**Supplementary Table S1**). All subjects provided informed consent before participation and the study was approved by Texas Woman's University Human Subjects Institutional Review Board.

Experimental Design

The investigation was a randomized-controlled, single-blinded study. After enrollment, participants were randomly assigned to one of two groups: anodal tDCS (i.e., genuine brain stimulation) or sham tDCS (i.e., placebo brain stimulation) group. Participants were blinded from their group assignments and had never previously enrolled in a tDCS study. The study design comprised two testing sessions on the same day: a "step training" session, followed by a "skill retention" session (**Figure 1A**). During the "step training" session, subjects completed a total of 100 stepping trials. Our pilot research demonstrated that healthy adults would be fully accustomed to this step task within 50 trials, as evidenced by minimal changes in stepping performance. Thus, all subjects first completed 50 step

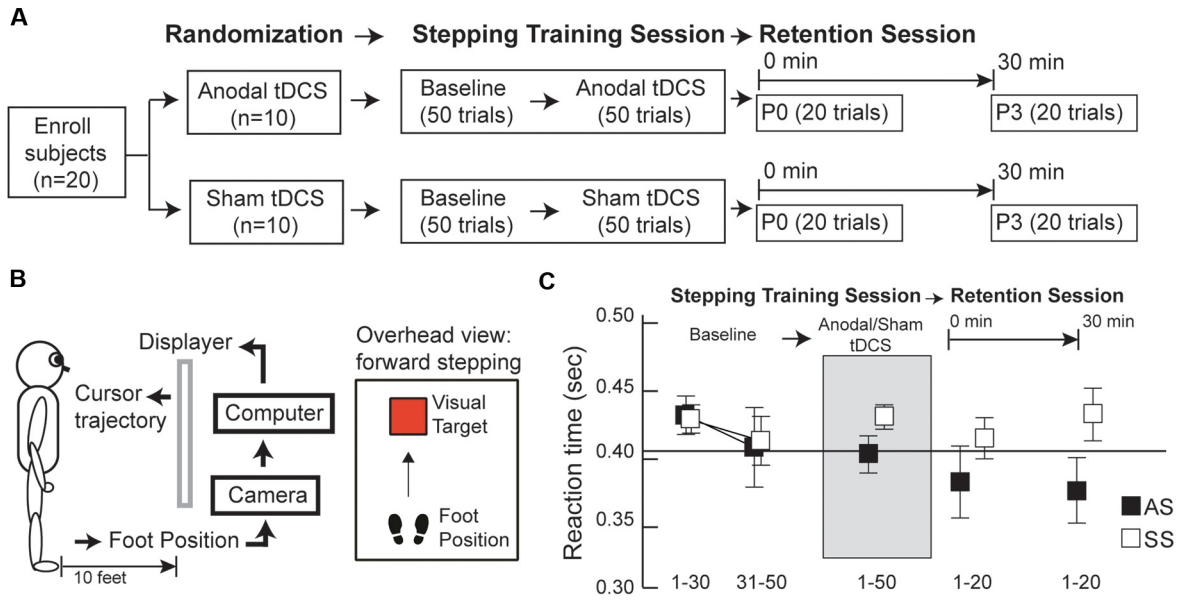

FIGURE 1 | (A) Experimental design, **(B)** visuomotor step task setup, **(C)** average reaction times (RTs) for anodal and sham transcranial direct current stimulation (tDCS) groups (AS and SS, respectively) before, during, and after tDCS. **(A)** Subjects were randomly assigned to one of two tDCS groups (anodal or sham tDCS) and underwent two sessions: a training session followed by a retention session. During the training session, subjects first completed 50 stepping trials before tDCS (baseline, BS) and additional 50 stepping trials, combined with either anodal or sham tDCS. In the retention session, 20 stepping trials were conducted at two time-points post-tDCS: 0 and 30 min after tDCS (P0 and P3, respectively). **(B)** Subjects learned to move the foot cursor to a visual target using real-time visual feedback. **(C)** Group average RTs were calculated before, during, and after tDCS. Before tDCS, the average of the last 20 trials at BS was comparable between the anodal and sham groups. After tDCS, anodal the tDCS group exhibited continually decreasing RT values over time, whereas the opposite trend of changes in RT was observed in the sham group. Error bars, ±1 SEM.

trials before brain stimulation (i.e., baseline, BS), followed by 50 trials with brain stimulation; subjects were seated while the brain stimulation apparatus was set up and run for approximately 5 min, to check the contact quality of the electrodes and assess safety, comfort levels, and tolerance of tDCS. Thereafter, all subjects continued to participate. A 1 min break was included for every block of 10 step trials, to minimize the effects of fatigue throughout the entire "step training" session. In the "skill retention" session, step performance was re-tested at two time-points: (1) 0 min post-tDCS (P0), when 20 step trials were recorded, to quantify immediate effects of brain stimulation on "online learning"; and (2) 30 min post-tDCS (P3), when an additional 20 step trials were conducted, to assess the after-effects of brain stimulation on "offline" learning.

tDCS Protocols

After completion of the first 50 stepping trials, 20 min of brain stimulation (either sham or anodal tDCS) was delivered through a pair of saline-soaked sponge electrodes (5 cm by 7 cm) using a Soterix 1 × 1 Medical tDCS Low-Intensity Stimulator (Model 1300A, Soterix Medical Inc., New York, NY, USA). Based on the EEG-electrode positions of the international 10/20 system, the medial edge of the anodal or sham electrode was placed lateral to the vertex (Cz) to target the leg area of the primary motor cortex (M1), which controls muscle activations of the stepping leg, and the reference electrode was placed over the supraorbital ridge ipsilateral to the stepping leg (Jeffery et al., 2007; Madhavan and Stinear, 2010). The skin was cleaned before stimulation, to reduce resistance to the electrical current. For **anodal stimulation**, the stimulus intensity was set to 2 mA (current density = 0.057 mA/cm^2) over a 20-min period. For **sham stimulation**, the direct current was first ramped up to 2 mA, within 30 s at the start of stimulation, immediately followed by a 20-s period when the current continued to ramp down from 2 mA to 0 mA. Subsequently, the current output was decreased to 0 mA over the remainder of the 20-min period. Subjects were informed that it is normal for the perception of brain stimulation (i.e., tingling sensation) to decrease over time, as a result of sensory adaptation to the same stimulation, and were not informed as to whether they were assigned to sham or anodal stimulation during the step test.

Stepping Task

Subjects were instructed to maintain a normal quiet standing position and were given real-time visual feedback about their leg movements *via* a foot cursor (7 cm by 5 cm) displayed on the wall 10 feet away from the front view (**Figure 1B**). A reflecting marker was attached to the base of the second toe of the stepping foot (i.e., the preferred, leg for step initiation, SI) to indicate the real-time cursor location on the display and the task was to move the cursor from a starting location to a target. In each trial, the target was presented on the screen at a pre-determined distance, equal to 40% of the individual's body

height (Tseng et al., 2009, 2010), and subjects were instructed to initiate a forward step with the preferred stepping leg, to move the cursor onto a visual target as soon as they saw the target, followed by another forward step made by the other leg to move the whole body from the starting location to the target location.

Data Collection

A three-dimensional camera system (Flex 13 OptiTrack, NaturalPoint Inc., Corvallis, OR, USA) recorded real-time marker locations during each stepping trial. Customized programming in Visual C++ (Microsoft visual studio, Microsoft Inc., Albuquerque, NM, USA) was used to control real-time cursor motion, as well as the location of the visual target displayed on the wall screen. All data were collected at 100 Hz. Each subject completed the "step training" sessions (including 50 trials before tDCS and 50 trials during tDCS) in approximately 30 min, followed by the "retention" session completed in approximately 40 min (20 trials at 0 min and 20 trials at 30 min post tDCS).

Data Analysis

A custom Matlab program (MathWorks, Natick, MA, USA) was used for all data processing and analyses. Offline foot position data were filtered using a 2nd-order Butterworth zero phase-lag low-pass filter, with a cut-off frequency of 10 Hz (Tseng et al., 2009). SI was defined as the time when the linear velocity in the forward/backward direction exceeded 1% of its maximal value and the linear velocity continued to increase for more than a second during a forward step. This velocity threshold was determined based on our previous pilot research and coincided with the onset of the lifting of the stepping foot. Step RT was calculated as the time interval between the onset of visual target appearance and the onset of SI in each stepping trial. Average RT values were calculated from the 20 stepping trials across the three time points: (1) BS (average of the last 20 trials); (2) P0; and (3) P3.

To compare the effects of anodal vs. sham tDCS on online and offline skill learning, we calculated the percentage change in RT after, relative to before, tDCS, normalized to the average of the last 20 baselines RTs (Devanathan and Madhavan, 2016). This allowed us to account for differences among individuals, thereby comparing changes in RT due to tDCS (anodal vs. sham). A percentage of 0 indicates no change in the reaction after tDCS. Group means were calculated for each time point (BS, P0, and P3).

To quantify changes in stepping performance before and after tDCS, average movement time (MT) and step accuracy (SA) were calculated across the first 20 trials in BS, the last 20 trials in BS, P0, and P3. Step termination (ST) was defined as the time when the linear velocity in the forward/backward direction fell below 1% of its maximal value and the linear velocity continued to decrease for more than a second during foot landing. MT was determined as the time duration between SI and ST. SA was quantified by the linear distance between the end-point foot position during a forward step and the location of the visual target in the horizontal plane referred to absolute error.

Statistical Analysis

Statistical comparisons were made using SAS/STAT software (SAS, Cary, NC, USA). A two-way (group × time) mixed-model ANOVA, with repeated measures on one factor (time), was used to test for the effects of time (BS, P0, and P3) and group (anodal vs. sham tDCS). If a significant interaction was present, *post hoc* analyses were performed using Tukey's Honest Significant Difference test. The level for statistical significance was set at $P \leq 0.05$.

RESULTS

Group averages of RT data for conditions (BS, during tDCS, P0, and P3) are presented in **Figure 1C**. At baseline, RT averages for the last 20 trials were comparable between the anodal and sham tDCS groups (**Supplementary Table S2**); indicating all participants were accustomed to the step test before tDCS. Interestingly, RTs post-tDCS showed distinctively different patterns of change in the two groups. After tDCS, the anodal group had decreased RT values at P0 and P3, relative to baseline whereas the sham group showed increased RT at P0 and P3 relative to baseline Comparison of RT values across the three time points (BS, P0, and P3) revealed a significant group × time interaction effect ($F_{(2,36)} = 6.38$, $P = 0.009$, $\eta^2 = 0.02$; **Figure 2A**); however, there were no primary effects of group ($F_{(1,18)} = 1.04$, $P = 0.32$, $\eta^2 = 0.05$) or time ($F_{(2,36)} = 1.00$, $P = 0.39$, $\eta^2 = 0.005$). In the anodal tDCS group, RT values declined continuously post-stimulation; however, RT at P0 did not differ significantly from baseline (*post hoc* $P = 0.28$); however, at P3 the RT value was significantly lower than baseline (*post hoc* $P = 0.047$). In the sham tDCS group, there were no significant differences in RT from baseline at either P0 or P3 (*post hoc* $P = 1.0$ and $P = 0.4$, respectively).

After normalization to baseline RT, the percent change in RT in the anodal tDCS group exhibited a continuous decline of up to 30 min after brain stimulation, whereas the sham tDCS group showed no decrease in RT after stimulation (**Figure 2B**). In the anodal tDCS group, RT values were decreased by 5.74% and 7.41% at P0 and P3 from the pre-stimulation baseline value. In contrast, RTs in the sham tDCS group increased by 0.98% and 4.86% at P0 and P3 from the pre-stimulation baseline value. Comparison of percent change in RT across the three time points (BS, P0, and P3) revealed a significant group × time interaction effect ($F_{(2,36)} = 4.92$, $P = 0.013$, $\eta^2 = 0.13$) and primary effect of group ($F_{(1,18)} = 10.09$, $P = 0.005$, $\eta^2 = 0.20$). However, there was no primary effect of time ($F_{(2,36)} = 0.74$, $P = 0.48$, $\eta^2 = 0.02$).The percentage change in RT at P0 did not differ significantly between the anodal and sham groups (*post hoc* $P = 0.24$); however, the difference between the groups became significant at P3 (*post hoc*, $P = 0.002$). Taken together, these findings suggest that anodal tDCS does not cause an immediate reduction in RT value; however, it does reduce RT at 30 min post-stimulation. The

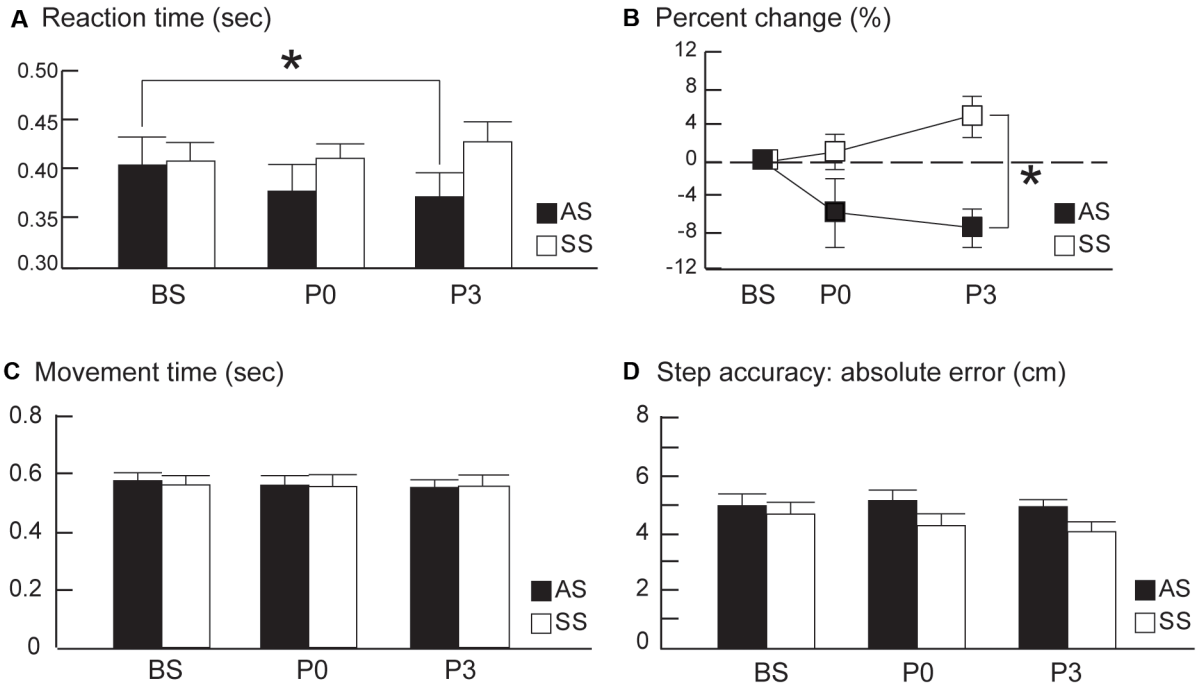

FIGURE 2 | (A) Average stepping reaction times (RTs). **(B)** Average percent changes from the baseline RTs, **(C)** average movement time, and **(D)** average step accuracy from pre- to post-tDCS in the anodal and sham tDCS groups (AS and SS, respectively) before (baseline, BS) and 0 and 30 min after tDCS (P0 and P3, respectively). The averages of the last 20 trials at BS were compared to the averages of 20 trials at P0 and P3 between the two groups. Error bars, ±1 SEM. Asterisks (*) indicate significant *post hoc* differences between conditions.

lower percentage change in RT during the retention phase (i.e., P3) is likely attributable to the persistent effects of anodal tDCS.

MT, RT, and SA were significantly improved from the first 20 baseline trials to the last 20 baseline trials of BS for both anodal and sham groups, indicating a training effect for this stepping task before tDCS (**Supplementary Table S2**). After tDCS, MT and SA remained at the similar levels at P0 and P3 relative to the mean of last 20 baseline trials (**Figures 2C,D**) for both groups, suggesting stepping movements became automatic after baseline training. For MT, there were no effects of group ($F_{(1,18)}$ = 0.01, P = 0.91, η^2 = 0.0006) or time ($F_{(2,36)}$ = 0.63, P = 0.54, η^2 = 0.003); nor was interaction effect of group by time ($F_{(2,36)}$ = 0.29, P = 0.75, η^2 = 0.002). For SA, there were no effects of group $F_{(1,18)}$ = 2.27, P = 0.15, η^2 = 0.08), time $F_{(2,36)}$ = 0.95, P = 0.39, η^2 = 0.01), or interaction effect $F_{(2,36)}$ = 1.01, P = 0.38, η^2 = 0.01).

DISCUSSION

To our knowledge, this study is the first to demonstrate that the co-application of anodal tDCS and visuomotor step training significantly reduces stepping RT in healthy adults. In this study, we investigated the effects of anodal tDCS on RTs during learning of a visual stepping task in healthy adults. The results showed that stepping RT was significantly reduced at 30 min post-anodal tDCS, while there was no significant decrease at 0 min post-stimulation. These findings suggest that anodal tDCS over the M1 leg area, paired with the learning of a visual stepping task, was effective in promoting skill retention in healthy adults. Future studies should determine the long-term effects of anodal tDCS combined with visuomotor step training on cortical and spinal excitability, to develop therapeutic strategies to enhance the health of people with neurological disorders.

Significant After-Effect of Anodal tDCS on Stepping Reaction

The significant decrease in stepping RT detected 30 min post-stimulation can likely be attributed to an after-effect associated with anodal tDCS. Previous studies have demonstrated that increased M1 excitability persists, even after cessation of stimulation, referred to as a long-lasting "after-effect" induced by anodal tDCS (Nitsche and Paulus, 2000, 2001). Although the exact neurophysiological mechanisms underlying this effect are incompletely understood, evidence supports that tDCS can modulate neural excitability of the cerebral cortex in rats and humans by changing the polarity of the resting membrane potential in the nervous system (Bindman et al., 1962, 1964; Nitsche and Paulus, 2000, 2001; Nitsche et al., 2005). Specifically, anodal tDCS increases the neural excitability of the stimulation area, whereas cathodal tDCS decreases the neural excitability of the stimulation area. The mechanism underlying the associated polarity-dependent modulations is that anodal tDCS shifts the resting membrane potential closer

to the depolarization threshold, thereby increasing neural excitability and firing rate (Bindman et al., 1962, 1964). In contrast, cathodal tDCS shifts the resting membrane potential further away from the depolarization threshold, resulting in hyperpolarization and a decrease in neural excitability and firing rate. Furthermore, in healthy adults, Nitsche and Paulus (2001) first demonstrated that a single session of anodal tDCS over the hand area of the M1 can produce a persistent after-effect, which increased neural excitation to up to 150% of its baseline value; this excitatory effect lasted for approximately 90 min after the end of stimulation. Such after-effects are partially controlled by modulation of N-methyl-d-aspartate (NMDA) receptor efficiency (Liebetanz et al., 2002; Nitsche et al., 2005). Similar to the findings from studies of the upper extremities mentioned above, Jeffery et al. (2007) was the first group to investigate the effects of anodal tDCS on neural excitability of the M1 leg area, which is located at a deeper position, relative to the M1 hand area in humans. These researchers showed that anodal tDCS (2 mA, 10 min) was effective in increasing motor evoked potentials (MEPs) in the M1 leg area of up to 140% of its baseline value 30 min post-stimulation; this excitatory effect continued for approximately 60 min after cessation of stimulation. Data from this study indicate that a 20 min anodal tDCS over the M1 leg area produces similar long-lasting after-effect of increased cortical neural excitability, which is responsible for the observed decrease in stepping RT 30 min post-stimulation.

No Immediate Effect of Anodal tDCS on Stepping Reaction

Interestingly, in this study, anodal tDCS did not induce a significant decrease in stepping RT immediately after stimulation; however, a significant decrease in RT was observed at 30 min post-stimulation. This finding may indicate that the changes in cortical excitability induced by anodal tDCS did not reach a maximum immediately after cessation of the stimulation and that the anodal tDCS-induced increase in cortical excitability required several minutes to elapse to reach its peak (Bindman et al., 1964; Jeffery et al., 2007). Bindman et al. (1964) showed that, in rats, a higher positive current flow passing through the somatosensory cortex can result in the complete abolition of the evoked potentials (referred to as cortical depression); however, the potentials gradually recovered during the next 30 min and reached a peak value around 30 min after stimulation. Notably, the amplitude of evoked potentials was significantly increased once they returned 30 min later, despite the period of depression. It is possible that, in this study, the positive current of 2 mA flowing over the M1 leg area continuously for 20 min may cause temporary cortical depression, leading to the lack of a significant decrease in RT immediately after brain stimulation. Nevertheless, following anodal stimulation, cortical excitability gradually increased and peaked at 30 min post-anodal tDCS, thereby contributing to the observed significant decrease in RT 30 min later. Jeffery et al. (2007) reported no significant increase in MEPs in the M1 leg area, relative to its baseline value, immediately after 10 min of anodal tDCS over the M1 leg area; however, MEPs continued to increase over the subsequent 60 min, becoming significantly different from the baseline value from 10 min post-stimulation. Behaviorally, Devanathan and Madhavan (2016) have reported that healthy young adults showed decreased RT for ankle choice reaction task 5 min after a single anodal tDCS session whereas prolonged RT was observed after a single sham tDCS session.

Limitations of This Study

It is difficult to ascribe specific neuronal mechanisms to the findings of this study, due to several limitations. Although evidence indicates that anodal tDCS is responsible for long-lasting after-effects of increased cortical and spinal neuronal excitability in humans (Nitsche and Paulus, 2000, 2001; Lang et al., 2005; Nitsche et al., 2005, 2007; Jeffery et al., 2007; Roche et al., 2009, 2011), we did not measure changes in MEPs before and after the 20 min anodal and sham tDCS while learning a visuomotor stepping task. Therefore, we have limited understanding of the extent of changes in cortical excitability induced by this stepping task combined with anodal tDCS during the training session and the after-effects associated with anodal tDCS in the retention session. Future studies should include transcranial magnetic stimulation (TMS) to quantify the changes in MEPs induced by tDCS during learning of a visual stepping task.

Although a considerable effort was devoted to controlling for the variability attributable to the individual participants, we acknowledge that stepping performance can be influenced by various factors, thereby affecting the RT calculation (Li et al., 2015). It is possible that our participants became bored or fatigued after repeatedly performing the same stepping task, which, in turn, influenced their stepping RTs. It is established that anodal tDCS over the M1 area can improve endurance time and negate fatigue effects (Cogiamanian et al., 2007; Devanathan and Madhavan, 2016). Also, the single-blinded randomized-controlled study protocol used in this study may result in biased outcomes because the researchers were likely to be biased in favor of the intervention they were performing. Furthermore, tDCS may induce widespread cortical changes in the adjacent area of M1 including supplementary motor area and alter functional connectivity between the M1 and motor association cortices, due to its low spatial focality, derived from the relatively large stimulation electrode (35 cm^2) and dispersed electrical field (Lang et al., 2005; Nitsche et al., 2007). The findings from this study may be attributable to the sum of cortical, subcortical, and spinal neural modulations, rather than only changes in M1 leg area excitability (Lang et al., 2005; Nitsche et al., 2007; Roche et al., 2009, 2011; Polanía et al., 2011; Mizuguchi et al., 2019).

Clinical Implications for Motor Learning and Gait Rehabilitation

This study advances understanding of the aggregate effects of anodal tDCS and step training on a group of healthy subjects. We demonstrate the feasibility of using anodal tDCS as an adjuvant to step training to reduce stepping RTs and enhance skill retention in healthy adults. These findings may have important clinical implications for the geriatric population

and individuals with neurological disorders, whose stepping RTs are significantly longer than those of healthy adults, leading to a limited ability to initiate stepping strategies in response to balance threats and increased risk of falling (Luchies et al., 1994; Maki and McIlroy, 1997, 2006; Tseng et al., 2009; Melzer et al., 2007; Peterson et al., 2016). Furthermore, it has been suggested that age-related slowing in volitional stepping is an important indicator of declined mobility, impaired balance, and increased risk of falling in the elderly population (Lord and Fitzpatrick, 2001; Cho et al., 2004; Maki and McIlroy, 2006; Melzer et al., 2007; Tisserand et al., 2016). The current study demonstrates that combining anodal tDCS and visuomotor step training can reduce stepping RT and therefore this approach may mitigate age-related stepping slowness, whether triggered by external perturbations or self-initiated.

In motor learning, skill acquisition (online learning) and retention (offline learning) were enhanced in healthy adults when anodal tDCS was co-applied with visuomotor hand skill training (Reis et al., 2009, 2015; Reis and Fritsch, 2011; Stagg et al., 2011). Behaviorally, tDCS-induced improvements in visuomotor skill, dependent on the passage of time after training, but not on overnight sleep (Reis et al., 2015). Reis et al. (2015) showed that co-application of tDCS and skill training is essential for the promotion of offline skill gains and prevention of skill loss after training; whereas application of tDCS alone after skill training did not lead to the acquisition of any offline gains; however, the majority of learning studies investigated skill gains in the upper extremities (Reis et al., 2009, 2015; Borich and Kimberley, 2011; Reis and Fritsch, 2011; Stagg et al., 2011; Cantarero et al., 2013). More evidence is needed to determine whether the co-application of anodal tDCS and lower extremity motor training can enhance online and offline skill gains. The results of this study are consistent with those of previous studies of visuomotor hand skill learning, which showed that that co-application of tDCS and skill training is essential to promote offline skill gains and prevent skill loss after training (Reis et al., 2015). Although findings from this study are exploratory, they raise the possibility that repetitive use of anodal tDCS combined with lower extremity motor skill training could help to restore walking function in individuals with neurological disorders, including chronic stroke. Future studies are necessary to understand whether regular anodal tDCS and locomotor training may influence the excitatory state of the M1 leg and spinal neuronal networks in healthy adults, as well as individuals with neurological disorders.

DATA AVAILABILITY STATEMENT

All data generated or analyzed during this study are included in this published article and its **Supplementary Material**.

ETHICS STATEMENT

The studies involving human participants were reviewed and approved by Texas Woman's University IRB Houston. The participants provided their written informed consent to participate in this study.

AUTHOR CONTRIBUTIONS

S-CT and S-HC contributed to the conception and design of the study. KH, A-TN, and DP conducted the study. S-CT contributed to data analysis and writing the manuscript.

FUNDING

This study was supported in part by research grant awards to S-CT from Texas Woman's University Research Enhancement Program.

ACKNOWLEDGMENTS

We would like to thank Jeremy Tzou for assistance with C^{++} software implementation.

SUPPLEMENTARY MATERIAL

The Supplementary Material for this article can be found online at: https://www.frontiersin.org/articles/10.3389/fnhum.2020.00251/full#supplementary-material.

REFERENCES

Bindman, L. J., Lippold, O. C., and Redfearn, J. W. (1962). Long-lasting changes in the level of the electrical activity of the cerebral cortex produced bypolarizing currents. *Nature* 196, 584–585. doi: 10.1038/196584a0

Bindman, L. J., Lippold, O. C., and Redfearn, J. W. (1964). The action of brief polarizing currents on the cerebral cortex of the rat (1) during current flow and (2) in the production of long-lasting after-effects. *J. Physiol.* 172, 369–382. doi: 10.1113/jphysiol.1964.sp007425

Borich, M. R., and Kimberley, T. J. (2011). Both sleep and wakefulness support consolidation of continuous, goal-directed, visuomotor skill. *Exp. Brain Res.* 214, 619–630. doi: 10.1007/s00221-011-2863-0

Cantarero, G., Tang, B., O'Malley, R., Salas, R., and Celnik, P. (2013). Motor learning interference is proportional to occlusion of LTP-like plasticity. *J. Neurosci.* 33, 4634–4641. doi: 10.1523/JNEUROSCI.4706-12.2013

Cho, B. L., Scarpace, D., and Alexander, N. B. (2004). Tests of stepping as indicators of mobility, balance, and fall risk in balance-impaired older adults. *J. Am. Geriatr. Soc.* 52, 1168–1173. doi: 10.1111/j.1532-5415.2004.52317.x

Cogiamanian, F., Marceglia, S., Ardolino, G., Barbieri, S., and Priori, A. (2007). Improved isometric force endurance after transcranial direct current stimulation over the human motor cortical areas. *Eur. J. Neurosci.* 26, 242–249. doi: 10.1111/j.1460-9568.2007.05633.x

Dayan, E., and Cohen, L. G. (2011). Neuroplasticity subserving motor skill learning. *Neuron* 72, 443–454. doi: 10.1016/j.neuron.2011.10.008

Devanathan, D., and Madhavan, S. (2016). Effects of anodal tDCS of the lower limb M1 on ankle reaction time in young adults. *Exp. Brain Res.* 234, 377–385. doi: 10.1007/s00221-015-4470-y

Jeffery, D. T., Norton, J. A., Roy, F. D., and Gorassini, M. A. (2007). Effects of transcranial direct current stimulation on the excitability of the leg motor cortex. *Exp. Brain Res.* 182, 281–287. doi: 10.1007/s00221-007-1093-y

King, B. R., Saucier, P., Albouy, G., Fogel, S. M., Rumpf, J. J., Klann, J., et al. (2017). Cerebral activation during initial motor learning forecasts subsequent sleep-facilitated memory consolidation in older adults. *Cereb. Cortex* 27, 1588–1601. doi: 10.1093/cercor/bhv347

Krakauer, J. W., and Shadmehr, R. (2006). Consolidation of motor memory. *Trends Neurosci.* 29, 58–64. doi: 10.1016/j.tins.2005.10.003

Lang, N., Siebner, H. R., Ward, N. S., Lee, L., Nitsche, M. A., Paulus, W., et al. (2005). How does transcranial DC stimulation of the primary motor cortex alter regional neuronal activity in the human brain? *Eur. J. Neurosci.* 22, 495–504. doi: 10.1111/j.1460-9568.2005.04233.x

Li, L. M., Uehara, K., and Hanakawa, T. (2015). The contribution of interindividual factors to variability of response in transcranial direct current stimulation studies. *Front. Cell. Neurosci.* 9:181. doi: 10.3389/fncel.2015.00181

Liebetanz, D., Nitsche, M. A., Tergau, F., and Paulus, W. (2002). Pharmacological approach to the mechanisms of transcranial DC-stimulation-induced after-effects of human motor cortex excitability. *Brain* 125, 2238–2247. doi: 10.1093/brain/awf238

Lord, S. R., and Fitzpatrick, R. C. (2001). Choice stepping reaction time: a composite measure of falls risk in older people. *J. Gerontol. A Biol. Sci. Med. Sci.* 56, M627–632. doi: 10.1093/gerona/56.10.m627

Luchies, C. W., Alexander, N. B., Schultz, A. B., and Ashton-Miller, J. (1994). Stepping responses of young and old adults to postural disturbances: kinematics. *J. Am. Geriatr. Soc.* 42, 506–512. doi: 10.1111/j.1532-5415.1994.tb04972.x

Madhavan, S., and Stinear, J. W. (2010). Focal and bi-directional modulation of lower limb motor cortex using anodal transcranial direct current stimulation. *Brain Stimul.* 3:42. doi: 10.1016/j.brs.2009.06.005

Maki, B. E., and McIlroy, W. E. (1997). The role of limb movements in maintaining upright stance: the "change-in-support" strategy. *Phys. Ther.* 77, 488–507. doi: 10.1093/ptj/77.5.488

Maki, B. E., and McIlroy, W. E. (2006). Control of rapid limb movements for balance recovery: age-related changes and implications for fall prevention. *Age Ageing* 35, ii12–ii18. doi: 10.1093/ageing/afl078

Melzer, I., Kurz, I., Shahar, D., Levi, M., and Oddsson, L. (2007). Application of the voluntary step execution test to identify elderly fallers. *Age Ageing* 36, 532–537. doi: 10.1093/ageing/afm068

Mizuguchi, N., Maudrich, T., Kenville, R., Carius, D., Maudrich, D., Villringer, A., et al. (2019). Structural connectivity prior to whole-body sensorimotor skill learning associates with changes in resting state functional connectivity. *NeuroImage* 197, 191–199. doi: 10.1016/j.neuroimage.2019.04.062

Nitsche, M. A., Doemkes, S., Karaköse, T., Antal, A., Liebetanz, D., Lang, N., et al. (2007). Shaping the effects of transcranial direct current stimulation of the human motor cortex. *J. Neurophysiol.* 97, 3109–3117. doi: 10.1152/jn.01312.2006

Nitsche, M. A., and Paulus, W. (2000). Excitability changes induced in the human motor cortex by weak transcranial direct current stimulation. *J. Physiol.* 527, 633–639. doi: 10.1111/j.1469-7793.2000.t01-1-00633.x

Nitsche, M. A., and Paulus, W. (2001). Sustained excitability elevations induced by transcranial DC motor cortex stimulation in humans. *Neurology* 57, 1899–1901. doi: 10.1212/wnl.57.10.1899

Nitsche, M. A., Seeber, A., Frommann, K., Klein, C. C., Rochford, C., Nitsche, M. S., et al. (2005). Modulating parameters of excitability during and after transcranial direct current stimulation of the human motor cortex. *J. Physiol.* 568, 291–303. doi: 10.1113/jphysiol.2005.092429

Peterson, D. S., Huisinga, J. M., Spain, R. I., and Horak, F. B. (2016). Characterization of compensatory stepping in people with multiple sclerosis. *Arch. Phys. Med. Rehabil.* 97, 513–521. doi: 10.1016/j.apmr.2015.10.103

Polanía, R., Paulus, W., Antal, A., and Nitsche, M. A. (2011). Introducing graph theory to track for neuroplastic alterations in the resting human brain: a transcranial direct current stimulation study. *NeuroImage* 54, 2287–2296. doi: 10.1016/j.neuroimage.2010.09.085

Reis, J., and Fritsch, B. (2011). Modulation of motor performance and motor learning by transcranial direct current stimulation. *Curr. Opin. Neurol.* 24, 590–596. doi: 10.1097/wco.0b013e32834c3db0

Reis, J., Fischer, J. T., Prichard, G., Weiller, C., Cohen, L. G., and Fritsch, B. (2015). Time- but not sleep-dependent consolidation of tDCS-enhanced visuomotor skills. *Cereb. Cortex* 25, 109–117. doi: 10.1093/cercor/bht208

Reis, J., Schambra, H. M., Cohen, L. G., Buch, E. R., Fritsch, B., Zarahn, E., et al. (2009). Noninvasive cortical stimulation enhances motor skill acquisition over multiple days through an effect on consolidation. *Proc. Natl. Acad. Sci. U S A* 106, 1590–1595. doi: 10.1073/pnas.0805413106

Roche, N., Lackmy, A., Achache, V., Bussel, B., and Katz, R. (2009). Impact of transcranial direct current stimulation on spinal network excitability in humans. *J. Physiol.* 587, 5653–5664. doi: 10.1113/jphysiol.2009.177550

Roche, N., Lackmy, A., Achache, V., Bussel, B., and Katz, R. (2011). Effects of anodal transcranial direct current stimulation over the leg motor area on lumbar spinal network excitability in healthy subjects. *J. Physiol.* 589, 2813–2826. doi: 10.1113/jphysiol.2011.205161

Sarlegna, F. R., and Sainburg, R. L. (2009). The roles of vision and proprioception in the planning of reaching movements. *Adv. Exp. Med. Biol.* 629, 317–335. doi: 10.1007/978-0-387-77064-2_16

Seidel, O., and Ragert, P. (2019). Effects of transcranial direct current stimulation of primary motor cortex on reaction time and tapping performance: a comparison between athletes and non-athletes. *Front. Hum. Neurosci.* 13:103. doi: 10.3389/fnhum.2019.00103

Shabbott, B. A., and Sainburg, R. L. (2009). On-line corrections for visuomotor errors. *Exp. Brain Res.* 195, 59–72. doi: 10.1007/s00221-009-1749-x

Stagg, C. J., Jayaram, G., Pastor, D., Kincses, Z. T., Matthews, P. M., and Johansen-Berg, H. (2011). Polarity and timing-dependent effects of transcranial direct current stimulation in explicit motor learning. *Neuropsychologia* 49, 800–804. doi: 10.1016/j.neuropsychologia.2011.02.009

Tisserand, R., Robert, T., Chabaud, P., Bonnefoy, M., and Cheze, L. (2016). Elderly fallers enhance dynamic stability through anticipatory postural adjustments during a choice stepping reaction time. *Front. Hum. Neurosci.* 10:613. doi: 10.3389/fnhum.2016.00613

Tseng, S. C., Stanhope, S. J., and Morton, S. M. (2009). Impaired reactive stepping adjustments in older adults. *J. Gerontol. A Biol. Sci. Med. Sci.* 64, 807–815. doi: 10.1093/gerona/glp027

Tseng, S. C., Stanhope, S. J., and Morton, S. M. (2010). Visuomotor adaptation of voluntary step initiation in older adults. *Gait Posture* 31, 180–184. doi: 10.1016/j.gaitpost.2009.10.001

Zimerman, M., Heise, K. F., Hoppe, J., Cohen, L. G., Gerloff, C., and Hummel, F. C. (2012). Modulation of training by single-session transcranial direct current stimulation to the intact motor cortex enhances motor skill acquisition of the paretic hand. *Stroke* 43, 2185–2191. doi: 10.1161/STROKEAHA.111.645382

Conflict of Interest: The authors declare that the research was conducted in the absence of any commercial or financial relationships that could be construed as a potential conflict of interest.

frontiers in Human Neuroscience

ORIGINAL RESEARCH
published: 26 June 2020
doi: 10.3389/fnhum.2020.00248

Non-invasive Brain Stimulation of the Posterior Parietal Cortex Alters Postural Adaptation

David R. Young[1]*, *Pranav J. Parikh*[1] and *Charles S. Layne*[1,2]

[1]Center for Neuromotor and Biomechanics Research, Department of Health and Human Performance, University of Houston, Houston, TX, United States, [2]Center for Neuro-Engineering and Cognitive Science, University of Houston, Houston, TX, United States

Effective central sensory integration of visual, vestibular, and proprioceptive information is required to promote adaptability in response to changes in the environment during postural control. Patients with a lesion in the posterior parietal cortex (PPC) have an impaired ability to form an internal representation of body position, an important factor for postural control and adaptation. Suppression of PPC excitability has also been shown to decrease postural stability in some contexts. As of yet, it is unknown whether stimulation of the PPC may influence postural adaptation. This investigation aimed to identify whether transcranial direct current stimulation (tDCS) of the bilateral PPC could modulate postural adaptation in response to a bipedal incline postural adaptation task. Using young, healthy subjects, we delivered tDCS over bilateral PPC followed by bouts of inclined stance (incline-interventions). Analysis of postural after-effects identified differences between stimulation conditions for maximum lean after-effect (LAE; p = 0.005) as well as a significant interaction between condition and measurement period for the average position (p = 0.03). We identified impaired postural adaptability following both active stimulation conditions. Results reinforce the notion that the PPC is involved in motor adaptation and extend this line of research to the realm of standing posture. The results further highlight the role of the bilateral PPC in utilizing sensory feedback to update one's internal representation of verticality and demonstrates the diffuse regions of the brain that are involved in postural control and adaptation. This information improves our understanding of the role of the cortex in postural control, highlighting the potential for the PPC as a target for sensorimotor rehabilitation.

Keywords: adaptation, transcranial direct current stimulation, posterior parietal cortex, posture, after-effects, sensory integration, proprioception

OPEN ACCESS

Edited by:
Giovanni Di Pino,
Campus Bio-Medico University, Italy

Reviewed by:
Junhong Zhou,
Harvard Medical School, United States
Leif Johannsen,
RWTH Aachen University, Germany
Michael Vesia,
University of Michigan, United States

***Correspondence:**
David R. Young
daryoung@ucdavis.edu

Specialty section:
This article was submitted to Motor Neuroscience, a section of the journal Frontiers in Human Neuroscience

Received: *29 March 2020*
Accepted: *03 June 2020*
Published: *26 June 2020*

Citation:
Young DR, Parikh PJ and Layne CS (2020) Non-invasive Brain Stimulation of the Posterior Parietal Cortex Alters Postural Adaptation. Front. Hum. Neurosci. 14:248. doi: 10.3389/fnhum.2020.00248

INTRODUCTION

Central integration of visual, vestibular, and proprioceptive sensory information is critical for successful postural control and the maintenance of upright stance (Peterka, 2002). Another important component of successful postural control is adaptability. Postural adaptation requires the updating of one's internal representation of their position and movement within the environment (Head and Holmes, 1911; Chritchley, 1953). The internal representation can adapt in response to changes in sensory feedback and/or the external environment. These changes occur slowly and

correspond with changes in behavior which gradually reduce movement errors (Gurfinkel et al., 1995). Once original conditions are restored, there is an after-effect while the internal representation recalibrates to its previous state (Kluzik et al., 2005; Ivanenko and Gurfinkel, 2018). After-effects dissipate over the course of seconds to minutes as prior experience and sensory feedback reverts the adapted internal representation to baseline (Wierzbicka et al., 1998; Kluzik et al., 2005). This investigation sought to improve our general understanding of how the posterior parietal cortex (PPC) is involved in postural adaptation.

Multisensory integration is impaired in individuals with lesions of the PPC (Derouesné et al., 1984). This suggests that the PPC is a sensory association area, where signals from multiple sensory systems (i.e., the visual, vestibular, and somatosensory systems) are integrated (Edwards et al., 2019). The PPC performs calculations, transforming sensory signals into sensorimotor representations of the body position to create an internal representation of our position in space (Sober and Sabes, 2003; Sabes, 2011; Findlater et al., 2016).

There is some evidence of the left hemisphere parietal lobe dominance in motor adaptation. Specifically, Mutha et al. (2011) identified that brain damage to the left PPC (lPPC) decreased visuomotor adaptation but damage to the right PPC (rPPC) did not. Newport et al. (2006) found that a bilateral lesion of the PPC, primarily in the left hemisphere, led to an inability to adapt to visual perturbations in a pair of 2006 case studies (Newport and Jackson, 2006; Newport et al., 2006). Other investigators have shown that disruptive TMS of the left PPC can impair adaptive reaching during a right-handed task (Desmurget et al., 1999). Alternatively, there is evidence that the right hemisphere parietal lobe, as part of a network with the right inferior frontal cortex, dominates processing of positional illusions induced by tendon vibration (Naito et al., 2007; Takeuchi et al., 2019). Still, others have found some level of bilateral activity associated with positional illusions generated by tendon vibration (Amemiya and Naito, 2016; Naito et al., 2016).

While the effects of brain stimulation of the PPC have yet to be explored regarding postural adaptation, previous research has demonstrated PPC involvement during postural control tasks with additional sensory integration demands (Ishigaki et al., 2016; Kaulmann et al., 2017). Both Ishigaki et al. (2016) and Kaulmann et al. (2017) identified that inhibition of the PPC *via* non-invasive brain stimulation altered the effects of augmented sensory feedback on postural stability. There is also evidence that the bilateral PPC is involved in continuous postural control during periods of sensory conflict (Goel et al., 2019). Based on the fact that the PPC is involved in upper body motor adaptation, processing of proprioceptive perturbations, and sensory integration during postural control, it is reasonable to hypothesize that the PPC is also involved in postural adaptation. Furthermore, a previous investigation by Heinen et al. (2016) identified that bilateral stimulation of the PPC was more effective at eliciting changes in working memory than unilateral stimulation. Thus, the bilateral role of the PPC should be investigated within the scope of postural adaptation. It is important to understand if there are hemisphere-specific roles of the PPC in postural adaptation or if the involvement is part of a more diffuse cortical network that requires bilateral PPC input.

To identify if relative facilitation or inhibition of the PPC alters postural adaptation, we employed bilateral transcranial direct current stimulation (tDCS). tDCS provides low-intensity stimulation, flowing from anodal to the cathodal electrode(s), which results in slight alterations in the excitability of underlying cortical tissue (Lefaucheur and Wendling, 2019). Anodal stimulation leads to a relative excitation of the underlying tissue while cathodal stimulation leads to a relative depression. Sham stimulation does not alter cortical excitability (Lefaucheur and Wendling, 2019). While there is no consensus, some previous investigations have found behavioral differences between sham and cathodal, but not a sham and anodal stimulation (Grundmann et al., 2011; Foerster et al., 2017). Improving the understanding of the PPC's role in postural adaptation will improve the basic understanding of cortical influences on postural control and may have clinical implications for use of non-invasive brain stimulation to improve adaptability in fall-risk populations.

To identify differences in postural adaptation resulting from tDCS of the PPC, this investigation utilized an incline-intervention adaptation paradigm. Incline-interventions involve prolonged stance on an inclined surface and result in a postural after-effect known as lean after-effect (LAE), which is an anterior shift in position that can persist for several minutes (Kluzik et al., 2005; Chong et al., 2014, 2017). Lean after-effect reflects a change in the internal relationship between gravitational vertical and elected postural orientation. This incongruence is corrected over time as subjects reorient to gravity (Kluzik et al., 2005). The current investigation sought to determine the effects of bilateral tDCS stimulation of the PPC on adaptation to the inclined surface, as well as on de-adaptation once conditions return to normal. It was hypothesized that active tDCS would alter LAE, however, based on previous literature, it was not feasible to hypothesize about hemisphere-specific effects.

MATERIALS AND METHODS

Subjects

Fifteen subjects were recruited to perform postural control tasks after tDCS stimulation across three data collection sessions. An additional 15 subjects participated in a control experiment without stimulation. All subjects provided their written informed consent following the Helsinki Declaration. Consenting documents were approved by the University of Houston institutional review board for experimental studies. Inclusion criteria included subjects being between 18–35 years of age, ability to stand without assistance, no history of neurological or musculoskeletal dysfunction, and no known contraindications to tDCS stimulation such as metallic implants, history of seizures or brain damage (Datta et al., 2011). Physical preparedness was assessed using a PAR-Q (Thomas et al., 1992).

Protocol

Subjects participated in three sessions, which were separated by a minimum of 48 h. The greatest period between sessions

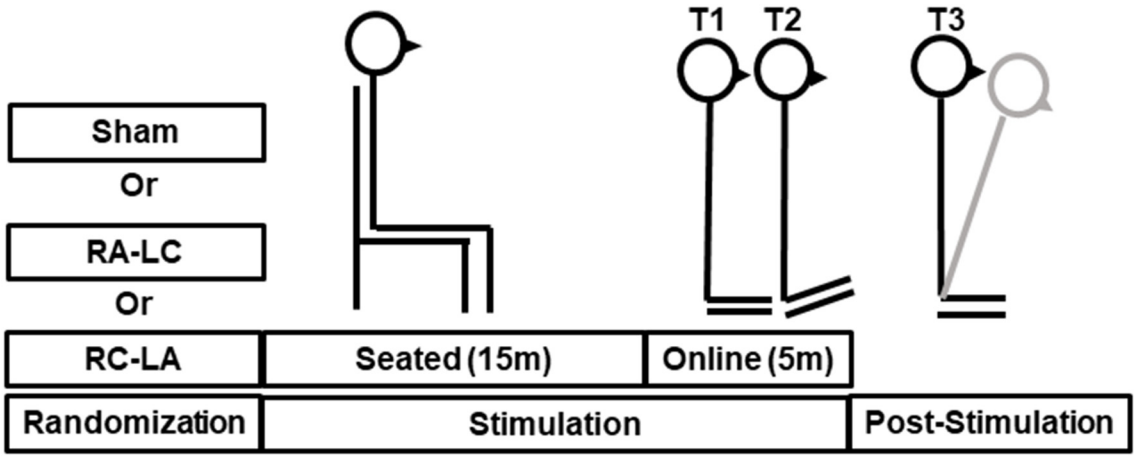

FIGURE 1 | Illustrative representation of stimulation and tasks during T1 (baseline), T2 (incline-intervention) and T3, (lean after-effect period). Transcranial direct current stimulation (tDCS) stimulation was started offline while the subject remained quietly seated. After 15 min the subject immediately proceeded through the T1-T3 tasks. The total stimulation duration was 20 min. The gray line shown during T3 reflects a typical response to incline-intervention, lean after-effect (LAE).

was 14 days [average 5.3 ± 4.1 days (mean ± SD)]. During each session, subjects performed an incline-intervention, which consisted of three trials (**Figure 1**). First, subjects performed a 30 s baseline trial of quiet stance (T1) on a horizontal surface. Next, they moved atop an inclined surface set to an angle of 10° for 5 min (T2). Last, subjects returned to standing on the horizontal surface (T3) where they stood for a final 5 min (**Figure 1**). Throughout the task, subjects were instructed to keep their eyes closed, place their arms across their chest, and stand naturally without, "resisting any pulls they felt on their body or temptation to lean." tDCS was applied at the beginning of each session and was administered in random order. Stimulation was administered in three conditions: Right Anodal-Left Cathodal (RA-LC), designed to slightly depolarize tissue in the rPPC while slightly hyperpolarizing tissue in the lPPC. Right Cathodal-Left Anodal (RC-LA), designed to do the opposite, and Sham, where the current was ramped up for 30 s and ramped down after 30 s of stimulation to simulate the scalp sensation of active stimulation without injecting sufficient current to alter cortical excitability (**Table 1**). For all conditions, stimulation was initiated before the incline-intervention (i.e., before T1). For the first 15 min of stimulation, the subject sat quietly, then, at the 15-min mark, subjects began to perform the protocol. First, subjects performed the baseline trial (T1), then immediately moved atop the inclined surface for T2, then immediately began T3. Stimulation was terminated at the end of T2, resulting in a total stimulation duration of 20 m. The stimulation order was double-blinded to the subject and the administrator of the experiment. A stimulation model can be seen in **Figure 2**.

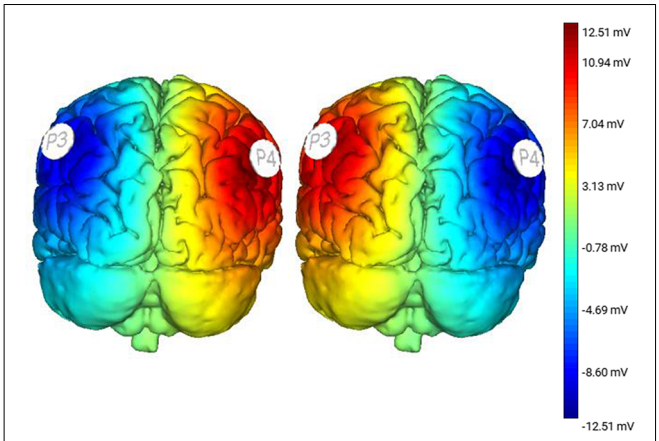

FIGURE 2 | Stimulation modeling illustrating modeled changes in cortical excitability resulting from Right Anodal-Left Cathodal (RA-LC) and Right Cathodal-Left Anodal (RC-LA) stimulation.

Instrumentation

Incline-interventions were performed on a surface set to an incline angle of 10° (ASAHI Corporation, Gifu, Japan). Kinematic experimental data were collected using a 12-Camera Vicon motion capture system. Subjects were measured and outfitted with reflective markers based on Vicon Nexus's Full Body Plug-in Gait Marker Set (Vicon, Oxford, UK). Kinematic data from all trials were captured at a rate of 100 Hz. Subjects also wore earmuffs to minimize auditory feedback. tDCS stimulation was performed using an eight-channel Starstim tDCS Device (Neuroelectrics, Spain). Saline soaked 25 cm^2 sponges were placed at P3 and P4 using the international 10-20 system (Homan et al., 1987). For both active conditions, stimulation was applied at 1.5 mA.

Data Processing

Kinematic data collected during the experiment were exported from Vicon Nexus and analyzed using custom MATLAB scripts (Mathworks, Inc., Natick, MA, USA). Marker trajectories of the legs and torso were utilized to compute the anterior-posterior (AP) center of gravity (COG) measurement. Based on previous literature, data derived from incline-interventions was filtered using a 4th order low-pass Butterworth filter with a cut-off

frequency of 0.1 Hz. This design can isolate changes in the mean center of gravity while eliminating signal higher frequency COG fluctuations during prolonged trials (Kluzik et al., 2005).

T1 AP-COG was baseline corrected. Raw signals were set to a position of zero at the start of T1. Because the subjects physically moved to and from the inclined surface to undergo T2, T3 AP-COG measures also required a baseline correction. To achieve this, upon returning to a horizontal stance, subjects stood with their eyes open for 5 s. Data during this time was averaged and that average was set to zero to ascertain lean after-effect related shift in COG while ignoring minute changes that may have occurred while the subject moved to and from the inclined surface. The subjects' eyes remained open during the initial 5 s of T3 because the opening of the eyes has been shown to extinguish LAE (Earhart et al., 2010). Data reflected that this was the case, with lean after-effect onset occurring once the eyes were closed. Thus, any anterior measure of COG is relative to the pre-adaptation stance, not an absolute position. We conducted a control experiment where 15 additional participants experienced the incline-intervention (i.e., T1-T3) without receiving tDCS to determine if experiencing active or sham tDCS influenced baseline (i.e., flat surface) stance.

We computed the mean position (Average AP-COG), the standard deviation of position, path length, and root mean square of position in the AP direction to compare baseline stance between stimulation conditions and the control condition (unstimulated). The COG data derived from the baseline-corrected post-inclined stance (T3) was used to calculate several outcome measures reflecting the magnitude of postural adaptation (LAE). Before any further calculations, two time periods were identified, the first 30 s of T3 was defined as the Early LAE period while the final 30 s was defined as the Late LAE period. The Max LAE was also calculated, which was defined as the maximum anterior AP-COG. Average AP-COG (Ave-COG) position during the Early and Late periods of T3 was also calculated to identify the magnitude of LAE present during each period. **Figure 2** describes these outcome measures visually (**Figure 3**). Finally, Off-Set Time, the first sample following Max LAE in which the subject returned to an average position within two standard deviations (SD) of their baseline position for a period of 10 s was calculated to identify what, if any, effect stimulation condition had on the time-course of recalibration to upright stance (Kluzik et al., 2005, 2007).

Statistical Analysis

To verify that tDCS did not alter baseline stance, average position in the AP direction, the standard deviation of AP position, AP-path length, and root mean square (RMS) of AP position were compared between stimulation conditions during T1. An additional sample of baseline measures from 15 subjects who did not receive tDCS stimulation was also included in the comparison to verify that Sham stimulation did not alter an unperturbed stance. Comparisons were made using separate repeated measures analysis of variance (rm-ANOVA) for each variable. Next, to identify the effects of tDCS stimulation on lean after-effect (LAE), a two-way rm-ANOVA (Condition by Time) was performed to compare average AP-COG during three time periods. First, the baseline position (T1), next during the Early period of T3, and last during the Late period of T3 to compare lean after-effect between the stimulation conditions. Follow-up one-way ANOVAs were utilized to compare average AP-COG during Early and Late LAE periods as well as for Max LAE and Off-Set Time between stimulation conditions. Pairwise comparisons for analyses were made using Bonferroni *post hoc* adjustments. For all analyses, significant findings were defined by an alpha value of $p < 0.05$. Effect sizes, derived from partial eta squared (η_p^2) for main effects and Hedge's G (HG) for pairwise differences were also derived in cases of significant findings. Statistical analyses were performed using SPSS (Version 25.0. IBM Corp., Armonk, NY, USA).

RESULTS

Fifteen subjects, eight females and seven males completed the study. Subjects were aged 23.4 ± 4.2 years, were 165.6 ± 12.6 cm tall, and weighed 77.4 ± 18.3 kg. When asked at the end of each session to identify what stimulation condition they had received, subjects guessed correctly 1.0 ± 0.78 times out of three indicating that subjects were generally unaware of what stimulation condition they were experiencing. Results of one-way rm-ANOVAs revealed no difference between stimulation conditions for the mean position ($F_{(3,12)} = 0.59$, $p = 0.63$, $\eta^2 = 0.13$), standard deviation of position ($F_{(3,12)} = 0.24$, $p = 0.74$, $\eta^2 = 0.09$), AP path length ($F_{(3,12)} = 0.14$, $p = 0.93$, $\eta^2 = 0.03$) or RMS of AP position ($F_{(3,12)} = 0.29$, $p = 0.83$, $\eta^2 = 0.07$) during baseline (T1) trials. This analysis included results from 15 pilot subjects who received no brain stimulation (i.e., unstimulated), demonstrating that tDCS did not alter the characteristics of stance during the baseline trial T1 and that the Sham condition can serve as effective control.

Analysis of COG data derived from the lean after-effect periods revealed that tDCS stimulation altered responses to inclined stance. Individual data can be found in **Table 2**. This is shown by differences in lean after-effect during T3 (**Figure 4**). Results of a two-way rm-ANOVA comparing Ave-COG during Baseline, Early and Late LAE periods between stimulation conditions revealed a significant overall effect of condition ($F_{(2,13)} = 7.61$, $p = 0.008$, $\eta^2 = 0.52$) no significant effect of time ($F_{(1,14)} = 5.2$, $p = 0.19$, $\eta^2 = 0.23$) but a significant interaction effect between time and condition ($F_{(2,13)} = 3.96$, $p = 0.03$, $\eta^2 = 0.59$). Additional analyses identified a significant main effect of stimulation conditions for Ave-COG during Early LAE ($F_{(2,13)} = 3.93$, $p = 0.046$, $\eta^2 = 0.38$), but pairwise comparisons using Bonferroni *post hoc* adjustments revealed no specific differences between stimulation conditions (Sham to RA-LC $p = 0.07$, Sham to RC-LA $p = 0.14$, RA-LC to RC-LA $p = 1$; **Figure 4B**). The condition also influenced the Ave-COG during the Late LAE period ($F_{(2,13)} = 8.47$, $p = 0.004$, $\eta^2 = 0.57$). Subsequent pairwise comparisons revealed that the RA-LC and RC-LA conditions each exhibited significantly less Ave-COG during Late LAE compared to the Sham condition

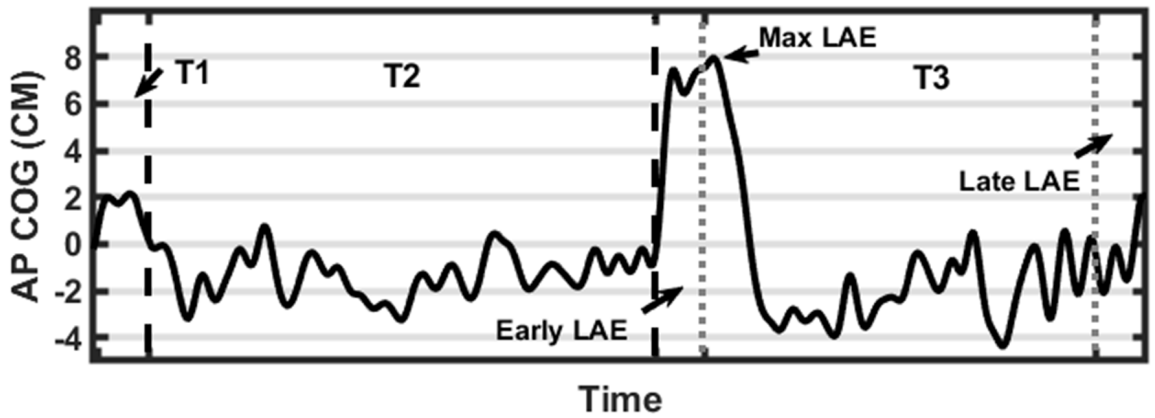

FIGURE 3 | Graphical representation of data processing parameters. Black dashed lines indicate transitions between trials (first line from T1-T2 and a second line from T2-T3). Gray dotted lines indicate measurement periods reflecting average anterior-posterior center of gravity (AP-COG) in during Early and Late LAE periods. The data presented are from one representative trial.

TABLE 1 | Definitions.

Center of graviy	COG	Approximation of one's overall position in space
Lean after-effect	LAE	Postural after-effect indicating adaptation, specifically adaptation to an incline-intervention
Posterior parietal cortex	PPC	Hub of multisensory integration in the cortex
Transcranial direct current stimulation	tDCS	Leads to depolarization or hyperpolarization of local brain tissue based on stimulation condition
Cathodal	RC or LC	Leads to relative hyperpolarization
Anodal	RA or LA	Leads to relative depolarization
Sham	Sham	Placebo

TABLE 2 | Postural adaptation outcomes.

	Maximum LAE			Average COG early			Average COG late			Off-set time		
Participant	**Sham**	**RA-LC**	**RC-LA**	**Sham**	**RA-LC**	**RC-LA**	**Sham**	**RA-LC**	**RC-LA**	**Sham**	**RA-LC**	**RC-LA**
1	2.44	0.95	0.63	1.00	0.09	0.57	0.31	0.02	−0.45	55.98	57.17	8.55
2	1.09	1.80	2.71	−1.40	−1.51	−0.55	1.71	−1.47	−1.43	37.28	50.92	48.55
3	1.17	1.88	1.45	0.80	1.60	0.39	0.82	0.30	0.53	42.34	42.25	0.55
4	2.34	1.15	1.19	0.44	0.27	−0.13	−1.21	−0.73	−2.63	13.83	11.61	13.41
5	5.01	1.43	2.90	4.79	1.14	−0.47	1.76	−0.74	0.20	37.42	5.87	38.43
6	3.60	0.82	0.47	2.15	0.13	−3.79	2.44	−1.57	−0.76	300	0.34	0.02
7	3.71	3.01	1.88	2.43	1.41	0.99	1.05	−1.52	0.43	36.55	63.48	166.99
8	8.73	5.52	9.41	6.05	2.89	8.50	2.01	−2.47	−4.93	61.71	72.38	115.13
9	1.17	3.02	2.52	0.59	0.63	2.30	0.04	−0.68	−0.18	117.91	172.19	92.77
10	2.93	1.98	2.14	1.47	0.62	0.53	1.12	−0.54	−0.64	230.14	257	76.61
11	0.27	−0.24	−0.34	0.13	−0.33	−0.99	−0.99	−1.47	−2.03	0.69	0.02	0.02
12	5.41	4.75	4.52	1.16	0.74	1.36	3.51	1.17	3.00	300	173.64	180.15
13	1.24	0.82	1.00	0.72	0.50	0.26	0.72	0.34	−0.27	122.14	48.37	39.49
14	2.72	2.69	1.06	0.65	1.41	−0.09	2.94	1.04	−1.75	55.81	38.76	77.09
15	2.15	0.15	0.50	1.02	−0.30	−1.00	0.50	0.22	1.33	45.57	17.35	22.95
Mean	2.93	1.98	2.14	1.47	0.62	0.53	1.12	−0.54	−0.64	97.16	67.42	58.71
SD	2.17	1.60	2.35	1.84	1.02	2.59	1.33	1.05	1.83	99.44	75.07	58.84

(p = 0.008, HG = 0.94; p = 0.003, HG = 0.98, respectively). The Ave-COG in the Late LAE for both active stimulation conditions were posterior to baseline (**Figure 4C**). Again, the average COG during the Late LAE period was not different between active conditions (p = 1). Time series data representing the lean after-effect between conditions can be observed in (**Figure 5**). A one-way rm-ANOVA of the maximum AP-COG (Max COG) again revealed a main effect of tDCS stimulation ($F_{(2,13)}$ = 8.33, p = 0.005, η^2 = 0.356; **Figure 6**). *Post hoc* comparisons found that both active stimulation conditions exhibited significantly less maximum forward lean than Sham (RA-LC p = 0.009 HG = 0.61; RC-LA p = 0.03 HG = 0.42), but there was again no difference between the two-active stimulation conditions (RA-LC to RC-LA p = 1). There were no differences in Off-Set Time between the three stimulation conditions ($F_{(2,13)}$ = 0.99, p = 0.397, η^2 = 0.13).

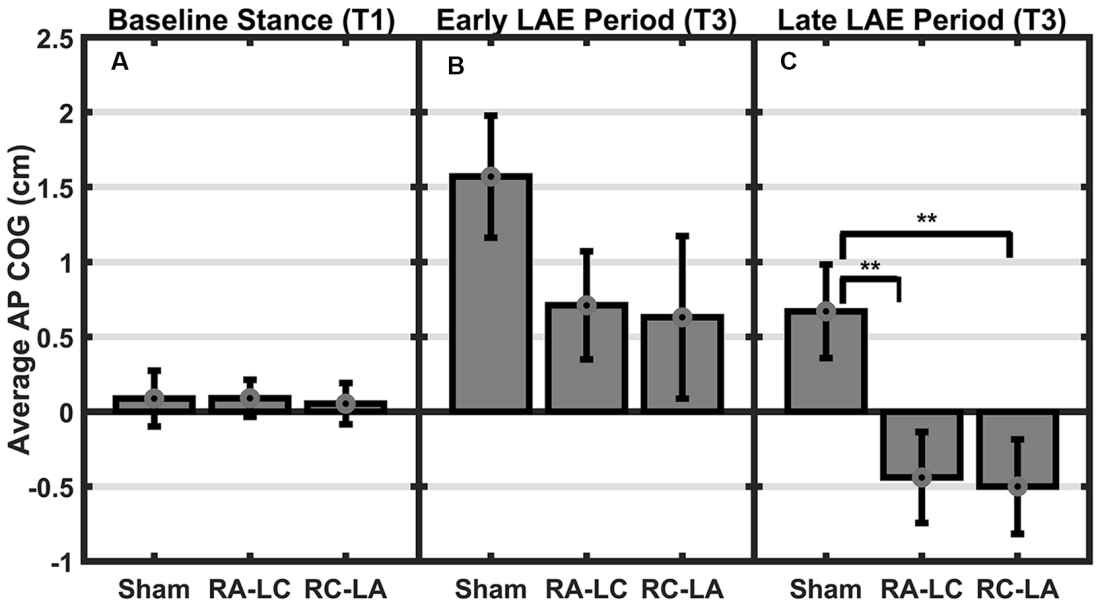

FIGURE 4 | Mean AP COG ± 1 SEM. Active stimulation significantly altered the lean after-effect. A significant effect of condition ($p = 0.008$) and condition by time interaction effect ($p = 0.03$) was found. No differences were observed during baseline stance ($p = 0.63$; **A**). A significant main effect of condition on average LAE during the early period **(B)** was found ($p = 0.046$) but no pairwise differences. Both active conditions exhibited lesser LAE than Sham during the Late LAE **(C)** period than Sham ($p = 0.004$; RA-LC $p = 0.008$ RC-LA $p = 0.003$), $^{**}p < 0.01$.

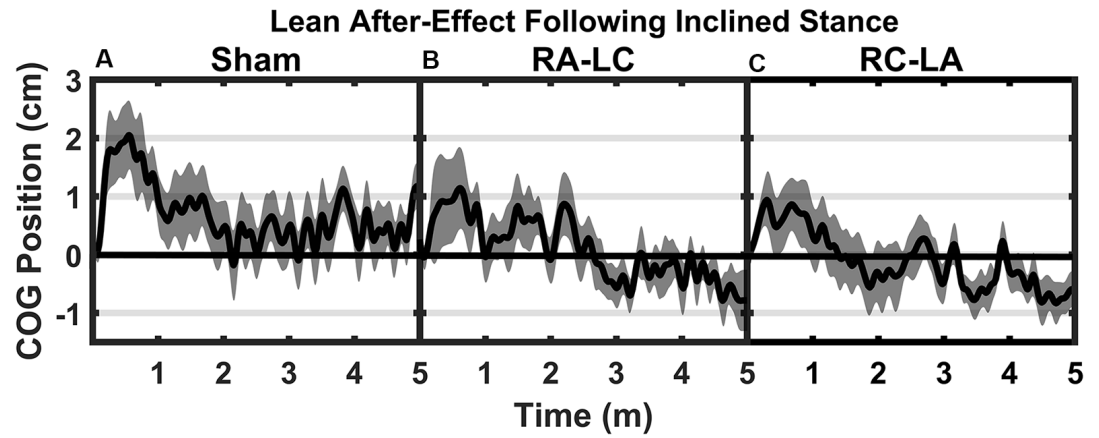

FIGURE 5 | Mean AP COG ± 1 SEM position during T3 after Sham **(A)**, RA-LC **(B)**, and RC-LA **(C)** stimulation.

DISCUSSION

The current investigation was designed to assess the role of the PPC in postural adaptation within a group of 15 healthy, young adults. Neuromodulation was applied in three conditions: RA-LC, RC-LA, and Sham in a random, double-blind fashion. Postural adaptation, measured by lean after-effect, was decreased in both active stimulation conditions compared to Sham. These findings demonstrate that active stimulation decreased initial adaptation to the incline-intervention (i.e., less forward lean). Off-Set Time was not different between conditions, which shows that while the magnitude of the adaptation was affected, the time course necessary to re-orient to gravity was not. These findings suggest impaired adaptability of the internal representation of one's body position following active stimulation of the PPC, regardless of which hemisphere was inhibited and which was excited. Additionally, the lack of differences between conditions in the Off-Set Time measure suggests that the time course associated with return to baseline may result from central processing occurring in areas of the cortex other than the PPC.

Evidence indicates that PPC integrates sensory information from the visual, vestibular, and proprioceptive systems to

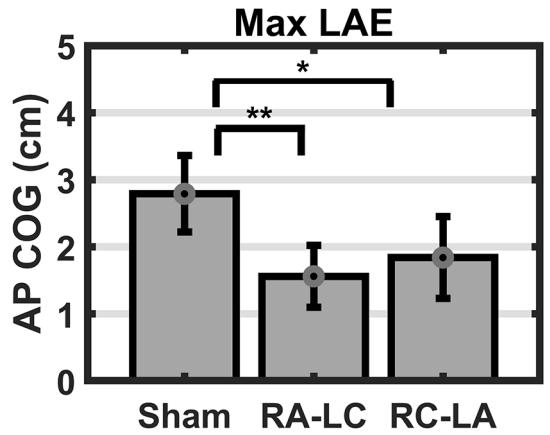

FIGURE 6 | Mean AP COG ±1 SEM. Active stimulation decreased the maximum lean after-effect ($p = 0.005$). Both active conditions exhibited smaller Max LAE than Sham (RA-LC $p = 0.009$; RC-LA $p = 0.03$), $^{*}p < 0.05$, $^{**}p < 0.01$.

maintain an internal representation of one's posture, which is continuously updated to influence motor commands (Andersen et al., 2004; Buneo and Andersen, 2006). During this experiment, we observed no difference in LAE between active stimulation conditions (i.e., RA-LC and RC-LA). This finding is of interest because some experiments have sought to identify hemisphere-specific roles of the PPC. Studies have suggested that the right hemisphere may be activated to a greater extent than the left in response to proprioceptive manipulations leading to movement illusions, such as tendon vibration (Hagura et al., 2009; Amemiya and Naito, 2016; Naito et al., 2016, 2017). In a series of studies, Naito et al. (2017) identified increased activity in the right inferior parietal lobule (IPL) during tendon vibration, which they identify as part of a frontoparietal network involved in proprioceptive processing to maintain a sense of position. According to the same group, the left IPL may be biased towards computations that associate self-position and the external environment and may be less sensitive to proprioceptive perturbations (Naito et al., 2016). Conversely, the left hemisphere PPC has been suggested to be an area closely associated with motor adaptation.

In a pair of case studies, Newport et al. (2006) identified impaired prism adaptation in a patient with bilateral damage to the PPC, with greater damage in the left hemisphere (Newport and Jackson, 2006; Newport et al., 2006). Later, these results were clarified by Mutha et al. (2011). In their study, Mutha et al. (2011) found that visuomotor adaptation was hindered in subjects with lesions of the left, but not right parietal region. The authors argued that the left parietal region is involved in modifying the internal representation of self-position, and the relationship between movement and the environment (Mutha et al., 2011). While Mutha et al. (2011) suggested that the left parietal region was more important for visuomotor adaptation, the current investigation found decreased postural adaptation through inhibition of either hemisphere. There are several possible reasons for these findings.

For many visuomotor adaptation experiments, a unilateral upper limb task has been employed, which could induce greater activation in the contralateral hemisphere than a bilateral task. Simply by the nature of postural control as a bilateral task, there may be increased bilateral input from several cortical areas. Postural adaptation tasks also include stability demands, unlike upper body adaptation tasks. Sensory processing may be altered by additional stability related requirements including the updating of the internal representation of the body and its relationship to gravitational space. Previous investigations have found increased PPC activation during difficult postural control tasks when exposed to multiple sensory perturbations (Takakura et al., 2015). Unfortunately, Takakura et al. (2015) were only able to record hemodynamics from the right hemisphere and were unable to identify if bilateral increases in activity were present. In healthy subjects, Ishigaki et al. (2016) found altered sensory integration of augmented feedback from cathodal tDCS stimulation of the lPPC during postural control, however, their study utilized light touch only on the right hand (Ishigaki et al., 2016). Johannsen et al. (2015) also identified that normal postural control involves parietal representation and that modulation of these regions can alter postural dynamics during periods of altered sensory feedback.

As the PPC has not previously been studied through the lens of postural adaptation, it was not apparent if there would be hemisphere specific contributions in response to a postural incline task. While the results of the current investigation cannot delineate the specific roles of the hemispheres, the results suggest that both hemispheres are involved in postural adaptation. This may be due to the reciprocal connections which exist between the bilateral PPC and the cerebellum (Amino et al., 2001). Specifically, the IPL, which compares perceived body positions to extra personal space is innervated by the cerebellum (Clower et al., 2001). The PPC utilizes sensory feedback as well as the efferent copy provided by the cerebellum to maintain an internal representation of limb positions and the body in space, what could be described as body ownership or the body schema (Amino et al., 2001; Dijkerman and de Haan, 2007; Kammers et al., 2009; Parkinson et al., 2010; van Stralen et al., 2011). Recent publications have even gone so far as to identify the PPC as the home for the "posture cells of the brain" (Chen, 2018; Mimica et al., 2018). The current study reinforces the notion of the bilateral PPC's role in monitoring and updating the internal representation.

This investigation identified decreased postural adaptation following active stimulation of the bilateral PPC. This study employed a paradigm that stimulated the bilateral PPC instead of placing the return electrode on another brain region (i.e., the supraorbital foramen; Ishigaki et al., 2016) to contain stimulation to the PPC and not alter the excitability of other brain regions such as the somatosensory or motor cortices. Because of this, as one hemisphere received inhibitory stimulation, the other received excitatory stimulation. Previously, some studies have shown that healthy young subjects experience alteration of sensory detection thresholds following cathodal,

but not anodal stimulation of S1 (Grundmann et al., 2011). Additionally, it has been shown that cathodal stimulation of the cerebellum decreases postural stability while anodal does not change stability in young subjects (Foerster et al., 2017). Other studies have shown the effects of anodal, but not cathodal stimulation in healthy subjects when stimulation was performed over motor areas (Carter et al., 2015). Additionally, it is possible that by utilizing a stimulation paradigm that required current to cross between hemispheres, our stimulation led intra-hemispheric interactions that cannot be fully explained by describing the sum of anodal and cathodal stimulation (Lindenberg et al., 2013). There is also some evidence that the inhibitory stimulus can lead to improved performance. Inhibitory stimulation could suppress neural noise, which can improve the signal to noise ratio, and facilitate the function of the affected cortical structures (Antal et al., 2004; Filmer et al., 2013). Therefore, we can only speculate as to whether the decreased adaptability observed in our study is due to the inhibitory nature of cathodal stimulation, or excitatory nature of anodal stimulation. Regardless, the current study does demonstrate that stimulation designed to alter PPC excitability does alter adaptability overall. The present results also indicate that stimulation does not serve to disrupt the time course of postural de-adaptation suggesting the magnitude of LAE is a separate process from the temporal characteristics of LAE. Future investigations should be conducted to explore this possibility.

In the future, designs may confirm these findings using techniques such as disruptive transcranial magnetic stimulation (rTMS) because more focal stimulation is less likely to alter the excitability of other brain regions. A previous publication by Johannsen et al. (2015) has illustrated the possibility of the use of rTMS to investigate parietal processes involved in postural control. The group performed 1,200 pulses of inhibitory rTMS at a frequency of 1 Hz to disrupt the left inferior parietal gyrus and identified that this disruption altered the body-sway response to altered sensory feedback during the posture. These results verify the possibility of using rTMS to probe the parietal lobes in the field of postural control (Johannsen et al., 2015). Also, while this study involved neuromodulation of the PPC, no recordings of brain activity were obtained. Future investigations are needed to verify the effects of tDCS on PPC excitability in postural adaptation. The brain is a complex and dynamic organ. As such, the brain's state during stimulation can influence the effects of non-invasive brain stimulation. Future research should endeavor to utilize neuroimaging (i.e., EEG) to optimize stimulation parameters to elicit the desired cortical changes (Bergmann, 2018). This study is important because while upper body motor adaptation research is critical for understanding the dynamics of human sensorimotor control, postural adaptation is more directly linked to public health due to fall risk. Therefore, this investigation provides novel information that may lead future experimentation to what efficacy there may be for non-invasive brain stimulation as a therapeutic measure to improve adaptability during postural control, decreasing fall risk. Future investigations should include clinical populations to identify the viability of tDCS of the PPC as a rehabilitative mechanism as well as include neuroimaging techniques.

DATA AVAILABILITY STATEMENT

The original contributions presented in the study are included in the article (**Table 2**), further inquiries can be directed to the corresponding author.

ETHICS STATEMENT

The studies involving human participants were reviewed and approved by University of Houston Committee for the Protection of Human Subjects. The patients/participants provided their written informed consent to participate in this study.

AUTHOR CONTRIBUTIONS

DY, PP, and CL contributed to the study design. DY recruited the subjects and was involved in the informed consent process, processed, and analyzed data and wrote the first draft of the manuscript. All authors contributed to data interpretation and manuscript revision, and all read and approved the submitted version.

ACKNOWLEDGMENTS

We would like to acknowledge the contributions of Beom-Chan Lee and Benjamin Tamber-Rosenau in refining the project as well as Hidetaka Hibino and Daisey Vega in assisting in the double-blinding process.

REFERENCES

Amemiya, K., and Naito, E. (2016). Importance of human right inferior frontoparietal network connected by inferior branch of superior longitudinal fasciculus tract in corporeal awareness of kinesthetic illusory movement. *Cortex* 78, 15–30. doi: 10.1016/j.cortex.2016.01.017

Amino, Y., Kyuhou, S. I., Matsuzaki, R., and Gemba, H. (2001). Cerebello-thalamo-cortical projections to the posterior parietal cortex in the macaque monkey. *Neurosci. Lett.* 309, 29–32. doi: 10.1016/s0304-3940(01)02018-3

Andersen, R., Meeker, D., Pesaran, B., Breznen, B., Buneo, C., and Scherberger, H. (2004). "Sensorimotor transformations in the posterior parietal cortex," in *The Cognitive Neurosciences III*, ed. M. Gazzaniga (Cambridge MA: MIT Press), 463–474. Available online at: http://authors.library.caltech.edu/19261/1/Andersen2004p10934Cognitive_Neurosciences_Iii_Third_Edition.pdf.

Antal, A., Nitsche, M. A., Kruse, W., Kincses, T. Z., Hoffmann, K. P., and Paulus, W. (2004). Direct current stimulation over V5 enhances visuomotor coordination by improving motion perception in humans. *J. Cogn. Neurosci.* 16, 521–527. doi: 10.1162/089892904323057263

Bergmann, T. O. (2018). Brain state-dependent brain stimulation. *Front. Psychol.* 9:2108. doi: 10.3389/fpsyg.2018.02108

Buneo, C. A., and Andersen, R. A. (2006). The posterior parietal cortex: sensorimotor interface for the planning and online control of visually guided

movements. *Neuropsychologia* 44, 2594–2606. doi: 10.1016/j.neuropsychologia.2005.10.011

Carter, M. J., Maslovat, D., and Carlsen, A. N. (2015). Anodal transcranial direct current stimulation applied over the supplementary motor area delays spontaneous antiphase-to-in-phase transitions. *J. Neurophysiol.* 113, 780–785. doi: 10.1152/jn.00662.2014

Chen, B. G. (2018). Identifying posture cells in the brain. *Science* 3788, 2017–2019. doi: 10.1126/science.aav3819

Chong, R. K., Adams, K., Fenton, K., Gibson, M., Hodges, K., Horne, J., et al. (2014). Postural adaptation to a slow sensorimotor set-changing task in Parkinson's disease. *Comprehensive Psychol.* 3:9. doi: 10.2466/15.26.cp.3.9

Chong, R., Berl, B., Cook, B., Turner, P., and Walker, K. (2017). Individuals with a vestibular-related disorder use a somatosensory-dominant strategy for postural orientation after inclined stance. *Acta Neurol. Scand.* 135, 635–640. doi: 10.1111/ane.12658

Chritchley, M. (1953). *The Parietal Lobes.* Baltimore: The Williams and Wilkins Company.

Clower, D. M., West, R. A., Lynch, J. C., and Strick, P. L. (2001). The inferior parietal lobule is the target of output from the superior colliculus, hippocampus, and cerebellum. *J. Neurosci.* 21, 6283–6291. doi: 10.1523/JNEUROSCI.21-16-06283.2001

Datta, A., Bikson, M., and Fregni, F. (2011). Transcranial direct current stimulation in patients with skull defects and skull plates: high-resolution computational FEM study of factors altering cortical current flow. *NeuroImage* 52, 1268–1278. doi: 10.1016/j.neuroimage.2010.04.252

Derouesné, C., Mas, J. L., Bolgert, F., and Castaigne, P. (1984). Pure sensory stroke caused by a small cortical infarct in the middle cerebral artery territory. *Stroke* 15, 660–662. doi: 10.1161/01.str.15.4.660

Desmurget, M., Epstein, C. M., Turner, R. S., Problanc, C., Alexander, G. E., and Grafton, S. T. (1999). Role of the posterior parietal cortex in updating reaching movements to a visual target. *Nat. Neurosci.* 2, 563–567. doi: 10.1038/9219

Dijkerman, H. C., and de Haan, E. H. F. (2007). Somatosensory processes subserving perception and action. *Behav. Brain Sci.* 30, 189–201. doi: 10.1017/s0140525x07001392

Earhart, G. M., Henckens, J. M., Carlson-Kuhta, P., and Horak, F. B. (2010). Influence of vision on adaptive postural responses following standing on an incline. *Exp. Brain Res.* 203, 221–226. doi: 10.1007/s00221-010-2208-4

Edwards, L. L., King, E. M., Buetefisch, C. M., and Borich, M. R. (2019). Putting the 'sensory' into sensorimotor control: the role of sensorimotor integration in goal-directed hand movements after stroke. *Front. Integr. Neurosci.* 13:16. doi: 10.3389/fnint.2019.00016

Filmer, H. L., Mattingley, J. B., and Dux, P. E. (2013). Improved multitasking following prefrontal TDCS. *Cortex* 49, 2845–2852. doi: 10.1016/j.cortex.2013.08.015

Findlater, S. E., Desai, J. A., Semrau, J. A., Kenzie, J. M., Rorden, C., Herter, T. M., et al. (2016). Central perception of position sense involves a distributed neural network—evidence from lesion-behavior analyses. *Cortex* 79, 42–56. doi: 10.1016/j.cortex.2016.03.008

Foerster, Á., Melo, L., Mello, M., Castro, R., Shirahige, L., Rocha, S., et al. (2017). Cerebellar transcranial direct current stimulation (CtDCS) impairs balance control in healthy individuals. *Cerebellum* 16, 872–875. doi: 10.1007/s12311-017-0863-8

Goel, R., Nakagome, S., Rao, N., Paloski, W. H., Contreras-Vidal, J. L., and Parikh, P. J. (2019). Fronto-parietal brain areas contribute to the online control of posture during a continuous balance task. *Neuroscience* 413, 135–153. doi: 10.1016/j.neuroscience.2019.05.063

Grundmann, L., Rolke, R., Nitsche, M. A., Pavlakovic, G., Happe, S., Detlef Treede, R., et al. (2011). Effects of transcranial direct current stimulation of the primary sensory cortex on somatosensory perception. *Brain Stimul.* 4, 253–260. doi: 10.1016/j.brs.2010.12.002

Gurfinkel, V. S., Ivanenko, Y. P., Levik, Y. S., and Babakova, I. A. (1995). Kinesthetic reference for human orthograde posture. *Neuroscience* 68, 229–243. doi: 10.1016/0306-4522(95)00136-7

Hagura, N., Oouchida, Y., Aramaki, Y., Okada, T., Matsumura, M., Sadato, N., et al. (2009). Visuokinesthetic perception of hand movement is mediated by cerebro-cerebellar interaction between the left cerebellum and right parietal cortex. *Cereb. Cortex* 19, 176–186. doi: 10.1093/cercor/bhn068

Head, H., and Holmes, H. (1911). Sensory disturbances from cerebral lesions. *Brain* 34, 102–254. doi: 10.1093/brain/34.2-3.102

Heinen, K., Sagliano, L., Candini, M., Husain, M., Cappelletti, M., and Zokaei, N. (2016). Cathodal transcranial direct current stimulation over posterior parietal cortex enhances distinct aspects of visual working memory. *Neuropsychologia* 87, 35–42. doi: 10.1016/j.neuropsychologia.2016.04.028

Homan, R. W., Herman, J., and Purdy, P. (1987). Cerebral location of international 10–20 system electrode placement. *Electroencephalogr. Clin. Neurophysiol.* 66, 376–382. doi: 10.1016/0013-4694(87)90206-9

Ishigaki, T., Imai, R., and Morioka, S. (2016). Cathodal transcranial direct current stimulation of the posterior parietal cortex reduces steady-state postural stability during the effect of light touch. *Neuroreport* 27, 1050–1055. doi: 10.1097/wnr.0000000000000654

Ivanenko, Y., and Gurfinkel, V. S. (2018). Human postural control. *Front. Neurosci.* 12:171. doi: 10.3389/fnins.2018.00171

Johannsen, L., Hirschauer, F., Stadler, W., and Hermsdörfer, J. (2015). Disruption of contralateral inferior parietal cortex by 1Hz repetitive TMS modulates body sway following unpredictable removal of sway-related fingertip feedback. *Neurosci. Lett.* 586, 13–18. doi: 10.1016/j.neulet.2014.11.048

Kammers, M. P. M., Verhagen, L., Dijkerman, H. C., Hogendoorn, H., De Vignemont, F., and Schutter, D. J. L. G. (2009). Is this hand for real? Attenuation of the rubber hand illusion by transcranial magnetic stimulation over the inferior parietal lobule. *J. Cogn. Neurosci.* 21, 1311–1320. doi: 10.1162/jocn.2009.21095

Kaulmann, D., Hermsdörfer, J., and Johannsen, L. (2017). Disruption of right posterior parietal cortex by continuous theta burst stimulation alters the control of body balance in quiet stance. *Eur. J. Neurosci.* 45, 671–678. doi: 10.1111/ejn.13522

Kluzik, J., Horak, F. B., and Peterka, R. J. (2005). Differences in preferred reference frames for postural orientation shown by after-effects of stance on an inclined surface. *Exp. Brain Res.* 162, 474–489. doi: 10.1007/s00221-004-2124-6

Kluzik, J., Peterka, R. J., and Horak, F. B. (2007). Adaptation of postural orientation to changes in surface inclination. *Exp. Brain Res.* 178, 1–17. doi: 10.1007/s00221-006-0715-0

Lefaucheur, J.-P., and Wendling, F. (2019). Mechanisms of action of TDCS: a brief and practical overview. *Neurophysiol. Clin.* 49, 269–275. doi: 10.1016/j.neucli.2019.07.013

Lindenberg, R., Nachtigall, L., Meinzer, M., Sieg, M. M., and Flöel, A. (2013). Differential effects of dual and unihemispheric motor cortex stimulation in older adults. *J. Neurosci.* 33, 9176–9183. doi: 10.1523/JNEUROSCI.0055-13.2013

Mimica, B., Dunn, B. A., Tombaz, T., Srikanth Bojja, V. P. T. N. C., and Whitlock, J. R. (2018). Efficient cortical coding of 3D posture in freely behaving rats. *BioRxiv* [Preprint]. doi: 10.1101/307785

Mutha, P. K., Sainburg, R. L., and Haaland, K. Y. (2011). Left parietal regions are critical for adaptive visuomotor control. *J. Neurosci.* 31, 6972–6981. doi: 10.1523/JNEUROSCI.6432-10.2011

Naito, E., Morita, T., and Amemiya, K. (2016). Body representations in the human brain revealed by kinesthetic illusions and their essential contributions to motor control and corporeal awareness. *Neurosci. Res.* 104, 16–30. doi: 10.1016/j.neures.2015.10.013

Naito, E., Morita, T., Saito, D. N., Ban, M., Shimada, K., Okamoto, Y., et al. (2017). Development of right-hemispheric dominance of inferior parietal lobule in proprioceptive illusion task. *Cereb. Cortex* 27, 5385–5397. doi: 10.1093/cercor/bhx223

Naito, E., Nakashima, T., Kito, T., Aramaki, Y., Okada, T., and Sadato, N. (2007). Human limb-specific and non-limb-specific brain representations during kinesthetic illusory movements of the upper and lower extremities. *Eur. J. Neurosci.* 25, 3476–8347. doi: 10.1111/j.1460-9568.2007.05587.x

Newport, R., Brown, L., Husain, M., Mort, D., and Jackson, S. R. (2006). The role of the posterior parietal lobe in prism adaptation: failure to adapt to optical prisms in a patient with bilateral damage to posterior parietal cortex. *Cortex* 42, 720–729. doi: 10.1016/s0010-9452(08)70410-6

Newport, R., and Jackson, S. R. (2006). Posterior parietal cortex and the dissociable components of prism adaptation. *Neuropsychologia* 44, 2757–2765. doi: 10.1016/j.neuropsychologia.2006.01.007

Parkinson, A., Condon, L., and Jackson, S. R. (2010). Parietal cortex coding of limb posture: in search of the body-schema. *Neuropsychologia* 48, 3228–3234. doi: 10.1016/j.neuropsychologia.2010.06.039

Peterka, R. J. (2002). Sensorimotor integration in human postural control. *J. Neurophysiol.* 88, 1097–1118. doi: 10.1152/jn.2002.88.3.1097

Sabes, P. N. (2011). Sensory integration for reaching: models of optimality in the context of behavior and the underlying neural circuits. *Prog. Brain Res.* 191, 195–209. doi: 10.1016/B978-0-444-53752-2.00004-7

Sober, S. J., and Sabes, P. N. (2003). Multisensory integration during motor planning. *J. Neurosci.* 23, 6982–6992. doi: 10.1523/JNEUROSCI.23-18-06982.2003

Takakura, H., Nishijo, H., Ishikawa, A., and Shojaku, H. (2015). Cerebral hemodynamic responses during dynamic posturography: Analysis with a multichannel near-infrared spectroscopy system. *Front. Hum. Neurosci.* 9:620. doi: 10.3389/fnhum.2015.00620

Takeuchi, N., Sudo, T., Oouchida, Y., Mori, T., and Ichi Izumi, S. (2019). Synchronous neural oscillation between the right inferior fronto-parietal cortices contributes to body awareness. *Front. Hum. Neurosci.* 13:330. doi: 10.3389/fnhum.2019.00330

Thomas, S., Reading, J., and Shephard, R. J. (1992). Revision of the physical activity readiness questionnaire (PAR-Q). *Can. J. Sport Sci.* 17, 338–345.

van Stralen, H. E., van Zandvoort, M. J. E., and Dijkerman, H. C. (2011). The role of self-touch in somatosensory and body representation disorders after stroke. *Philos. Trans. R. Soc. Lond. B Biol. Sci.* 366, 3142–3152. doi: 10.1098/rstb.2011.0163

Wierzbicka, M. M., Gilhodes, J. C., and Roll, J. P. (1998). Vibration-induced postural posteffects. *J. Neurophysiol.* 79, 143–150. doi: 10.1152/jn.1998.79.1.143

Conflict of Interest: The authors declare that the research was conducted in the absence of any commercial or financial relationships that could be construed as a potential conflict of interest.

frontiers in Human Neuroscience

ORIGINAL RESEARCH
published: 17 July 2020
doi: 10.3389/fnhum.2020.00282

Lesion Topography Impact on Shoulder Abduction and Finger Extension Following Left and Right Hemispheric Stroke

Silvi Frenkel-Toledo[1,2]*, *Shay Ofir-Geva*[2,3] *and Nachum Soroker*[2,3]

[1]*Department of Physical Therapy, School of Health Sciences, Ariel University, Ariel, Israel,* [2]*Department of Neurological Rehabilitation, Loewenstein Rehabilitation Hospital, Raanana, Israel,* [3]*Sackler Faculty of Medicine, Tel Aviv University, Tel Aviv, Israel*

The existence of shoulder abduction and finger extension movement capacity shortly after stroke onset is an important prognostic factor, indicating favorable functional outcomes for the hemiparetic upper limb (HUL). Here, we asked whether variation in lesion topography affects these two movements similarly or distinctly and whether lesion impact is similar or distinct for left and right hemisphere damage. Shoulder abduction and finger extension movements were examined in 77 chronic post-stroke patients using relevant items of the Fugl-Meyer test. Lesion effects were analyzed separately for left and right hemispheric damage patient groups, using voxel-based lesion-symptom mapping. In the left hemispheric damage group, shoulder abduction and finger extension were affected only by damage to the corticospinal tract in its passage through the corona radiata. In contrast, following the right hemispheric damage, these two movements were affected not only by corticospinal tract damage but also by damage to white matter association tracts, the putamen, and the insular cortex. In both groups, voxel clusters have been found where damage affected shoulder abduction and also finger extension, along with voxels where damage affected only one of the two movements. The capacity to execute shoulder abduction and finger extension movements following stroke is affected significantly by damage to shared and distinct voxels in the corticospinal tract in left-hemispheric damage patients and by damage to shared and distinct voxels in a larger array of cortical and subcortical regions in right hemispheric damage patients.

Keywords: stroke, upper extremity, shoulder, abduction, finger, extension, brain mapping

OPEN ACCESS

Edited by:
Marco Iosa,
Santa Lucia Foundation (IRCCS), Italy

Reviewed by:
Giovanni Morone,
Santa Lucia Foundation (IRCCS), Italy
Alessandro Picelli,
University of Verona, Italy

***Correspondence:**
Silvi Frenkel-Toledo
silvift@ariel.ac.il

Specialty section:
This article was submitted to Motor Neuroscience, a section of the journal Frontiers in Human Neuroscience

Received: *12 May 2020*
Accepted: *23 June 2020*
Published: *17 July 2020*

Citation:
Frenkel-Toledo S, Ofir-Geva S and Soroker N (2020) Lesion Topography Impact on Shoulder Abduction and Finger Extension Following Left and Right Hemispheric Stroke. Front. Hum. Neurosci. 14:282. doi: 10.3389/fnhum.2020.00282

INTRODUCTION

Stroke is a leading cause of adult acquired long-term motor disability (Langhorne et al., 2011). Up to 85% of post-stroke survivors present an initial upper limb (UL) motor deficit (Wade et al., 1983; Olsen, 1990), and up to 50% encounter UL function problems 4 years after stroke onset (Broeks et al., 1999). As a result, independence in activities of daily living, as well as the quality of life, remain reduced for most patients with severe hemiparesis (Urton et al., 2007). Upper limb rehabilitation trials designed to improve recovery rates have been largely unsuccessful (Krakauer and Carmichael, 2017), thus stressing the importance of obtaining a better understanding of the factors that limit and prevent the recovery process.

Recovery prediction for the hemiparetic upper limb (HUL) is important for setting a realistic rehabilitation goal, for planning a focused and personalized rehabilitation treatment program and for a more efficient allocation of resources. Early return of finger extension (FE; Fritz et al., 2005; Smania et al., 2007; Nijland et al., 2010; Stinear et al., 2012, 2017b; Winters et al., 2016; Snickars et al., 2017; Hoonhorst et al., 2018) and shoulder abduction (SA; Katrak et al., 1998; Nijland et al., 2010; Stinear et al., 2012, 2017b; Winters et al., 2016; Snickars et al., 2017; Hoonhorst et al., 2018) were found to be important prognostic determinants of subsequent HUL function after stroke. For example, in a cohort study, Nijland et al. (2010) found that stroke patients who exhibit some voluntary extension of the fingers and some abduction of the hemiplegic shoulder on day 2 have a 0.98 probability of regaining some dexterity at 6 months, whereas the probability was only 0.25 for those who did not exhibit this voluntary motor activity early after stroke onset. In another cohort study, Katrak et al. (1998) found that initial active shoulder abduction noted on average 11 days after stroke onset, predicted good hand movement at 1 month and hand function at 1 and 2 months. Bakker et al. (2019) even found that the ability of patients to voluntarily extend the fingers within 4 weeks after stroke was strongly related to Fugl-Meyer (FM) at 26 weeks after stroke, with no false-negative results and no additional value of the motor-evoked potential amplitude of the affected finger extension muscle for this clinical predictor. More recent studies have developed algorithms (also based on the scoring of SA and FE movements) to predict an individual's potential for UL recovery within a few months post-stroke (Stinear et al., 2012, 2017b) and 2 years post-stroke (Smith et al., 2019). The implementation of the "Predict Recovery Potential" (PREP) algorithm for prediction of UL functionality in stroke rehabilitation, which combines clinical measures and neurophysiological and neuroimaging biomarkers, modified therapy content and increased rehabilitation efficiency after stroke, without compromising clinical outcomes (Stinear et al., 2017a).

Recovery of HUL function is constrained by the location of the anatomical damage (Grefkes and Fink, 2012; Grefkes and Ward, 2014; Frenkel-Toledo et al., 2019). During the acute phase, the probability of HUL recovery was found to decrease progressively with lesion location as follows: cortex—corona radiata—posterior limb of the internal capsule (PLIC; Shelton and Reding, 2001). In the sub-acute phase, damage to subcortical structures showed a higher association with poor motor performance of the HUL (Feys et al., 2000). We recently used voxel-based lesion-symptom mapping (VLSM; Bates et al., 2003) to investigate the impact of stroke lesion topography on HUL function (Frenkel-Toledo et al., 2019). Unlike various previous studies, where patients with right and left hemispheric damage (RHD, LHD) were grouped, the analysis of each patient group was done separately, given the differences between the dominant left and the non-dominant right cerebral hemispheres in the functional neuroanatomy of motor control (Tretriluxana et al., 2009; Mani et al., 2013), and known differences in patterns of motor recovery (Zemke et al., 2003; Wu et al., 2015). We found that in the sub-acute phase, HUL motor ability following LHD, assessed using the FM test, is affected mainly by damage to white matter tracts, the putamen, and the insula. In the chronic phase, FM performance in LHD patients was affected only by damage to white matter tracts. In contrast, HUL function following RHD was affected in both phases by damage to a large array of cortical and subcortical structures, notably the basal ganglia, white matter tracts, and the insula (Frenkel-Toledo et al., 2019).

Patients' ability to execute voluntarily FE movement shortly after stroke onset is believed to depend on propagation of motor cortical impulses *via* the corticospinal tract (CST; Brodal, 2016; Stinear et al., 2017b), as the spinal motor neurons that innervate distal upper limb muscles are controlled almost exclusively by upper motor neurons of the lateral corticospinal system, which crossed from the contralateral side at the medullary level (Palmer and Ashby, 1992). By contrast, SA—a proximal UL movement, is likely to be controlled to some extent also by the anterior (ventral, non-crossing) CST and the descending brainstem tracts that maintain a more widespread bilateral innervation at the spinal level (Brodal, 2016). Despite this difference in innervation patterns, both early execution of FE and early execution of SA were found to constitute important prognostic determinants of HUL functional recovery, with quite similar sensitivity and specificity. For example, Snickars et al. (2017) found that a prognostic model based on FE at 3 days post-stroke onset plus stroke severity had sensitivity and specificity of 90.5% and 90.3%, respectively, and a model based on SA at 3 days and stroke severity had sensitivity and specificity of 85.7% and 82.3%, respectively.

The extremely high positive predictive value of early demonstration of SA and FE movement capacity (Katrak et al., 1998; Fritz et al., 2005; Smania et al., 2007; Nijland et al., 2010; Stinear et al., 2012, 2017b; Winters et al., 2016; Snickars et al., 2017; Hoonhorst et al., 2018) is likely to reflect the high correlation between the dynamics of SA and other shoulder-girdle movements, and high correlation of FE and other hand movements in the recovery process. This enables the use of these two movements as indicators of the capacity to move the proximal and distal segments of the HUL in activities of daily living. Unlike the high positive predictive value of SA and FE movements early after stroke onset (Nijland et al., 2010), the negative predictive value of these movements is much lower (i.e., lack of SA and FE movements early after onset does not preclude late recovery of HUL function). A substantial number of patients without initial voluntary FE movements experience a spontaneous return of these movements in the first 3 months post-stroke (Winters et al., 2016). According to the PREP-2 algorithm for prediction of HUL function at 3 months post-stroke, even in patients whose "SAFE" score at 3 days is poor (less than 5 of 10 Medical Research Council grades for SA plus FE), the combined use of the NIHSS score plus assessment of impulse propagation in the CST by transcranial magnetic stimulation (TMS), allows for the prediction of a poor, limited, or even good outcome (Stinear et al., 2017b).

The limited negative predictive power of SA and FE movement capacity early after stroke onset (Nijland et al., 2010; Stinear et al., 2012; Snickars et al., 2017) can be explained in different ways. One possibility is that HUL function recovers,

despite the early lack of these movements, by resolution of reversible neurophysiological dysfunction in the motor network. Another option is that such recovery results from structure-function re-mapping processes and network re-organization, compensating for permanent focal structural damage in the motor system. It is unclear yet which of these explanations provides a better account of the limited negative predictive power in the current case. This information is important for guiding the development of interventions aimed to increase the HUL functional level in the chronic stage despite an early lack of SA and FE movement capacity. For example, it is crucial to know whether truncated transmission in the CST (evidenced by TMS) results from a reversible process or permanent structural damage to the tract, as in the latter case functional improvement may depend largely on the development of homolateral corticospinal control (Ward et al., 2006; Stinear et al., 2012, 2017b; Bradnam et al., 2013). Thus, in the case of CST permanent structural damage (but not in the case of reversible physiological impairment to CST connectivity), therapeutic interventions like non-invasive brain stimulation may need to target the intact hemisphere in an excitatory manner (Bradnam et al., 2012, 2013; Carmel et al., 2014; Harrington et al., 2020).

Discrimination between reversible and permanent damage to corticospinal control mechanisms is not easily obtainable from lesion analysis conducted at the time when SA and FE are examined for prognostication purposes, i.e., in the first few days after stroke onset. At this time the demarcation of the area of structural damage is not yet complete, especially in hemorrhagic stroke, and the final lesion boundaries may not be visualized clearly in CT/MR scans (Mikhael, 1989). The use of follow-up scans is more likely to provide the needed information concerning the functional neuroanatomy of SA and FE and the neuroanatomical constraints dictating their final level of recovery.

It should be noted that while the functional integrity of the CST originating from the primary motor cortex of the damaged hemisphere is believed to be necessary for the execution of distal upper-limb movements (hand and fingers, including FE) after stroke onset (Brodal, 2016; Stinear et al., 2017b; Bakker et al., 2019), the brain structures underlying the capacity to execute proximal movements, like SA, are less clear. Also, while the amplitude of motor-evoked potentials (MEPs) recorded from FE muscles early after stroke onset correlates with late FM scores, it was claimed that MEPs lack a significant added value for prediction of long-term hand function over and above the clinical prediction method (Bakker et al., 2019). This however might result from stimulation power being insufficient to activate functionally depressed but structurally preserved cortical motor neurons or reflect recovery processes based on structure-function re-mapping and network reorganization, involving brain systems that are not directly connected to the corticospinal pathways. Lesion studies may provide complementary information about the importance of specific brain structures, beyond the CST, for the execution of SA and FE movements after completion of the recovery process.

In the current study, we examined, for the first time, the long term impact of stroke lesion topography on patients' capacity to execute SA and FE movements, beyond the time window where most neurological recovery occurs (Krakauer and Carmichael, 2017), that is—in the chronic phase of the disease, after completion of natural and treatment-related recovery, when patients' capacity or incapacity to execute SA and FE movements stabilizes. At this stage, when focal structural brain damage is highly correlated with impaired task performance, the integrity of the damaged part of the brain is conceived to be necessary for the normal performance of the behavioral task in question. Following an earlier demonstration of dissimilar LHD and RHD lesion effects on motor function (Frenkel-Toledo et al., 2019) we assumed that hemispheric differences will be revealed for SA and FE and conducted VLSM analyses separately for LHD and RHD patient groups. We hypothesized that SA and FE are constrained mainly by damage to cortical and subcortical structures directly involved in motor execution, i.e., the upper-limb part of the homunculus in the primary motor cortex (pre-central gyrus) and the CST in its passage through the corona radiata and the PLIC (Brodal, 2016). Also, as both SA and FE are important prognostic determinants of overall HUL function, with quite similar sensitivity and specificity values (Snickars et al., 2017), we hypothesized that damage to common brain voxels and not only to different brain voxels will affect the ability to perform these two movements.

MATERIALS AND METHODS

Participants

Seventy-seven first event stroke patients in the chronic stage (>1 year after onset) who were hospitalized in the subacute period at the Loewenstein Rehabilitation Hospital, Ra'anana, Israel, were recruited for the study. Patients were included if they did not suffer from previous psychiatric or neurological disorders, their language and cognitive status enabled comprehension of the task requirements and they did not have a subsequent stroke. The study was approved by the Ethics Review Board of the Loewenstein Hospital (approval number LOE-004-14). All participants were informed about the protocol and gave their written informed consent before inclusion in the study.

Clinical Assessment

The standardized FM test (Fugl-Meyer et al., 1975; Gladstone et al., 2002) was used for the evaluation of HUL motor impairment. The test contains 33 test items for the HUL. These items are divided into four subsections: shoulder-arm, wrist, hand, and upper-limb coordination. Each test item is scored on a 3-point ordinal scale (0 = no movement, 1 = partial movement, 2 = full movement), with a maximal total score of 66 points. The scale has proven to be sensitive, reliable, and valid (Platz et al., 2005). For the current study, we performed lesion-symptom analysis on two items of interest from the FM test—finger extension and shoulder abduction (Nijland et al., 2010; Snickars et al., 2017; Hoonhorst et al., 2018). The chosen item for assessing shoulder abduction was "shoulder abduction

0–90°," with starting position of the elbow at 0° and forearm in neutral position (and not the FM item that assesses abduction during flexor synergy), to assess a volitional movement with little or no synergy. Both finger extension and shoulder abduction were measured using the FM, similarly to the approach of Snickars et al. (2017).

Imaging

Follow-up CT scans dated on average 51 and 28 days post-stroke onset for the LHD and RHD groups, respectively, were carefully examined by a physician experienced in the analysis of neuroimaging data (author NS). This was done to ensure that lesion boundaries were clear and traceable and that the CT presents a stable pattern of tissue damage without a mass effect from residual edema. Author NS was blinded to all other participants' information.

Lesion Analysis

Lesion analyses were performed with the Analysis of Brain Lesions (ABLe) module implemented in MEDx software (Medical-Numerics, Sterling, VA, USA). Lesion delineation was made manually on the digitized CTs. ABLe characterizes brain lesions in MRI and CT scans of the adult human brain by spatially normalizing the lesioned brain into Talairach space using the Montreal Neurological Institute (MNI) template. It reports tissue damage in the normalized brain using an interface to the Talairach Daemon (San Antonio, TX, USA; Lancaster et al., 2000), Automated Anatomical Labeling (AAL) atlas (Tzourio-Mazoyer et al., 2002; Solomon et al., 2007), Volume Occupancy Talairach Labels (VOTL) atlas (Lancaster et al., 2000; Solomon et al., 2007) or the White Matter Atlas (Mori et al., 2008). Quantification of the amount of tissue damage within each structure/region of the atlas was obtained as described earlier (Haramati et al., 2008). In the current study, tissue damage in the normalized brain was reported using the interface to the AAL and white matter atlases. Registration accuracy of the scans to the MNI template (Solomon et al., 2007) across all subjects ranged from 89.3% to 95.8% ($94.2 \pm 1.3\%$, $94.5 \pm 0.8\%$ in LHD and RHD subjects, respectively).

Voxel-Based Lesion-Symptom Mapping (VLSM)

VLSM (Bates et al., 2003) was used to identify voxels ($2 \times 2 \times 2$ mm) of the normalized brain where damage has a significant impact on the SA and FE scores of the FM test. Voxel-by-voxel analysis was used to calculate the statistical significance of performance difference between subjects with and without damage in a given voxel, using the Mann-Whitney test. To avoid spurious results due to low numbers of lesioned voxels, only voxels lesioned in at least 10 subjects were tested (Rorden et al., 2007; Medina et al., 2010; Handelzalts et al., 2019) and at least 10 adjacent voxels had to show a statistically significant impact on performance for a cluster of voxels to be reported (McDonald et al., 2017). To correct for multiple comparisons, voxels with values exceeding a permutation threshold of $p < 0.05$ were considered significant (Mirman et al., 2018). Given the need to correct for multiple comparisons (as the basic anatomical unit in the analysis is a small volume of brain tissue, the voxel, of which there are hundreds of thousands in a brain), false-negative results are common in VLSM studies (Lorca-Puls et al., 2018). By setting a threshold of 10 subjects that had to have damage in a particular voxel for it to be included in the analyses, the number of comparisons that had to be corrected was reduced, thus increasing the statistical power of the analysis. Due to insufficient statistical power in one analysis, we also report anatomical regions containing clusters of at least 10 voxels, where patients affected in these voxels showed disadvantage relative to patients who were not affected in these voxels, using a lenient criterion of $p < 0.01$, which did not survive permutation correction for multiple comparisons (for a similar approach see references Schoch et al., 2006; Lo et al., 2010; Wu et al., 2015; Moon et al., 2016; Frenkel-Toledo et al., 2019). This information is provided under the assumption that in such cases VLSM points to possible trends. The maximum z-score is reported for each cluster of contiguous above-threshold voxels. Since, there may be multiple voxels with this maximum z-score in the cluster, we report the coordinates of the voxel that is most superior, posterior and left in its location within the cluster (the centroid of the cluster is not reported as it may not have the highest z-score value and it may not be an above-threshold voxel). The AAL atlas for gray matter and the White Matter Atlas (Lancaster et al., 2000; Tzourio-Mazoyer et al., 2002; Solomon et al., 2007; Mori et al., 2008) were used to identify the brain structures in which the significant clusters are located. Conjunction analysis was used to characterize voxels surpassing the VLSM thresholds (corresponding to z scores used for determining results that passed permutation correction for multiple comparisons or, in the case of FE in the LHD group, results that did not survive the permutation correction but passed the more lenient criterion of z score = 2.00) involved non-specifically in both the SA and FE and specifically in either the SA ($z = 3.26$ and $z = 2.91$ in LHD and RHD patient groups, respectively) or FE ($z = 2.00$ and $z = 2.76$ in LHD and RHD patient groups, respectively) by overlaying significant voxels from each analysis on the same template.

To rule out the possibility that the results were influenced differently in the RHD and LHD groups by demographic and clinical characteristics, gender, age, dominance, lesion type, time after stroke onset, lesion volume, SA and FE scores of the FM test, FM total score (FM T), Box and Blocks (B&B) and the FM sensation score were compared between groups, using *t*-tests or Mann-Whitney tests or Chi-square tests as required (normal group distribution of continuous data was assessed using Kolmogorov–Smirnov tests). A comparison was made also between the RHD and LHD groups concerning: (1) the proportion of subjects affected in each region of the AAL and WM atlases; and (2) the extent of damage in each region, using Chi-square/Fisher's exact tests, and Mann Whitney tests, respectively. Also, correlations between total lesion volume and SA or FE scores were calculated in both groups, using Spearman-rho. False Discovery Rate (FDR; Genovese et al., 2002) was used to correct for multiple comparisons. All the tests were done using SPSS (version 25.0) with significance levels of $p_{FDR} < 0.05$.

TABLE 1 | Demographic and clinical characteristics of participants.

	LHD group (n = 44)	RHD group (n = 33)	p-value
Gender (M/F)	32/12	25/8	0.764[a]
Age: Mean ± SD (range)	59.7 ± 10.5 (27.3–78.8)	63.2 ± 9.6 (26.7–73.2)	0.137[b]
Dominance (R/L/A)	41/2/1	30/2/1	0.934[a]
Lesion type (I/H/I>H)	2/41/1	2/30/1	0.633[a]
TAO (months): Mean ± SD (range)	27.5 ± 13.7 (12.0–59.8)	29.7 ± 13.9 (13.1–68.5)	0.510[c]
Lesion volume (cc): Mean ± SD (range)	26.4 ± 34.3 (0.4–182.3)	31.6 ± 41.8 (0.3–186.9)	0.853[c]
SA (0/1/2), Median (IQR)	12/8/24 2 (0–2)	11/1/21 2 (0–2)	0.743[c]
FE (0/1/2), Median (IQR)	8/9/27 2 (1–2)	9/5/19 2 (0–2)	0.573[c]
FM Total (X/66): Mean ± SD (range)	45.0 ± 18.6 (3–66)	43.3 ± 24.4 (4–66)	0.654[c]
B&B*: Mean ± SD (range)	29.9 ± 24.0 (0–67)	27.6 ± 23.0 (0–62)	0.585[c]
FM Sensation (X/12): Mean ± SD (range)	8.7 ± 4.2 (0–12)	8.6 ± 3.6 (2–12)	0.652[c]

*LHD, left hemisphere damage; RHD, right hemisphere damage; Gender, M, Male; F, Female; Dominance R, Right; L, Left; A, Ambidextrous; Lesion type I, Ischemic; H, Hemorrhagic; I>H, Ischemic with hemorrhagic transformation; TAO, Time after stroke onset—mean (SD); SA, Shoulder abduction; FE, Finger extension; IQR, interquartile range; FM, Fugl-Meyer; B&B, Box and Blocks; *Number of participants in the B&B test: n = 30 (right) and n = 35 (left); Number of participants in the FM sensation test: n = 30 (right) and n = 39 (left); [a]Chi-Square test, [b]t-test, [c]Mann Whitney test.*

RESULTS

As can be seen in **Table 1**, the demographic and clinical characteristics of the LHD and RHD patient groups are essentially similar. Individual data are displayed in the **Supplementary Table S1**.

The proportion of LHD and RHD subjects having a lesion (yes/no) in at least 1 voxel in each of the regions of the AAL (Tzourio-Mazoyer et al., 2002; Solomon et al., 2007), and White Matter (Mori et al., 2008) atlases was similar, except for a larger proportion of LHD patients with damage to the caudate nucleus (73% vs. 46%, p = 0.019; FDR corrected p = 1.00). The extent of damage in each region was similar in LHD and RHD groups. In the RHD group, total hemispheric volume loss correlated significantly with SA (Spearman-rho = −0.570; FDR corrected p = 0.002) and FE (Spearman-rho = −0.516; FDR corrected p = 0.002). In the LHD group, total hemispheric volume loss did not correlate with SA or FE. Overlay lesion maps (stroke lesion distribution) of LHD and RHD patients are shown in **Figure 1**. Individual lesion data are displayed in **Supplementary Figure S1**.

VLSM (Bates et al., 2003) identified clusters of voxels associated with poorer ability to perform SA and FE movements (**Figure 2**). **Tables 2**, **3** show the anatomical structures in the left and right hemispheres, respectively, where damage was found to exert a significant impact on the tested abilities. In the LHD group (**Table 2**), both SA and FE movements were affected only by damage to the CST in its passage through the superior part of the corona radiata (SCR). The VLSM result for FE did not survive the correction for multiple comparisons by permutation. In the RHD group (**Table 3**), the lesion effect differs from the pattern observed in the LHD group. Here SA and FE movements were affected mainly by CST damage within the PLIC and SCR, as well as by damage to the external capsule (EC), association fibers of the superior longitudinal fasciculus (SLF), the insular cortex and the putamen.

Tables 4, **5** show the anatomical structures in the left and right hemispheres, respectively, where VLSM conjunction analysis disclosed voxel clusters in which damage exerts a significant impact on SA only, FE only, and both SA and FE. The anatomical structures involved are shown in **Figure 3**. In the LHD group (**Table 4**), 50% of the voxels in which damage was shown to affect SA were involved selectively in SA, and 50% were involved both in SA and FE. In contrast, in 93% of the voxels in which damage affected FE performance, the impact of damage was specific to FE, while damage to only 7% of the voxels affected both SA and FE. As can be seen in **Table 4**, SA and FE movements were affected by lesions to common and distinct voxels of the SCR. In the RHD group (**Table 5**) the picture is different. In the large majority of voxels in which stroke lesion was shown to affect either SA or FE movements, the impact of structural damage was significant both to SA and FE. Moreover, in contrast to the findings of the LHD analysis where damage affecting both SA and FE was restricted to the CST in its passage through the corona radiata, in the RHD group, brain voxels in which damage affected both SA and FE were found in a large array of structures (**Table 5**). Selective impact on SA only was shown in 15% of the voxels where damage affected SA performance, and selective impact on FE only was shown in 9% of the voxels where damage affected FE performance. Thus, in the RHD group, the impact of damage to the large majority of "significant" voxels for either SA or FE was not specific and was noted in both SA and FE.

DISCUSSION

The current study aimed to assess the impact of lesion topography on the capacity of chronic stroke patients to execute SA and FE movements in the HUL. The interest in these two specific movements stems from the fact that they seem to represent successfully the recovery process of proximal and distal muscle groups, thus pointing to the functional level of the HUL as a whole. This is evidenced by the fact that a patient who demonstrates SA and FE movement capacity a few days after stroke onset has an extremely high likelihood to manifest good HUL functionality in the chronic stage (Katrak et al., 1998; Fritz et al., 2005; Smania et al., 2007; Nijland et al., 2010; Stinear et al., 2012, 2017b; Winters et al., 2016; Snickars et al., 2017; Hoonhorst et al., 2018).

We used VLSM (Bates et al., 2003), but unlike various earlier VLSM studies in which left- and right-hemisphere damage

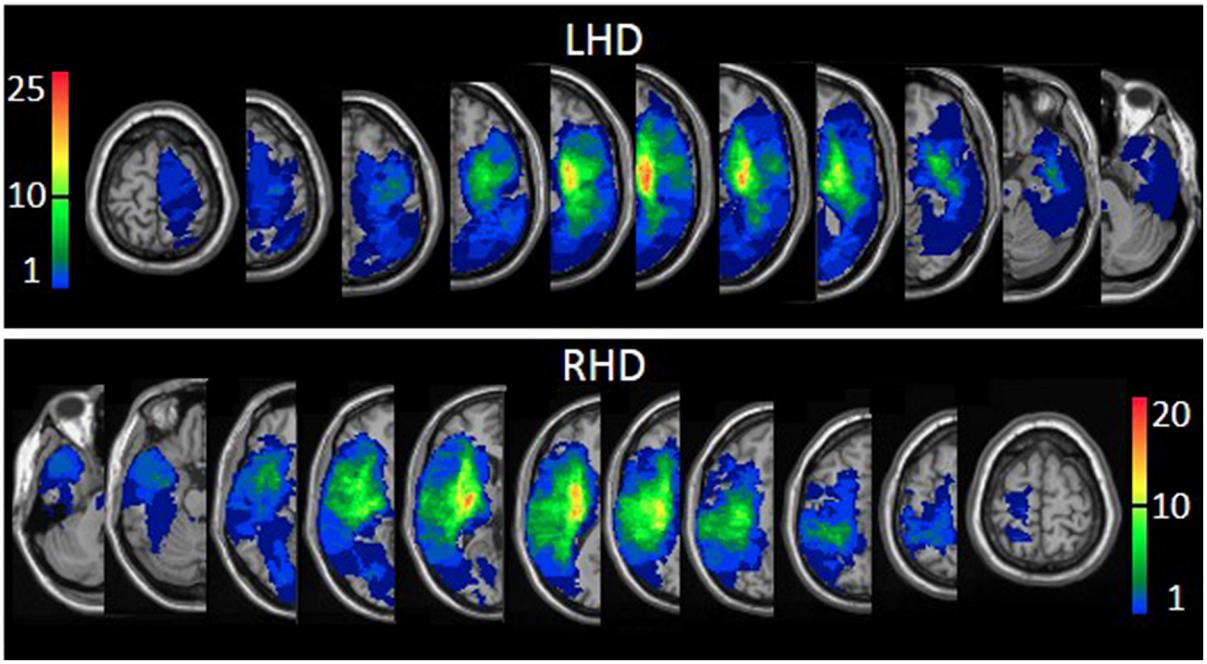

FIGURE 1 | Lesion overlay maps of left hemispheric damage (LHD; *n* = 44) and right hemispheric damage (RHD; *n* = 33) patient groups. The threshold for inclusion in the Voxel-based Lesion-Symptom Mapping (VLSM) analysis: at least 10 subjects had to have damage to a particular voxel for it to be included in the analysis. Representative normalized slices (out of 90 normalized slices employed) are displayed in radiological convention (right hemisphere on the left side and vice versa), with warmer colors indicating greater lesion overlap (units: number of patients with a lesion in this region).

data was treated jointly (Lo et al., 2010; Cheng et al., 2014; Meyer et al., 2016), this analysis was conducted separately for LHD and RHD patients. The decision to separate the analyses was made under the assumption that differences between the dominant left and the non-dominant right cerebral hemispheres in the functional neuroanatomy of motor control (Tretriluxana et al., 2009; Mani et al., 2013), and in patterns of motor recovery (Zemke et al., 2003; Wu et al., 2015), may be reflected also in a different impact for lesion topography on patients' capacity to execute SA and FE movements. Indeed, the analysis revealed marked differences between LHD and RHD patient groups in the impact of the lesion pattern on SA and FE expression. This finding is of special interest as it cannot be explained by group differences in baseline parameters. The two hemispheric groups did not differ in a series of demographic data (gender, age, and motor dominance distribution), lesion data (type and total hemispheric volume), time of clinical examination after stroke onset, and HUL impairment level (as reflected in the FM total score, B&B score, and the FM-sensation score). Moreover, the groups' scores of SA and FE movement capacity did not differ (**Table 1**), and the two groups showed a similar proportion of patients being affected in all the regions defined by the AAL

TABLE 2 | VLSM results in LHD patients (*n* = 44).

Test	Structure	*Z*-value	*X*	*Y*	*Z*	Voxels	% area
SA*	SCR	3.81	−24	−8	30	19	2.06
FE	SCR	3.36	−24	−12	26	59	6.39
		2.90	−28	−10	20	20	2.16

**SA results passed permutation correction for multiple comparisons (corresponding in this analysis to z scores of 3.269). FE did not survive the permutation correction but passed the more lenient criterion of z score = 2.00 or above. SCR, superior corona radiate.*

TABLE 3 | VLSM results in RHD patients (*n* = 33).

Test	Structure	*Z*-value	*X*	*Y*	*Z*	Voxels	% area
SA*	SCR	4.60	30	−16	30	171	18.59
	SLF	4.60	32	−16	30	151	18.30
	Insula	4.15	34	−12	16	143	8.08
	EC	3.83	32	−10	12	97	20.82
	Putamen	3.68	30	−10	6	71	6.67
		3.26	30	12	10	13	1.22
	PLIC	3.53	28	−14	18	40	7.98
	PCR	4.24	28	−22	26	26	5.75
	RLIC	3.68	28	−24	14	20	6.33
FE*	SCR	4.62	30	−14	30	174	18.91
	SLF	4.30	34	−12	30	142	17.21
	EC	3.39	30	−8	12	85	18.24
	Insula	3.67	34	−12	16	84	4.75
	Putamen	3.64	30	−10	6	75	7.05
		3.03	30	12	10	13	1.22
	PLIC	3.39	26	−8	14	60	11.98
	PCR	3.97	28	−22	26	24	5.31
	RLIC	3.64	28	−24	14	20	6.33
	ALIC	3.39	24	−4	18	11	2.70

**SA and FE results passed permutation correction for multiple comparisons (corresponding in these analyses to z scores of 2.917 and 2.763, respectively). EC, external capsule; SCR/PCR, superior/posterior corona radiata; PLIC/RLIC/ALIC, posterior/retro-lenticular/anterior limb of internal capsule; SLF, superior longitudinal fasciculus.*

TABLE 4 | Number of voxels in affected brain regions where the damage had a significant impact on SA only, FE only, and SA plus FE, in LHD patients (n = 44).

Areas	SA only	FE only	SA plus FE
SCR	6	63	6
Putamen		12	
EC		11	

Only structures with at least 10 voxels affecting performance in one or more of the three options are shown. SCR, superior corona radiata; EC, external capsule.

TABLE 5 | Number of voxels in affected brain regions where the damage had a significant impact on SA only, FE only, and SA plus FE, in RHD patients (n = 33).

Areas	SA only	FE only	SA plus FE
SLF	13	4	141
Putamen	8	13	76
EC	32	21	74
SCR	1	4	177
Insula	59	2	84
PLIC		20	40
RLIC			20
PCR	2		24

Only structures with at least 10 voxels affecting performance in one or more of the three options are shown. SLF, superior longitudinal fasciculus; EC, external capsule; SCR/PCR, superior/posterior corona radiata; PLIC/RLIC, posterior/retro-lenticular limb of internal capsule.

atlas (Tzourio-Mazoyer et al., 2002; Solomon et al., 2007) and the White-Matter atlas (Mori et al., 2008). The lesion overlay maps of LHD and RHD patient groups (**Figure 1**) demonstrate a typical stroke lesion pattern with dominant middle-cerebral artery territory damage in both groups.

Despite the above similarities between the groups in baseline parameters, patients with left hemiparesis (LHD) differed significantly from patients with right hemiparesis (RHD) in the impact of lesion topography on the capacity to execute SA and FE movements. In the LHD group, both SA and FE movements were affected mainly by damage to the CST in its passage through the corona radiata. In contrast, SA and FE movements were affected in the RHD group by CST damage both in the corona radiata and the PLIC, as well as by damage to intra-hemispheric association fibers, the insula, and the putamen. As can be seen in **Tables 2**, **3**, both SA and FE were sensitive, in RHD patients, to damage in a much larger array of brain structures, including many more "significant" voxels, compared to LHD patients. Also, the capacity to execute SA and FE movements correlated negatively with the total hemispheric volume loss in RHD but not in LHD. Given the similarity between the groups in baseline demographic, clinical, and lesion parameters, we interpret the salient difference in the impact of lesion topography on SA and FE expression in LHD and RHD as a reflection of a fundamental difference in structure-function relationships.

We propose that the scarcity of "significant" voxels (i.e., brain voxels in which the existence of damage is shown by VLSM to exert a significant impact on the examined behavior) in the LHD group relative to the RHD group, stems from the fact that in the dominant left hemisphere (most patients in both groups were right-handed), the processing of sensory-motor data is carried out by a more extensive and densely connected network (Guye et al., 2003), where damage to one component is more easily substituted by other network components. Earlier studies have shown that the primary motor cortex, descending corticospinal pathways, somatosensory association, and premotor cortices of the dominant and non-dominant hemispheres differ anatomically and functionally (Serrien et al., 2006). Such differences are reflected in the deeper central sulcus in the dominant hemisphere (Amunts et al., 1996), the more potent intracortical circuits in the primary motor cortex of the dominant hemisphere (Hammond et al., 2004), the more extensive connectivity of the left dominant M1 with other parts of the brain (Guye et al., 2003), the higher excitability of the corticospinal system on the dominant left hemisphere (De Gennaro et al., 2004), and the relationship between the lateralization of the motor network and the quality of performance of different motor tasks (Barber et al., 2012). Recently, we reported on asymmetrical lesion effects in LHD and RHD on overall HUL functioning (Fugl-Meyer and box-and-blocks test scores), which were found both in the sub-acute and the chronic phases following a stroke. As in the current study, the asymmetry reflected a relative paucity of "significant" voxels in the LHD group (Frenkel-Toledo et al., 2019). It should be noted, however, that the current cohort includes subjects who participated also in our aforementioned study, a fact that could contribute to pattern similarity. Our proposed interpretation of the differences between LHD and RHD in the relationship between lesion topography and motor performance relates to hemispheric dominance, thus applying to right-handed patients (forming 93% and 91% of the LHD and RHD cohorts, respectively). With a larger group of left-handed stroke patients, it will be possible to assess whether the above differences are maintained or not among left-handers.

In both left and right hemisphere strokes, damage to the CST affected the capacity to execute SA and FE movements. This finding was expected given the CST role as the main pathway for mediation of cerebral control on the motor neurons of the cervical spinal cord that activate upper limb muscles (Palmer and Ashby, 1992; Lindenberg et al., 2010; Lo et al., 2010; Puig et al., 2011). Earlier studies (e.g., Lo et al., 2010) found that the brain region where damage affects HUL function in the most severe and protracted manner is the area of convergence of the corona radiata into the CST before it enters into the internal capsule. In a recent study, we have found a strong impact on CST damage (in either the corona radiata or the PLIC) on HUL function, following both LHD and RHD. The detrimental effect of CST damage was noted both in the sub-acute and in the chronic phases (Frenkel-Toledo et al., 2019). Algorithms that predict the HUL functional outcome also emphasize the importance of CST integrity (Stinear et al., 2012, 2017b). For example, in the PREP algorithm, patients with a "SAFE score" (i.e., Medical Research Council grades for SA plus FE) higher than 8/10 within 72 h of stroke onset made a "complete" recovery of HUL function within 12 weeks. Patients with a "SAFE score" lower than 8/10, in whom propagation of impulses in the CST could be demonstrated by elicitation of MEPs had a "notable" functional recovery. In patients without elicitable MEPs, diffusion-weighted imaging was required to distinguish patients with "limited" recovery from those with no recovery at all. Thus, incorporation

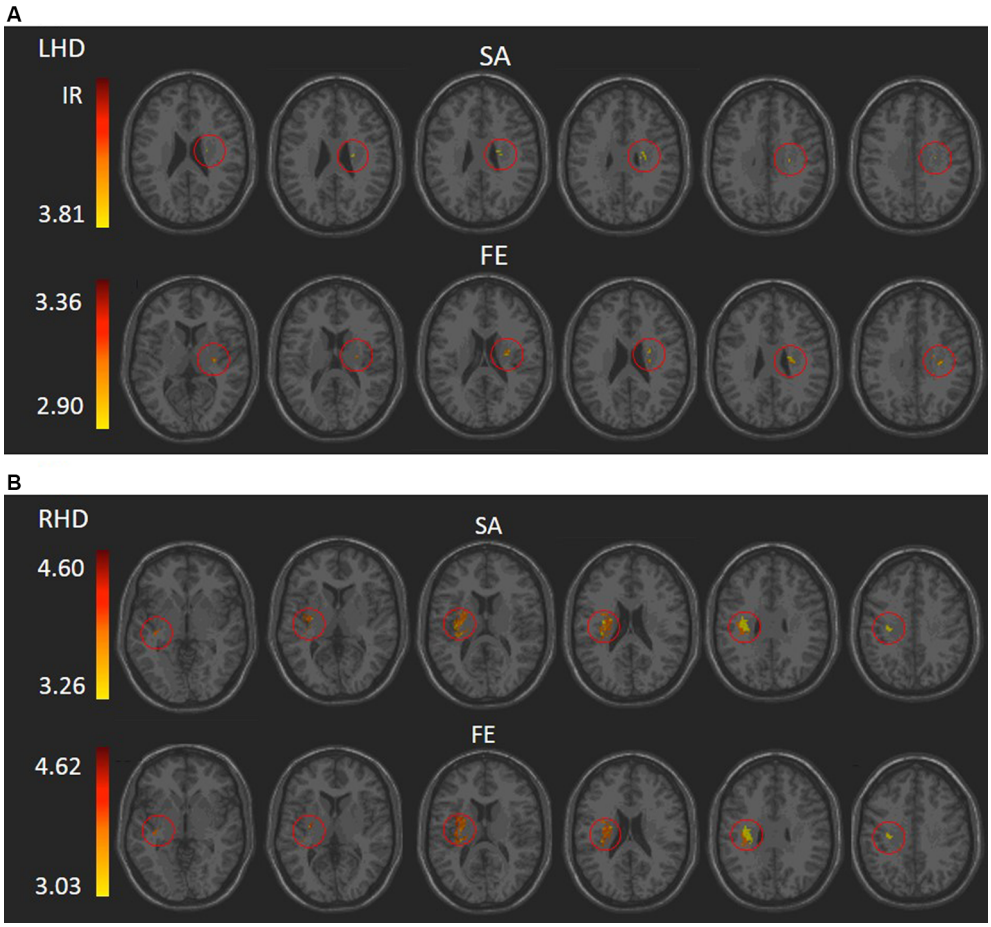

FIGURE 2 | VLSM analysis depicting areas where damage was significantly associated with a lower score of shoulder abduction (SA) and finger extension (FE) in the LHD **(A)** and RHD **(B)** groups, respectively (minimum cluster size: 10 voxels, minimum number of patients affected in a voxel: 10). Warmer colors indicate higher z-scores. The colored regions in SA and FE of the RHD group and SA of the LHD group survived permutation correction for multiple comparisons, and the colored regions in the FE of the LHD group did not but were based on a lenient criterion of z score ≥ 2.00 ($p \leq 0.01$). IR, irrelevant, all structures shared a single z score.

of neurophysiological and neuroimaging techniques to assess the functional integrity of the CST in the first days after onset enables an accurate prediction of HUL function at 3 months after stroke (Stinear et al., 2012).

Careful inspection of cluster coordinates in **Tables 2**, **3** reveals location differences when the "significant" voxels for SA and FE within a given structure are compared. To assess further the extent of voxel sharing between SA and FE, "conjunction" analyses were performed (**Figure 3**, **Tables 4**, **5**). These analyses differentiated between voxels in which damage affected SA only, FE only, or SA plus FE. The conjunction analyses pointed to a larger proportion of shared voxels in the RHD group (in this group most of the "significant" voxels, within all the involved structures, were shared by both SA and FE). In the LHD group, the number of "significant" voxels was much lower and the proportion of voxels that were found significant to either SA or FE but not to both movements was higher compared to the RHD group. In the LHD group, voxels in which damage affected specifically either SA or FE were found in the superior part of the corona radiata, i.e., near the primary motor cortex, where somatotopic organization separates the representations of proximal and distal upper-limb movements (Snell, 2010). The greater proportion in the LHD group of voxels in which the impact of damage was specific to either SA or FE may point to greater differentiation in the sensory-motor cortex of the dominant hemisphere. Motor dominance in humans (Amunts et al., 1996) and primates (Hopkins and Cantalupo, 2004; Margiotoudi et al., 2019) is attributed to hemispheric asymmetries in motor cortex architecture. On the other hand, the finding, especially following RHD, of voxel sharing for SA and FE (i.e., voxels in which damage affected significantly the capacity of patients to execute both SA and FE movements), reflects the importance of brain structures contributing to these movements in a less specific manner, i.e., both to proximal and distal upper limb movements. Previous research in subacute post-stroke patients found a similar reduction of the active range of motion in proximal and distal segments of the HUL (Beebe and Lang, 2008), while other studies (Colebatch and Gandevia, 1989) reported on greater strength deficits in the more distal HUL muscle groups. Such discordant findings may reflect variant

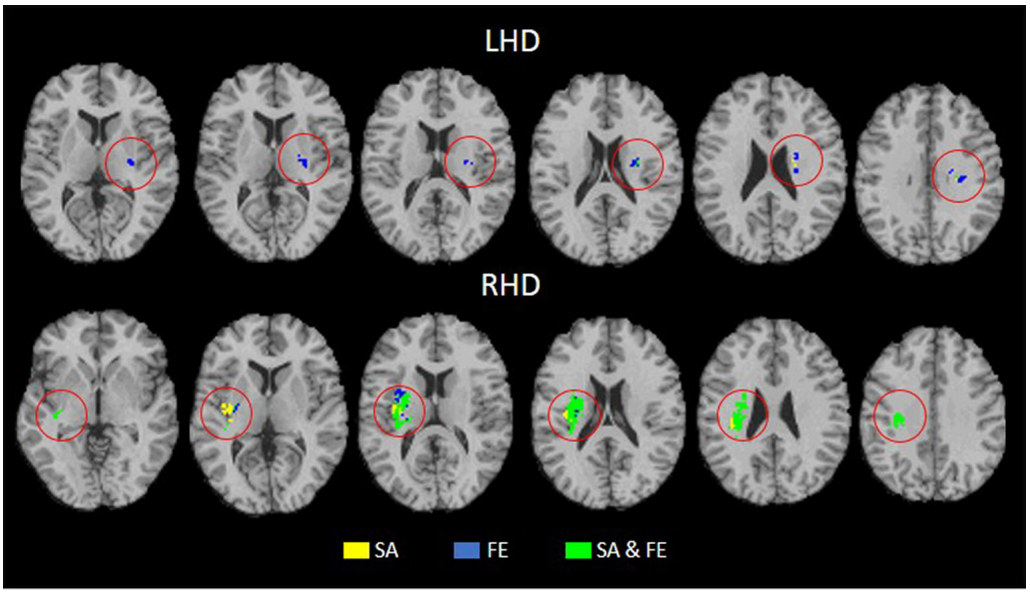

FIGURE 3 | Conjunction analysis depicting areas of brain damage that were associated with lower scores in the SA only, FE only, and both SA and FE, shown in yellow, blue, and green, respectively, in the LHD (n = 44) and RHD (n = 33) groups.

involvement in the stroke process of voxels which contribute to a given movement in a specific manner vs. voxels which contribute to movements in a non-specific manner. Alternatively, such discordant findings may point to the variant impact of damage to homologous voxels in the two hemispheres, as shown in the current study for LHD and RHD patient groups.

It should be noted that the high positive predictive power of SA and FE movement execution is based on the assessment done a few days after stroke onset, whereas the current analyses were conducted in the chronic stage when structure and function in the brain are expected to maintain a more stable relationship. As explained in the introduction section, transient physiological malfunction in "penumbra" regions and not necessarily permanent structural damage, could affect patients' capacity to execute SA and FE in the acute stage. Thus, theoretically, stroke patients may be unable to execute SA and FE movements in the acute stage even if none of the "significant" voxels disclosed in the current study was damaged permanently. This can explain the fact that early ability to execute SA and FE movements has a strong positive predictive power but a much weaker negative predictive power [for example, Winters et al. (2016) reported that 45% of the patients who could not show voluntary FE about a week after stroke onset, achieved later (at 6 months) a score equal or higher than 10 points in the Action Research Arm Test (ARAT), indicating at least partial HUL functionality]. Given that our lesion data were derived from follow-up brain scans and analyzed against behavioral information obtained months and years after the stroke, it points to structures whose integrity is necessary for the proper execution of SA and FE irrespective of the recovery type (resolution of reversible physiological dysfunction or long-term network re-organization) and magnitude of recovery. Based on the current findings we may assume those stroke patients who could execute SA and FE movements shortly after stroke onset, as well as those who could not execute it initially but regained later HUL dexterity, did not have a major involvement in the location of the "significant" voxel clusters found in the current study.

Limitations

Several limitations of the study should be acknowledged. First, to avoid spurious results in the VLSM analysis, only voxels damaged in at least 10 subjects were tested. Given the number of subjects in the current cohort (44 LHD, 33 RHD), this threshold precluded an assessment of the impact of damage to relevant brain voxels of the sensory-motor and adjacent cortical regions where the prevalence of damage was lower than this threshold. Also, the majority of the current cohort had strokes located within the MCA territory. This limited the possibility of identifying "significant" voxel clusters related to strokes in other vascular territories, including posterior-circulation brainstem strokes. It is assumed that these limitations lead to type-2 (false negative) errors.

Second, as most subjects had mild to moderate HUL motor impairment at the time of testing (FM scores of 45.0 $\pm$ 18.6 and 43.3 $\pm$ 24.4 in LHD and RHD groups, respectively; SA and FE median score = 2, for both), patients with more severe hemiparesis were under-represented in this study.

Third, the VLSM results for FE in the LHD group are based on a lenient criterion, as they did not survive the permutation correction for multiple comparisons. These results are likely to reflect a trend that may become significant with larger numbers of subjects, but it may also represent a type-1 (false positive) error.

Fourth, measuring the capacity to execute SA and FE movements using the Medical Research Council (MRC) method (i.e., on a 5-point ordinal scale, James, 2007), as done by Stinear et al. (2012, 2017b), is probably more sensitive to mild improvement compared to the 3-point ordinal scale of the FM used in the current study, and may affect the possibility of comparing the results of studies using these two methods for outcome measurement.

Fifth, data collection in this study was conducted when the participants were in the chronic stage, mostly being tested in their homes. This precluded control of residual aphasia among LHD patients and residual spatial neglect among RHD patients. Both residual aphasia and residual neglect could probably affect the results. For example, the fact that a much larger array of brain structures affected SA and FE movements in the RHD group may be related to residual neglect in part of the RHD cohort. Spatial neglect is known to imply poor functional outcomes for stroke survivors (Katz et al., 1999), emerging from dysfunction within large-scale networks involved in attention, motor, and multimodal sensory processing (Corbetta, 2014).

Implications

Our findings indicate that the capacity to execute SA and FE movements following stroke is affected differently by lesion topography in LHD and RHD patients. In both groups, these movements are sensitive to damage in brain voxels within the CST. However, in the RHD group, patients' capacity to execute the movements is affected also by damage to a large array of cortical and subcortical regions. This finding expands previous data pointing to differences between the dominant left and the non-dominant right cerebral hemispheres in the functional neuroanatomy of motor control (Tretriluxana et al., 2009; Mani et al., 2013) and patterns of motor recovery (Zemke et al., 2003; Wu et al., 2015). Our finding that damage to shared and not only to distinct brain voxels affects both SA and FE movement capacity is likely to relate to the quite similar sensitivity and specificity values of these two movements when used as prognostic determinants of overall HUL function (Snickars et al., 2017). Prognostication of HUL function may benefit from adding lesion information to clinical and physiological measures in use, provided that lesion boundaries are already clearly visible in the brain scan, enabling accurate delineation of the area of structural brain damage.

Summary and Conclusions

The current study sheds new light on the functional neuroanatomy of SA and FE movements. Our findings point to marked differences between left and right hemispheric damage: in the former, SA and FE are affected in the chronic stage mainly by CST damage, while in the latter, the capacity to execute SA and FE movements are affected in addition to CST damage, also by damage to white matter association tracts, the insula, and the putamen. In both groups, voxel clusters are found where damage affects SA and also FE, along with voxels where damage affects only one of the two movements. Voxel specificity is higher in LHD compared to RHD. In LHD, voxels specificity is much higher for FE compared to SA. We propose that the above differences between LHD and RHD stem from physiological differences related to hemispheric motor dominance.

DATA AVAILABILITY STATEMENT

The raw data supporting the conclusions of this article will be made available by the authors, without undue reservations.

ETHICS STATEMENT

The study was reviewed and approved by the Ethics Review Board of the Loewenstein Hospital (approval number LOE-004-14). The patients/participants provided their written informed consent to participate in this study.

AUTHOR CONTRIBUTIONS

SF-T was involved in planning and conducting the experiments as well as data analysis, interpretation, and drafting of the manuscript. SO-G was involved in conducting the experiments as well as data analysis, interpretation of data, and revising of the manuscript. NS was involved in subject medical screening, lesion delineation, planning the experiment, interpretation, and revising of the manuscript. All authors read and approved the final manuscript.

FUNDING

This work was supported in part by the Legacy Foundation, granted through the Loewenstein Rehabilitation Hospital, Israel to authors SF-T and NS.

ACKNOWLEDGMENTS

Gadi Bartur, Justine Lowenthal-Raz, Osnat Granot, Shir Ben-Zvi, Nurit Goldshuv-Ezra, and Shirley Handelzalts helped to analyze patients' imaging data used in this study.

SUPPLEMENTARY MATERIAL

The Supplementary Material for this article can be found online at: https://www.frontiersin.org/articles/10.3389/fnhum.2020.00282/full#supplementary-material.

REFERENCES

Amunts, K., Schlaug, G., Schleicher, A., Steinmetz, H., Dabringhaus, A., Roland, P. E., et al. (1996). Asymmetry in the human motor cortex and handedness. *NeuroImage* 4, 216–222. doi: 10.1006/nimg.1996.0073

Bakker, C. D., Massa, M., Daffertshofer, A., Pasman, J. W., Van Kuijk, A. A., Kwakkel, G., et al. (2019). The addition of the MEP amplitude of finger extension muscles to clinical predictors of hand function after stroke: a prospective cohort study. *Restor. Neurol. Neurosci.* 37, 445–456. doi: 10.3233/rnn-180890

Barber, A. D., Srinivasan, P., Joel, S. E., Caffo, B. S., Pekar, J. J., and Mostofsky, S. H. (2012). Motor "dexterity": evidence that left hemisphere lateralization of motor circuit connectivity is associated with better motor performance in children. *Cereb. Cortex* 22, 51–59. doi: 10.1093/cercor/bhr062

Bates, E., Wilson, S. M., Saygin, A. P., Dick, F., Sereno, M. I., Knight, R. T., et al. (2003). Voxel-based lesion-symptom mapping. *Nat. Neurosci.* 6, 448–450. doi: 10.1038/nn1050

Beebe, J. A., and Lang, C. E. (2008). Absence of a proximal to distal gradient of motor deficits in the upper extremity early after stroke. *Clin. Neurophysiol.* 119, 2074–2085. doi: 10.1016/j.clinph.2008.04.293

Bradnam, L. V., Stinear, C. M., Barber, P. A., and Byblow, W. D. (2012). Contralesional hemisphere control of the proximal paretic upper limb following stroke. *Cereb. Cortex* 22, 2662–2671. doi: 10.1093/cercor/bhr344

Bradnam, L. V., Stinear, C. M., and Byblow, W. D. (2013). Ipsilateral motor pathways after stroke: implications for non-invasive brain stimulation. *Front. Hum. Neurosci.* 7:184. doi: 10.3389/fnhum.2013.00184

Brodal, P. (2016). *The Central Nervous System. 5th Edn.* New York, NY: Oxford UP.

Broeks, J. G., Lankhorst, G. J., Rumping, K., and Prevo, A. J. (1999). The long-term outcome of arm function after stroke: results of a follow-up study. *Disabil. Rehabil.* 21, 357–364. doi: 10.1080/096382899297459

Carmel, J. B., Kimura, H., and Martin, J. H. (2014). Electrical stimulation of motor cortex in the uninjured hemisphere after chronic unilateral injury promotes recovery of skilled locomotion through ipsilateral control. *J. Neurosci.* 34, 462–466. doi: 10.1523/jneurosci.3315-13.2014

Cheng, B., Forkert, N. D., Zavaglia, M., Hilgetag, C. C., Golsari, A., Siemonsen, S., et al. (2014). Influence of stroke infarct location on functional outcome measured by the modified rankin scale. *Stroke* 45, 1695–1702. doi: 10.1161/strokeaha.114.005152

Colebatch, J. G., and Gandevia, S. C. (1989). The distribution of muscular weakness in upper motor neuron lesions affecting the arm. *Brain* 112, 749–763. doi: 10.1093/brain/112.3.749

Corbetta, M. (2014). Hemispatial neglect: clinic, pathogenesis, and treatment. *Semin. Neurol* 34, 514–523. doi: 10.1055/s-0034-1396005

De Gennaro, L., Cristiani, R., Bertini, M., Curcio, G., Ferrara, M., Fratello, F., et al. (2004). Handedness is mainly associated with an asymmetry of corticospinal excitability and not of transcallosal inhibition. *Clin. Neurophysiol.* 115, 1305–1312. doi: 10.1016/j.clinph.2004.01.014

Feys, H., Hetebrij, J., Wilms, G., Dom, R., and De Weerdt, W. (2000). Predicting arm recovery following stroke: value of site of lesion. *Acta Neurol. Scand.* 102, 371–377. doi: 10.1034/j.1600-0404.2000.102006371.x

Frenkel-Toledo, S., Fridberg, G., Ofir, S., Bartur, G., Lowenthal-Raz, J., Granot, O., et al. (2019). Lesion location impact on functional recovery of the hemiparetic upper limb. *PLoS One* 14:e0219738. doi: 10.1371/journal.pone.0219738

Fritz, S. L., Light, K. E., Patterson, T. S., Behrman, A. L., and Davis, S. B. (2005). Active finger extension predicts outcomes after constraint-induced movement therapy for individuals with hemiparesis after stroke. *Stroke* 36, 1172–1177. doi: 10.1161/01.str.0000165922.96430.d0

Fugl-Meyer, A. R., Jääskö, L., Leyman, I., Olsson, S., and Steglind, S. (1975). The post-stroke hemiplegic patient. 1. a method for evaluation of physical performance. *Scand. J. Rehabil. Med.* 7, 13–31.

Genovese, C. R., Lazar, N. A., and Nichols, T. (2002). Thresholding of statistical maps in functional neuroimaging using the false discovery rate. *NeuroImage* 15, 870–878. doi: 10.1006/nimg.2001.1037

Gladstone, D. J., Danells, C. J., and Black, S. E. (2002). The fugl-meyer assessment of motor recovery after stroke: a critical review of its measurement properties. *Neurorehabil. Neural Repair* 16, 232–240. doi: 10.1177/154596802401105171

Grefkes, C., and Fink, G. R. (2012). Disruption of motor network connectivity post-stroke and its noninvasive neuromodulation. *Curr. Opin. Neurol.* 25, 670–675. doi: 10.1097/wco.0b013e3283598473

Grefkes, C., and Ward, N. S. (2014). Cortical reorganization after stroke: how much and how functional? *Neuroscientist* 20, 56–70. doi: 10.1177/1073858413491147

Guye, M., Parker, G. J. M., Symms, M., Boulby, P., Wheeler-Kingshott, C. A. M., Salek-Haddadi, A., et al. (2003). Combined functional MRI and tractography to demonstrate the connectivity of the human primary motor cortex *in vivo*. *NeuroImage* 19, 1349–1360. doi: 10.1016/s1053-8119(03)00165-4

Hammond, G., Faulkner, D., Byrnes, M., Mastaglia, F., and Thickbroom, G. (2004). Transcranial magnetic stimulation reveals asymmetrical efficacy of intracortical circuits in primary motor cortex. *Exp. Brain Res.* 155, 19–23. doi: 10.1007/s00221-003-1696-x

Handelzalts, S., Melzer, I., and Soroker, N. (2019). Analysis of brain lesion impact on balance and gait following stroke. *Front. Hum. Neurosci.* 13:149. doi: 10.3389/fnhum.2019.00149

Haramati, S., Soroker, N., Dudai, Y., and Levy, D. A. (2008). The posterior parietal cortex in recognition memory: a neuropsychological study. *Neuropsychologia* 46, 1756–1766. doi: 10.1016/j.neuropsychologia.2007.11.015

Harrington, R. M., Chan, E., Rounds, A. K., Wutzke, C. J., Dromerick, A. W., Turkeltaub, P. E., et al. (2020). Roles of lesioned and nonlesioned hemispheres in reaching performance poststroke. *Neurorehabil. Neural Repair* 34, 61–71. doi: 10.1177/1545968319876253

Hoonhorst, M. H. J., Nijland, R. H. M., van den Berg, P. J. S., Emmelot, C. H., Kollen, B. J., and Kwakkel, G. (2018). Does transcranial magnetic stimulation have an added value to clinical assessment in predicting upper-limb function very early after severe stroke? *Neurorehabil. Neural Repair* 32, 682–690. doi: 10.1177/1545968318785044

Hopkins, W. D., and Cantalupo, C. (2004). Handedness in chimpanzees (Pan troglodytes) is associated with asymmetries of the primary motor cortex but not with homologous language areas. *Behav. Neurosci.* 118, 1176–1183. doi: 10.1037/0735-7044.118.6.1176

James, M. A. (2007). Use of the Medical Research Council muscle strength grading system in the upper extremity. *J. Hand Surg. Am.* 32, 154–156. doi: 10.1016/j.jhsa.2006.11.008

Katrak, P., Bowring, G., Conroy, P., Chilvers, M., Poulos, R., and McNeil, D. (1998). Predicting upper limb recovery after stroke: the place of early shoulder and hand movement. *Arch. Phys. Med. Rehabil.* 79, 758–761. doi: 10.1016/s0003-9993(98)90352-5

Katz, N., Hartman-Maeir, A., Ring, H., and Soroker, N. (1999). Functional disability and rehabilitation outcome in right hemisphere damaged patients with and without unilateral spatial neglect. *Arch. Phys. Med. Rehabil.* 80, 379–384. doi: 10.1016/s0003-9993(99)90273-3

Krakauer, J. W., and Carmichael, S. T. (2017). *Broken Movement: The Neurobiology of Motor Recovery After Stroke.* Cambridge, MA: MIT Press.

Lancaster, J. L., Woldorff, M. G., Parsons, L. M., Liotti, M., Freitas, C. S., Rainey, L., et al. (2000). Automated Talairach atlas labels for functional brain mapping. *Hum. Brain Mapp.* 10, 120–131. doi: 10.1002/1097-0193(200007)10:3<120::aid-hbm30>3.0.co;2-8

Langhorne, P., Bernhardt, J., and Kwakkel, G. (2011). Stroke rehabilitaiton. *Lancet* 377, 1693–1702. doi: 10.1016/S0140-6736(11)60325-5

Lindenberg, R., Renga, V., Zhu, L. L., Betzler, F., Alsop, D., and Schlaug, G. (2010). Structural integrity of corticospinal motor fibers predicts motor impairment in chronic stroke. *Neurology* 74, 280–287. doi: 10.1212/wnl.0b013e3181ccc6d9

Lo, R., Gitelman, D., Levy, R., Hulvershorn, J., and Parrish, T. (2010). Identification of critical areas for motor function recovery in chronic stroke subjects using voxel-based lesion symptom mapping. *NeuroImage* 49, 9–18. doi: 10.1016/j.neuroimage.2009.08.044

Lorca-Puls, D. L., Gajardo-Vidal, A., White, J., Seghier, M. L., Leff, A. P., Green, D. W., et al. (2018). The impact of sample size on the reproducibility of voxel-based lesion-deficit mappings. *Neuropsychologia* 115, 101–111. doi: 10.1016/j.neuropsychologia.2018.03.014

Mani, S., Mutha, P. K., Przybyla, A., Haaland, K. Y., Good, D. C., and Sainburg, R. L. (2013). Contralesional motor deficits after unilateral stroke reflect hemisphere-specific control mechanisms. *Brain* 136, 1288–1303. doi: 10.1093/brain/aws283

Margiotoudi, K., Marie, D., Claidière, N., Coulon, O., Roth, M., Nazarian, B., et al. (2019). Handedness in monkeys reflects hemispheric specialization within the central sulcus. An *in vivo* MRI study in right- and left-handed olive baboons. *Cortex* 118, 203–211. doi: 10.1016/j.cortex.2019.01.001

McDonald, V., Hauner, K. K., Chau, A., Krueger, F., and Grafman, J. (2017). Networks underlying trait impulsivity: evidence from voxel-based lesion-symptom mapping. *Hum. Brain Mapp.* 38, 656–665. doi: 10.1002/hbm.23406

Medina, J., Kimberg, D. Y., Chatterjee, A., and Coslett, H. B. (2010). Inappropriate usage of the Brunner-Munzel test in recent voxel-based lesion-symptom mapping studies. *Neuropsychologia* 48, 341–343. doi: 10.1016/j.neuropsychologia.2009.09.016

Meyer, S., Kessner, S. S., Cheng, B., Bönstrup, M., Schulz, R., Hummel, F. C., et al. (2016). Voxel-based lesion-symptom mapping of stroke lesions underlying somatosensory deficits. *NeuroImage Clin.* 10, 257–266. doi: 10.1016/j.nicl.2015.12.005

Mikhael, M. A. (1989). "Neuroradiology of cerebral infarction," in *Imaging of Non-Traumatic Ischemic and Hemorrhagic Disorders of the Central Nervous System*, eds M. Sarwar and S. Batnitzky (Boston, MA: Springer), 193–220.

Mirman, D., Landrigan, J. F., Kokolis, S., Verillo, S., Ferrara, C., and Pustina, D. (2018). Corrections for multiple comparisons in voxel-based lesion-symptom mapping. *Neuropsychologia* 115, 112–123. doi: 10.1016/j.neuropsychologia.2017.08.025

Moon, H. I., Pyun, S. B., Tae, W. S., and Kwon, H. K. (2016). Neural substrates of lower extremity motor, balance and gait function after supratentorial stroke using voxel-based lesion symptom mapping. *Neuroradiology* 58, 723–731. doi: 10.1007/s00234-016-1672-3

Mori, S., Oishi, K., Jiang, H., Jiang, L., Li, X., Akhter, K., et al. (2008). Stereotaxic white matter atlas based on diffusion tensor imaging in an ICBM template. *NeuroImage* 40, 570–582. doi: 10.1016/j.neuroimage.2007.12.035

Nijland, R. H. M., Van Wegen, E. E. H., Harmeling-Van Der Wel, B. C., and Kwakkel, G. (2010). Presence of finger extension and shoulder abduction within 72 hours after stroke predicts functional recovery: Early prediction of functional outcome after stroke: The EPOS cohort study. *Stroke* 41, 745–750. doi: 10.1161/strokeaha.109.572065

Olsen, T. S. (1990). Arm and leg paresis as outcome predictors in stroke rehabilitation. *Stroke* 21, 247–251. doi: 10.1161/01.str.21.2.247

Palmer, E., and Ashby, P. (1992). Corticospinal projections to upper limb motoneurons in humans. *J. Physiol.* 448, 397–412. doi: 10.1113/jphysiol.1992.sp019048

Platz, T., Pinkowski, C., van Wijck, F., Kim, I. H., Di Bella, P., and Johnson, G. (2005). Reliability and validity of arm function assessment with standardized guidelines for the Fugl-Meyer Test, Action Research Arm Test and Box and Block Test: a multicentre study. *Clin. Rehabil.* 19, 404–411. doi: 10.1191/0269215505cr832oa

Puig, J., Pedraza, S., Blasco, G., Daunis-I-Estadella, J., Prados, F., Remollo, S., et al. (2011). Acute damage to the posterior limb of the internal capsule on diffusion tensor tractography as an early imaging predictor of motor outcome after stroke. *Am. J. Neuroradiol.* 32, 857–863. doi: 10.3174/ajnr.A2400

Rorden, C., Karnath, H. O., and Bonilha, L. (2007). Improving lesion-symptom mapping. *J. Cogn. Neurosci.* 19, 1081–1088. doi: 10.1162/jocn.2007.19.7.1081

Schoch, B., Dimitrova, A., Gizewski, E. R., and Timmann, D. (2006). Functional localization in the human cerebellum based on voxelwise statistical analysis: a study of 90 patients. *NeuroImage* 30, 36–51. doi: 10.1016/j.neuroimage.2005.09.018

Serrien, D. J., Ivry, R. B., and Swinnen, S. P. (2006). Dynamics of hemispheric specialization and integration in the context of motor control. *Nat. Rev. Neurosci.* 7, 160–167. doi: 10.1038/nrn1849

Shelton, F. N., and Reding, M. J. (2001). Effect of lesion location on upper limb motor recovery after stroke. *Stroke* 32, 107–112. doi: 10.1161/01.str.32.1.107

Smania, N., Paolucci, S., Tinazzi, M., Borghero, A., Manganotti, P., Fiaschi, A., et al. (2007). Active finger extension: a simple movement predicting recovery of arm function in patients with acute stroke. *Stroke* 38, 1088–1090. doi: 10.1161/01.str.0000258077.88064.a3

Smith, M. C., Ackerley, S. J., Barber, P. A., Byblow, W. D., and Stinear, C. M. (2019). PREP2 algorithm predictions are correct at 2 years poststroke for most patients. *Neurorehabil. Neural Repair* 33, 635–642. doi: 10.1177/1545968319860481

Snell, R. S. (2010). *Clinical Neuroanatomy*. Philadelphia, PA: Lippincott Williams and Wilkins.

Snickars, J., Persson, H. C., and Sunnerhagen, K. S. (2017). Early clinical predictors of motor function in the upper extremity one month post-stroke. *J. Rehabil. Med.* 49, 216–222. doi: 10.2340/16501977-2205

Solomon, J., Raymont, V., Braun, A., Butman, J. A., and Grafman, J. (2007). User-friendly software for the analysis of brain lesions (ABLe). *Comput. Methods Programs Biomed.* 86, 245–254. doi: 10.1016/j.cmpb.2007.02.006

Stinear, C. M., Barber, P. A., Petoe, M., Anwar, S., and Byblow, W. D. (2012). The PREP algorithm predicts potential for upper limb recovery after stroke. *Brain* 135, 2527–2535. doi: 10.1093/brain/aws146

Stinear, C. M., Byblow, W. D., Ackerley, S. J., Barber, P. A., and Smith, M. C. (2017a). Predicting recovery potential for individual stroke patients increases rehabilitation efficiency. *Stroke* 48, 1011–1019. doi: 10.1161/strokeaha.116.015790

Stinear, C. M., Byblow, W. D., Ackerley, S. J., Smith, M. C., Borges, V. M., and Barber, P. A. (2017b). PREP2: a biomarker-based algorithm for predicting upper limb function after stroke. *Ann. Clin. Transl. Neurol.* 4, 811–820. doi: 10.1002/acn3.488

Tretriluxana, J., Gordon, J., Fisher, B. E., and Winstein, C. J. (2009). Hemisphere specific impairments in reach-to-grasp control after stroke: Effects of object size. *Neurorehabil. Neural Repair* 23, 679–691. doi: 10.1177/1545968309332733

Tzourio-Mazoyer, N., Landeau, B., Papathanassiou, D., Crivello, F., Etard, O., and Delcroix, N. (2002). Automated anatomical labeling of activations in SPM using a macroscopic anatomical parcellation of the MNI MRI single-subject brain. *NeuroImage* 15, 273–289. doi: 10.1006/nimg.2001.0978

Urton, M. L., Kohia, M., Davis, J., and Neill, M. R. (2007). Systematic literature review of treatment interventions for upper extremity hemiparesis following stroke. *Occup. Ther. Int.* 14, 11–27. doi: 10.1002/oti.220

Wade, D. T., Langton-Hewer, R., Wood, V. A., Skilbeck, C. E., and Ismail, H. M. (1983). The hemiplegic arm after stroke: measurement and recovery. *J. Neurol. Neurosurg. Psychiatry.* 46, 521–524. doi: 10.1136/jnnp.46.6.521

Ward, N. S., Newton, J. M., Swayne, O. B., Lee, L., Thompson, A. J., Greenwood, R. J., et al. (2006). Motor system activation after subcortical stroke depends on corticospinal system integrity. *Brain* 129, 809–819. doi: 10.1093/brain/awl002

Winters, C., Kwakkel, G., Nijland, R., and Van Wegen, E. (2016). When does return of voluntary finger extension occur post-stroke? A prospective cohort study. *PLoS One* 11:e0160528. doi: 10.1371/journal.pone.0160528

Wu, O., Cloonan, L., Mocking, S. J. T., Bouts, M. J., Copen, W. A., Cougo-Pinto, P. T., et al. (2015). Role of acute lesion topography in initial ischemic stroke severity and long-term functional outcomes. *Stroke* 46, 2438–2444. doi: 10.1161/strokeaha.115.009643

Zemke, A. C., Heagerty, P. J., Lee, C., and Cramer, S. C. (2003). Motor cortex organization after stroke is related to side of stroke and level of recovery. *Stroke* 34, e23–e38. doi: 10.1161/01.str.0000065827.35634.5e

Conflict of Interest: The authors declare that the research was conducted in the absence of any commercial or financial relationships that could be construed as a potential conflict of interest.

frontiers in Human Neuroscience

BRIEF RESEARCH REPORT
published: 06 October 2020
doi: 10.3389/fnhum.2020.567177

Effects of Diazepam on Reaction Times to Stop and Go

*Swagata Sarkar[1,2†], Supriyo Choudhury[1†], Nazrul Islam[3], Mohammad Shah Jahirul Hoque Chowdhury[3], Md Tauhidul Islam Chowdhury[3], Mark R. Baker[4,5,6], Stuart N. Baker[6] and Hrishikesh Kumar[1]**

[1]Department of Neurology, Institute of Neurosciences Kolkata, Kolkata, India, [2]Department of Physiology, University of Calcutta, Kolkata, India, [3]Department of Neurology, National Institute of Neurosciences and Hospital, Dhaka, Bangladesh, [4]Department of Neurology, Royal Victoria Infirmary, Newcastle upon Tyne, United Kingdom, [5]Department of Clinical Neurophysiology, Royal Victoria Infirmary, Newcastle upon Tyne, United Kingdom, [6]The Medical School, Newcastle University, Newcastle upon Tyne, United Kingdom

Introduction: The ability to stop the execution of a movement in response to an external cue requires intact executive function. The effect of psychotropic drugs on movement inhibition is largely unknown. Movement stopping can be estimated by the Stop Signal Reaction Time (SSRT). In a recent publication, we validated an improved measure of SSRT (optimum combination SSRT, ocSSRT). Here we explored how diazepam, which enhances transmission at $GABA_A$ receptors, affects ocSSRT.

Methods: Nine healthy individuals were randomized to receive placebo, 5 mg or 10 mg doses of diazepam. Each participant received both the dosage of drug and placebo orally on separate days with adequate washout. The ocSSRT and simple reaction time (RT) were estimated through a stop-signal task delivered *via* a battery-operated box incorporating green (Go) and red (Stop) light-emitting diodes. The task was performed just before and 1 h after dosing.

Result: The mean change in ocSSRT after 10 mg diazepam was significantly higher (+27 ms) than for placebo (−1 ms; $p = 0.012$). By contrast, the mean change in simple response time remained comparable in all three dosing groups ($p = 0.419$).

Conclusion: Our results confirm that a single therapeutic adult dose of diazepam can alter motor inhibition in drug naïve healthy individuals. The selective effect of diazepam on ocSSRT but not simple RT suggests that GABAergic neurons may play a critical role in movement-stopping.

Keywords: benzodiazepine, Diazepam, SSRT, motor stopping, GABA

OPEN ACCESS

Edited by:
Giovanni Di Pino,
Campus Bio-Medico University, Italy

Reviewed by:
Alessandro Gulberti,
University Medical Center Hamburg-Eppendorf, Germany
Dominic M. D. Tran,
The University of Sydney, Australia
Nahian Chowdhury,
The University of Sydney, Australia

****Correspondence:***
Hrishikesh Kumar
rishi_medicine@yahoo.com

†These authors have contributed equally to this work

Specialty section:
This article was submitted to Motor Neuroscience, a section of the journal Frontiers in Human Neuroscience

Received: *29 May 2020*
Accepted: *31 August 2020*
Published: *06 October 2020*

Citation:
Sarkar S, Choudhury S, Islam N, Chowdhury MSJH, Chowdhury MTI, Baker MR, Baker SN and Kumar H (2020) Effects of Diazepam on Reaction Times to Stop and Go. Front. Hum. Neurosci. 14:567177. doi: 10.3389/fnhum.2020.567177

INTRODUCTION

Real-life environments require us to build or adapt different movement control strategies to accomplish a task goal or to respond rapidly to a fast-moving visual and/or auditory stimulus. During our engagement in these complex scenarios, we must be able to prioritize different actions (Mückschel et al., 2014). Response inhibition (or movement stopping) is a key component of executive control, providing the ability to suppress an action that has already been initiated but which is no longer required (Logan et al., 1984).

Day-to-day life has numerous examples where such response control is needed, for example avoiding touching a hot pan, or stopping before crossing a road when a car is approaching at speed. A range of psychopathological and impulse control disorders severely impair response inhibition, for example, attention-deficit/hyperactivity disorder, obsessive-compulsive disorder, substance abuse, pathological gambling, and eating disorders (Bechara et al., 2006). Experimental studies in patients have helped to define the contribution of subcortical structures to response inhibition, specifically fronto-basal interactions (Whelan et al., 2012). Evidence from these studies suggest that the connection between supplementary motor area/inferior frontal gyrus and sub-thalamic nucleus (Inase et al., 1999; Aron et al., 2007) is crucial in controlling response inhibition (Aron and Poldrack, 2006; Frank, 2006; Li et al., 2008; Hikosaka and Isoda, 2010; Munakata et al., 2011; Forstmann et al., 2012)

The stop-signal paradigm is well-suited for laboratory investigation of response inhibition. Participants perform a reaction time (RT) task in response to a Go cue. Occasionally, the Go signal is followed by a stop signal after a variable delay (the stop signal delay). Using the probability of an inappropriate response after the stop signal, and the distribution of RTs on Go trials, this paradigm allows estimation of the covert latency of the stopping process, or stop signal reaction time (SSRT). This has been used extensively to explore the cognitive and neural mechanisms of response inhibition (Hanes and Schall, 1996; Aron and Poldrack, 2006; Verbruggen et al., 2014; Debey et al., 2015). Studies with SSRT have found correlations between individual differences in stopping and behavior such as risk-taking, substance abuse, and control of impulses/urges (Schachar and Logan, 1990; Ersche et al., 2012; Whelan et al., 2012). Moreover, movement stopping can be enhanced or impaired by a variety of factors. The drug methylphenidate enhances stopping (Tannock et al., 1995), whereas by contrast, in long-term users, cocaine impairs response inhibition (Fillmore et al., 2002). Increased motivational incentives can enhance stopping (Boehler et al., 2014).

Recently we have developed an improved index by applying Bayesian statistics to SSRT estimation. This index, which appears to have significantly higher reproducibility (Choudhury et al., 2019), is known as optimum combination SSRT (ocSSRT).

Those who abuse drugs often develop impairments in performance and attention, and increases in impulsive behavior (Heishman et al., 1997; De Wit and Richards, 2004). Evidence from animal studies has shown that D2 receptors are essential both for psychostimulant activity and motor response inhibition (Dalley et al., 2007). Methylphenidate is a dopamine and noradrenaline reuptake inhibitor; it has varied effects on movement stopping, not all of which are reversed by blocking dopaminergic receptors (Eagle et al., 2007). This suggests that other monoaminergic transmitters may also play a role in motor response inhibition. In the cerebral cortex, around 10–15% of neurons in the cerebral cortex are GABAergic inhibitory interneurons, which can be sub-divided into multiple cell types (Ascoli et al., 2008). In the STN, around 7.5% of cells are GABAergic (Lévesque and Parent, 2005). The major components of the known neural circuitry for response inhibition (Aron et al., 2014) should therefore be susceptible to GABAergic modulation. Diazepam is a widely prescribed anxiolytic, muscle relaxant, and anticonvulsant that is commonly abused (Woods et al., 1987; Gelkopf et al., 1999). Diazepam administered at standard therapeutic doses (5–10 mg) reportedly did not affect measures of behavioral inhibition including delay discounting, a Go/No-Go task, or the stop signal reaction task, despite the drug-producing prototypical sedative-like effects (Reynolds et al., 2004). At higher doses (20 mg) it did impair performance on both Go/No-Go and stop-signal tasks but did not affect measures of delay discounting (Acheson et al., 2006). Here, we aimed to assess the impact of a benzodiazepine on movement stops. We conducted a randomized, placebo-control, cross-sectional, double-blinded trial, which compared the effect of two therapeutic doses of diazepam (5 and 10 mg) on the improved novel measure ocSSRT.

MATERIALS AND METHODS

Population and Trial Protocol

Twelve potential participants were initially screened for this pilot study. We did not perform a prior power calculation to determine the number of participants, as we had no information on the expected effect size. Three were excluded as one had a drug allergy, one was taking a benzodiazepine as a medication already, and one discontinued because of personal reasons. The nine remaining subjects came from our research laboratory (five male and four female, including two authors of this report; age 27 $\pm$ 4 years, mean $\pm$ SD), all educated to post-graduate degree level or higher with no known underlying neurological disorder, and were randomly assigned to three groups. The order in which the three conditions (placebo; 5 mg diazepam; or 10 mg diazepam) were recorded was counterbalanced across groups. Study participants received no financial compensation. Each participant received both the dosage of drug and placebo orally on separate days with an adequate washout interval (1 week). The estimation of ocSSRT was performed through a stop-signal task (see below), immediately before and 1 h after dosing (peak plasma concentration of diazepam is achieved approximately 1 h after ingestion, Mandelli et al., 1978). The trial protocol is summarized schematically in **Figure 1**. We measured ocSSRT and RT, where ocSSRT represents movement stopping and RT is the simple response time.

Experiments were conducted in a tertiary care neurology center in Eastern India. Written informed consent was obtained from each participant before the study following the Declaration of Helsinki. Protocols and procedures were approved by the Institutional Ethics Committee (reference number I-NK/IEC/99/2019 ver.1. dated 29 April 2019) and the trial was registered prospectively with the Clinical Trials Registry-India (CTRI), registration number CTRI/2020/02/023530 on 24 February 2020.

Device

We used a custom-built battery-powered device housed in a plastic case, which the subject held comfortably in two hands (Choudhury et al., 2019). One red and one green

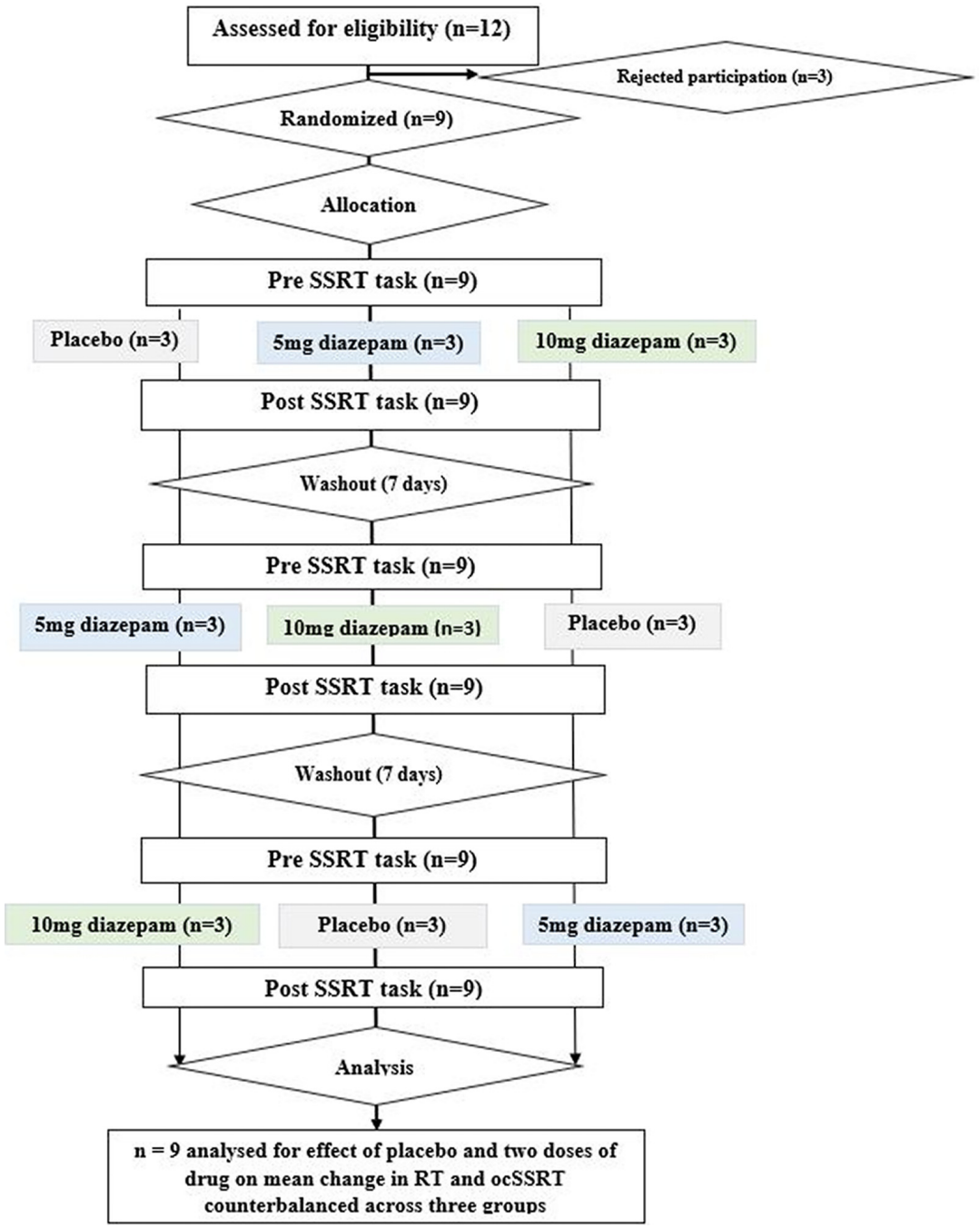

FIGURE 1 | Consort diagram for the study, depicting randomization, group allocation, washout periods, and data analysis.

light-emitting diode (LED, 5 mm diameter) mounted on the front of this box indicated Stop and Go respectively; a press button (2 cm diameter) positioned beneath the LEDs was depressed and held or released by the subject depending on the instructions encoded by the sequence of LED flashes. A four-line liquid crystal display (LCD) screen providing a textual status display during the test was positioned above the LEDs. A microcontroller (dsPIC30F6012A, Microchip Inc.) programmed with custom firmware written in C using the MPLAB development environment within the device determined the task sequence, measured RTs (1 ms precision) and response probabilities, and computed the SSRT. The Task outcome as a numerical value of the estimated ocSSRT and RT was then displayed on the LCD screen and copied to a laboratory notebook, and thence to a spreadsheet, by the experimenter. The device did not keep a permanent record of single-trial responses.

Mathematical details of the calculation of ocSSRT are provided in Choudhury et al. (2019), which should be consulted for a full description. Briefly, for a given stop-signal delay (SSD), the number of inappropriate responses M and the total number of trials tested with that delay N was determined. Instead of simply estimating response probability p as M/N, a Bayesian approach was used to estimate the likelihood of a particular response probability p, assuming that the response number M followed a binomial distribution. To calculate SSRT for a particular response probability p, we found the point in the distribution of RTs to a Go cue alone where a fraction p of RTs were smaller (RT) and subtracted the stop signal delay SSD, so $SSRT = RT - SSD$. This allowed calculation of the likelihood of a range of SSRT values. SSRT likelihood curves were found for each of the four SSD values, and then a combined SSRT likelihood curve computed from the product of the individual curves. The mean of this distribution gave the ocSSRT. This approach is an improvement over simpler approaches that average single estimates of SSRT for each SSD, as it naturally takes account of the reliability of each estimate.

Detailed Test Procedure

Study participants were randomized to each interventional group by a computer-generated random sequence generator (Random Allocation, Ver. 2.0 software). Investigators and participants were blinded to the group allocation during the entire study period. The study drugs were dispensed by an unblinded study coordinator who was not involved in any of the assessment procedures or analyses. The placebo (ascorbic acid 500 mg) and the active compound (Valium 5 diazepam tablets, Abbott) had the same external appearance. To mask any differences in taste, participants were requested to swallow the tablets with a strongly flavored lemon drink.

All participants sat comfortably in a semi-illuminated, quiet room holding the task device. Participants were asked to respond to a Go cue as fast as they could, but to inhibit their responses on the trials when a Stop cue appeared. A trial was initiated by pressing and holding the response button with the index finger or thumb of the dominant hand (dominant side as subjectively reported by the participants). The LCD screen then showed the instruction "release on the green, hold on red." The green LED illuminated after a delay (chosen from a uniform random distribution between 1 and 2.638 s). No other LED illuminated on 75% of trials, and the subject was required to release the button to respond (a Go trial). In 25% of trials, the green LED extinguished and the red LED illuminated (a Stop trial). For correct performance, the subject was required not to release the button. Four different SSDs (between the illumination of green and red LED) were used: 5 ms; 65 ms; 130 ms; and 195 ms. Trials were presented in blocks of 32, with 24 Go trials and eight Stop trials (two for each delay) within a block. The order was adjusted so that a Stop trial was always preceded and followed by a Go trial. There was a 1.3 s delay after each button release and before the next trial started. A Stop trial was considered successful if the button was not released for 0.7 s after the green LED illuminated; the next trial started after a 2 s delay. The task was paused for 60 s to allow the subject to rest after two blocks of 32 trials. Subjects could also pause the test at any point by releasing the button, as the next trial did not start until the button was depressed. Subjects sometimes did this for a few seconds, for example, to adjust their posture to be more comfortable, but did not choose to take longer rests other than at the scheduled times at the end of a set of 64 trials. One complete measurement typically lasted around 15 min. To aid with familiarization on the task, naïve subjects were allowed to complete 64 trials as practice; results from these were discarded.

The total duration of the study protocol was 2 weeks. During this time and 1 week before day one, the participants were not allowed to take any prescription or over the counter medications with potential neurotropic actions (e.g., anti-depressants, anxiolytics, sedatives, anti-tussives, common cold remedies).

Statistical Analysis

Summary statistics of numerical variables were presented as mean and standard deviation (SD) for categorical variables. The normality of the data was tested using the Shapiro–Wilk test. Mean changes in RT, ocSSRT for placebo, 5 mg diazepam, and 10 mg diazepam were compared using repeated-measures ANOVA. Pairwise comparisons were completed by applying *post hoc* t-tests, with significance levels adjusted by a Bonferroni correction to account for the three comparisons (placebo vs. 5 mg diazepam, placebo vs. 10 mg diazepam, 5 mg vs. 10 mg diazepam). A corrected p-value of less than 0.05 was considered significant. All statistical analysis was performed using the SPSS 20 statistical package (SPSS, Chicago, IL, USA). As a pilot study, formal statistical calculation of sample size was not performed and convenience sampling was instead adopted.

RESULTS

Nine healthy individuals were randomly assigned to three groups, in which the order of testing the three conditions was counterbalanced. The baseline ocSSRT and RT (measured before ingestion of drug or placebo) were comparable between the three groups (**Table 1**). Subjects made inappropriate responses on between 0 and 73% of Stop trials, depending on the SSD. Changes in ocSSRT and RT from before to after placebo or drug ingestion were not distributed significantly differently from normal across the population (Shapiro–Wilk test statistic; $p < 0.8$ in all cases). Repeated measures ANOVA showed a significantly different effect of placebo and two doses of the drug on ocSSRT (**Figure 2A**; $F = 6.790$; $p = 0.007$). The further pairwise analysis revealed that the mean ocSSRT change (from baseline)

TABLE 1 | Comparison of baseline optimum combination Stop Signal Reaction Time (ocSSRT) and reaction time (RT) in three experimental sessions.

Baseline	Placebo	5 mg diazepam	10 mg diazepam	*p*-value
ocSSRT (ms)	190 ± 39	207 ± 44	204 ± 26	0.288
RT (ms)	408 ± 48	405 ± 27	412 ± 45	0.928

Values are given as means ± standard deviation. p-values determined from repeated measure ANOVA.

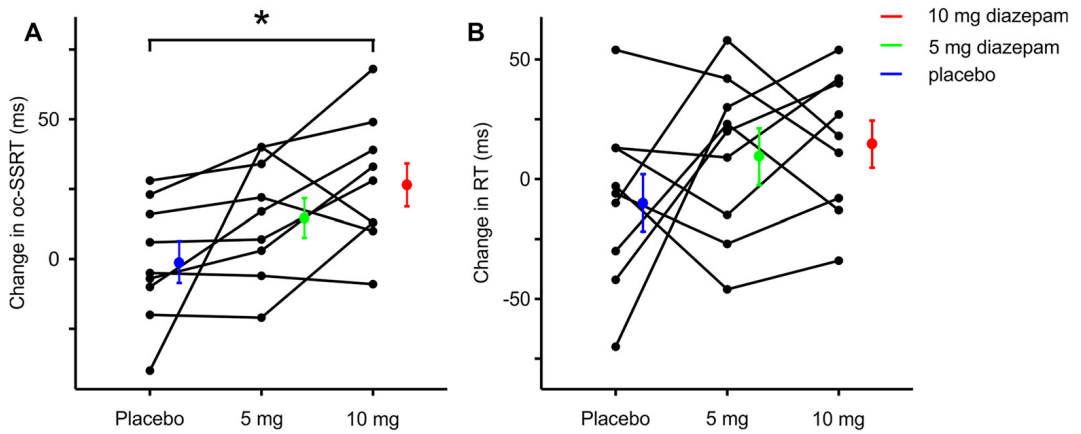

FIGURE 2 | Change in ocSSRT and simple reaction time (RT) with placebo, 5 mg, and 10 mg diazepam. **(A)** Mean change in ocSSRT and **(B)** mean change in RT, in nine individuals. Significant differences from placebo are indicated by * ($p < 0.05$, *t*-tests).

was significantly higher with the 10 mg dose of diazepam compared to placebo (+27 ms vs. −1 ms, $p = 0.012$). ocSSRT also increased after 5 mg diazepam (mean change 15 ms), but this failed to reach statistical significance relative to placebo ($p = 0.288$).

The change in RT from baseline (**Figure 2B**) was comparable after placebo, 5 mg and 10 mg of diazepam (mean changes −9, +10 and 15 ms, repeated measures ANOVA $F = 1.399$, $p = 0.276$; *t*-test between placebo and 5 mg, $p = 0.867$; *t*-test between placebo and 10 mg, $p = 0.603$).

It is important to consider the statistical power of our study, given the failure to detect a change in RT. We performed a *post hoc* power calculation for both ocSSRT and RT, using the measured standard deviation of the change in the experimental measure from before to after placebo (22 and 36 ms for ocSSRT and RT respectively), for a power level of 90%. With nine subjects, this indicated that we should detect a 27 ms change in ocSSRT, and a 45 ms change in RT, equivalent to 14% and 11% change respectively. We can therefore have confidence that any change in RT is likely to be smaller than this value.

Our results clearly show that even therapeutic doses of diazepam can affect stopping ability. Whilst we could not detect changes in a measure of simple motor response (RT), the ocSSRT was increased at the highest dose tested of 10 mg.

DISCUSSION

There are several ways to measure SSRT, and each may have advantages and disadvantages (Verbruggen et al., 2013; Leunissen et al., 2017). In this study, we used our recently-developed method exploiting portable equipment and an analytical approach which incorporates knowledge of the likely reliability of the response probability estimates. We have shown that this provides rapid SSRT measurements with high reproducibility (Choudhury et al., 2019). Regardless of any methodological differences, we can have high confidence in our results since this was a double-blind placebo-controlled trial, in which we demonstrated a significant difference between placebo and 10 mg diazepam.

Benzodiazepines are widely used psychotropic drugs. Medical indications for benzodiazepines are broad and include anxiety, insomnia, muscle relaxation, management of spasticity, and epilepsy. These drugs bind exclusively to and allosterically modulate $GABA_A$ receptors (the major inhibitory receptor of the CNS), acting as partial agonists (Downing et al., 2005; Gielen et al., 2012; Möhler, 2015). Diazepam is a long-acting, medium potency benzodiazepine and is thus generally used for its anti-convulsive and anxiolytic effects. Long term use of diazepam has been associated with cognitive impairment, presumably as a side effect of the non-selective binding to all synaptic $GABA_A$ subtypes (Rudolph and Knoflach, 2011). In the present study, we found that a single dose of diazepam impairs inhibitory control without significantly affecting RT.

Previously human studies showed that neural circuitry within the dorsolateral prefrontal cortex (Baker et al., 1996; Manes et al., 2002) and orbitofrontal cortex (Rogers et al., 1999) are involved in tests requiring planning and decision-making. Deakin et al. (2004) hypothesized that high doses of diazepam cause disinhibitory cognitive effects by impeding inhibitory networks within these cortical regions. They also speculated that diazepam can influence frontal lobe functions associated with decision making either by direct effects on $GABA_A$ receptors within the frontal cortex or by modulating activity in the ascending reticular system (Deakin et al., 2004). In a rodent study involving the punished behavior model, Ford et al. (1979) showed that diazepam and d-amphetamine when administered in combination increased punished responding in all the rats. Ljungberg et al. (1987) evaluated the dose-dependent effects of diazepam on decision making in rats, in a rewarding behavior rodent model with water restriction paradigm. They observed that lever-pressing behavior in rats was not affected at a diazepam dose of 2 mg/kg but reduced significantly

at doses of 5 mg/kg and 10 mg/kg. In a follow-up study, they found a selectively reduced tolerance of reward delay by diazepam (Ljungberg, 1990).

The phenomenon of response inhibition is not exclusively GABAergically mediated. Several rodent studies have shown that D2 receptor antagonism improves response inhibition when antagonists are infused into the prefrontal cortex, while a global reduction in 5HT impairs inhibition, suggesting an interaction between dopaminergic and serotonergic systems in response inhibition (Harrison et al., 1997; Granon et al., 2000; Winstanley et al., 2004; van Gaalen et al., 2006; Bari et al., 2011). Robbins (2000) noted that in marmosets manipulations of dopamine and noradrenaline tend to produce effects on tasks predominantly engaging the dorsolateral prefrontal cortex, but manipulations of the serotonergic system tend to alter performance in tests sensitive to orbitofrontal dysfunction. Interestingly, a recent study from our group (Choudhury et al., 2019) showed a significant reduction in SSRT after treatment with the dopamine precursor levodopa in Parkinson's patients, potentially supporting the contention that movement stopping is mediated by circuits involving the dorsolateral prefrontal cortex.

Previous work (Deakin et al., 2004; Acheson et al., 2006) found that behavioral inhibition in a decision-making task was only impaired at higher doses of diazepam (20 mg) and not at typical therapeutic doses of 5–10 mg. However, in our study even therapeutic doses of diazepam could impair response inhibition in healthy individuals, without compromising RT. This was presumably by modulating $GABA_A$ receptors in the frontal cortex or the basal ganglia.

Rather than manipulating $GABA_A$ efficacy as in this study, Hermans et al. (2018) measured endogenous GABA levels in the brain using magnetic resonance spectroscopy. Older adults had lower levels of GABA, and also slower SSRT than younger participants. The association between lower GABA and slower SSRT was also seen just within the older subject group. Chowdhury et al. (2019) used transcranial magnetic brain stimulation to measure short-interval intracortical inhibition (SICI) and also concluded that lower inhibition was associated with slower SSRT. The direction of this association is opposite to that which we observed: enhancing $GABA_A$ efficacy in our study led to slower SSRT. However, it should be remembered that GABAergic networks are far from simple. For example, in the cerebral cortex, GABAergic cells expressing vasoactive intestinal polypeptide (VIP) inhibit those expressing somatostatin, which in turn inhibit excitatory pyramidal neurons (Karnani et al., 2016). Both inhibition and disinhibition will be potentiated by diazepam. The level of GABA measured by magnetic resonance spectroscopy is a composite of the contributions from all inhibitory circuits in a given region; SICI measures inhibition of corticospinal pyramidal neurons. Differences in the sensitivity of circuits to each approach likely underlie the different direction of effects seen.

There are some reports of non-$GABA_A$ receptor occupancy (5HT, D2) by diazepam (Saner and Pletscher, 1979; Gomez et al., 2017; van der Kooij et al., 2018) raising the possibility that the effects we observed could be mediated *via* non-GABAergic mechanisms. However, this is unlikely to explain our results given that we observed effects at therapeutic doses of diazepam and that GABAergic networks are a crucial substrate of response inhibition (Nicholson et al., 2018).

CONCLUSION

Our results suggest that therapeutic doses of diazepam can significantly alter response inhibition. Inappropriate responses in a stop signal task are presumably mediated by inhibition of the prefrontal cortex, through GABAergic mechanisms. These changes occurred at doses that had no effect on the simple RT. This indicates that even a therapeutic dose of diazepam should be taken with adequate precaution, especially in cases where motor compromise is already a feature.

DATA AVAILABILITY STATEMENT

The raw data supporting the conclusions of this article will be made available by the authors on request, without undue reservation.

ETHICS STATEMENT

The studies involving human participants were reviewed and approved by Institutional Ethics Committee (reference number I-NK/IEC/99/2019 ver.1. dated 29 April 2019) Institute of Neurosciences Kolkata, Kolkata, India. The patients/participants provided their written informed consent to participate in this study.

AUTHOR CONTRIBUTIONS

SS and SC: study concept and design, acquisition of data, analysis, and interpretation, writing the first draft, and critical revision of the manuscript for important intellectual content. NI: acquisition of data, analysis, and interpretation, and critical revision of the manuscript for important intellectual content. MC and MdC: critical revision of the manuscript for important intellectual content. MB: study concept and design, acquisition of data, analysis, and interpretation, and critical revision of the manuscript for important intellectual content. SB: study concept and design, analysis and interpretation, critical revision of the manuscript for important intellectual content, and study supervision. HK: study concept and design, acquisition of data, analysis, and interpretation, critical revision of the manuscript for important intellectual content, and study supervision. All authors contributed to the article and approved the submitted version.

FUNDING

HK received an Institutional research fund, Institute of Neurosciences Kolkata, India. Partial funding for the study was provided by MRC Confidence in Concept grant number MC/PC/17168 and by MRC project grant number MR/P012922/1 to SB.

REFERENCES

Acheson, A., Reynolds, B., Richards, J. B., and de Wit, H. (2006). Diazepam impairs behavioral inhibition but not delay discounting or risk taking in healthy adults. *Exp. Clin. Psychopharmacol.* 14, 190–198. doi: 10.1037/1064-1297.14.2.190

Aron, A. R., Behrens, T. E., Smith, S., Frank, M. J., and Poldrack, R. A. (2007). Triangulating a cognitive control network using diffusion-weighted magnetic resonance imaging (MRI) and functional MRI. *J. Neurosci.* 27, 3743–3752. doi: 10.1523/JNEUROSCI.0519-07.2007

Aron, A. R., and Poldrack, R. A. (2006). Cortical and subcortical contributions to Stop signal response inhibition: role of the subthalamic nucleus. *J. Neurosci.* 26, 2424–2433. doi: 10.1523/JNEUROSCI.4682-05.2006

Aron, A. R., Robbins, T. W., and Poldrack, R. A. (2014). Inhibition and the right inferior frontal cortex: one decade on. *Trends Cogn. Sci.* 18, 177–185. doi: 10.1016/j.tics.2013.12.003

Ascoli, G. A., Alonso-Nanclares, L., Anderson, S. A., Barrionuevo, G., Benavides-Piccione, R., Burkhalter, A., et al. (2008). Petilla terminology: nomenclature of features of GABAergic interneurons of the cerebral cortex. *Nat. Rev. Neurosci.* 9, 557–568. doi: 10.1038/nrn2402

Baker, S. C., Rogers, R. D., Owen, A. M., Frith, C. D., Dolan, R. J., Frackowiak, R. S. J., et al. (1996). Neural systems engaged by planning: a PET study of the Tower of London task. *Neuropsychologia* 34, 515–526. doi: 10.1016/0028-3932(95)00133-6

Bari, A., Mar, A. C., Theobald, D. E., Elands, S. A., Oganya, K. C., Eagle, D. M., et al. (2011). Prefrontal and monoaminergic contributions to stop-signal task performance in rats. *J. Neurosci.* 31, 9254–9263. doi: 10.1523/JNEUROSCI.1543-11.2011

Bechara, A., Noel, X., and Crone, E. A. (2006). "Loss of willpower: abnormal neural mechanisms of impulse control and decision making in addiction," in *Handbook of Implicit Cognition and Addiction*, eds R. W. Wiers and A. W. Stacy (Thousand Oaks, CA: Sage Publications, Inc.), 215–232.

Boehler, C. N., Schevernels, H., Hopf, J. M., Stoppel, C. M., and Krebs, R. M. (2014). Reward prospect rapidly speeds up response inhibition *via* reactive control. *Cogn. Affect. Behav. Neurosci.* 14, 593–609. doi: 10.3758/s13415-014-0251-5

Choudhury, S., Roy, A., Mondal, B., Singh, R., Halder, S., Chatterjee, K., et al. (2019). Slowed movement stopping in Parkinson's disease and focal dystonia is improved by standard treatment. *Sci. Rep.* 9:19504. doi: 10.1038/s41598-019-55321-5

Chowdhury, N. S., Livesey, E. J., and Harris, J. A. (2019). Individual differences in intracortical inhibition during behavioural inhibition. *Neuropsychologia* 124, 55–65. doi: 10.1016/j.neuropsychologia.2019.01.008

Dalley, J. W., Fryer, T. D., Brichard, L., Robinson, E. S., Theobald, D. E., Laane, K., et al. (2007). Nucleus accumbens D2/3 receptors predict trait impulsivity and cocaine reinforcement. *Science* 315, 1267–1270. doi: 10.1126/science.1137073

Deakin, J. B., Aitken, M. R., Dowson, J. H., Robbins, T. W., and Sahakian, B. J. (2004). Diazepam produces disinhibitory cognitive effects in male volunteers. *Psychopharmacology* 173, 88–97. doi: 10.1007/s00213-003-1695-4

Debey, E., De Schryver, M., Logan, G. D., Suchotzki, K., and Verschuere, B. (2015). From junior to senior Pinocchio: a cross-sectional lifespan investigation of deception. *Acta Psychol.* 160, 58–68. doi: 10.1016/j.actpsy.2015.06.007

De Wit, H., and Richards, J. B. (2004). Dual determinants of drug use in humans: rewards and impulsivity. *Nebr. Sym. Motiv.* 50, 19–55.

Downing, S. S., Lee, Y. T., Farb, D. H., and Gibbs, T. T. (2005). Benzodiazepine modulation of partial agonist efficacy and spontaneously active $GABA^{(A)}$ receptors supports an allosteric model of modulation. *Br. J. Pharmacol.* 145, 894–906. doi: 10.1038/sj.bjp.0706251

Eagle, D. M., Tufft, M. R., Goodchild, H. L., and Robbins, T. W. (2007). Differential effects of modafinil and methylphenidate on stop-signal reaction time task performance in the rat and interactions with the dopamine receptor antagonist cis-flupenthixol. *Psychopharmacology* 192, 193–206. doi: 10.1007/s00213-007-0701-7

Ersche, K. D., Jones, P. S., Williams, G. B., Turton, A. J., Robbins, T. W., and Bullmore, E. T. (2012). Abnormal brain structure implicated in stimulant drug addiction. *Science* 335, 601–604. doi: 10.1126/science.1214463

Fillmore, M. T., Rush, C. R., and L, H. (2002). Acute effects of oral cocaine on inhibitory control of behavior in humans. *Drug Alcohol Depend.* 67, 157–167. doi: 10.1016/s0376-8716(02)00062-5

Ford, R. D., Rech, R. H., Commissaris, R. L., and Meyer, L. Y. (1979). Effects of acute and chronic interactions of diazepam and d-amphetamine on punished behavior of rats. *Psychopharmacology* 65, 197–204. doi: 10.1007/bf00433049

Forstmann, B. U., Keuken, M. C., Jahfari, S., Bazin, P. L., Neumann, J., Schäfer, A., et al. (2012). Cortico-subthalamic white matter tract strength predicts interindividual efficacy in stopping a motor response. *NeuroImage* 60, 370–375. doi: 10.1016/j.neuroimage.2011.12.044

Frank, M. J. (2006). Hold your horses: a dynamic computational role for the subthalamic nucleus in decision making. *Neural Netw.* 19, 1120–1136. doi: 10.1016/j.neunet.2006.03.006

Gelkopf, M., Bleich, A., Hayward, R., Bodner, G., and Adelson, M. (1999). Characteristics of benzodiazepine abuse in methadone maintenance treatment patients: a 1 year prospective study in an Israeli clinic. *Drug Alcohol Depend.* 55, 63–68. doi: 10.1016/s0376-8716(98)00175-6

Gielen, M. C., Lumb, M. J., and Smart, T. G. (2012). Benzodiazepines modulate $GABA_A$ receptors by regulating the preactivation step after GABA binding. *J. Neurosci.* 32, 5707–5715. doi: 10.1523/JNEUROSCI.5663-11.2012

Gomez, A. A., Fiorenza, A. M., Boschen, S. L., Sugi, A. H., Beckman, D., Ferreira, S. T., et al. (2017). Diazepam inhibits electrically evoked and tonic dopamine release in the nucleus accumbens and reverses the effect of amphetamine. *ACS Chem. Neurosci.* 8, 300–309. doi: 10.1021/acschemneuro.6b00358

Granon, S., Passetti, F., Thomas, K. L., Dalley, J. W., Everitt, B. J., and Robbins, T. W. (2000). Enhanced and impaired attentional performance after infusion of D1 dopaminergic receptor agents into rat prefrontal cortex. *J. Neurosci.* 20, 1208–1215. doi: 10.1523/JNEUROSCI.20-03-01208.2000

Hanes, D. P., and Schall, J. D. (1996). Neural control of voluntary movement initiation. *Science* 274, 427–430. doi: 10.1126/science.274.5286.427

Harrison, A. A., Everitt, B. J., and Robbins, T. W. (1997). Central 5-HT depletion enhances impulsive responding without affecting the accuracy of attentional performance: interactions with dopaminergic mechanisms. *Psychopharmacology* 133, 329–342. doi: 10.1007/s002130050410

Heishman, S. J., Arasteh, K., and Stitzer, M. L. (1997). Comparative effects of alcohol and marijuana on mood, memory, and performance. *Pharmacol. Biochem. Behav.* 58, 93–101. doi: 10.1016/s0091-3057(96)00456-x

Hermans, L., Leunissen, I., Pauwels, L., Cuypers, K., Peeters, R., Puts, N. A. J., et al. (2018). Brain GABA levels are associated with inhibitory control deficits in older adults. *J. Neurosci.* 38, 7844–7851. doi: 10.1523/JNEUROSCI.0760-18.2018

Hikosaka, O., and Isoda, M. (2010). Switching from automatic to controlled behavior: cortico-basal ganglia mechanisms. *Trends Cogn. Sci.* 14, 154–161. doi: 10.1016/j.tics.2010.01.006

Inase, M., Tokuno, H., Nambu, A., Akazawa, T., and Takada, M. (1999). Corticostriatal and corticosubthalamic input zones from the presupplementary motor area in the macaque monkey: comparison with the input zones from the supplementary motor area. *Brain Res.* 833, 191–201. doi: 10.1016/s0006-8993(99)01531-0

Karnani, M. M., Jackson, J., Ayzenshtat, I., Hamzehei Sichani, A., Manoocheri, K., Kim, S., et al. (2016). Opening holes in the blanket of inhibition: localized lateral disinhibition by VIP interneurons. *J. Neurosci.* 36, 3471–3480. doi: 10.1523/JNEUROSCI.3646-15.2016

Leunissen, I., Zandbelt, B. B., Potocanac, Z., Swinnen, S. P., and Coxon, J. P. (2017). Reliable estimation of inhibitory efficiency: to anticipate, choose or simply react? *Eur. J. Neurosci.* 45, 1512–1523. doi: 10.1111/ejn.13590

Lévesque, J. C., and Parent, A. (2005). GABAergic interneurons in human subthalamic nucleus. *Mov. Disord.* 20, 574–584. doi: 10.1002/mds.20374

Li, C. S., Yan, P., Sinha, R., and Lee, T. W. (2008). Subcortical processes of motor response inhibition during a stop signal task. *NeuroImage* 41, 1352–1363. doi: 10.1016/j.neuroimage.2008.04.023

Ljungberg, T. (1990). Diazepam and decision making in the rat: negative evidence for reduced tolerance to reward delay. *Psychopharmacology* 102, 117–121. doi: 10.1007/bf02245755

Ljungberg, T., Lidfors, L., Enquist, M., and Ungerstedt, U. (1987). Impairment of decision making in rats by diazepam: implications for the "anticonflict"

effects of benzodiazepines. *Psychopharmacology* 92, 416–423. doi: 10.1007/bf00176471

Logan, G. D., Cowan, W. B., and Davis, K. A. (1984). On the ability to inhibit simple and choice reaction time responses: a model and a method. *J. Exp. Psychol.* 10, 276–291. doi: 10.1037/0096-1523.10.2.276

Mandelli, M., Tognoni, G., and Garattini, S. (1978). Clinical pharmacokinetics of diazepam. *Clin. Pharmacokinet.* 3, 72–91. doi: 10.2165/00003088-197803010-00005

Manes, F., Sahakian, B., Clark, L., Rogers, R., Antoun, N., Aitken, M. R., et al. (2002). Decision-making processes following damage to the prefrontal cortex. *Brain* 125, 624–639. doi: 10.1093/brain/awf049

Möhler, H. (2015). The legacy of the benzodiazepine receptor: from flumazenil to enhancing cognition in Down syndrome and social interaction in autism. *Adv. Pharmacol.* 72, 1–36. doi: 10.1016/bs.apha.2014.10.008

Mückschel, M., Stock, A. K., and Beste, C. (2014). Psychophysiological mechanisms of interindividual differences in goal activation modes during action cascading. *Cereb. Cortex* 24, 2120–2129. doi: 10.1093/cercor/bht066

Munakata, Y., Herd, S. A., Chatham, C. H., Depue, B. E., Banich, M. T., and O'Reilly, R. C. (2011). A unified framework for inhibitory control. *Trends Cogn. Sci.* 15, 453–459. doi: 10.1016/j.tics.2011.07.011

Nicholson, M. W., Sweeney, A., Pekle, E., Alam, S., Ali, A. B., Duchen, M., et al. (2018). Diazepam-induced loss of inhibitory synapses mediated by PLCdelta/Ca^{2+}/calcineurin signalling downstream of $GABA_A$ receptors. *Mol. Psychiatry* 23, 1851–1867. doi: 10.1038/s41380-018-0100-y

Reynolds, B., Richards, J. B., Dassinger, M., and de Wit, H. (2004). Therapeutic doses of diazepam do not alter impulsive behavior in humans. *Pharmacol. Biochem. Behav.* 79, 17–24. doi: 10.1016/j.pbb.2004.06.011

Robbins, T. W. (2000). Chemical neuromodulation of frontal-executive functions in humans and other animals. *Exp. Brain Res.* 133, 130–138. doi: 10.1007/s002210000407

Rogers, R. D., Owen, A. M., Middleton, H. C., Williams, E. J., Pickard, J. D., Sahakian, B. J., et al. (1999). Choosing between small, likely rewards and large, unlikely rewards activates inferior and orbital prefrontal cortex. *J. Neurosci.* 20, 9029–9038. doi: 10.1523/JNEUROSCI.19-20-09029.1999

Rudolph, U., and Knoflach, F. (2011). Beyond classical benzodiazepines: novel therapeutic potential of $GABA_A$ receptor subtypes. *Nat. Rev. Drug Discov.* 10, 685–697. doi: 10.1038/nrd3502

Saner, A., and Pletscher, A. (1979). Effect Of diazepam on cerebral 5-hydroxytryptamine synthesis. *Eur. J. Pharmacol.* 55, 315–318. doi: 10.1016/0014-2999(79)90200-0

Schachar, R., and Logan, G. D. (1990). Impulsivity and inhibitory control in normal development and childhood psychopathology. *Dev. Psychol.* 26, 710–720. doi: 10.1037/0012-1649.26.5.710

Tannock, R., Schachar, R., and Logan, G. D. (1995). Methylphenidate and cognitive flexibility: dissociated dose effects in hyperactive children. *J. Abnorm. Child Psychol.* 23, 235–266. doi: 10.1007/bf01447091

van der Kooij, M. A., Hollis, F., Lozano, L., Zalachoras, I., Abad, S., Zanoletti, O., et al. (2018). Diazepam actions in the VTA enhance social dominance and mitochondrial function in the nucleus accumbens by activation of dopamine D1 receptors. *Mol. Psychiatry* 23, 569–578. doi: 10.1038/mp.2017.135

van Gaalen, M. M., Brueggeman, R. J., Bronius, P. F., Schoffelmeer, A. N., and Vanderschuren, L. J. (2006). Behavioral disinhibition requires dopamine receptor activation. *Psychopharmacology* 187, 73–85. doi: 10.1007/s00213-006-0396-1

Verbruggen, F., Chambers, C. D., and Logan, G. D. (2013). Fictitious inhibitory differences: how skewness and slowing distort the estimation of stopping latencies. *Psychol. Sci.* 24, 352–362. doi: 10.1177/0956797612457390

Verbruggen, F., Stevens, T., and Chambers, C. D. (2014). Proactive and reactive stopping when distracted: an attentional account. *J. Exp. Psychol. Hum. Percept. Perform.* 40, 1295–1300. doi: 10.1037/a0036542

Whelan, R., Conrod, P. J., Poline, J. B., Lourdusamy, A., Banaschewski, T., Barker, G. J., et al. (2012). Adolescent impulsivity phenotypes characterized by distinct brain networks. *Nat. Neurosci.* 15, 920–925. doi: 10.1038/nn.3092

Winstanley, C. A., Theobald, D. E., Dalley, J. W., Glennon, J. C., and Robbins, T. W. (2004). 5-HT2A and 5-HT2C receptor antagonists have opposing effects on a measure of impulsivity: interactions with global 5-HT depletion. *Psychopharmacology* 176, 376–385. doi: 10.1007/s00213-004-1884-9

Woods, J. R., Plessinger, M. A., and Clark, K. E. (1987). Effect of cocaine on uterine blood flow and fetal oxygenation. *JAMA* 257, 957–961. doi: 10.1001/jama.1987.03390070077027

Conflict of Interest: The authors declare that the research was conducted in the absence of any commercial or financial relationships that could be construed as a potential conflict of interest.

Advantages of publishing in Frontiers

OPEN ACCESS
Articles are free to read for greatest visibility and readership

FAST PUBLICATION
Around 90 days from submission to decision

HIGH QUALITY PEER-REVIEW
Rigorous, collaborative, and constructive peer-review

TRANSPARENT PEER-REVIEW
Editors and reviewers acknowledged by name on published articles

Frontiers
Avenue du Tribunal-Fédéral 34
1005 Lausanne | Switzerland

Visit us: www.frontiersin.org
Contact us: frontiersin.org/about/contact

REPRODUCIBILITY OF RESEARCH
Support open data and methods to enhance research reproducibility

DIGITAL PUBLISHING
Articles designed for optimal readership across devices

FOLLOW US
@frontiersin

IMPACT METRICS
Advanced article metrics track visibility across digital media

EXTENSIVE PROMOTION
Marketing and promotion of impactful research

LOOP RESEARCH NETWORK
Our network increases your article's readership